Award Number: W81XWH-12-1-0224

TITLE: "Prostate Cancer Diagnostics and Prognostics Based on Interphase Spatial Genome Positioning"

PRINCIPAL INVESTIGATOR: Thomas Misteli

CONTRACTING ORGANIZATION: The Geneva Foundation
Tacoma, WA 98402

REPORT DATE: March 2016

TYPE OF REPORT: Final report

PREPARED FOR: U.S. Army Medical Research and Materiel Command Fort Detrick, Maryland 21702-5012

REPORT DOCUMENTATION PAGE

Form Approved OMB No. 0704-0188

1. REPORT DATE	2. REPORT TYPE	3. DATES COVERED
March 2016	Final	1 July 2012 - 31 Dec 2015

4. TITLE AND SUBTITLE

"Prostate Cancer Diagnostics and Prognostics Based on Interphase Spatial Genome Positioning"

5a. CONTRACT NUMBER

5b. GRANT NUMBER
W81XWH-12-1-0224

5c. PROGRAM ELEMENT NUMBER

6. AUTHOR(S)
Thomas Misteli, Karen Meaburn

E-Mail: mistelit@mail.nih.gov; meaburnk@mail.nih.gov

5d. PROJECT NUMBER

5e. TASK NUMBER

5f. WORK UNIT NUMBER

7. PERFORMING ORGANIZATION NAME(S) AND ADDRESS(ES)

The Geneva Foundation 917
Pacific Ave, Suite 600
Tacoma, WA 98402

8. PERFORMING ORGANIZATION REPORT NUMBER

9. SPONSORING / MONITORING AGENCY NAME(S) AND ADDRESS(ES)

U.S. Army Medical Research and Materiel Command
Fort Detrick, Maryland 21702-5012

10. SPONSOR/MONITOR'S ACRONYM(S)

11. SPONSOR/MONITOR'S REPORT NUMBER(S)

12. DISTRIBUTION / AVAILABILITY STATEMENT

Approved for Public Release; Distribution Unlimited

13. SUPPLEMENTARY NOTES

14. ABSTRACT

We are aiming to develop a novel strategy for the diagnosis and prognosis of prostate cancer. Our approach takes advantage of the non-random spatial organization of the genome in human cell nuclei. It is well established that individual gene loci can undergo changes in their spatial position during disease. We have previously exploited these changes in spatial positioning patterns as a novel tool for the detection of invasive breast cancer, and we are now extending these studies to prostate cancer. We have screened 48 genes in a panel of normal, cancer and hyperplasic human prostate tissues. We have identified three genes as potential prostate cancer biomarkers (*FLI1*, *MMP2* and *MMP9*), based on changes in their spatial positioning patterns in cancerous tissues, compared to normal. *FLI1* and *MMP9* repositioning is specific to cancer, and does not occur in benign disease. The positioning pattern of *MMP2* is a biomarker for prostate disease in general, since *MMP2* also repositions, albeit to a smaller degree, in benign disease. Changes in spatial positioning do not correlate with copy number changes or prognostic status. If validated, these three gene positioning biomarkers represent a novel class of biomarkers for the detection of prostate cancer and prostate disease. Further, we identified a fourth gene, *SP100*, which may have prognostic potential, since it repositions in low grade Gleason score cancers, but not intermediate Gleason grade cancers.

15. SUBJECT TERMS
Prostate Cancer; Cancer Diagnosis; Spatial Gene Positioning; Nuclear Architecture.

16. SECURITY CLASSIFICATION OF:			17. LIMITATION OF ABSTRACT	18. NUMBER OF PAGES	19a. NAME OF RESPONSIBLE PERSON
a. REPORT	b. ABSTRACT	c. THIS PAGE			USAMRMC
Unclassified	Unclassified	Unclassified	Unclassified	137	19b. TELEPHONE NUMBER *(include area code)*

Table of Contents

Page

1. Introduction

Prostate cancer is one of the most prevalent cancers in the United States, where there are more than 180,000 new cases diagnosed each year and 1 in 7 men develop prostate cancer during their lifetime (*1*). Over 26,000 men die annually from prostate cancer, accounting for 8% of all male cancer deaths (*1*). Diagnosis of prostate relies on histological analysis of biopsies, which uses subjective morphological and histological criteria. Only neoplastic changes that result in clear histological defects can be detected. Moreover, currently there is a lack of reliable prognostic markers to distinguish latent prostate cancers, where a watch-and-wait approach is the best strategy for the patient, from aggressive tumors, which require treatment as early in the cancers life as possible. During the DoD Prostate Cancer Idea Award funding period, our objective was to test the feasibility of using the differential non-random spatial organization of the genome between normal and cancer tissue as the basis of a novel, molecularly defined, diagnostic and prognostic test. Our method is based on the fact that genomes are non-randomly organized with individual chromosomes and genes occupying preferred positions within interphase nuclei (*2-4*). Changes to these positioning patterns can occur in cancer (*5, 6*). For example, in pancreatic cancer, chromosome 8 shifts to a more peripheral location (*7*). Similarly, chromosomes 18 and 19 change nuclear location in several cancers types, including cervical, thyroid and colon (*8, 9*). We have previously discovered several genes that are repositioned in breast cancer, but, importantly, not in non-cancerous breast diseases (*10-12*). Such changes in spatial positioning patterns are not a reflection of a global reorganization of the genome during carcinogenesis and are instead loci-specific, with the position of many genomic regions remaining conserved in cancer (*7, 11, 12*). For the DoD Prostate Cancer Idea Award, we aimed to exploit spatial genome reorganization events for the diagnosis and, subsequently, prognosis of prostate cancer.

2. Key Words

Prostate Cancer; Cancer Diagnosis; Spatial Gene Positioning; Nuclear Architecture; Cancer Biomarkers, Prognosis; *FLI1; MMP9*; *MMP2*; *SP100*.

3. Overall Project Summary

Gene positioning methodology (all tasks)

The aim of this project was to identify genes that occupy distinct intra-nuclear positions in normal and malignant cells and to explore the usability of these markers for diagnostic purposes. The methods are described in full in the accompanying copies of the published articles generated from this work (*10, 13*) (see Appendices). Briefly, we performed fluorescence *in situ* hybridization (FISH) to detect individual genes in 4-5μm thick formalin fixed, paraffin embedded human prostate tissue sections, using protocols established for breast tissues and optimized for prostate tissues (*10, 11, 13, 14*) (Fig. 1. A, B). The radial position of a gene was determined using a previously developed image analysis method (*10, 11, 13*). Radial positioning describes the location of a gene locus along the axis from the center of the nucleus to the nuclear periphery (edge). To account for the fact that nuclei are not always a regular elliptical shape, a method was developed in which the binary Euclidean distance transform (EDT) was computed for each nucleus (*10, 11, 13*). The EDT is a morphological operation that assigns each pixel in a nucleus a value that equals the shortest distance to the edge of the nucleus. To account for variations in nuclear size, the EDT of the geometric gravity center of a FISH signal is normalized to the maximum EDT value for the given nucleus. Using this method, no assumption regarding nuclear shape is made when

determining the radial position of a gene, allowing accurate comparisons between tissues, even if there are differences or irregularities in nuclear shape or size. All alleles in a nucleus were included in the analysis and nuclei were included regardless of the number of alleles present, unless no gene signals were present in a nucleus. For each sample, data from 89-263 epithelial nuclei, which were acquired from multiple randomly selected regions of the tissue sample, were analyzed and combined to determine the cumulative relative radial distribution (RRD) for each gene in a tissue. The RRD is a standard measure of a genes position in a population and is defined as the statistical distribution of the radial position of all alleles in a cell population. RRDs were statistically compared to each other using the two-sample 1-D Kolmogorov-Smirnov test (KS; $P < 0.01$).

Figure 1.

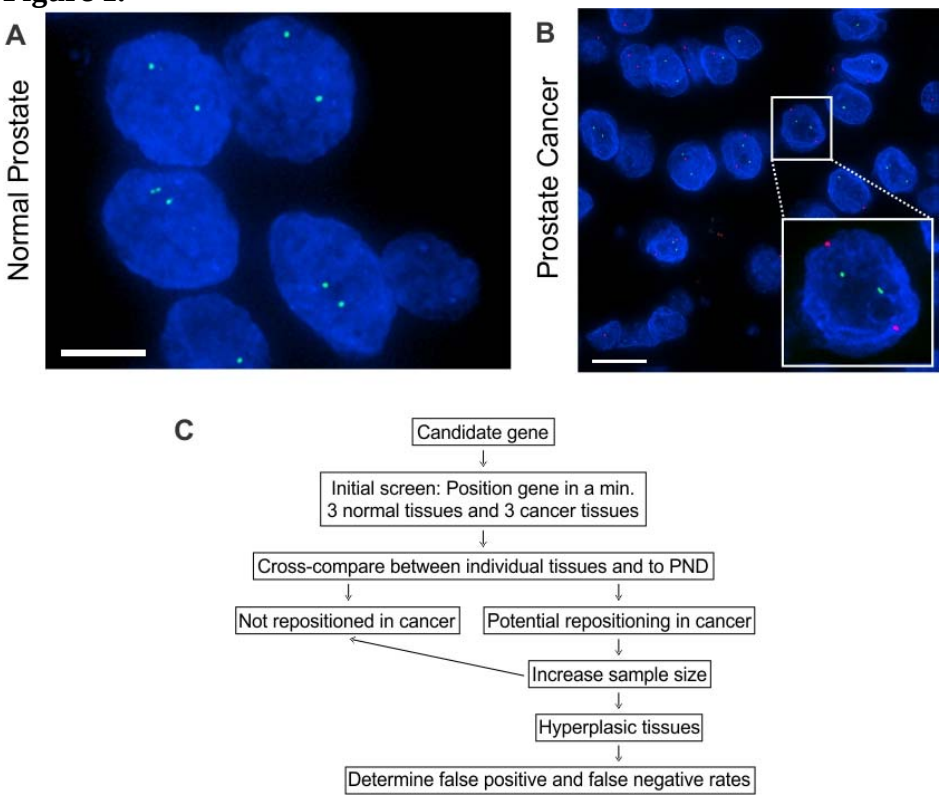

Fig 1. FISH was used to detect gene loci in FFPE tissue sections. Blue, DAPI nuclear counterstain. Projected image stacks of represented FISH are shown. (A) *HES5* (green) in a normal prostate tissue. Scale bar, 5µm. (B) *EGFR* (red) and *SPDEF* (green) gene loci, in a malignant prostate tissue. Bar, 10µm. (C) Outline of the screening strategy used to identify genes that reposition in prostate cancer. PND: Pooled normal distribution. Fig adapted from (*10, 13*)

For this DoD funded study, we analyzed the RRDs of 48 genes (Table 1) in a panel of human prostate tissues (Table 2). We have previously identified a set of eight genes (*AKT1*, *CSF1R, ERBB2*, *FOL2, HES5, HSP90AA1, MYC* and *TGFB3*) that reposition in breast cancer (*11*), which we refer to as breast GBPs (Gene Positioning Biomarkers). To determine if breast GPBs would also be useful markers of prostate cancer we analyzed the positions of the breast GPBs in prostate tissues (Published (*10*), appendix). We also screened a wide range of genes in prostate tissues, which included many of the most important genes related to prostate cancer, such as genes that have been reported mis-regulated in prostate cancer or participate in translocations, as well as a set of randomly selected genes, which were selected independently of known changes in activity

or involvement in prostate cancer development or progression. Moreover, the test set included genes from 21 different chromosomes (Published (*13*), appendix).

Table 1. Candidate genes positioned in human prostate tissues

	Gene	Chromosomal location	BAC	Number of nuclei in PND
a	*AKT1*	14q32.33	RP11-477I4	465
	CSF1R	5q32	RP11-21I20	1397
	ERBB2	17q21	RP11-62N23	515
	FOSL2	2p23.2	RP11-373D23	1090
	HES5	1p36.32	RP3-395M20	798
	HSP90AA1	14q32.31	RP11-367F11	880
	MYC	8q24.21	RP11-237F24	648
	TGFB3	14q24.3	RP11-270M14	741
b	*AR*	Xq12	RP11-479J1	752
	BCL2	18q21.33	RP11-299P2	489
	BRCA2	13q13.1	RP11-37E23	518
	CCND1	11q13	RP11-300I6	508
	DCN	12q21.33	RP11-644B23	461
	EGFR	7p11.2	RP11-815K24	612
	ERG	21q22.2	RP11-95I21	646
	ESR2	14q23.2-q23.3	RP11-14C21	641
	ETV1	7p21.2	RP11-692L4	569
	FGFR1	8p11.23-p11.22	RP11-100B16	716
	FGFR2	10q26.13	RP11-300A10	740
	FLI1	11q24.3	RP11-744N12	1047
	FOXA1	14q21.1	RP11-606C5	411
	FUT4	11q21	RP11-42H7	449
	GREB1	2p25.1	RP11-50E1	523
	HOXA9	7p15.2	RP11-1132K14	505
	KLK3 (PSA)	19q13.33	RP11-795B6	541
	LMNA	1q22	RP11-35P22	481
	MATR3	5q31.2	RP11-815G18	488
	MMP1	11q22.2	RP11-686G6	303
	MMP14	14q11.2	RP11-885L10	324
	MMP2	16q12.2	RP11-90H1	791
	MMP9	20q13.12	RP11-465L10	1128
	NPM1	5q35.1	RP11-117L6	311
	NUMA1	11q13.4	RP11-449G14	514
	PADI4/6	1p36.13	RP11-1119C2	647
	PTEN	10q23.31	RP11-383D9	391
	RAF1	3p25.2	RP11-148M13	1027
	SATB1	3p24.3	RP11-1021J5	610
	SERPINB2	18q21.33	RP11-75O12	380
	SLC45A3	1q32.1	RP11-6B6	727
	SP100	2q37.1	RP11-727M18	615
	SPDEF	6p21.31	RP11-375E1	517
	TGFB1	19q13.2	RP11-1012F23	433
	THBS1	15q14	RP11-590D2	630
	TIMP2	17q25.3	RP11-72M9	697
	TIMP3	22q12.3	RP11-641L14	760
	TMPRSS2	21q22.3	RP11-671L10	1260
	VEGFA	6p21.1	RP11-1152J4	1375
	VIM	10p13	RP11-1122I7	631

a) Breast cancer GPBs b) remaining genes. BAC, Bacterial artificial chromosome. PND, pooled normal distribution. Table from (*10, 13*)

Table 2. Characterization of human prostate tissues

a. Analysis of breast cancer GPBs in prostate tissue

Sample code	Pathology	Age (years)	Vol of cancer (cc)	Weight of prostate (g)	Stage	Gleason Score	TNM	Metastatic	Source	Source specimen ID
P-C1	Adenocarcinoma	73			II	6 (3+3)	T2N0M0	No	Biomax	HuCAT371
P-C2	Adenocarcinoma								L.D.T.	UW7
P-C3	Adenocarcinoma								L.D.T.	UW8
P-C4	Adenocarcinoma	75							Biomax	HuCAT376
P-C5	Adenocarcinoma	72							Biomax	HuCAT367
P-C6	Adenocarcinoma	80							Biomax	HuCAT366
P-C7	Adenocarcinoma								L.D.T.	UW3
P-C8	Adenocarcinoma	58			II	6 (3+3)	T2N0M0	No	Biomax	TMA: PR632, core F3
P-C9	Adenocarcinoma	73			II	5 (2+3)	T2N0M0	No	Biomax	TMA: PR632, core F5
P-C10	Adenocarcinoma								L.D.T.	UW24
P-C11	Adenocarcinoma	50’s	5.5	36		7	T3N0		L.D.T.	UW18
P-C12	Adenocarcinoma								L.D.T.	UW19
P-C13	Adenocarcinoma	50's	0.5	30		6	T2N0		L.D.T.	UW5
P-C14	Adenocarcinoma	60's	1	33		7	T2N0		L.D.T.	UW11
P-C15	Adenocarcinoma	50's	2	40		7	T2N0		L.D.T.	UW13
P-C16	Adenocarcinoma	50's	3	31		6	T2N0		L.D.T.	UW15
P-C17	Adenocarcinoma	50's	0.6	26		7	T2N0		L.D.T.	UW9
P-C18	Adenocarcinoma	50's	4.5	38		7	T2N0		L.D.T.	UW12
P-C19	Adenocarcinoma	50's	1.2	32		6	T2N0		L.D.T.	UW14
P-C20	Adenocarcinoma	40’s	3.5	37		7	T2N0		L.D.T.	UW16
P-B1	Hyperplasia; same individual as C3	50's							L.D.T.	UW20
P-B2	Hyperplasia	73							Biomax	TMA: PR632, core D1, D2, D3 #
P-B3	Hyperplasia	74							Biomax	TMA: PR632, core E1, E2 #
P-B4	Hyperplasia	78							Biomax	TMA: PR632, cores E7, E8 #
P-N1	Normal	28							Biomax	HuFPT141
P-N2	Normal	54							Imgenex	IMH-1035
P-N3	Normal	35							Biomax	TMA: PR632, core B2

P-N4	Normal	37		TMA: PR632, core B8
P-N5	Normal	35	Biomax	TMA: PR632, core C4 or C6
P-N6	Normal	48/35[a]	Biomax	HuFPT143
P-N7	Normal	64	BioChain	T2234201
P-N8	Normal	43	Biomax	HuFPT142
P-N9	Normal		L.D.T.	UW21
P-N10	Normal		L.D.T.	UW22
P-N11	Normal		L.D.T.	UW24
P-N12	NAT (of P-C2)		L.D.T.	UW7
P-N13	NAT (of P-C3)		L.D.T.	UW8
P-N14	NAT (of P-C10)		L.D.T.	UW17
P-N15	NAT (of P-C11)	50s	L.D.T.	UW18
P-N16	NAT (of P-C12)		L.D.T.	UW19
P-N17	NAT (of P-C13)	50's	L.D.T.	UW5
P-N18	NAT (of P-C14)	60's	L.D.T.	UW11
P-N19	NAT (of P-C15)	50's	L.D.T.	UW13
P-N20	NAT (of P-C16)	50's	L.D.T.	UW15
P-N21	NAT (of P-C18)	50's	L.D.T.	UW12
P-N22	NAT (of P-C19)	50's	L.D.T.	UW14
P-N23	NAT (of P-C20)	40’s	L.D.T.	UW16
P-N24	NAT (of P- C17)	50's	L.D.T.	UW9

b) Analysis of other genes

Sample code	Pathology	Age (years)	Vol of cancer (cc)	Weight of prostate (g)	Stage	Gleason Score	TNM	Metastatic?	Source	Source specimen ID
C1	Adenocarcinoma	40's	1	36		7	T2N0		L.D.T.	UW1
C2	Adenocarcinoma	60's	1.6	47		9	T2N0		L.D.T.	UW2
C3	Adenocarcinoma								L.D.T.	UW3
C4	Adenocarcinoma	60's	0.6	40		7	T2N0		L.D.T.	UW4
C5	Adenocarcinoma	50's	0.5	30		6	T2N0		L.D.T.	UW5
C6	Adenocarcinoma	73			II	6 (3+3)	T2N0M0	No	Biomax	HuCAT371
C7	Adenocarcinoma	58			II	6 (3+3)	T2N0M0	No	Biomax	TMA: PR632, core F3
C8	Adenocarcinoma	73			II	5 (2+3)	T2N0M0	No	Biomax	TMA: PR632, core F5
C9	Adenocarcinoma	62			II	7 (3+4)	T2N0M0	No	Biomax	TMA: PR632, core G2
C10	Adenocarcinoma	71			II	8 (4+4)	T2N0M0	No	Biomax	TMA: PR632, core G8
C11	Adenocarcinoma	62			IV	7 (3+4)	T3N1M1b	Yes	Biomax	TMA: T196, core A6
C12	Adenocarcinoma	69			II	6 (3+3)	T2N0M0	No	Biomax	TMA: T196, core B6

C13	Adenocarcinoma	60			IV	8 (3+5)	T3N1M1b	Yes	Biomax	TMA: T196, core D2
C14	Adenocarcinoma	64			IV	7 (3+4)	T3N0M1b	Yes	Biomax	TMA: T196, core D4
C15	Adenocarcinoma	60's	3.5	36		7	T3bN0		L.D.T.	UW6
C16	Adenocarcinoma								L.D.T.	UW7
C17	Adenocarcinoma								L.D.T.	UW8
C18	Adenocarcinoma	50's	0.6	26		7	T2N0		L.D.T.	UW9
C19	Adenocarcinoma	60's	2.5	30		7	T3N0		L.D.T.	UW10
C20	Adenocarcinoma	60's	1	33		7	T2N0		L.D.T.	UW11
C21	Adenocarcinoma	50's	4.5	38		7	T2N0		L.D.T.	UW12
C22	Adenocarcinoma	50's	2	40		7	T2N0		L.D.T.	UW13
C23	Adenocarcinoma	50's	1.2	32		6	T2N0		L.D.T.	UW14
C24	Adenocarcinoma	50's	3	31		6	T2N0		L.D.T.	UW15
C25	Adenocarcinoma	40’s	3.5	37		7	T2N0		L.D.T.	UW16
C26	Adenocarcinoma								L.D.T.	UW17
C27	Adenocarcinoma	75							Biomax	HuCAT376
C28	Adenocarcinoma	50’s	5.5	36		7	T3N0		L.D.T.	UW18
C29	Adenocarcinoma	72							Biomax	HuCAT367
C30	Adenocarcinoma								L.D.T.	UW19
B1	Hyperplasia; same individual as C3	50's							L.D.T.	UW20
B2	Hyperplasia	70							Biomax	TMA: PR632, core D6
B3	Hyperplasia	76							Biomax	TMA: PR632, cores D9, D8, D7 #
B4	Hyperplasia	78							Biomax	TMA: PR632, cores E7, E8 #
B5	Hyperplasia	74							Biomax	TMA: PR632, core E2
N1	Normal	28							Biomax	TMA: PR632, core A9
N2	Normal	35							Biomax	TMA: PR632, core B2
N3	Normal	35							Biomax	TMA: PR632, core C6
N4	Normal	38							Biomax	TMA: PR632, core C7
N5	Normal	28							Biomax	HuFPT141
N6	Normal	43/31[a]							Biomax	HuFPT142
N7	Normal	48/35[a]							Biomax	HuFPT143
N8	Normal								L.D.T.	UW21
N9	Normal								L.D.T.	UW22
N10	Normal								L.D.T.	UW23
N11	Normal	54							Imgenex	IMH-1035
N12	NAT (of C1)	40's							L.D.T.	UW1
N13	NAT (of C2)	60's							L.D.T.	UW2
N14	NAT (of C4)	60's							L.D.T.	UW4

N15	NAT (of C5)	50's	L.D.T.	UW5
N16	NAT (of C15)	60's	L.D.T.	UW6
N17	NAT (of C16)		L.D.T.	UW7
N18	NAT (of C17)		L.D.T.	UW8
N19	NAT (of C18)	50's	L.D.T.	UW9
N20	NAT (of C19)	60's	L.D.T.	UW10
N21	NAT (of C20)	60's	L.D.T.	UW11
N22	NAT (of C21)	50's	L.D.T.	UW12
N23	NAT (of C22)	50's	L.D.T.	UW13
N24	NAT (of C23)	50's	L.D.T.	UW14
N25	NAT (of C24)	50's	L.D.T.	UW15
N26	NAT (of C25)	40's	L.D.T.	UW16
N27	NAT (of C26)		L.D.T.	UW17
N28	NAT (of C28)	50s	L.D.T.	UW18
N29	NAT (of C30)		L.D.T.	UW19

Biomax, US Biomax Inc; Imgenex, Imgenex corporation; L.D.T., Dr. Lawrence True; NAT, Normal Adjacent to Tumor; Normal, Normal tissue taken from cancer free prostates; TMA, Tissue microarray; Vol, volume; #, Multiple cores of the same tissue were used for analysis; [a]The individual used for these two catalogue numbers changed with subsequent purchases, consequently it is not always tissue from the same individual used between the different genes for these sample codes. Tables from (*10, 13*)

We used the same approach that led to the identification of positioning marker genes for breast cancer to search for gene positioning biomarkers (GPBs) for prostate cancer (Fig. 1 C). For an initial screen of candidate genes, we assessed the position of each gene in 3-6 cancer and 3-6 normal tissues. In our work on breast cancer, we established that this sample size accurately predicts if the given gene has promise to be a cancer GPB (*11*). We focused on aggressive cancers for this initial screen, with the majority of cancers used being Gleason score ≥7. We did this to bias our results to find markers of aggressive cancers, the most clinically relevant subtype of prostate cancer, since the best marker currently available for the aggressiveness of a prostate cancer is its Gleason score, with Gleason score ≥7 is considered an aggressive cancer. Promising candidate genes were further characterized in a larger cancer tissue set, which included cancers with Gleason scores of 5 and 6. This will enable us to assess if the genes position can be used as a marker of prostate cancer in general or specifically of aggressive cancer.

Task1: Identification of candidate makers based in radial positioning.
Tasks 4 and 5: Validation in normal and cancerous tissues.

Conservation of positioning patterns in morphologically normal prostate tissues

It is currently unknown how similar positioning patterns are between prostate tissues from different individuals. Potential variability of positioning patterns is particularly relevant in prostate, since the position of several genes has been shown to be sensitive to androgen (*15, 16*). Genes that are highly variable between individuals, in non-diseased tissues, will not be useful as cancer biomarkers since they are likely to generate high false positive rates. To determine the degree of variability in gene localization amongst individuals, we compared the positioning pattern of our set of 48 genes in morphologically normal prostate tissues (*10, 13*). For most of the genes analyzed the radial distribution of the gene between normal prostate tissues was similar (Table 3, 4, Fig. 2, 3,4, (*10, 13*). For 12 out of 48 (25.0%) genes the RRDs were statistically identical between all individuals ($P > 0.01$; Table 3, Fig. 2, 3,4). A further 25 genes (52.1%), although not identical between all comparisons, were very similarly positioned between most individuals, with less than 33.4% of cross-comparisons being statistically significantly different ($P < 0.01$). The position of 22.9% of genes (11/44; *FOL2*, *CSF1R, HSP90AA1, CCND1, ERG, LMNA, TGFB1, TIMP2, TIMP3, TMPRSS2* and *VIM*) were highly variable between individuals, with 38.9-70% of the individual cross-comparison between normal tissues being significantly different *FOL2*, *CSF1R* and *HSP90AA1*) (*10, 13*).

As another measure of conservation in positioning patterns between individuals, we compared the RRD of each gene in each normal tissue to a pooled normal distribution (PND), generated by combining the RRDs from all normal tissues analyzed into a single distribution for each gene, as previously described (*11*). Again we found a high level of similarity between individuals (Table 4, Figs. 2-4) (*10, 13*). For 30 of the 48 (62.5%) genes, no individual's normal tissue was significantly different than the PND (Table 4, Figs. 2-4) (*10, 13*). A further nine (18.8%) genes had only a single normal tissue significantly different to the PND (7.7-25% of normal tissues); while five genes, *CSF1R*, *FOSL2*, *FGFR1*, *TMPRSS2* and *RAF1* had ~one third (27.3-37.5%) of normal tissues significantly different to the PND (Table 4, Figs. 2-4) (*10, 13*). Four genes (*HSP90AA1*, *CCND1*, *TIMP2* and *TIMP3*) (4/48; 8.3%), however should substation intra-individual variation, and were significantly different to the PND in 42.9-66.7% of normal tissues

(Table 4, Figs. 2-4) (*10, 13*). Taken together, these data demonstrate that the radial positions of most genes are conserved amongst prostate tissue from different individuals. However, the position of a subset of genes is variable between individuals.

Figure 2.

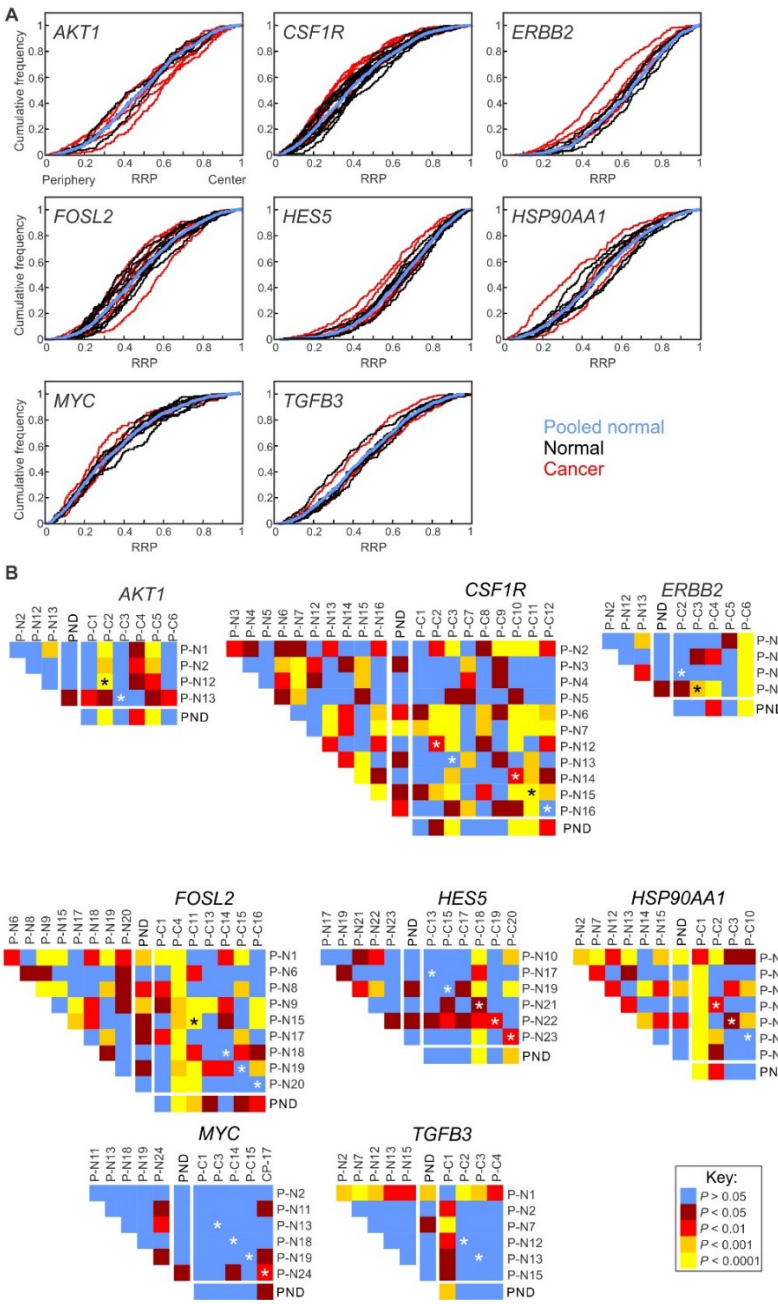

Fig.2. Breast cancer GPBs do not reposition in prostate cancer. (a) Cumulative RRDs for the indicated genes in prostate cancer, normal tissues and the pooled normal distribution (PND). (b) Heat maps representing the pair-wise statistical comparisons of positioning patterns of indicated genes between tissues, using the two-sample 1D KS test. P-N1 - P-N24, normal prostate tissues; P-C1 - P-C20, cancerous prostate tissues Black or white asterisks indicate a cross-comparison between a normal and cancer specimen from the same individual. Fig adapted from (*10*).

Table 3. Cross-comparisons between individual tissues for breast cancer GPB genes

	Gene	Number of tissues		% (and number) of SD cross-comparison between:	
		Normal	Cancer	Individual normal tissues	Individual normal and cancer tissues
a	*AKT1*	4	6	16.7% (1/6)	37.5% (9/24)
	CSF1R	11	9	41.8% (23/55)	38.4% (38/99)
	ERBB2	4	5	33.3% (2/6)	35.0% (7/20)
	FOSL2	9	7	38.9% (14/36)	47.6% (30/63)
	HES5	6	6	20.0% (3/15)	27.8% (10/36)
	HSP90AA1	7	4	57.1% (12/21)	46.4% (13/28)
	MYC	6	5	6.7% (1/15)	3.3% (1/30)
	TGFB3	6	4	33.3% (5/15)	25.0% (6/24)
b	*AR*	7	6	9.5% (2/21)	16.7% (7/42)
	BCL2	4	4	0.0% (0/6)	0.0% (0/16)
	BRCA2	4	3	0.0% (0/6)	0.0% (0/12)
	CCND1	4	4	50.0% (3/6)	37.5% (6/16)
	DCN	5	3	20.0% (2/10)	0.0% (0/15)
	EGFR	6	4	0.0% (0/15)	0.0% (0/24)
	ERG	5	3	50.0% (5/10)	40.0% (6/15)
	ESR2	5	4	0.0% (0/10)	0.0% (0/20)
	ETV1	5	3	0.0% (0/10)	0.0% (0/15)
	FGFR1	7	5	28.6% (6/21)	22.9% (8/35)
	FGFR2	6	4	33.3% (5/15)	41.7% (10/24)
	FLI1	8	14	7.1% (2/28)	60.7% (68/112)
	FOXA1	4	4	0.0% (0/6)	0.0% (0/16)
	FUT4	4	3	0.0% (0/6)	0.0% (0/12)
	GREB1	4	3	16.7% (1/6)	25.0% (3/12)
	HOXA9	4	3	0.0% (0/6)	8.3% (1/12)
	KLK3	5	4	20.0% (2/10)	30% (6/20)
	LMNA	4	3	50.0% (3/6)	16.7% (2/12)
	MATR3	4	3	33.3% (2/6)	0.0% (0/12)
	MMP1	3	3	33.3% (1/3)	11.1% (1/9)
	MMP14	3	3	33.3% (1/3)	44.4% (4/9)
	MMP2	8	16	7.1% (2/28)	48.4% (62/128)
	MMP9	10	19	17.8% (8/45)	44.2% (84/190)
	NPM1	3	3	33.3% (1/3)	33.3% (3/9)
	NUMA1	4	4	0.0% (0/6)	12.5% (2/16)
	PADI4/6	6	6	13.3% (2/15)	5.6% (2/36)
	PTEN	3	3	0.0% (0/3)	22.2% (2/9)
	RAF1	8	5	32.1% (9/28)	30.0% (12/40)
	SATB1	5	4	20.0% (2/10)	15.0% (3/20)
	SERPINB2	4	4	16.7% (1/6)	6.3% (1/16)
	SLC45A3	5	0	0.0% (0/10)	ND
	SP100	5	4	0.0% (0/10)	20.0% (4/20)
	SPDEF	5	4	10.0% (1/10)	5.0% (1/20)
	TGFB1	4	4	50.0% (3/6)	30.0% (5/16)
	THBS1	5	4	20.0% (2/10)	30.0% (6/20)
	TIMP2	6	7	53.3% (8/15)	33.3% (14/42)
	TIMP3	6	4	60.0% (9/15)	58.3% (14/24)
	TMPRSS2	6	4	60.0% (9/15)	50.0% (12/24)
	VEGFA	13	7	24.4% (19/78)	47.3% (43/91)
	VIM	5	4	70.0% (7/10)	40.0% (8/20)

a) Breast cancer GPBs b) remaining genes.SD, significantly different, based on a two-sample 1D KS test, $P < 0.01$. Tables from (*10, 13*)

Identification of repositioned genes in prostate cancer

Having established limited variability in gene positioning amongst individuals, we screened for genes that reposition in prostate cancer. To this end, we compared the RRDs of 47 genes in multiple cancer tissue to individual normal tissues and to the PND (Tables 3,4, Figures 2-4) (*10, 13*). First, we determined how many of the previously identified breast GPBs (*AKT1, CSF1R, ERBB2, FOL2, HES5, HSP90AA1, MYC* and *TGFB3 (11)*) reposition in prostate cancer, to assess if they would also be useful markers of prostate cancer. We find that none of these breast GPBs robustly reposition in prostate cancer tissue (Tables 3a, 4a, Fig. 2) (*10*). The majority of cross-comparisons between normal and prostate cancer tissues were not significantly different for any of the genes with between 3.3%-47.6% cross-comparisons being significantly different. For most genes the number of significantly different cross-comparisons between normal and malignant prostate tissues was similar or less than the proportion (16.7%-57.1%) of cross-comparisons between normal tissues that were significantly different, suggesting that the repositioning was not cancer specific but rather related to the variability in positioning patterns between individuals (Table 3a, Fig. 2) (*10*). Comparing the position of genes in prostate cancer specimens to their PND also identified only a limited amount of repositioning of these genes in prostate cancer (Table 4a, Fig. 2) (*10*). *MYC, TGFB3* and *HES5* repositioned in 0-33.3% prostate adenocarcinoma's compared to their PNDs and *ERBB2, FOL2, CSF1R, AKT1* and *TGFB3* in 40.0-50.0% of cancer tissues compared to their PND (Table 4a, Fig. 2) (*10*).

Next, we positioned our remaining 39 genes in cancerous prostate tissue to identify prostate cancer biomarkers (*13*). While the position of nine genes (23.1%) were indistinguishable in all cross-comparisons between individual normal and cancer tissues and an additional 19 genes (48.7%) had only limited variability between normal and cancer tissues, with 5.0-33.4% of cross-comparisons reaching significance, nine genes (23.1%; *CCND1, ERG, VIM, FGFR2, MMP9, MMP14, VEGFA, MMP2* and *TMPRSS2*) were differently positioned in 33.4-50.0% comparisons. Two genes (5.1%; *TIMP3* and *FLI1*) were repositioned in ~60% of cross-comparisons between normal and malignant prostate tissues (Table 3b, Figs. 3,4) (*13*). For most genes the number of significantly different cross-comparisons between normal and cancer specimens was not above that of the cross-comparisons between normal tissues, suggesting that the repositioning was not cancer specific (Table 3b) (*13*). For example, while *TIMP3* was differently positioned in 58.3% (14/24) of the cross-comparisons between individual normal and cancer tissues, 60.0% (9/15) of cross-comparisons were statistically different when normal tissues were cross-compared to each other. Taking into consideration the degree of positioning changes in all cross-comparisons and the inter-individual variability of candidates, we identified three genes, *MMP2*, *MMP9* and *FLI1*, which exhibited robust differential positioning between normal and cancer tissues. For these genes, the percentage of cross-comparisons between normal and cancer tissues were higher by > 25% compared to when normal tissues were compared to each other (48.4% vs 7.1%; 44.2% vs 17.8% and 60.7% vs 7.1%, respectively; Table 3b, Figs. 3,4) (*13*).

Figure 3.

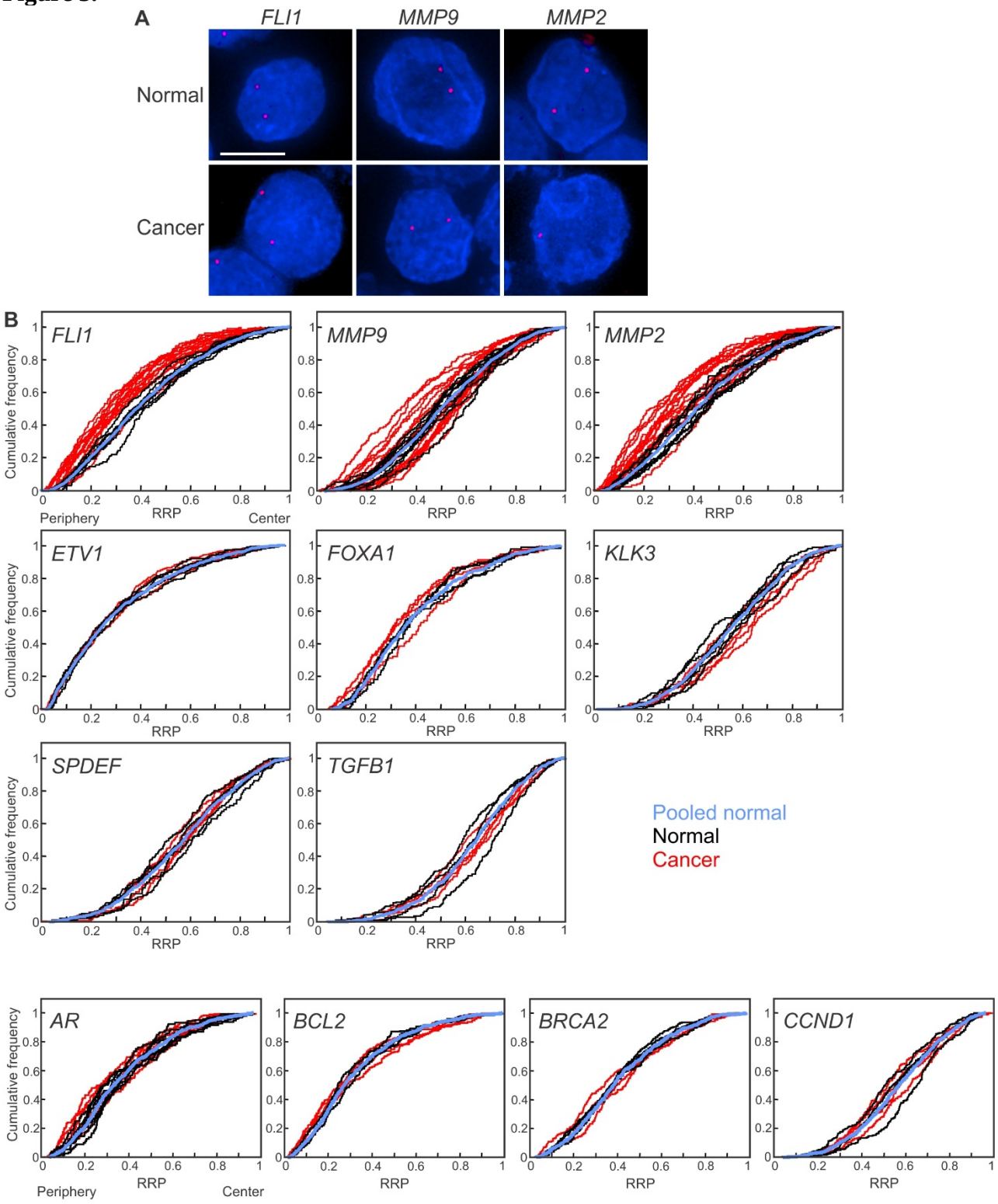

Fig. continued on next page

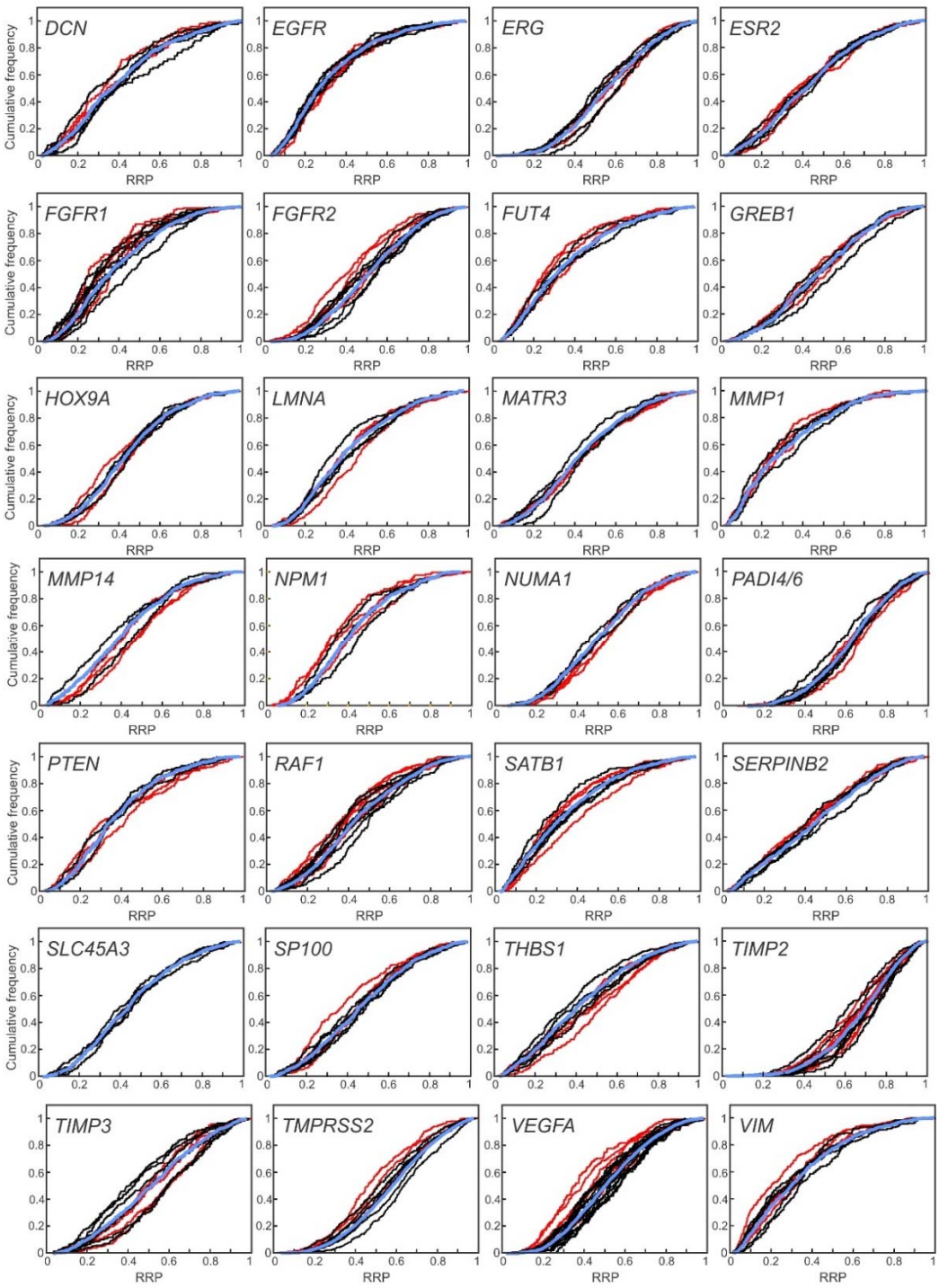

Fig. 3. Gene specific spatial reorganization of the genome in prostate cancer. Gene loci were detected by FISH in FFPE prostate tissue sections. Blue, DAPI nuclear counterstain. Projected image stacks are shown. (A) FLI1, MMP9 and MMP2 gene loci (red) in normal and cancer tissues. Bar, 5µm. (B) Cumulative RRDs for the indicated genes in prostate cancer (red), normal tissues (black) and the pooled normal distribution (PND, blue). The positioning patterns of some, but not all, genes are different in prostate cancer compared to normal tissues. RRP, relative radial position. Figure adapted from (*13*).

Figure 4.

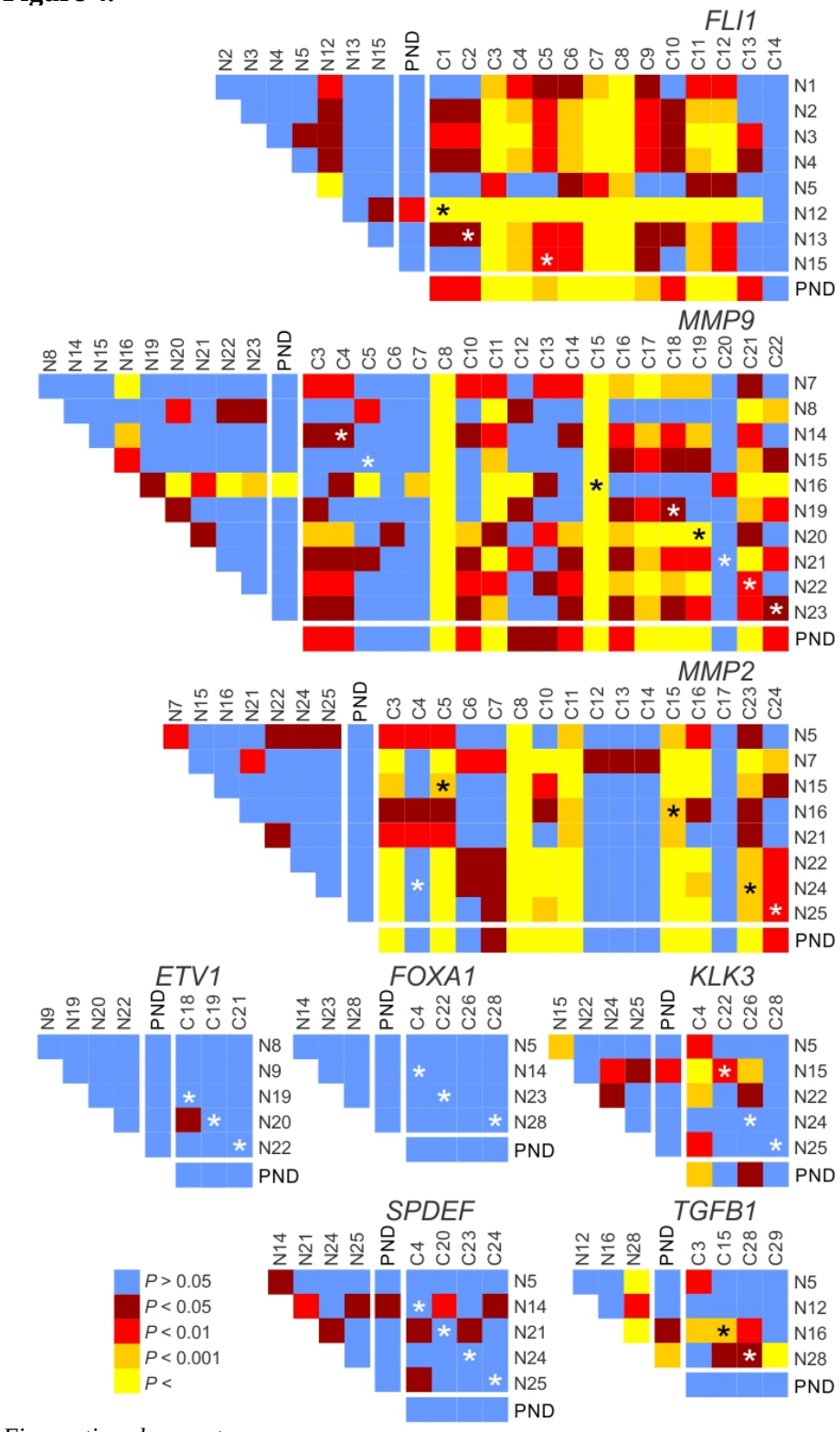

Fig. continued on next page

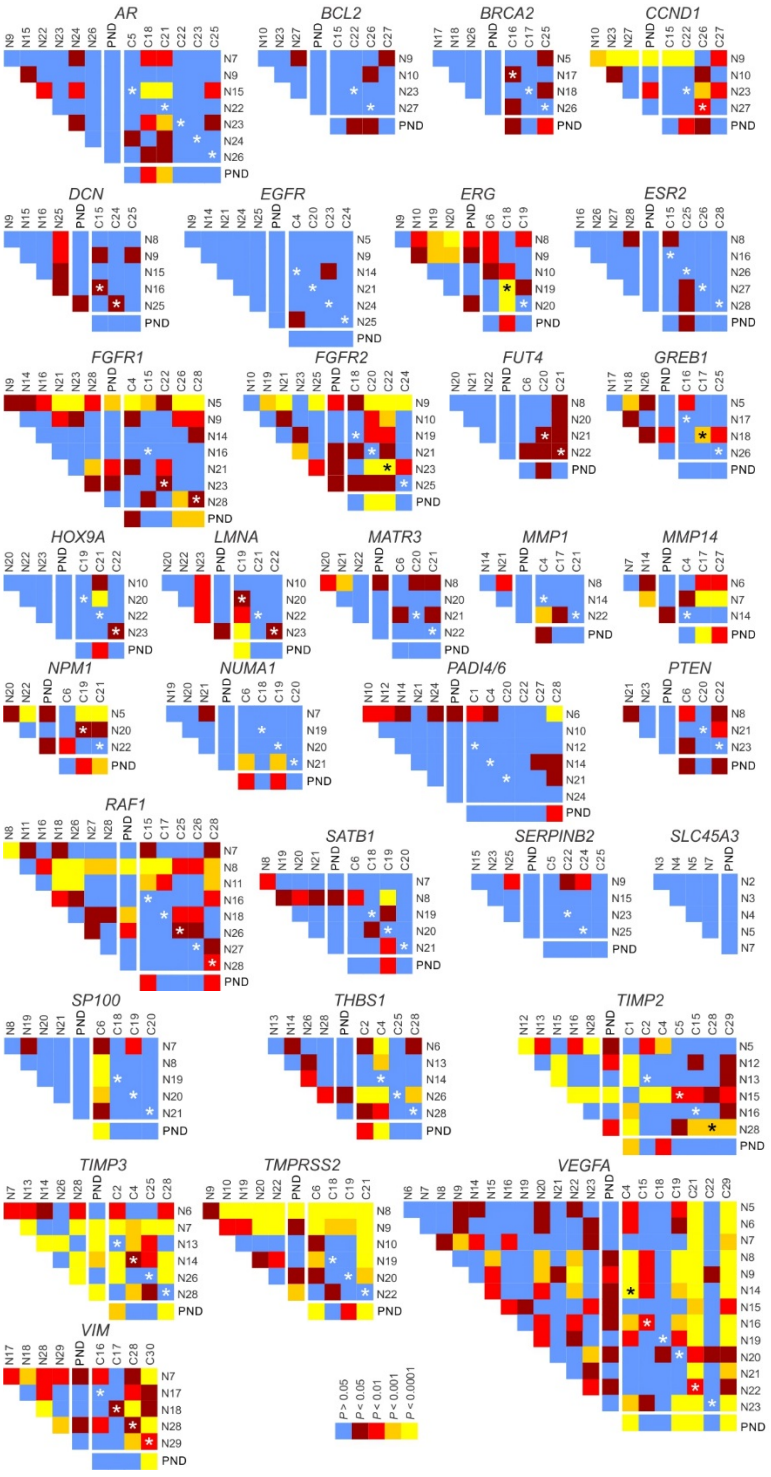

Fig 4. Gene specific repositioning in prostate cancer. Heat maps representing the pair-wise statistical comparisons of positioning patterns of indicated genes between tissues, using the two-sample 1D KS test. While positioning patterns are statistically similar (blue, brown) between most normal tissues (N1-N28), they can be divergent (red, orange, yellow) in cancer tissues (C1-C24). Black or white asterisks indicate a cross-comparison between a normal and cancer specimen from the same individual. PND, pooled normal distribution. Fig. adapted from (*13*).

Table 4. Comparison of individual tissues to a pooled normal

a)

Gene	% (and number) of SD cross-comparison between: Individual normal tissues and pooled normal	Individual cancer tissues and pooled normal
AKT1	0.0% (0/4)	50.0% (3/6)
CSF1R	27.3% (3/11)	44.4% (4/9)
ERBB2	0.0% (0/4)	40.0% (2/5)
FOSL2	33.3% (3/9)	42.9% (3/7)
HES5	0.0% (0/6)	33.3% (2/6)
HSP90AA1	42.9% (3/7)	50.0% (2/4)
MYC	0.0% (0/6)	0.0% (0/5)
TGFB3	16.7% (1/6)	25.0% (1/4)

b)

Gene	% (and number) of SD cross-comparison between: Individual normal tissues and pooled normal	Individual cancer tissues and pooled normal
AR	0.0% (0/7)	33.3% (2/6)
BCL2	0.0% (0/4)	0.0% (0/4)
BRCA2	0.0% (0/4)	33.3% (1/3)
CCND1	50.0% (2/4)	25.0% (1/4)
DCN	0.0% (0/5)	0.0% (0/3)
EGFR	0.0% (0/6)	0.0% (0/4)
ERG	20.0% (1/5)	33.3% (1/3)
ESR2	0.0% (0/5)	0.0% (0/4)
ETV1	0.0% (0/5)	0.0% (0/3)
FGFR1	28.6% (2/7)	40.0% (2/5)
FGFR2	16.7% (1/6)	50.0% (2/4)
FLI1	12.5% (1/8)	92.9 (13/14)
FOXA1	0.0% (0/4)	0.0% (0/4)
FUT4	0.0% (0/4)	0.0% (0/3)
GREB1	25.0% (1/4)	0.0% (0/3)
HOXA9	0.0% (0/4)	33.3% (1/3)
KLK3	20.0% (1/5)	25.0% (1/4)
LMNA	0.0% (0/4)	33.3% (1/3)
MATR3	0.0% (0/4)	0.0% (0/3)
MMP1	0.0% (0/3)	0.0% (0/3)
MMP14	0.0% (0/3)	66.7% (2/3)
MMP2	0.0% (0/8)	56.3% (9/16)
MMP9	10.0% (1/10)	68.4% (13/19)
NPM1	0.0% (0/3)	66.7% (2/3)
NUMA1	0.0% (0/4)	50.0% (2/4)
PADI4/6	0.0% (0/6)	16.7% (1/6)
PTEN	0.0% (0/3)	0.0% (0/3)
RAF1	37.5% (3/8)	40.0% (2/5)
SATB1	0.0% (0/5)	25.0% (1/4)
SERPINB2	0.0% (0/4)	0.0% (0/4)
SLC45A3	0.0% (0/5)	ND
SP100	0.0% (0/5)	25.0% (1/4)
SPDEF	0.0% (0/5)	0.0% (0/4)
TGFB1	25.0% (1/4)	0.0% (0/4)
THBS1	0.0% (0/5)	50.0% (2/4)
TIMP2	50.0% (3/6)	28.6% (2/7)
TIMP3	66.7% (4/6)	50.0% (2/4)
TMPRSS2	33.3% (2/6)	75.0% (3/4)
VEGFA	7.7% (1/13)	57.1% (4/7)
VIM	0.0% (0/5)	25.0% (1/4)

SD, significantly different, based on a KS test, $P < 0.01$. ND, not determined. Tables adapted from (*10, 13*).

Repositioning of *MMP2*, *MMP9* and *FLI1* were confirmed by analysis of their distributions in individual cancer samples to their PNDs. Most genes in the test set displayed limited repositioning in prostate cancer tissues when compared to their PNDs. Two-thirds (26) of genes were repositioned in 0-33.3% of cancer tissues, compared to the PND and six genes repositioned in 40-50% of cancers (Table 4b, Figs 3,4) (*13*). As observed in the cross-comparison analysis, *FLI1*, *MMP9* and *MMP2* showed robust repositioning in prostate cancer, and their distributions were distinct from their PNDs in 92.9% (13/14 cancers), 68.4% (13/19) and 56.3% (9/16) of cancers, respectively (Table 4b, Figs 3,4) (*13*). Although a further four genes were also repositioned in more than 50% of cancers compared to the PND (*VEGF*: 57.1% (4/7), *MMP14*: 66.7% (2/3); *NPM1*: 66.7% (2/3); *TMPRSS2*: 75% (3/4)) (Table 4b, Figs 3,4) (*13*), they are not robustly repositioned in prostate cancer given that visual inspection of the cumulative frequency distribution plots reveals that no more than a few distributions in cancer tissues fall outside the range of all normal tissues (Table 4b (*13*). In the vast majority (96/125; 76.8%) of cases there was a similar repositioning behavior when a cancer was compared to its matched NAT or to the PND (Figs 3,4) (*13*). This observation suggests that repositioning, if present in a patient, is limited to the cancer tissue itself and that comparison to the PND is suitable to assess if a gene is repositioned in cancer, even when no normal tissues from the same individual is available. We conclude *MMP2*, *MMP9* and *FLI1* undergo positional changes in prostate cancer (*13*).

We were unable to define any feature of a prostate cancer that predicted the likelihood of a gene repositioning within it. For example, the genes that reposition map to different chromosomes (*FLI1*: HSA11, *MMP9*: HSA20 and *MMP2*: HSA16). The repositioning of FLI1, at least, is unlikely to reflect whole chromosome movements since the other four genes analyzed that located on HSA11 (*CCND1, FUT4, MMP1* and *NUMA1*) did not repositioned in prostate cancer. Biological function or known relevance to tumorigenesis of genes also did not predict repositioning behavior. Many of the genes we positioned that are commonly implicated in prostate cancer (e.g. *KLK3* (PSA), *AR*, *PTEN*, *TGFB1*, *VEGFA* and *BCL2)*, and the commonly translocated genes in prostate cancer (*TMPRSS2, ERG* and *ETV1*), do not spatially reposition in prostate cancers. Although an increase in *MMP9* and *MMP2* expression has been linked to poor prognosis in prostate cancer, both genes are predominantly expressed by the stromal cells and not by the tumor cells (*17*), which we analyzed. Other MMP family members or regulators (e.g. *MMP14, MMP1 TIMP2, TIMP3* and *SPDEF* do not reposition in prostate cancer, further reducing a link between function and cancer-associated gene repositioning. A lack of a link between gene function and an altered radial position in cancer is in line with multiple studies that find no correlation between changes in gene expression and changes radial positioning patterns, including a cell culture model of early breast cancer (*12, 18-20*). Moreover, only two of the eleven marker genes that robustly reposition in either breast or prostate cancer (18.2%; *MMP9* and *FLI1*; Table 5, Fig. 5) reposition in both breast and prostate cancer (*10, 11, 13*), demonstrating that cancer-related repositioning is not a gene-intrinsic feature, or a more general response to disease in general, but that distinct sets of genes reposition in cancer in a tissue-of-origin specific manner.

Table 5. A comparison of the number of breast and prostate cancers with gene repositioning events

Gene	% (and number) of SD cross-comparison between individual cancer tissues and PND	
	Breast cancer	Prostate cancer
AKT1	64.3% (9/14)	50.0% (3/6)
CSF1R	69.2% (9/13)	44.4% (4/9)
ERBB2	71.4% (10/14)	40.0% (2/5)
FLI1	100.0% (10/10)	92.9% (13/14)
FOSL2	69.2% (9/13)	42.9% (3/7)
HES5	100.0% (13/13)	33.3% (2/6)
HSP90AA1	81.8% (9/11)	50.0% (2/4)
MMP2	0.0% (0/6)	56.3% (9/16)
MMP9	83.3% (10/12)	68.4% (13/19)
MYC	72.7% (8/11)	0.0% (0/5)
TGFB3	78.6% (11/14)	25.0% (1/4)
BCL2	16.7% (1/6)	0.0% (0/4)
CCND1	33.3% (2/6)	25.0% (1/4)
MMP1	33.3% (1/3)	0.0% (0/3)
VEGF	50.0% (3/6)	57.1% (4/7)

SD, significantly different, based on a two-sample 1D KS test, $P < 0.01$. PND, pooled normal distribution. Red, the gene has been classified as being repositioned in breast and/or prostate cancer. Data from (*10*, *11*, *13*), table from (*10*).

Figure 5

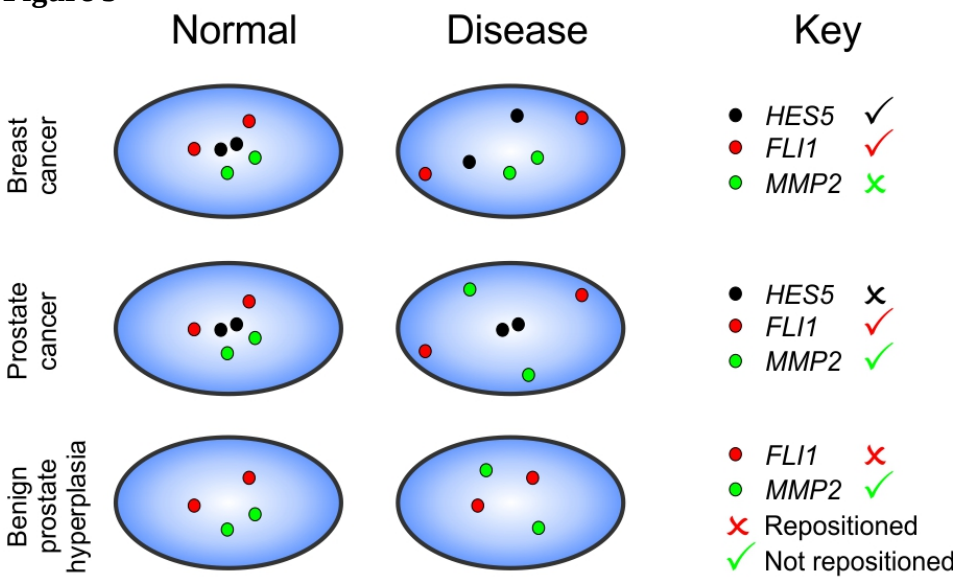

Figure 5: Certain loci adopt alternative nuclear positions in disease (tick) compared to normal cells, whilst the positions of other loci are conserved in disease (cross). The repositioning of some loci is disease specific, and although a gene repositions in one disease, it may not in another disease. For example, *FLI1* repositions in breast and prostate cancer, whereas *MMP2* repositions in prostate disease but not breast cancer. Blue = Nucleus. (Fig adapted from Meaburn, K.J. The Emerging Role of Spatial Genome Organization as a Diagnosis Tool. Frontiers in genetics. *Under review*.

Moreover, the propensity of the three marker genes to reposition in a given cancer was not linked to changes in copy number (Table 6) (*10, 13*). Consequently, our data demonstrates that even in the background of genetic instability it is still possible to use gene positioning for cancer diagnostics.

Table 6. Repositioning events are not due to variations in copy number

Cancer	*FLI1*	*MMP9*	*MMP2*	Non-cancer	*FLI1*	*MMP9*	*MMP2*
C1	- 58.6%			N1			
C2	- 64.8%			N2			
C3	- 49.2%	- 49.0%	- 58.3%	N3			
C4	- 66.4%	- 50.0%	- 87.2%	N4			
C5	- 77.8%	- 58.1%	- 52.7%	N5	- 40.8%		
C6			- 87.5%	N7			- 55.8%
C7	+ 40.8%	++ 69.6%	+ 40.3%	N8			
C8				N12	- 54.0%		
C9				N13	- 64.5%		
C10	- 55.4%			N14		- 63.6%	
C11				N15	- 52.4%	- 55.2%	- 48.5%
C12	++ 57.3%	+ 45.1%	+ 31.6%	N16		- 59.2%	- 73.2%
C13	+ 31.9%			N19			
C14	- 47.4%		- 50.9%	N20			
C15		- 56.4%	- 60.6%	N21			- 66.3%
C16		- 50.0%	- 64.4%	N22			- 61.4%
C17		- 46.0%	- 61.5%	N23		- 47.3%	
C18		+ 48.4%		N24			- 52.5%
C19		++ 60.6%		N25			- 64.2%
C20		- 40.3%		PND			- 55.1%
C21		- 44.9%		B1	- 58.6%	- 48.0%	- 56.2%
C22		- 46.0%		B2			
C23			- 62.6%	B3			
C24			- 74.1%	B4			
				B5			

A comparison of the incidence of gene repositioning with the number of FISH signals detected for a gene in a given tissue. Black box: the gene was reposition compared to the pooled normal distribution ($P < 0.01$; KS test); grey box: no repositioning compared to the pooled normal ($P > 0.01$); white box: gene positioning not determined. The copy number of a gene was diploid unless otherwise stated. Copy number changes are denoted by: +, 20-49.9% of nuclei had ≥3 gene FISH signals; ++, ≥ 50% of nuclei had ≥3 gene signal; -, ≥40% of nuclei had a single FISH signal. The percentage of nuclei with the corresponding number of FISH signals (+/++/-) is also displayed. PND, Pooled normal distribution. N1-8, Normal tissue, from cancer free prostates; N12-N25 = NAT; B1-5, hyperplasia. Tissues are color-coded to indicate tissues from the same individual (e.g. N12 is the NAT from cancer C1). With the exception of C3/B1, analysis for these pairs of normal and cancer tissues was performed on the same slide (same 4-5µm tissue section), for a given gene. Table from (*13*).

Task 3: High-throughput software

A major bottleneck in the analysis of these samples is the image analysis. We have relied on a semi-manual method to identify nuclei and FISH signals in the tissue sample, the large number of individual nuclei (100 per tissue sample, several hundred tissues) exceeded our analysis capacity. In this semi-automated analysis nuclei must be manually identified and segmented. To try to overcome this problem, we have, in close collaboration with Dr. Stephen Lockett, NCI, been developing a novel image analysis tool. However, so far we have been unable to develop a tool that could segment nuclei with a high enough precision for our use. Since the automated software was unable perform at a high enough level we were unable to perform high-throughput automated image analysis and had to only use manual analysis. This significantly slowed down our throughput, and we have been unable to validate the genes in a large number of specimens (*Task 4-10*).

Task 4: Validation in benign tissue

Cancer specificity of *FLI1* and *MMP9* repositioning

Given that loci can alter their nuclear location in diseases other than cancer (*11, 21, 22*), we sought to determine if the repositioning of *FLI1*, *MMP9* and *MMP2* was specific to cancer or was a more general feature of prostate disease. We compared the positioning patterns of these genes in five benign hyperplastic tissues with the positioning patterns of normal prostate tissues, and between multiple hyperplasia tissues (Table 7 and Figure 6) (*13*). *MMP9* and *MMP2* were positioned identically in all hyperplastic tissues (Table 7 and Figure 6) (*13*). The position of *FLI1* is similarly conserved between hyperplastic tissues, with only a single cross-comparison reaching significance (1/10; Table 7 and Figure 6). *FLI1* and *MMP9* did not reposition in hyperplasia compared with normal tissues, since the positioning of both genes was indistinguishable from the PND in all five hyperplasia tissues (Table 7 and Figure 6) and only 10% (4/40) and 12% (6/50) of the cross-comparisons between individual normal tissues reached significance, respectively. These findings, combined with the low repositioning rate in normal tissue, suggests that *FLI1* and *MMP9* repositioning is specific to cancer. In contrast, compared to normal tissues *MMP2* was repositioned in both prostate cancer and in hyperplasia. *MMP2* was in a significantly different position in 80% (4/5) of the hyperplastic tissues compared to the PND and in 45.0% (18/40) of cross-comparisons between hyperplasic and normal tissues (Table 6 and Figure 7) (*13*), suggesting that the repositioning of *MMP2* is common in prostate disease, and not limited to malignancy. We had access to both hyperplastic and cancer tissue from the same prostate (B1 and C3, respectively; Table 2, (*13*)); in keeping with the comparisons between hyperplasia and normal tissue, *FLI1* and *MMP9* occupied significantly different positions in the cancer and hyperplasic tissue (I = 0.004 and 0.002, respectively), whereas *MMP2* was in a similar position in the two disease states (P = 0.516), for this individual. We conclude that repositioning of *MMP9* and *FLI1* is cancer specific, whereas *MMP2* repositions in both benign disease and cancer (Fig. 5) (*13*).

Figure 6

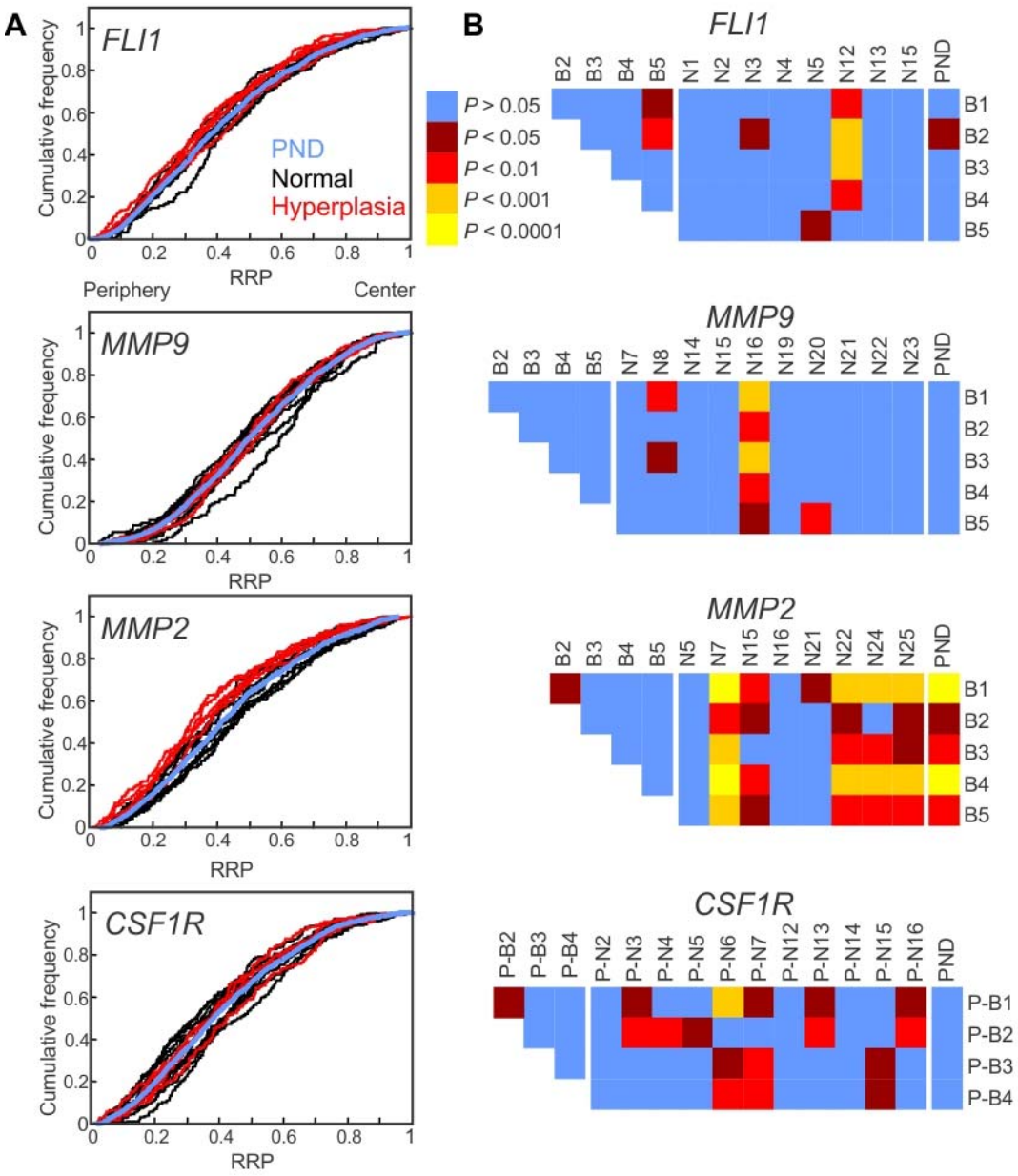

Fig. 6. Gene positioning in benign disease. Positions of indicated genes were compared between hyperplasia (B1-B5) and normal prostate tissue. (A) Cumulative RRDs for the indicated genes in hyperplasia (red), normal tissues (black) and the pooled normal distribution (PND; blue). (B) Pairwise statistical comparisons of RRDs between hyperplasic tissues and normal tissues and amongst hyperplasic tissues, using the two-sample 1D KS test. All three genes are similarly positioned between hyperplasic tissues and only *MMP2* repositions in hyperplasic compared to normal tissues. RRP, relative radial position. Figure adapted from (*10, 13*).

Normal and NAT prostate tissue often contain small areas of mild hyperplasic morphology. Therefore, as a control to ensure the heterogeneity in positioning patterns for some genes in normal prostate tissues was not a reflection of the inclusion of abnormal tissue, we positioned one of the genes with a high level of variability between individuals, *CSF1R*, in hyperplasic prostate tissues. *CSF1R* was positioned identically amongst all hyperplasic prostate tissues (Table 7, Fig. 6) (*10*). Similarly, the position of *CSF1R* was also similar between hyperplasic and normal tissues with all four hyperplasic prostate tissues distributions statistically similar to the PND and only 18.2% (8/44) of cross-comparisons between hyperplasic and individual normal tissues being significantly different (Table 7, Fig. 6) (*10*). This suggests that the presence of hyperplasic nuclei within a normal tissue RRD is not skewing spatial positioning patterns.

Table 7. Comparison of gene positioning in benign tissues

Gene	% (and number) of SD cross-comparison between:		
	Individual hyperplasia tissues	Individual normal and hyperplasia tissues	Individual hyperplasia tissues and pooled normal
FLI1	10.0% (1/10)	10.0% (4/40)	0.0% (0/5)
MMP9	0.0% (0/10)	12.0% (6/50)	0.0% (0/5)
MMP2	0.0% (0/10)	45.0% (18/40)	80.0% (4/5)
CSF1R	0.0% (0/6)	18.2% (8/44)	0.0% (0/4)

SD, significantly different, based on a two-sample 1D KS test, $P < 0.01$. Table adapted from (*10, 13*)

Task 1, 4, 5

High-confidence detection of prostate cancers using multiplexed positioning biomarkers

Since *FLI1* and *MMP9* repositioning occurs predominantly in cancer tissues, we determined their false positive and false negative rates as a preliminary step towards assessing their potential as biomarkers for prostate cancer. We defined a false positive reading as repositioning of the marker gene in a non-malignant (normal or hyperplastic) tissue compared to the PND, thus incorrectly classifying the tissue as cancer. Conversely, we defined a false negative reading as a lack of repositioning of the marker gene in a cancer, leading to incorrect classification of the tissue as non-malignant. As expected due to its high rate of repositioning in hyperplasia, *MMP2* had a high false positive rate (30.8%; Table 8) (*13*). This finding, combined with its high false negative rate (43.8%; Table 9) (*13*) suggests that *MMP2* would not be a useful biomarker for prostate cancer. In contrast, *FLI1* had both a low false negative and false positive rate (7.1% and 7.7% respectively; Tables 8 and 9) (*13*). *MMP9* had a fairly high false negative rate (31.6%; Table 9) (*13*), but a low false positive rate (6.7%; Table 8) (*13*).

Table 8. False positive rates

Gene	Normal tissue false positives	Benign tissue false positives	Total false positives
FLI1	12.5% (1/8)	0.0% (0/5)	7.7% (1/13)
MMP9	10.0% (1/10)	0.0% (0/5)	6.7% (1/15)
MMP2	0.0% (0/8)	80.0% (4/5)	30.8% (4/13)

The percentage (and number) of tissues that give a false positive result. A false positive is scored when a gene has a statistically significant different RRD in a normal or hyperplastic tissue compared to the pooled normal ($P < 0.01$; KS test). Table from (*13*).

Table 9 False negative rates for single and multiplexed genes

Gene(s)	False negative rate
Single gene	
FLI1	7.1% (1/14)
MMP9	31.6% (6/19)
MMP2	43.8% (7/16)
Multiplexed genes	
FLI1 and *MMP9*	0.0% (0/11)
FLI1 and *MMP2*	9.1% (1/11)
MMP9 and *MMP2*	28.6% (4/14)

The percentage (and number) of tissues that give a false negative result. A false negative is scored when the RRD of a gene in a cancer tissue is similar to that of the pooled normal distribution (KS test, $P > 0.01$). For multiplexed genes, a false positive is scored when neither gene in the pair is repositioned compared to the pooled normal distribution ($P > 0.01$, KS test). Only tissues where both genes of the pair were positioned have been included. Table from (*13*).

None of the genes we tested repositioned in all prostate cancer tissues. However, at least one repositioned gene was present in every prostate cancer tissue analyzed (30/30 cancers; Fig. 4) (*13*). Given the low false positive rate of *FLI1* and *MMP9*, we explored the possibility of using these two genes in a multiplex format for the detection of cancer samples. When analyzed together, *FLI1* or *MMP9* (or both) repositioned in all (11/11) cancers (Table 10, Fig. 4) (*13*). Consequently, multiplexing *FLI1* and *MMP9* reduced the false negative rate to 0% (0/11; Table 9) (*13*). We conclude that in combination *FLI1* and *MMP9* are strong potential biomarkers for prostate cancer (*13*).

Table 10. Gene Multiplexing

Gene	*MMP9*	*MMP2*
FLI1	100.0% (11/11)	90.9% (10/11)
MMP9		71.4% (10/14)

The percentage (and number) of cancers where at least one of the indicated pair of genes repositioned, compared to the pooled normal distribution ($P < 0.01$, KS test). Only tissues where both genes of the pair have been positioned are included. Table from (*13*).

Determination of prognostic potential for spatial genome organization biomarkers

Since none of our prostate cancer GPBs. *FLI1*, *MMP9* and *MMP9*, repositioned in all cancers we further characterized their spatial repositioning patterns to determine if they were candidate biomarkers for prognostic applications.

Task 6: Marker of tumor grade

We first asked if gene repositioning could distinguish between Gleason grades. *FLI1* and *MMP2* cannot distinguish between Gleason grade, and were repositioned, when compared to the PND, at a similar frequency between Gleason grades (Table 2, 11, Figure 2-4, 7) (*13*). *FLI1* repositioned in 5 out of 5 Gleason grade 5 and 6 cancers, 4/5 Gleason grade cancers and 3/3 Gleason grade 8

and 9 cancers (Table 11) (*13*). Similarly, *MMP2* repositioned in 4/7 Gleason grade 5 and 6 cancers, 2/4 Gleason grade cancers and 1/2 Gleason grade 8 and 9 cancers (Table 11) (*13*). Conversely, *MMP9* showed an increase incidence of repositioning in Gleason grade 7 cancers (8/9; 88.9%) compared to low Gleason score cancers (1/5; 20%) (Table 11) (*13*). We also selected an additional gene for further analysis. Form our initial analysis *SP100* repositioned in one Gleason score 6 cancer but not in three Gleason score 7 cancers (*13*). We increased the number of normal and cancer tissues analyzed (Fig. 8 and 9). As further evidence that the PND's sample size appropriate, the addition of two normal tissues (239 nuclei) gave a statically identical PND to our original PND (P 0.83, Fig. 8; unpublished data). As opposed to *MMP9, SP100* repositioned in low score (5-6) but not intermediate score (7) prostate cancers (Fig. 9, unpublished data) *SP100* repositioned in 66.7% (4/6) Gleason score ≤6 cancers, but does not reposition in Gleason score 7 cancers (0/3; Fig. 9, Unpublished data). Future studies are required, to increase the sample size, and to increase the range of Gleason scores compared.

Figure 7

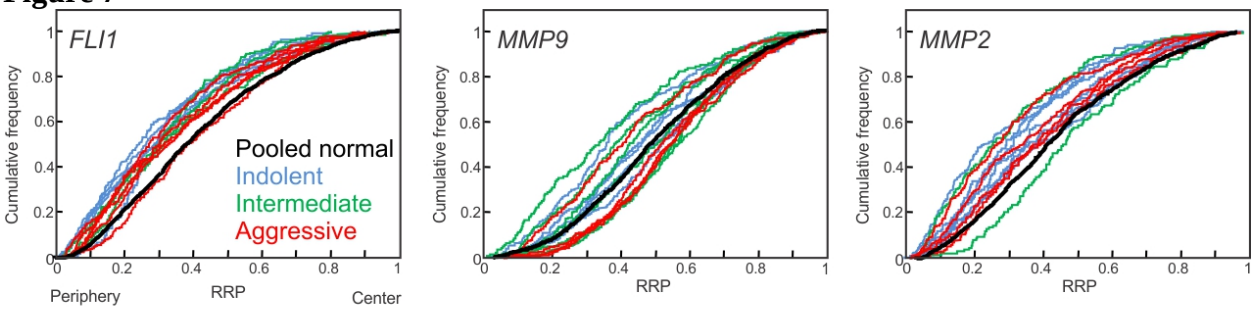

Fig. 7. Gene repositioning in prostate cancer is not linked to prognostic status. Cumulative RRDs are color-coded according to the prognostic status of the cancer: Blue, indolent prostate cancers (Gleason score ≤6, without metastasis); green, intermediate cancers (Gleason score 7, without metastasis) and red, aggressive cancers (Gleason score ≥8, and/or metastasis). The pooled normal distribution (black) is included for comparison. RRP, relative radial position. Figure adapted from (*13*).

Figure 8

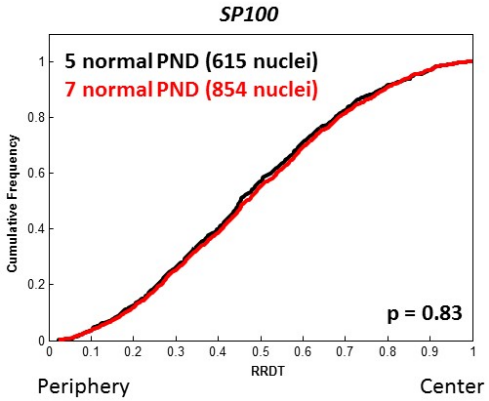

Fig. 8. Cumulative RRDs for the of *SP100* when 5 (black (*13*)) or 7 (red (unpublished data)) normal tissues are used to generate the pooled normal distribution (PND). Statistical comparison by two-sample 1D KS test. RRP, relative radial position.

Table 11. Characterization of repositioning events by Gleason grade and other markers of risk.

Gene	Total	Gleason score (GS) 7	GS 5 or 6	GS 8 or 9	Met	T3	"aggressive" / "high risk"	Unknown
AR	6 (2)	4 (2)	2					
BCL2	4 (0)	2				1	**1**	2
BRCA2	3 (1)	1 (1)						2
CCND1	4 (1)	2 (1)				1	**1**	2
DCN	3 (0)	2	1			1	**1**	
EGFR	4 (0)	2	2					
ERG	3 (1)	2 (1)	1					
ESR2	4 (0)	3				2	**2**	1
ETV1	3 (0)	3						
FGFR1	5 (2)	4 (1)				2 (1)	**2 (1)**	1 (1)
FGFR2	4 (2)	3 (2)	1					
FLI1	14 (13)	5 (4)	5 (5)	3 (3)	3 (2)	3 (2)	**5 (4)**	1
FOXA1	4 (0)	3 (2)				1	**1**	1
FUT4	3 (0)	2	1					
GREB1	3 (0)	1						2
HOXA9	3 (1)	3 (1)				1	**1**	
KLK3 (PSA)	4 (1)	2 (1)	1			1	**1**	1
LMNA	3 (1)	3 (1)				1 (1)	**1 (1)**	
MATR3	3 (0)	2	1					
MMP1	3 (0)	2						1
MMP14	3 (2)	1						2 (2)
MMP2	16 (9)	4 (2)	7 (4)	2 (1)	3 (1)	4 (2)	**5 (3)**	3 (2)
MMP9	19 (13)	9 (8)	5 (1)	2 (1)	3 (2)	5 (4)	**6 (5)**	3 (3)
NPM1	3 (2)	2 (2)	1			1 (1)	**1 (1)**	
NUMA1	4 (2)	3 (1)	1 (1)			2 (1)	**2 (1)**	
PADI4/6	6 (1)	5 (1)				1 (1)	**1 (1)**	1
PTEN	3 (0)	2	1					
RAF1	5 (2)	3 (2)				2 (2)	**2 (2)**	3
SATB1	4 (1)	3 (1)	1			1 (1)	**1 (1)**	
SERPINB2	4 (0)	2	2					
SP100	4 (1)	3	1 (1)			1	**1**	
SPDEF	4 (0)	2	2					
TGFB1	4 (0)	2				2	**2**	2
THBS1	4 (2)	3 (1)		1 (1)		1	**2 (1)**	
TIMP2	7 (2)	4 (2)	1	1		2	**3**	1
TIMP3	4 (2)	3 (1)		1 (1)		1 (1)	**2 (2)**	
TMPRSS2	4 (3)	3 (2)	1 (1)			1 (1)	**1 (1)**	
VEGFA	7 (4)	6 (3)				2	**2 (1)**	1 (1)
VIM	4 (1)	1				1	**1**	3 (1)
AKT1	6 (3)		1					5 (3)
CSF1R	9 (4)	1 (1)	3					5 (3)
ERBB2	5 (2)							5 (2)
FOSL2	7 (3)	3 (1)	3 (1)					1 (1)
HES5	6 (2)	4 (2)	2					
HSP90AA1	4 (2)		1 (1)					3 (1)
MYC	5 (0)	3	1					1
TGFB3	4 (1)		2 (1)					2

The number of tissue analyzed for each gene. The numbers in parentheses indicate the number of cancers where the gene repositioned, compared to the pooled normal distribution ($P < 0.01$, KS test). Where there is no parentheses the gene did not repositioned in any cancers analyzed. GS, Gleason score, Met, metastatic cancer, T3, TNM classification, T3 is a marker of a cancer at high risk. Table using data from (*10, 13*).

Figure 9

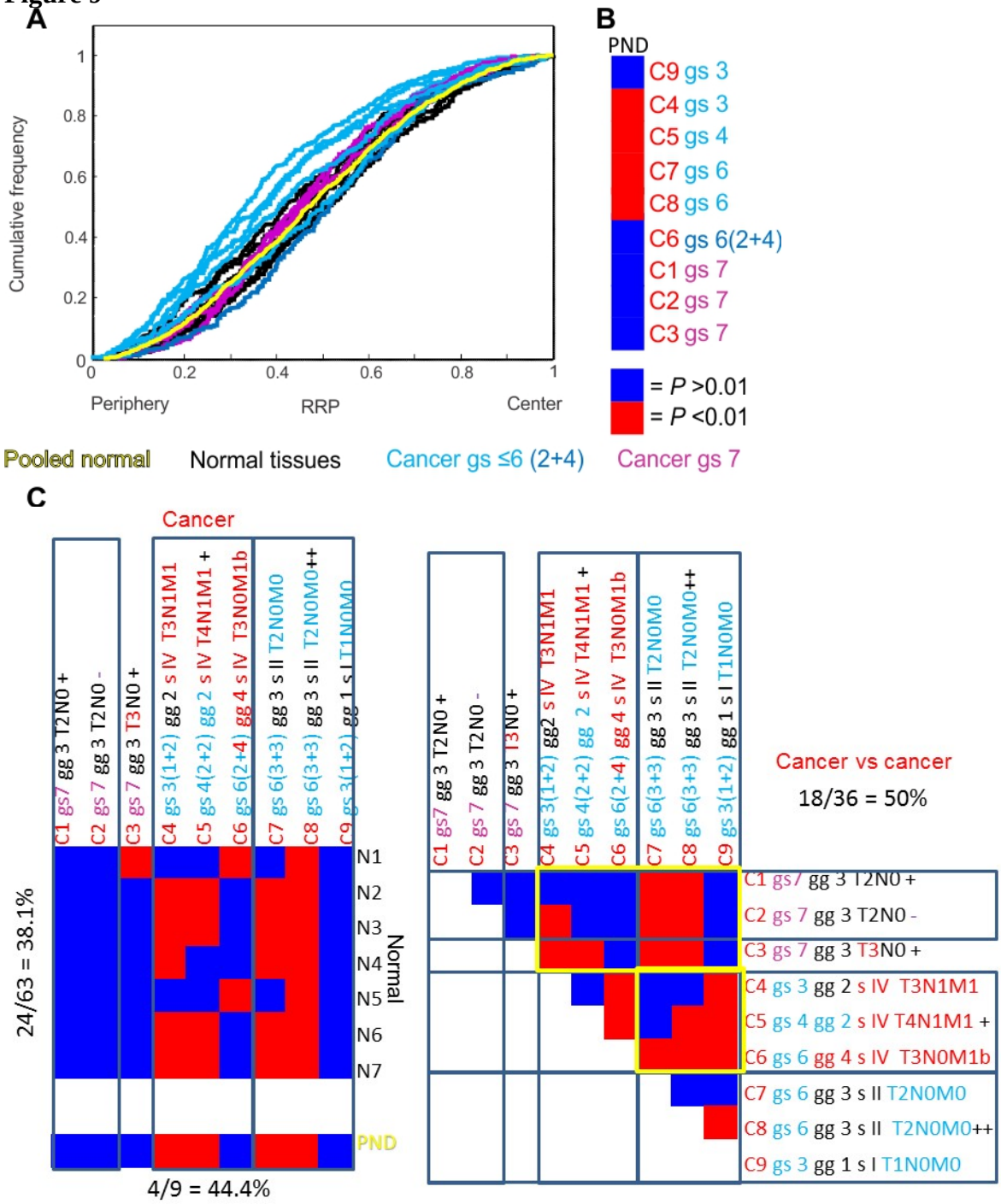

Fig. 9. The spatial position of *SP100* is a marker of Gleason score, but not aggressive prostate cancer. A) Cumulative RRDs are color-coded according to the Gleason score (gs) of the cancer: Gleason score 5 or 6 (blue), Gleason score 7 (purple), normal tissues (black) and the pooled normal distribution (PND; yellow). Pairwise statistical comparisons of RRDs between (B) cancer tissues and the PND, or (C) individual normal and cancer tissues, using the two-sample 1D KS test. RRP, relative radial position; gg, Gleason grade; s, Stage, +, 20-49.9% of nuclei had ≥3 gene FISH signals; ++, ≥ 50% of nuclei had ≥3 gene signal; -, ≥40% of nuclei had a single FISH signal. Unpublished Data.

Task 7. Detection of early cancer

Prostate cancers with Gleason scores of ≤6 are classified as low grade, early cancers. Therefore, given the results described above *SP100* and *MMP9* are candidate markers to distinguish early prostate cancer, since *SP100* repositions in ≤6 prostate cancers, but not in Gleason score 7 cancers and, conversely, *MMP9* predominantly repositions in Gleason score ≥7 cancers (Table 11, Fig 2-4, 9) (*13*) (unpublished data). Future studies will be required to validate this finding in larger numbers of tissues, particularly in cancers with a large range of Gleason scores. Most likely, the combined use of these 2 genes will be a stronger biomarker than either used singularly.

Task 9: metastatic marker potential

The variation in the positioning patterns of *FLI1*, *MMP9*, *MMP2* and *SP100* did not correlate with the clinicopathologically defined aggressiveness of the cancer (Table 11, Fig. 7 and 9) (*13*) (Unpublished data). Neither the propensity to reposition nor the direction/degree of repositioning could be used to distinguish metastatic cancers from non-metastatic cancers using the radial positioning patterns of *FLI1*, *MMP9*, *MMP2* or *SP100* (Table 11, Fig. 7 and 9) (*13*) (Unpublished data).

Task 2, 8 ,10: Nothing to report.

No cost extension tasks:

Task11: Grant reports finalized.

Task 12: The 2 manuscripts based on aims 1 and 2 were successfully finalized, and have now been published in peer-review journals, *Molecular Biology of the Cell* and *Histochem Cell Biol* (*10, 13*) (Appendix). Additional data generated for this task is included in the above discussion of the resulsts, since this data was the analysis of the positioning of our candidate genes additional tissues.

Task13: *SP100* data as presented in Task 6 and 9.

Summary

We have identified two genes, *MMP9* and *FLI1,* which undergo cancer-specific repositioning, which can be used to distinguish cancerous prostate tissue from normal/hyperplasic tissue with high accuracy. We conclude that the spatial positioning patterns of *MMP9* and *FLI1,* especially when used in combination, are strong candidate biomarkers for use in cancer diagnosis (*13*). Future large-scale studies will be required to further validate their diagnostic potential.

4. Key Research Accomplishments

- Interphase spatial positioning patterns of 48 genes have been screened in a panel of normal and cancerous human prostate tissues to identify candidate marker genes for prostate cancer detection.
- Demonstration of minimal variation in the spatial position of a most gene amongst normal individuals. Thus, any repositioning between normal and cancer tissues, for most genes, are specific to disease and are not a consequence of inter-individual differences in positioning patterns.
- Demonstration of gene-specific repositioning events associated with prostate carcinogenesis.
- Demonstration of an absence of global genome reorganization in prostate cancer cells.
- Identification of three potential prostate cancer maker genes (*FLI1*, *MMP9*, *MMP2*).
- Demonstration that the repositioning events in cancer are not a consequence of genomic instability.
- Establishment of a pooled normal distribution for use as a standard for comparison with unknown samples.
- Determination of false positive/negative rates.
- Demonstration that multiplexing improves sensitivity.
- Determination that different sets of genes reposition in breast and prostate cancer.
- Validation that *FLI1* and *MMP9* gene repositioning events are specific to cancer, whereas *MMP2* repositioning events are specific to disease.
- Proof-of-principle that spatial gene positioning has prognostic potential since *SP100* and *MMP9* differentially repositions in low grade and intermediate grade prostate cancers.

5. Conclusions

We have developed a strategy to identify a novel class of prostate cancer biomarkers, based on the differential spatial localization of genes within the cell nucleus. Application of this strategy has led to the identification and partial characterization of three promising novel prostate cancer biomarkers (*FLI1, MMP9, MMP2*), which warrant further investigation. We tested their usefulness in human prostate formalin-fixed paraffin embedded tissues. We adapted the approach to the requirements in a clinical setting by developing a normalized standard reference distribution (PND) for each gene. We found that *FLI1*, *MMP9* and *MMP2* repositioned in a significant fraction of prostate cancers, compared to the normal standard. The sensitivity of detecting prostate cancer was markedly improved by multiplexing markers. The repositioning of *FLI1* and *MMP9* was specific to cancer, and had low false positive rates. *MMP2* spatial positioning is a marker of prostatic disease, but not specifically cancer, since it also repositioned in BPH. Spatial gene

repositioning in prostate cancer is highly gene specific, and not a reflection of a global reorganization of the genome. These repositioning events were also not due to inter-individual variations in gene positioning, since the positioning pattern of most genes was highly similar between normal tissues from different individuals. Nor were the repositioning events correlated with genomic instability. We also provide, for the first time, a proof-of-principle that spatial positioning of the genome has can be used to stratify prostate cancers, and therefore are potential prognostic markers, since *SP100* only repositioned in Gleason score 5 and 6 cancers, whereas *MMP9* repositioned more frequently in Gleason score 7 cancers. Further large-scale studies, using a wide range of cancers, are required to validate our findings and to identify prognostic makers.

In the long-term, our efforts should lead to the development of a robust, standardized method for the detection of prostate cancer in a routine diagnostic laboratory setting. While conventional prostate cancer diagnosis is largely based on qualitative morphological criteria, our assay provides highly quantitative method for the detection of cancerous cells. Analysis of gene positioning patterns promises to be a sensitive and effective diagnostic approach for prostate cancer. Although the marker genes thus far identified did not, spatial positioning patterns also have the promise to stratify aggressive and indolent prostate cancer and to act as robust prognostic markers. Consistent with this hypothesis, we find differences in gene positioning patterns between individual cancers, different genes reposition in prostate cancers to those that reposition in breast cancer and, most importantly, the positioning patterns of *MMP9* and *SP100* can be used to sub-type Gleason score 5 and 6 cancer from Gleason score 7 cancers. Our approach overcomes several of the limitations of current and currently proposed diagnostic tests since it is i) highly quantitative, ii) based on single cell analysis, iii) applicable to extremely small tissue samples, thus reducing the requirement for additional exploratory invasive procedures, iv) is independent from the generation of metaphase chromosome, which can be difficult to obtain from solid tumors and v) is insensitive to protein and RNA degradation, which commonly occurs during biopsy sample handling, unlike immunohistochemistry-, PCR-, or microarray-based diagnostic approaches. Moreover, our method of diagnostics can easily be integrated into clinical laboratories as an extension to existing routine cytogenetic procedures using FISH to detect gene amplifications in solid tumors. Our assay will extend and complement conventional morphology-based diagnostics and it is anticipated that the combined use of standard pathological indicators and our method will be a highly accurate, quantitative and powerful diagnostic approach.

6. Publications, Abstracts, and Presentations

Lay Press:
Nothing to report

Peer-reviewed journal publications:

1. Leshner, M., Devine, M., Roloff, G.W., True, L.D. and Misteli, T., and Meaburn, K.J.. Locus-specific gene repositioning in prostate cancer. Mol. Biol. Cell. 27(2): 236-246, 2016.
2. Meaburn, K.J. Agunloye, O., Devine, M., Leshner, M., Roloff, G.W., True, L.D., and Misteli, T. Tissue-of-origin specific gene repositioning in breast and prostate cancer. Histochemistry and Cell Biology. 145(4):433-46., 2016.

Invited Articles:

1. Meaburn, K.J. The Emerging Role of Spatial Genome Organization as a Diagnosis Tool. Frontiers in genetics. *Under review.*
2. Meaburn, K.J., Burman, B., and Misteli, T. Genome organization in disease. In: The Functional nucleus, Dellaire, G., Bazett-Jones, D. (Eds.) Springer, New York. *Accepted for publication*

Abstracts:
Nothing to report

Presentations:
Oral Meeting and Seminar presentations:

- Predictive Cancer Biomarkers, Next Generation Diagnostics Summit, Washington, DC. August 26, 2016
- NIH, NCI, LGCP, Bethesda, January 12, 2016
- Florida State University, Distinguished Lecturer "Spatial genome organization:, January 8, 2015
- International Microscopy Congress, Prague, Czech Republic, September 7-12, 2014
- Nuclear Organization & Function meeting. Cold Spring Harbor Laboratory, NY, USA. August 19-23, 2014.
- The 6th UK Nuclear Envelope and Chromatin Organisation Brunel University, Middlesex, UK. September 25-26 2013.
- NCI "Molecular Oncology" Strategy workshop, Bethesda, MD, February 18, 2013.
- Olson Memorial Lecture, St. Louis University, March 28, 2013.
- 30th FEBS Congress, St. Petersburg, Russia, July 6-11, 2013.

Poster presentations:

- Post-baccalaureate Poster Day 2014. NIH, Bethesda, MD. USA. May 3, 2015.
- Post-baccalaureate Poster Day 2013. NIH, Bethesda, MD. USA. May 1, 2013.

Personnel receiving pay from the research effort:
Karen Meaburn, PhD
Bharat Burman, PhD

7. Inventions, Patents and Licenses

Nothing to report

8. Reportable outcomes

Results demonstrate a proof-of-principle that spatial genome organization can be developed into a diagnostic tool for cancer detection.

9. Other Achievements

Funding awarded based on work supported by the grant:
Department of Defense, Prostate Cancer Idea Development Award.
Project: Prostate cancer prognostics based on genome architecture (W81XWH-15-1-0322).

Degrees obtained supported by this award:
Bharat Burman PhD

10. References

1. R. L. Siegel, K. D. Miller, A. Jemal, Cancer statistics, 2016. *CA: a cancer journal for clinicians* **66**, 7-30 (2016).
2. C. Ferrai, I. J. de Castro, L. Lavitas, M. Chotalia, A. Pombo, Gene positioning. *Cold Spring Harbor perspectives in biology* **2**, a000588 (2010).
3. K. Meaburn, B. Burman, T. Misteli, in *The functional Nucleus,* G. Dellaire, D. Bazett-Jones, Eds. (Springer DE, 2016), pp. in press.
4. T. Misteli, Beyond the sequence: cellular organization of genome function. *Cell* **128**, 787-800 (2007).
5. K. J. Meaburn, T. Misteli, Cell biology: chromosome territories. *Nature* **445**, 379-781 (2007).
6. D. Zink, A. H. Fische, J. A. Nickerson, Nuclear structure in cancer cells. *Nat Rev Cancer* **4**, 677-687 (2004).
7. T. Wiech *et al.*, Human archival tissues provide a valuable source for the analysis of spatial genome organization. *Histochem Cell Biol* **123**, 229-238 (2005).
8. M. Cremer *et al.*, Inheritance of gene density-related higher order chromatin arrangements in normal and tumor cell nuclei. *The Journal of cell biology* **162**, 809-820 (2003).
9. S. Murata *et al.*, Conservation and alteration of chromosome territory arrangements in thyroid carcinoma cell nuclei. *Thyroid : official journal of the American Thyroid Association* **17**, 489-496 (2007).
10. K. J. Meaburn *et al.*, Tissue-of-origin-specific gene repositioning in breast and prostate

cancer. *Histochem Cell Biol* **145**, 433-446 (2016).
11. K. J. Meaburn, P. R. Gudla, S. Khan, S. J. Lockett, T. Misteli, Disease-specific gene repositioning in breast cancer. *The Journal of cell biology* **187**, 801-812 (2009).
12. K. J. Meaburn, T. Misteli, Locus-specific and activity-independent gene repositioning during early tumorigenesis. *The Journal of cell biology* **180**, 39-50 (2008).
13. M. Leshner *et al.*, Locus-specific gene repositioning in prostate cancer. *Molecular biology of the cell* **27**, 236-246 (2016).
14. K. J. Meaburn, Fluorescence in situ hybridization on 3D cultures of tumor cells. *Methods in molecular biology* **659**, 323-336 (2010).
15. C. Lin *et al.*, Nuclear receptor-induced chromosomal proximity and DNA breaks underlie specific translocations in cancer. *Cell* **139**, 1069-1083 (2009).
16. R. S. Mani *et al.*, Induced chromosomal proximity and gene fusions in prostate cancer. *Science* **326**, 1230 (2009).
17. M. Egeblad, Z. Werb, New functions for the matrix metalloproteinases in cancer progression. *Nat Rev Cancer* **2**, 161-174 (2002).
18. L. Harewood *et al.*, The effect of translocation-induced nuclear reorganization on gene expression. *Genome research* **20**, 554-564 (2010).
19. T. Takizawa, P. R. Gudla, L. Guo, S. Lockett, T. Misteli, Allele-specific nuclear positioning of the monoallelically expressed astrocyte marker GFAP. *Genes & development* **22**, 489-498 (2008).
20. R. R. Williams *et al.*, Neural induction promotes large-scale chromatin reorganisation of the Mash1 locus. *J Cell Sci* **119**, 132-140 (2006).
21. J. Borden, L. Manuelidis, Movement of the X chromosome in epilepsy. *Science* **242**, 1687-1691 (1988).
22. K. J. Meaburn *et al.*, Primary laminopathy fibroblasts display altered genome organization and apoptosis. *Aging cell* **6**, 139-153 (2007).

11. Appendices

Reprints/original copies of the journal articles and invited book chapter supported by this grant:

1. Leshner, M., Devine, M., Roloff, G.W., True, L.D. and Misteli, T., and Meaburn, K.J. Locus-specific gene repositioning in prostate cancer. Mol. Biol. Cell. 27(2): 236-246, 2016.
2. Meaburn, K.J. Agunloye, O., Devine, M., Leshner, M., Roloff, G.W., True, L.D., and Misteli, T. Tissue-of-origin specific gene repositioning in breast and prostate cancer. Histochemistry and Cell Biology. 145(4):433-46., 2016.
3. Meaburn, K.J., Burman, B., and Misteli, T. Genome organization in disease. In: The Functional nucleus, Dellaire, G., Bazett-Jones, D. (Eds.) Springer, New York. *Accepted for publication*
4. Meaburn, K.J. The Emerging Role of Spatial Genome Organization as a Diagnosis Tool. Frontiers in genetics. *Under review.*

Locus-specific gene repositioning in prostate cancer

Marc Leshner[a], Michelle Devine[a], Gregory W. Roloff[a], Lawrence D. True[b], Tom Misteli[a], and Karen J. Meaburn[a]

[a]National Cancer Institute, National Institutes of Health, Bethesda, MD 20892; [b]Department of Pathology, University of Washington, Seattle, WA 98195

ABSTRACT **Genes occupy preferred spatial positions within interphase cell nuclei. However, positioning patterns are not an innate feature of a locus, and genes can alter their localization in response to physiological and pathological changes. Here we screen the radial positioning patterns of 40 genes in normal, hyperplasic, and malignant human prostate tissues. We find that the overall spatial organization of the genome in prostate tissue is largely conserved among individuals. We identify three genes whose nuclear positions are robustly altered in neoplastic prostate tissues. *FLI1* and *MMP9* position differently in prostate cancer than in normal tissue and prostate hyperplasia, whereas *MMP2* is repositioned in both prostate cancer and hyperplasia. Our data point to locus-specific reorganization of the genome during prostate disease.**

Monitoring Editor
Orna Cohen-Fix
National Institutes of Health

Received: May 22, 2015
Revised: Sep 28, 2015
Accepted: Nov 5, 2015

INTRODUCTION

The interphase nucleus is a highly organized organelle, with genes and chromosomes occupying preferred locations within the cell nucleus (Ferrai *et al.*, 2010; Meaburn *et al.*, 2016). Although the spatial organization of the genome is largely conserved among individuals (Borden and Manuelidis, 1988; Wiech *et al.*, 2005; Murata *et al.*, 2007; Meaburn *et al.*, 2009; Timme *et al.*, 2011), nuclear location is not an inherent feature of a locus, since gene loci can occupy distinct positions depending on context or conditions. For example, gene positions may differ among tissue types during differentiation or as cells become quiescent or senescent (Bridger *et al.*, 2000; Boyle *et al.*, 2001; Kosak *et al.*, 2002; Parada *et al.*, 2004; Meaburn and Misteli, 2008; Meaburn *et al.*, 2016; Takizawa *et al.*, 2008a; Ferrai *et al.*, 2010; Peric-Hupkes *et al.*, 2010; Foster *et al.*, 2012). Although the molecular mechanisms that govern the nuclear position of a gene are unknown, changes in gene positioning are sometimes, but not always, correlated with functional changes, such as altered transcription levels or replication timing or with epigenetic changes to chromatin (Kosak *et al.*, 2002; Williams *et al.*, 2006; Hiratani *et al.*, 2008; Meaburn and Misteli, 2008; Meaburn *et al.*, 2016; Takizawa *et al.*, 2008a; Morey *et al.*, 2009; Ferrai *et al.*, 2010; Peric-Hupkes *et al.*, 2010; Towbin *et al.*, 2012; Kind *et al.*, 2013; Therizols *et al.*, 2014; Rafique *et al.*, 2015).

There is accumulating evidence that spatial reorganization of the genome is a pathological feature, with repositioning of individual genes or genomic regions detected in a wide range of diseases, including epilepsy (Borden and Manuelidis, 1988), laminopathies (Meaburn *et al.*, 2007; Mewborn *et al.*, 2010; Mehta *et al.*, 2011), parasitic or viral infection (Li *et al.*, 2010; Knight *et al.*, 2011; Arican-Goktas *et al.*, 2014), Down syndrome (Paz *et al.*, 2015), endometriosis (Mikelsaar *et al.*, 2014), and cancer (Cremer *et al.*, 2003; Murata *et al.*, 2007; Meaburn and Misteli, 2008; Meaburn *et al.*, 2009; Zeitz *et al.*, 2013). For example, in cultured fibroblasts from laminopathy patients, some chromosomes, such as chromosomes (HSAs) 13 and 18, occupy altered nuclear positions, although others, including HSAX and HSA4, are unaffected (Meaburn *et al.*, 2007; Mewborn *et al.*, 2010; Mehta *et al.*, 2011). Similarly, in brain tissue from epilepsy patients, the centromere of HSAX is relocated but 1q12, 9q12, and Y12 are not (Borden and Manuelidis, 1988).

Spatial genome reorganization has been associated with cancer. HSA18 and HSA19, which in many cell types are peripherally and

This article was published online ahead of print in MBoC in Press (http://www.molbiolcell.org/cgi/doi/10.1091/mbc.E15-05-0280) on November 12, 2015.

Address correspondence to: Tom Misteli (mistelit@mail.nih.gov), Karen J. Meaburn (meaburnk@mail.nih.gov).

Abbreviations used: EDT, Euclidean distance transform; FFPE, Formalin-fixed, paraffin-embedded; FISH, fluorescence in situ hybridization; HSA, human chromosome; KS, Kolmogorov–Smirnov; NAT, normal adjacent to tumor; PND, pooled normal distribution; RRD, relative radial distribution.

Supplemental Material can be found at:
http://www.molbiolcell.org/content/suppl/2015/11/09/mbc.E15-05-0280v1.DC1.html

internally located, respectively, broadly maintained their positions in cell lines derived from various cancers, including colon and cervical cancer, melanoma, and Hodgkin's disease, although they tend to be in closer proximity, and a small fraction of nuclei have inverted the locations of these two chromosomes (Boyle *et al.*, 2001; Cremer *et al.*, 2003; Meaburn *et al.*, 2007). Similarly, HSA19 is also shifted to a more peripheral position in tumors of a subset of thyroid cancer patients (Murata *et al.*, 2007). Moreover, HSA18 and the *BCL2* gene are shifted to a more peripheral position in invasive cervical squamous carcinoma compared with the apical, but not basal, layer of nonneoplastic squamous epithelium (Wiech *et al.*, 2009). In both an in vitro model of breast cancer and breast cancer tissues, ~40% of the tested genes were in altered locations (Meaburn and Misteli, 2008; Meaburn *et al.*, 2009). Of importance, most of these gene-repositioning events are specific to the oncogenic state and do not occur in benign breast disease (Meaburn *et al.*, 2009). Not only might the position of a genomic region change in relation to the nuclear edge or center (radial positioning) in cancer, but its position relative to its neighbors might also be affected. For instance, the group of loci that are in close spatial proximity to the *IGFBP3* locus is significantly changed in breast cancer cell lines compared with a normal control (Zeitz *et al.*, 2013).

Spatial genome reorganization in cancer, however, is not a global event. The positions of many genomic regions remain conserved in cancer (Kozubek *et al.*, 2002; Parada *et al.*, 2002; Wiech *et al.*, 2005; Meaburn and Misteli, 2008; Meaburn *et al.*, 2009; Timme *et al.*, 2011). For example, the radial position of HSA8 in pancreatic cancer (Timme *et al.*, 2011) and HSA10 in most thyroid cancers (Murata *et al.*, 2007) is similar to that in normal tissue, and the position of the majority of genes analyzed in breast cancer (Wiech *et al.*, 2005; Meaburn and Misteli, 2008; Meaburn *et al.*, 2009) and leukemia (Kozubek *et al.*, 2002) are unaffected. Similarly, the preferred clustering of chromosomes 12, 14, and 15 is maintained in a mouse lymphoma cell line compared with cultured spleenocytes (Parada *et al.*, 2002).

Prostate cancer is highly prevalent. In the United States alone, >220,000 new cases are diagnosed each year, with one in seven men developing prostate cancer during their lifetime, and there are >27,500 deaths from it annually, accounting for 9% of all male cancer deaths (Siegel *et al.*, 2015). A major challenge in the treatment of prostate cancer patients is the difficulty of distinguishing indolent from aggressive cancer. As a result, a large number of patients receive unnecessary treatment for cancers that will likely remain asymptomatic during their lifetime (Draisma *et al.*, 2009; Cooperberg *et al.*, 2010). There is also a subset of patients with high-risk prostate cancer who are undertreated and are not receiving the treatment their cancer requires to ensure disease-free survival (Cooperberg *et al.*, 2010). Emerging evidence suggests that changes in nuclear architecture features, such as nuclear shape or global levels and patterns of histone modifications and nuclear lamin proteins, may have a clinical value for prostate cancer detection and prognosis (Veltri and Christudass, 2014). However, whereas spatial (re)organization of the genome has been proposed to have diagnostic potential for breast cancer (Meaburn and Misteli, 2008; Meaburn *et al.*, 2009), little is known about spatial genome organization in prostate cancer.

We performed an unbiased screen of the position of 40 genes in Formalin-fixed, paraffin- embedded (FFPE) human prostate tissues. Although we find limited variability in gene positioning patterns among individuals and general conservation of positioning patterns in cancer, we identified three genes that undergo disease-specific repositioning in prostate cancer.

RESULTS

Comprehensive mapping of gene positioning in prostate tissue

Analogous to our approach with regard to breast cancer (Meaburn *et al.*, 2009), we screened the positioning patterns of 40 genes (Supplemental Table S1) in prostate specimens to identify genes that reposition in prostate cancer. To this end, to map comprehensively the spatial position of genes in normal and malignant prostate tissue, we combined fluorescence in situ hybridization (FISH) with quantitative imaging to map the nuclear positions of our set of genes in 4- to 5-µm-thick FFPE human prostate tissues (Supplemental Table S2). The panel of tissues used includes 30 prostate carcinomas, five hyperplasic (nonmalignant abnormality) tissues, and 29 normal or normal adjacent to tumor (NAT) tissues (Supplemental Table S2). The eight genes previously identified to reposition in breast cancer tissues (Meaburn *et al.*, 2009), do not reposition in prostate (unpublished data), and we were unable to identify any particular characteristics of repositioning genes in breast cancer that predicted repositioning potential (Meaburn *et al.*, 2009). Therefore we screened a wide range of genes in prostate tissues, which included many of the most important genes related to prostate cancer, such as genes reported to be misregulated in prostate cancer or to participate in translocations, as well as a set of randomly selected genes, which were selected independently of known changes in activity or involvement in prostate cancer development or progression. The test set included genes from 21 different chromosomes (Supplemental Table S1). To map the nuclear locations of individual genes in a given tissue, we determined the radial position of each allele in typically 100–200 randomly selected epithelial nuclei on projections of three-dimensional image stacks using Euclidean distance transform (EDT) after automated FISH signal detection, as previously described (Meaburn *et al.*, 2009; see *Materials and Methods* for details). For each candidate gene, the positions, normalized to the nuclear radius to eliminate nuclear size effects, of all measured alleles in a tissue were combined and represented as a cumulative relative radial distribution (RRD). Statistical difference between the cumulative RRDs of different samples was assessed using the nonparametric two-sample one-dimensional (1D) Kolmogorov–Smirnov (KS) test as previously described (Meaburn *et al.*, 2009; see *Materials and Methods*).

To screen for genes that specifically reposition in prostate cancer, we used a previously described screening strategy (Meaburn *et al.*, 2009). Briefly, gene positions were first compared in at least three normal and three cancerous prostate tissues (Table 1 and Supplemental Figure 1A). Genes that repositioned in the majority of cancers, in the absence of a large variability among normal tissues, were then screened in a larger number of tissues (Table 1 and Supplemental Figure 1A). Finally, the sensitivity and specificity of the repositioning events of the top hits were assessed by positioning these genes in hyperplasic tissues and determining false-positive and false-negative rates (Supplemental Figure 1A; see later discussion for details).

Conservation of positioning patterns in morphologically normal prostate tissues

It is unknown how similar positioning patterns are between prostates from different individuals, yet knowing the level of interindividual variability in the positioning pattern of a given gene is critical in determining whether any repositioning detected in cancer tissues is specific to cancer or simply a product of interindividual variability. Potential variability of positioning patterns is particularly relevant in the prostate, since the position of several genes has been shown to

Gene	Number of tissues		Percentage (number) of SD cross-comparisons among:	
	Normal	Cancer	Individual normal tissues	Individual normal and cancer tissues
AR	7	6	9.5 (2/21)	16.7 (7/42)
BCL2	4	4	0.0 (0/6)	0.0 (0/16)
BRCA2	4	3	0.0 (0/6)	0.0 (0/12)
CCND1	4	4	50.0 (3/6)	37.5 (6/16)
DCN	5	3	20.0 (2/10)	0.0 (0/15)
EGFR	6	4	0.0 (0/15)	0.0 (0/24)
ERG	5	3	50.0 (5/10)	40.0 (6/15)
ESR2	5	4	0.0 (0/10)	0.0 (0/20)
ETV1	5	3	0.0 (0/10)	0.0 (0/15)
FGFR1	7	5	28.6 (6/21)	22.9 (8/35)
FGFR2	6	4	33.3 (5/15)	41.7 (10/24)
FLI1	8	14	7.1 (2/28)	60.7 (68/112)
FOXA1	4	4	0.0 (0/6)	0.0 (0/16)
FUT4	4	3	0.0 (0/6)	0.0 (0/12)
GREB1	4	3	16.7 (1/6)	25.0 (3/12)
HOXA9	4	3	0.0 (0/6)	8.3 (1/12)
KLK3	5	4	20.0 (2/10)	30 (6/20)
LMNA	4	3	50.0 (3/6)	16.7 (2/12)
MATR3	4	3	33.3 (2/6)	0.0 (0/12)
MMP1	3	3	33.3 (1/3)	11.1 (1/9)
MMP14	3	3	33.3 (1/3)	44.4 (4/9)
MMP2	8	16	7.1 (2/28)	48.4 (62/128)
MMP9	10	19	17.8 (8/45)	44.2 (84/190)
NPM1	3	3	33.3 (1/3)	33.3 (3/9)
NUMA1	4	4	0.0 (0/6)	12.5 (2/16)
PADI4/6	6	6	13.3 (2/15)	5.6 (2/36)
PTEN	3	3	0.0 (0/3)	22.2 (2/9)
RAF1	8	5	32.1 (9/28)	30.0 (12/40)
SATB1	5	4	20.0 (2/10)	15.0 (3/20)
SERPINB2	4	4	16.7 (1/6)	6.3 (1/16)
SLC45A3	5	0	0.0 (0/10)	ND
SP100	5	4	0.0 (0/10)	20.0 (4/20)
SPDEF	5	4	10.0 (1/10)	5.0 (1/20)
TGFB1	4	4	50.0 (3/6)	30.0 (5/16)
THBS1	5	4	20.0 (2/10)	30.0 (6/20)
TIMP2	6	7	53.3 (8/15)	33.3 (14/42)
TIMP3	6	4	60.0 (9/15)	58.3 (14/24)
TMPRSS2	6	4	60.0 (9/15)	50.0 (12/24)
VEGFA	13	7	24.4 (19/78)	47.3 (43/91)
VIM	5	4	70.0 (7/10)	40.0 (8/20)

SD, significantly different, based on a KS test, $p < 0.01$. ND, not determined.

TABLE 1: Cross-comparisons among individual tissues.

be sensitive to androgen (Lin *et al.*, 2009; Mani *et al.*, 2009). To determine the degree of variability in gene localization among individuals, we compared the positioning pattern of our set of 40 genes among morphologically normal prostate tissues. For most of the genes analyzed, the radial distribution of the gene among normal prostate tissues was similar (Table 1, Figures 1 and 2, and Supplemental Figures S1 and S2). For 12 of 40 (30.0%) genes, the RRDs were statistically identical among all individuals ($p > 0.01$; Table 1, Figures 1 and 2, and Supplemental Figures S1 and S2). An additional 20 genes (50.0%), although not identical among all comparisons, were very similarly positioned among most individuals, with <33.4% of cross-comparisons being statistically significantly different ($p < 0.01$; Table 1, Figures 1 and 2, and Supplemental Figures S1 and S2). The position of 20% of genes (8 of 40; *CCND1* [3 of 6 cross-comparisons], *ERG* [5 of 10], *LMNA* [3 of 6], *TGFB1* [3 of 6], *TIMP2* [8 of 15], *TIMP3* [9 of 15], *TMPRSS2* [9 of 15] and *VIM* [7of 10]) were highly variable among individuals, with 50–70% of the cross-comparisons among normal tissues being significantly different (Table 1, Figures 1 and 2, and Supplemental Figures S1 and S2).

Because the position of a gene in a given tissue can be significantly different from some but not all other tissues, as an additional measure of conservation in positioning patterns among individuals, we compared the RRD of each gene in each normal tissue to a pooled normal distribution (PND). The PND is used as a standardized "average" position of a gene within normal tissues and was generated by combining the RRDs from all normal tissues analyzed into a single distribution for each gene, as previously described (Meaburn *et al.*, 2009; see *Materials and Methods*). Again we found a high level of similarity among individuals (Table 2, Figures 1 and 2, and Supplemental Figures S1 and S2). For 26 of the 40 (65.0%) genes, no individual's normal tissue was significantly different from the PND, and an additional eight (20.0%) genes had only a single normal tissue significantly different to the PND (7.7–25% of normal tissues; Table 2, Figures 1 and 2, and Supplemental Figures S1 and S2). On the other hand, three genes (3 of 40; 7.5%)—*FGFR1* (2 of 7 normal tissues), *TMPRSS2* (2 of 6), and *RAF1* (3 of 8)—had approximately one-third (28.6–37.5%) of normal tissues significantly different from the PND, and an additional three genes (*CCND1* [2 of 4], *TIMP2* [3 of 6], and *TIMP3* [4 of 6]) were significantly different from the PND in 50.0–66.7% of normal tissues (Table 2 and Supplemental Figures S1 and S2). Taken together, these data demonstrate that the radial positions of most genes are conserved among prostate tissue from different individuals. However, the position of a subset of genes is variable among individuals.

Identification of repositioned genes in prostate cancer

Having established limited variability in gene positioning among individuals, we screened for genes that reposition in prostate cancer. We compared the RRDs of 39 genes in multiple cancer tissues to individual normal tissues and to the PND (Tables 1 and 2, Figures 1 and 2, and Supplemental Figures S1 and S2). The position of nine genes (23.1%) was indistinguishable in all cross-comparisons among individual normal and cancer tissues, and an additional 19 genes (48.7%) had only limited variability between normal and cancer tissues, with 5.0–33.3% of cross-comparisons reaching significance. Nine genes (23.1%; *CCND1* [6 of 16 comparisons], *ERG* [6 of 15], *VIM* [43 of 91], *FGFR2* [10 of 24], *MMP9* [84 of 190], *MMP14* [4 of 9], *VEGFA* [43 of 91], *MMP2* [62 of 128], and *TMPRSS2* [12 of 24]) were differently positioned in 37.5–50.0% of cross-comparisons. Two genes (5.1%; *TIMP3* [14 of 24] and *FLI1* [68 of 112]) were repositioned in ~60% of cross-comparisons between normal and malignant prostate tissues (Table 1, Figures 1 and 2, and Supplemental

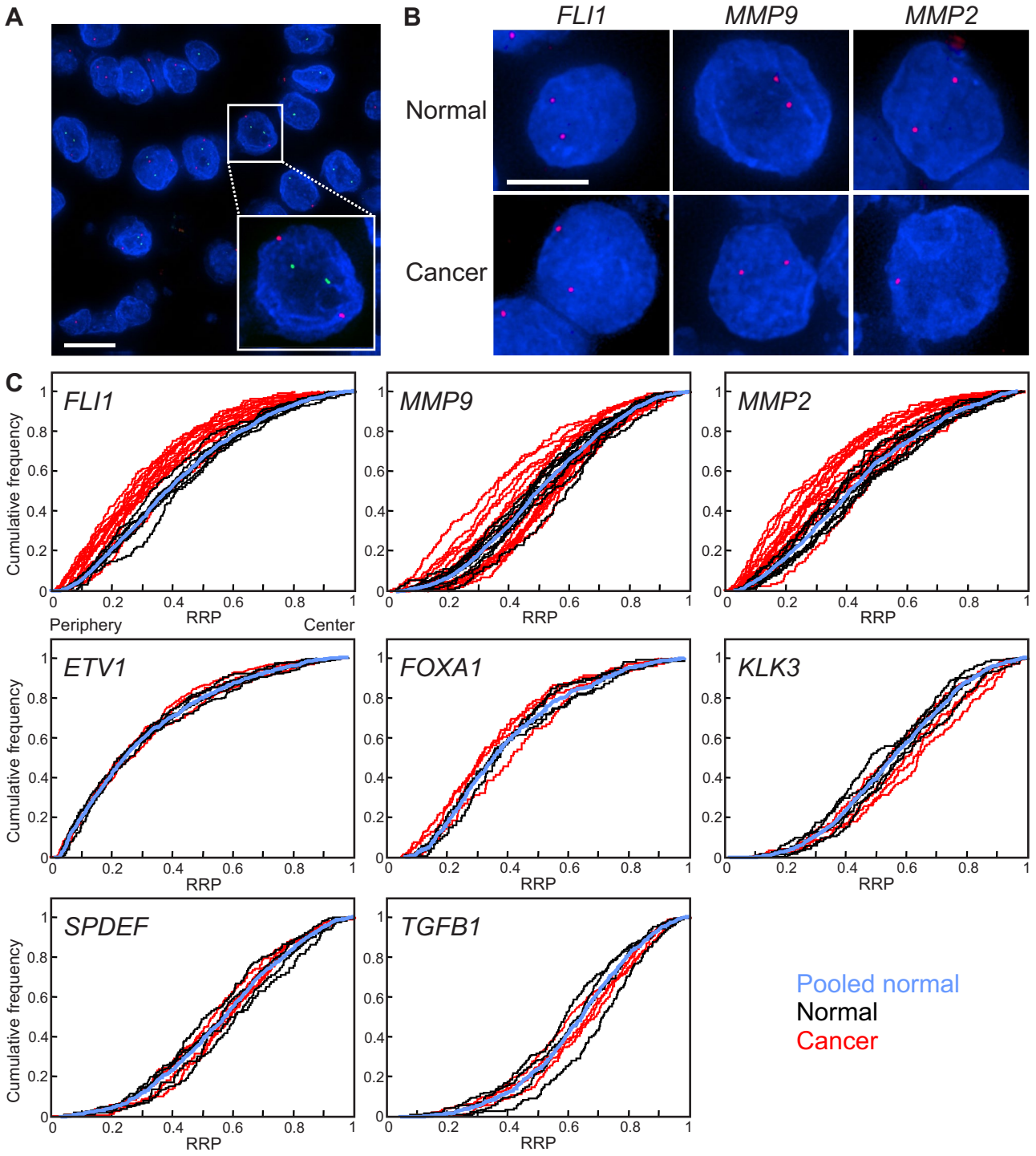

FIGURE 1: Gene-specific spatial reorganization of the genome in prostate cancer. (A, B) Gene loci were detected by FISH in FFPE prostate tissue sections. Blue, 4′,6-diamidino-2-phenylindole nuclear counterstain. Projected image stacks. (A) *EGFR* (red) and *SPDEF* (green) gene loci, in a malignant prostate tissue. Bar, 10 µm. (B) *FLI1*, *MMP9*, and *MMP2* gene loci (red) in normal and cancer tissues. Bar, 5 µm. (C) Cumulative RRDs for the indicated genes in prostate cancer (red), normal prostate tissues (black), and the pooled normal distribution (PND, blue). The positioning patterns of some but not all genes are different in prostate cancer compared with normal tissues. RRP, relative radial position.

Figures S1 and S2). For most genes, the number of significantly different cross-comparisons between normal and cancer specimens was not greater than that of the cross-comparisons among normal tissues, suggesting that the repositioning was not cancer specific (Table 1). For example, whereas *TIMP3* was differently positioned in 58.3% (14 of 24) of the cross-comparisons between individual normal and cancer tissues, 60.0% (9 of 15) of cross-comparisons were statistically different when normal tissues were cross-compared with each other (Table 1 and Supplemental Figure S2). Taking into consideration the degree of positioning changes in all cross-comparisons and the interindividual variability of candidates, we identified three genes—*MMP2*, *MMP9*, and *FLI1*—that exhibited robust

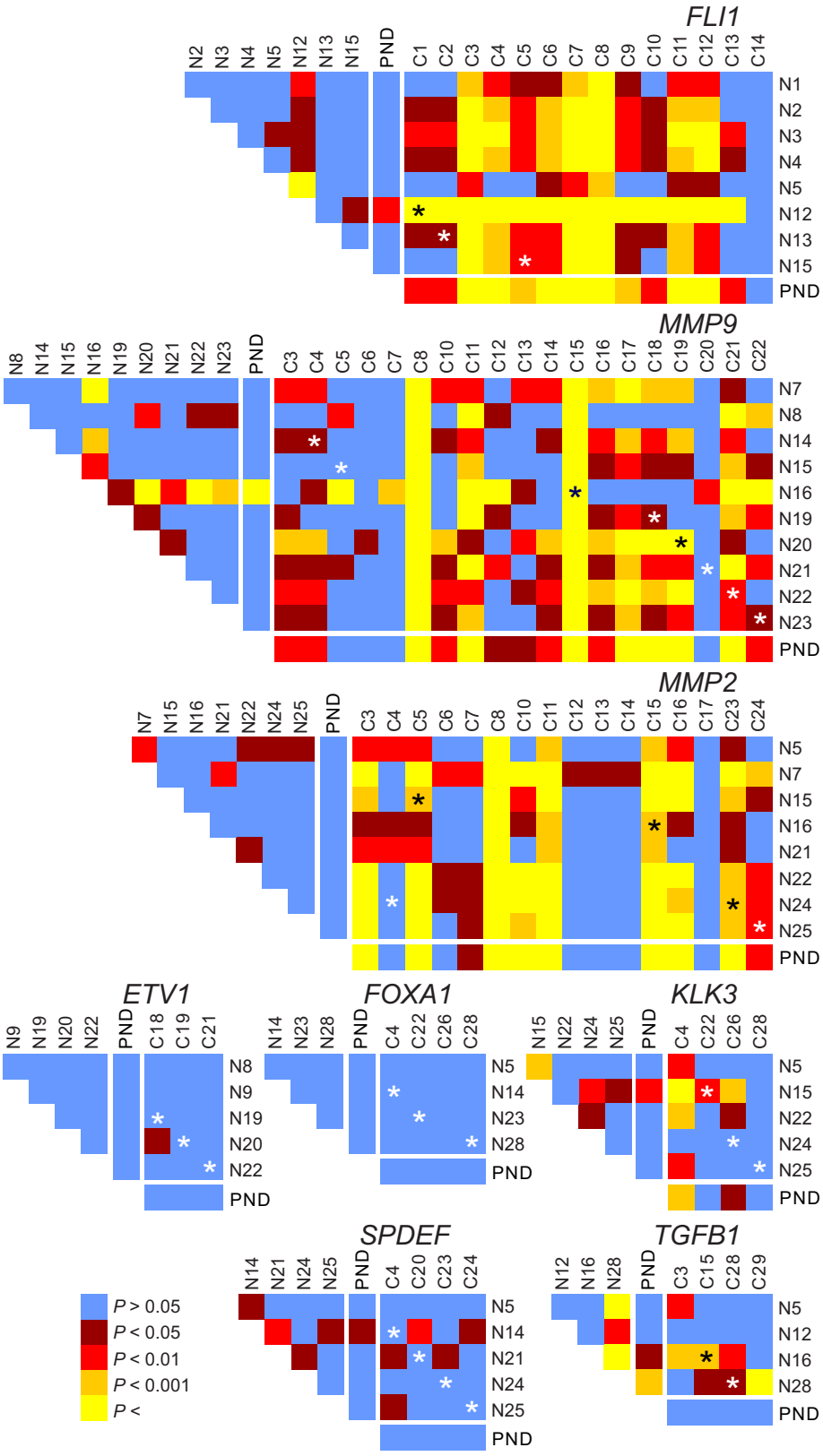

FIGURE 2: Gene-specific repositioning in prostate cancer. Heat maps representing the pairwise statistical comparisons of radial positioning patterns of indicated genes among tissues using the two-sample 1D KS test. Although positioning patterns are statistically similar (blue, brown) among most normal tissues (N1–N28; see Supplemental Table S2), they can be divergent (red, orange, yellow) in cancer tissues (C1–C24; see Supplemental Table S2). Black and white asterisks indicate a cross-comparison between a normal and cancer specimens from the same individual. PND, pooled normal distribution.

differential radial positioning between normal and cancer tissues. For these genes, the percentage of cross-comparisons between normal and cancer tissues was higher by >25% than when normal tissues were compared with each other (48.4 vs. 7.1%, 44.2 vs. 17.8%, and 60.7 vs. 7.1%, respectively; Table 1 and Figure 2).

Repositioning of *FLI1*, *MMP9*, and *MMP2* in prostate cancers was confirmed by analysis of their distributions in individual cancer samples to their PNDs. Most genes in the test set displayed limited repositioning in prostate cancer tissues compared with their PNDs. Two-thirds (26) of genes were repositioned in 0–33.3% of cancer tissues compared with the PND, and six genes repositioned in 40–50% of cancers (Table 2, Figures 1 and 2, and Supplemental Figures S1 and S2). As observed in the cross-comparison analysis, *FLI1*, *MMP9*, and *MMP2* showed robust repositioning in prostate cancer, and their distributions were distinct from their PNDs in 92.9% (13 of 14 of cancer tissues), 68.4% (13 of 19), and 56.3% (9 of 16) of cancers, respectively (Table 2 and Figures 1 and 2). Although an additional four genes were also repositioned in >50% of cancers compared with the PND (*VEGF*, 57.1% [4 of 7]; *MMP14*, 66.7% [2 of 3]; *NPM1*, 66.7% [2 of 3]; and *TMPRSS2*, 75% [3 of 4]; Table 2 and Supplemental Figures S1 and S2), we classified these genes as low-priority hits and did not pursue them further because the percentage of cross-comparisons between normal and cancer tissues was not significantly higher than the variability detected among normal tissues and visual inspection of the cumulative frequency distribution plots revealed that only a small number of the distributions in cancer tissues fell outside the range of the normal tissues (Supplemental Figure S1).

In the vast majority (96 of 125; 76.8%) of cases, there was a similar repositioning behavior when a cancer was compared with its matched NAT or with the PND (Figure 2 and Supplemental Figure S2). This observation suggests that repositioning, if present in a patient, is limited to the cancer tissue itself and that comparison to the PND is suitable to assess whether a gene is repositioned in cancer, even when no normal tissue from the same individual is available.

We were unable to define any feature of a prostate cancer that predicted the likelihood of a gene repositioning within it. The propensity of the three marker genes to reposition in a given cancer was not linked to changes in copy number (Supplemental Table S3), nor was the variation in their positioning patterns correlated with the

Gene	Percentage (number) of SD cross-comparisons between: Individual normal tissues and pooled normal	Individual cancer tissues and pooled normal
AR	0.0 (0/7)	33.3 (2/6)
BCL2	0.0 (0/4)	0.0 (0/4)
BRCA2	0.0 (0/4)	33.3 (1/3)
CCND1	50.0 (2/4)	25.0 (1/4)
DCN	0.0 (0/5)	0.0 (0/3)
EGFR	0.0 (0/6)	0.0 (0/4)
ERG	20.0 (1/5)	33.3 (1/3)
ESR2	0.0 (0/5)	0.0 (0/4)
ETV1	0.0 (0/5)	0.0 (0/3)
FGFR1	28.6 (2/7)	40.0 (2/5)
FGFR2	16.7 (1/6)	50.0 (2/4)
FLI1	12.5 (1/8)	92.9 (13/14)
FOXA1	0.0 (0/4)	0.0 (0/4)
FUT4	0.0 (0/4)	0.0 (0/3)
GREB1	25.0 (1/4)	0.0 (0/3)
HOXA9	0.0 (0/4)	33.3 (1/3)
KLK3	20.0 (1/5)	25.0 (1/4)
LMNA	0.0 (0/4)	33.3 (1/3)
MATR3	0.0 (0/4)	0.0 (0/3)
MMP1	0.0 (0/3)	0.0 (0/3)
MMP14	0.0 (0/3)	66.7 (2/3)
MMP2	0.0 (0/8)	56.3 (9/16)
MMP9	10.0 (1/10)	68.4 (13/19)
NPM1	0.0 (0/3)	66.7 (2/3)
NUMA1	0.0 (0/4)	50.0 (2/4)
PADI4/6	0.0 (0/6)	16.7 (1/6)
PTEN	0.0 (0/3)	0.0 (0/3)
RAF1	37.5 (3/8)	40.0 (2/5)
SATB1	0.0 (0/5)	25.0 (1/4)
SERPINB2	0.0 (0/4)	0.0 (0/4)
SLC45A3	0.0 (0/5)	ND
SP100	0.0 (0/5)	25.0 (1/4)
SPDEF	0.0 (0/5)	0.0 (0/4)
TGFB1	25.0 (1/4)	0.0 (0/4)
THBS1	0.0 (0/5)	50.0 (2/4)
TIMP2	50.0 (3/6)	28.6 (2/7)
TIMP3	66.7 (4/6)	50.0 (2/4)
TMPRSS2	33.3 (2/6)	75.0 (3/4)
VEGFA	7.7 (1/13)	57.1 (4/7)
VIM	0.0 (0/5)	25.0 (1/4)

SD, significantly different, based on a KS test, $p < 0.01$. ND, not determined.

TABLE 2: Comparison of individual tissues to a pooled normal distribution.

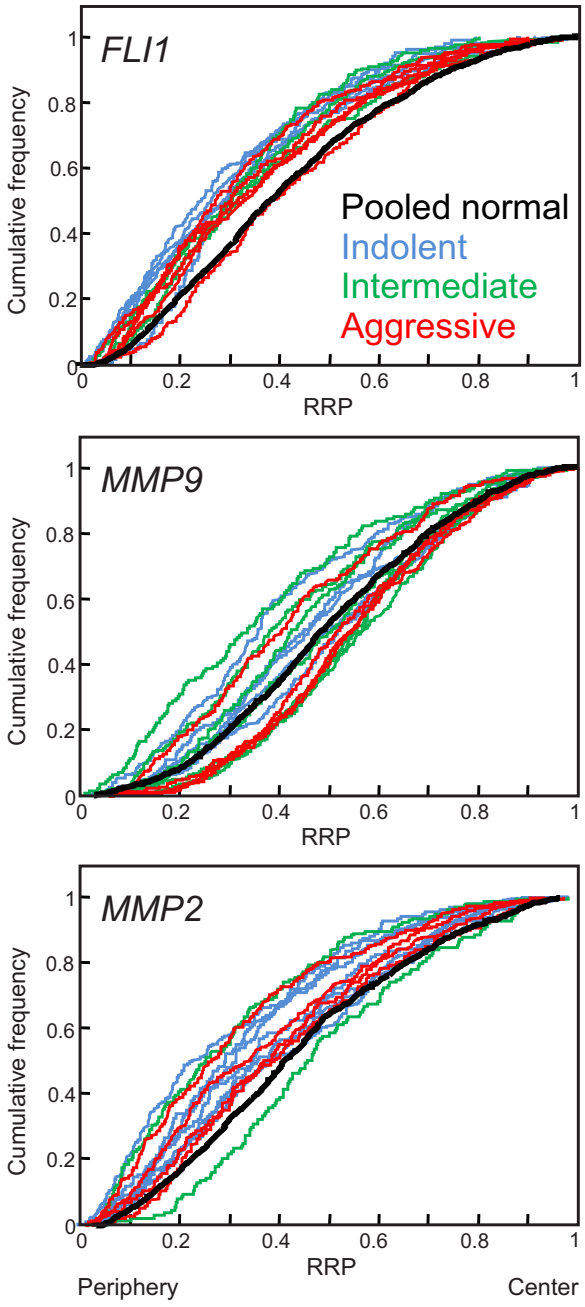

FIGURE 3: Gene repositioning in prostate cancer is not linked to prognostic status. Cumulative RRDs are color coded according to the prognostic status of the cancer: blue, indolent prostate cancers (Gleason score ≤6, without metastasis); green, intermediate cancers (Gleason score 7, without metastasis); red, aggressive cancers (Gleason score ≥8, and/or metastasis). The pooled normal distribution (black) is included for comparison. RRP, relative radial position.

clinicopathologically defined aggressiveness of the cancer (Supplemental Table S2 and Figure 3).

Cancer specificity of *FLI1* and *MMP9* repositioning

Given that loci can alter their nuclear location in diseases other than cancer (Borden and Manuelidis, 1988; Meaburn *et al.*, 2007, 2009), we sought to determine whether the repositioning of *FLI1*, *MMP9*, and *MMP2* was specific to cancer or was a more general feature of prostate disease. We compared the radial positioning patterns of

Gene	Percentage (number) of SD cross-comparison among:		
	Individual hyperplasia tissues	Individual normal and hyperplasia tissues	Individual hyperplasia tissues and pooled normal
FLI1	10.0 (1/10)	10.0 (4/40)	0.0 (0/5)
MMP9	0.0 (0/10)	12.0 (6/50)	0.0 (0/5)
MMP2	0.0 (0/10)	45.0 (18/40)	80.0 (4/5)

SD, significantly different, based on a two-sample 1D KS test, $p < 0.01$.

TABLE 3: Comparison of gene positioning in benign tissues.

these genes in five benign hyperplastic tissues with the positioning patterns of normal prostate tissues and among multiple hyperplasia tissues (Table 3 and Figure 4). *MMP9* and *MMP2* were positioned identically in all hyperplastic tissues (Table 3 and Figure 4). The position of *FLI1* is similarly conserved among hyperplastic tissues, with only a single cross-comparison reaching significance (1 of 10; Table 3 and Figure 4). *FLI1* and *MMP9* did not reposition in hyperplasia compared with normal tissues, since the positioning of both genes was indistinguishable from the PND in all five hyperplasia tissues (Table 3 and Figure 4), and only 10% (4 of 40) and 12% (6 of 50) of the cross-comparisons among individual normal tissues reached significance, respectively. These findings, combined with the low repositioning rate in normal tissue, suggests that *FLI1* and *MMP9* repositioning is specific to cancer. In contrast, compared with normal tissues, *MMP2* was repositioned in both prostate cancer and hyperplasia. *MMP2* was in a significantly different position in 80% (4 of 5) of the hyperplastic tissues compared with the PND and in 45% (18 of 40) of cross-comparisons between hyperplasic and normal tissues (Table 3 and Figure 4), suggesting that the repositioning of *MMP2* is common in prostate disease and not limited to malignancy. We had access to both hyperplastic and cancer tissue from the same prostate (B1 and C3, respectively; Supplemental Table S2). In keeping with the comparisons between hyperplasia and normal tissue, *FLI1* and *MMP9* occupied significantly different positions in the cancer and hyperplasic tissue ($p = 0.004$ and 0.002, respectively), whereas

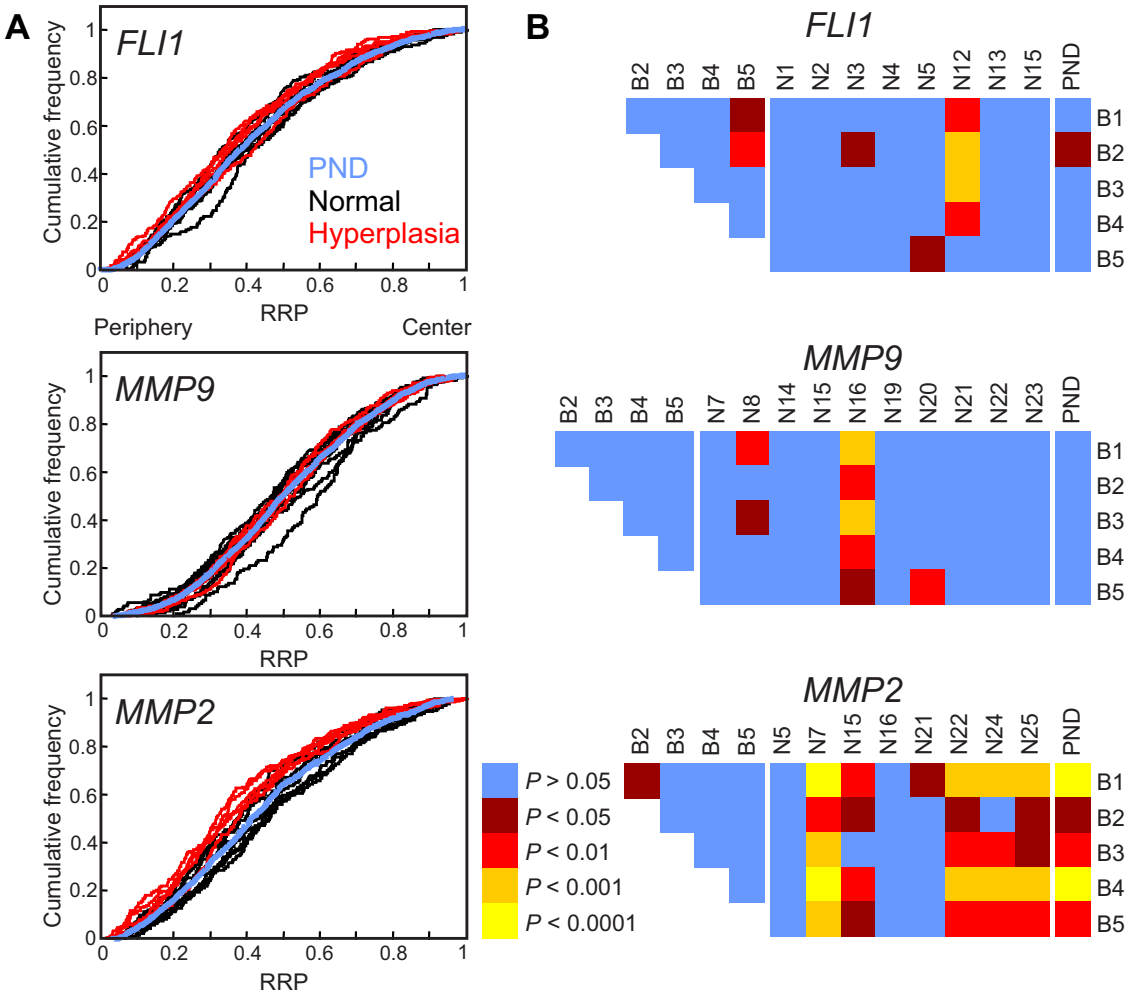

FIGURE 4: Gene positioning in benign disease. Positions of indicated genes were compared between hyperplasia (B1–B5) and normal prostate tissue (N1–N25). (A) Cumulative RRDs for the indicated genes in hyperplasia (red), normal tissues (black), and the pooled normal distribution (PND; blue). (B) Pairwise statistical comparisons of RRDs between hyperplasic tissues and normal tissues and among hyperplasic tissues, using the two-sample 1D KS test. All three genes are similarly positioned between hyperplasic tissues and only *MMP2* repositions in hyperplasic compared with normal tissues. RRP, relative radial position.

Gene	Normal-tissue false positives	Benign-tissue false positives	Total false positives
FLI1	12.5% (1/8)	0.0% (0/5)	7.7% (1/13)
MMP9	10.0% (1/10)	0.0% (0/5)	6.7% (1/15)
MMP2	0.0% (0/8)	80.0% (4/5)	30.8% (4/13)

The percentage (number) of tissues that give a false-positive result. A false positive is scored when a gene has a statistically significant different RRD in a normal or hyperplastic tissue compared with the pooled normal ($p < 0.01$; KS test).

TABLE 4: False-positive rates.

MMP2 was in a similar position in the two disease states ($p = 0.516$) for this individual.

High-confidence detection of prostate cancers using multiplexed positioning biomarkers

Because *FLI1* and *MMP9* repositioning occurs predominantly in cancer tissues, we determined their false-positive and false-negative rates as a preliminary step toward assessing their potential as biomarkers for prostate cancer. A false positive was defined as repositioning ($p > 0.01$; KS test) of the marker gene in a nonmalignant (normal or hyperplastic) tissue compared with the PND, thus incorrectly classifying the tissue as cancer. Conversely, a false negative was defined as lack of repositioning ($p < 0.01$) of the marker gene in a cancer, leading to incorrect classification of the tissue as nonmalignant. As expected due to its high rate of repositioning in hyperplasia, *MMP2* had a high false-positive rate (30.8% [4 of 13 nonmalignant tissues]; Figures 2 and 4 and Table 4). This finding, combined with its high false-negative rate (43.8% [7 of 16 cancer tissues]; Figure 2 and Table 5), suggests that *MMP2* would not be a useful biomarker for prostate cancer. In contrast, *FLI1* had low false-negative and false-positive rates (7.1% [1 of 14 cancer tissues] and 7.7% [1 of 13 nonmalignant tissues], respectively; Figures 2 and 4 and Tables 4 and 5). *MMP9* had a fairly high false-negative rate (31.6% [6 of 19 cancer tissues]; Figure 2 and Table 5) but a low false-positive rate (6.7% [1 of 15 nonmalignant tissues]; Figures 2 and 4 and Table 4).

None of the genes we tested repositioned in all prostate cancer tissues. However, at least one repositioned gene was present in every prostate cancer tissue analyzed (30 of 30 cancers; Figure 2 and Supplemental Figure S2). Given the low false-positive rate of *FLI1* and *MMP9*, we explored the possibility of using these two genes in a multiplex format for the detection of cancer samples. When analyzed together, *FLI1* or *MMP9*, or both, repositioned in all (11 of 11) cancers (Figure 2 and Supplemental Table S4). Consequently, multiplexing *FLI1* and *MMP9* reduced the false-negative rate to 0% (0 of 11; Table 5). We conclude that in combination, *FLI1* and *MMP9* are strong potential biomarkers for prostate cancer.

Gene(s)	False-negative rate
Single gene	
FLI1	7.1% (1/14)
MMP9	31.6% (6/19)
MMP2	43.8% (7/16)
Multiplexed genes	
FLI1 and *MMP9*	0.0% (0/11)
FLI1 and *MMP2*	9.1% (1/11)
MMP9 and *MMP2*	28.6% (4/14)

The percentage (number) of tissues that give a false-negative result. A false negative is scored when the RRD of a gene in a cancer tissue is similar to that of the pooled normal distribution (KS test, $p > 0.01$). For multiplexed genes, a false positive is scored when neither gene in the pair is repositioned compared with the pooled normal distribution ($p > 0.01$, KS test). Only tissues in which both genes of the pair were positioned are included.

TABLE 5: False-negative rates for single and multiplexed genes.

DISCUSSION

This study was designed to identify gene loci that undergo repositioning during prostate carcinogenesis. Spatial mapping of the radial position of 40 genes by FISH identified two genes that robustly reposition in prostate cancer and a third gene that repositions in both prostate cancer and benign prostate disease. The vast majority of analyzed genes, however, did not undergo significant cancer-specific repositioning, pointing to considerable conservation of spatial genome organization in prostate cancer.

In keeping with previous studies on positioning of select genes and of whole chromosomes in brain (Borden and Manuelidis, 1988), pancreas (Timme *et al.*, 2011), thyroid (Murata *et al.*, 2007), and breast (Wiech *et al.*, 2005; Meaburn *et al.*, 2009), we find that the spatial positioning of most genes tested in normal prostate tissue is generally well conserved among individuals. Of 40 genes analyzed, only three (*CCND1*, *TIMP2*, and *TIMP3*) were highly variable among individuals. A prerequisite of a useful cancer biomarker is conservation among individuals in nonmalignant tissues because such variability leads to low sensitivity and specificity of the marker. Therefore some genes will not be suitable for diagnostic purposes due to variable positioning patterns among individuals. The variability in the position of some genes in normal prostate tissue is higher than previously detected for 15 genes in morphologically normal breast tissue (Meaburn *et al.*, 2009). The reasons for this difference between the two tissue types are not known. One possibility is that some glands within normal prostate tissues have preneoplastic features. For example, proliferative inflammatory atrophy, which is regarded as a histologically distinctive pattern of benign glands, has some of the molecular features of prostate neoplasia (De Marzo *et al.*, 1999). In contrast, there is no reported counterpart lesion of mammary glands. Another possibility is that these prostate glands could have included low-grade prostatic intraepithelial neoplasia, which is challenging to recognize in dark-field FISH preparations. In addition, some genes could be more susceptible to interindividual variations in their positioning patterns, which could be either a general feature of the locus or tissue specific. For example, the position of *CCND1* was similar among normal breast tissues (Meaburn *et al.*, 2009) but varied among individuals in the prostate, pointing to a potential tissue-specific driver to interindividual positioning patterns. Because CCND1 is a cell cycle regulator and epithelial cells are largely quiescent in normal breast and prostate tissues, a direct link between CCND1 function and tissue specificity seems unlikely.

We identified three genes that consistently reposition in prostate cancer. The repositioning of *FLI1* and *MMP9* was specific to cancer, as it did not occur in benign disease, in line with earlier observations in breast, where gene repositioning was generally limited to cancerous tissue (Meaburn *et al.*, 2009). In contrast, *MMP2* repositioned in cancer as well as in hyperplasic prostate tissue. Our findings are in line with previous studies in other types of cancer, for which repositioning of some loci and concurrent conservation in the positioning patterns of others have been reported (Croft *et al.*, 1999; Parada *et al.*, 2002; Cremer *et al.*, 2003; Wiech *et al.*, 2005, 2009; Murata *et al.*, 2007; Meaburn and Misteli, 2008; Meaburn *et al.*, 2009;

Harewood *et al.*, 2010). Of interest, *FLI1* and *MMP9* also reposition in breast cancer (unpublished data), suggesting that they are multitissue markers of cancer. Not all genes that reposition in cancer are general markers of a malignant state, however, since an additional eight genes that reposition in breast cancer (Meaburn *et al.*, 2009) do not reposition in prostate cancer (unpublished data).

We did not identify any common features shared among repositioning genes in prostate cancer. For example, the genes that reposition map to different chromosomes (*FLI1*, HSA11; *MMP9*, HSA20; and *MMP2*, HSA16). The repositioning of *FLI1*, at least, is unlikely to reflect whole-chromosome movements, since of five genes located on HSA11 (*FLI1*, *CCND1*, *FUT4*, *MMP1*, and *NUMA1*), only *FLI1* robustly repositioned in prostate cancer. In addition, biological function or known relevance to tumorigenesis of genes does not predict repositioning behavior. Many of the genes we positioned that are commonly implicated in prostate cancer, such as *KLK3* (prostate-specific antigen), *AR, PTEN, TGFB1, VEGFA,* and *BCL2* (Bok and Small, 2002; Ferte *et al.*, 2010; Lawrence *et al.*, 2010; Shen and Abate-Shen, 2010), and the commonly translocated genes in prostate cancer, the androgen-regulated *TMPRSS2* and the ETS transcription factors *ERG* and *ETV1* (Tomlins *et al.*, 2005), do not spatially reposition in prostate cancers. Yet the ETS transcription factor *FLI1*, which forms rare translocations in prostate cancer (Paulo *et al.*, 2012), does. *MMP9* and *MMP2*, which belong to the same class of matrix metallopeptidases (MMPs) and are involved in the breakdown of extracellular matrix, which is important to cancer- associated processes such as angiogenesis and metastasis (Egeblad and Werb, 2002), reposition in prostate cancer, and yet the potential functional relevance of the cancer-association gene repositioning is unclear. Although an increase in MMP9 and MMP2 expression has been linked to poor prognosis in prostate cancer, both genes are predominantly expressed by the stromal cells and not by the tumor cells (Egeblad and Werb, 2002). Other MMP family members, such as *MMP14*, and the genomic loci containing a cluster of MMP genes, including *MMP1*, did not reposition. Moreover, genes coding the MMP-regulating proteins *TIMP2, TIMP3* (Egeblad and Werb, 2002), and *SPDEF* (Johnson *et al.*, 2010), another ETS transcription factor, do not reposition in prostate cancer, further reducing a link between function and cancer-associated gene repositioning. A lack of a link between gene function and an altered radial position in cancer is in line with multiple studies that find no correlation between changes in gene expression and changes in radial positioning patterns, including a cell culture model of early breast cancer (Williams *et al.*, 2006; Meaburn and Misteli, 2008; Takizawa *et al.*, 2008b; Morey *et al.*, 2009; Harewood *et al.*, 2010; Shachar *et al.*, 2015). Although we focused on radial positioning patterns to identify cancer-specific spatial genome-repositioning events, relative positioning of loci to other genomic loci or nuclear landmarks, such as nuclear bodies, may be a promising alternative parameter to characterize the spatial reorganization of gene loci in cancer.

Repositioning did not correlate with gene copy number or the presence of translocations. For example, *FLI1* repositioned in both cancers with and without amplified *FLI1*, and we found *FLI1* repositioning in 13 of 14 prostate cancers, yet the *SLC45A3-FLI1* translocation occurs in only 1 in 200 prostate cancers (Paulo *et al.*, 2012). Although it is possible that translocations could affect the position of genomic regions beyond the translocating region, even on chromosomes not involved in the translocation, our data demonstrate that in the background of genetic instability, it is still possible to use gene positioning for cancer diagnostics.

As previously observed for breast cancer (Meaburn *et al.*, 2009), we find that combinatorial analysis of multiple genes results in detection of cancer with high accuracy. Whereas neither *MMP9* nor *FLI1* alone was repositioned in all prostate tumor samples, at least one of the two was repositioned in all cancer samples analyzed. Our observation of cancer-specific repositioning of these two genes, combined with their relatively low false-positive detection rate, makes *MMP9* and *FLI1* strong candidates for combinatorial use in cancer diagnosis.

MATERIALS AND METHODS

Tissues

To detect individual genes, FISH was performed on a panel of 4- to 5-µm-thick FFPE human prostate tissue sections, which consisted of 30 prostate cancers, 29 normal and NAT prostate tissues, and five hyperplasic tissues (Supplemental Table S2). Prostate tissues were obtained from the University of Washington (Seattle, WA) under the guidelines and approval of the Institutional Review Board of the University of Washington (#00-3449). These specimens were reviewed by a single genitourinary pathologist (L.D.T.). Additional tissues were purchased from US Biomax (Rockville, MD) and Imgenex (San Diego, CA; Supplemental Table S2). All specimens were deidentified.

FISH

FISH probes were produced by using nick translation to label DNA purified from bacterial artificial chromosome clones (BACPAC Resources Center [Oakland, CA]; Supplemental Table S1) with either biotin- or digoxigenin-conjugated dUTPs (Roche, Indianapolis, IN), as detailed in Meaburn (2010). An identical dual-probe FISH procedure was performed on all specimens as previously described (Meaburn *et al.*, 2009), with the exceptions that 1) the 60°C slide baking step, before xylene (Avantor Performance Materials, Center Valley, PA) treatment, was omitted, 2) the time the tissue sections were incubated in 0.25 mg/ml Proteinase K (Sigma-Aldrich, St. Louis, MO) was increased to 15–20 min, and 3) 0.5 mg/ml Proteinase K was often required for single-tissues slides obtained from Biomax (but not tissue microarray slides).

Image acquisition and FISH analysis

Image accusation was performed essentially as described in Meaburn *et al.* (2009). Briefly, tissue sections were imaged with an IX70 (Olympus, Waltham, MA) DeltaVision (Applied Precision-GE Healthcare Bio-Sciences, Pittsburgh, PA) system, using a 60×/1.42 numerical aperture oil objective lens (Olympus) and an auxiliary magnification of 1.5. Image stacks were acquired with a 0.5-µm step interval along the *z*-axis. If mixed morphologies were present in a tissue section, before imaging, the tissue was visually inspected at low resolution (10× lens; Olympus) to identify malignant, normal, or hyperplastic regions. In these cases, hematoxylin and eosin–stained tissue slides that had been marked by a pathologist (L.D.T.) were used as a guide to ensure correct classification of different regions of a tissue. Image stacks were deconvolved and converted into maximum intensity projections using SoftWoRx (Applied Precision).

Image analysis was performed as previously described (Meaburn *et al.*, 2009). Images were contrast enhanced based on visual inspection, and individual nuclei were manually delineated in Photoshop 7.0 (Adobe, San Jose, CA), with each nucleus saved in a separate image file. To determine the relative radial positioning of a gene in a given tissue, 91–263 randomly selected interphase epithelial nuclei were run though a custom-made image analysis software package (P. Gudla and S. Lockett, National Cancer Institute, Bethesda, MD; Meaburn *et al.*, 2009) in MATLAB (MathWorks, Natick, MA) using the PRTools and DIPImage toolboxes (Delft University of Technology, Delft, Netherlands). The software automatically identified FISH

signals (>99% of FISH signals detected, with a false-positive rate of <1%; Takizawa *et al.*, 2008a) and determined both the binary EDT of the geometric gravity center of each FISH signal and the number of FISH signals in a nucleus for both genes visualized by FISH. In EDT, each pixel in a nucleus is assigned a value that equals the shortest distance to the nuclear edge. EDT values are then normalized to the maximum EDT value of a given nucleus to account for variations in nuclear size. Using this method, no assumption regarding nuclear shape or size is made when determining the radial position of a gene, allowing accurate comparisons between tissues even if there are differences or irregularities in nuclear shape or size. The relative radial positions of individual nuclei from the same specimen for each histologic entity were combined to generate a RRD for a gene. All alleles in a nucleus were included for analysis, and nuclei were analyzed regardless of the number of alleles present, unless there were no signals for either gene. Because some nuclei contained FISH signals for only one gene, when the number of nuclei analyzed is indicated, only nuclei containing FISH signals for the indicated gene are included. To generate PNDs, normalized EDTs from all nuclei from all normal tissues analyzed for a given gene were combined into a single data set (see Table 1 for the number of normal tissues analyzed for each gene and Supplemental Table S1 for the number of nuclei used to generate each gene's PND). Finally, cumulative RRDs from different samples were statistically compared using the nonparametric two-sample 1D KS test. The null hypothesis that the samples are from the same distribution was rejected if $p < 0.01$.

ACKNOWLEDGMENTS

We thank Prabhakar Gudla and Stephen Lockett for help with image analysis; Olufunmilayo Agunloye for technical assistance; Delft University of Technology for providing the DIPImage and PRTools toolboxes; and Tatiana Karpova for microscopy support. We also thank Kathy Doan for help in identifying and obtaining tissue used for this study. Fluorescence imaging was performed at the National Cancer Institute Fluorescence Imaging Facility (Bethesda, MD). This work was supported by Department of Defense Idea Award W81XWH-12-1-0224, the National Cancer Institute, National Institutes of Health, under Pacific Northwest Prostate Cancer SPORE Grant P50CA097186, and, in part, by the Intramural Research Program of the National Institutes of Health, National Cancer Institute, Center for Cancer Research.

REFERENCES

Arican-Goktas HD, Ittiprasert W, Bridger JM, Knight M (2014). Differential spatial repositioning of activated genes in Biomphalaria glabrata snails infected with Schistosoma mansoni. PLoS Negl Trop Dis 8, e3013.

Bok RA, Small EJ (2002). Bloodborne biomolecular markers in prostate cancer development and progression. Nat Rev Cancer 2, 918–926.

Borden J, Manuelidis L (1988). Movement of the X chromosome in epilepsy. Science 242, 1687–1691.

Boyle S, Gilchrist S, Bridger JM, Mahy NL, Ellis JA, Bickmore WA (2001). The spatial organization of human chromosomes within the nuclei of normal and emerin-mutant cells. Hum Mol Genet 10, 211–219.

Bridger JM, Boyle S, Kill IR, Bickmore WA (2000). Re-modelling of nuclear architecture in quiescent and senescent human fibroblasts. Curr Biol 10, 149–152.

Cooperberg MR, Broering JM, Carroll PR (2010). Time trends and local variation in primary treatment of localized prostate cancer. J Clin Oncol 28, 1117–1123.

Cremer M, Kupper K, Wagler B, Wizelman L, von Hase J, Weiland Y, Kreja L, Diebold J, Speicher MR, Cremer T (2003). Inheritance of gene density-related higher order chromatin arrangements in normal and tumor cell nuclei. J Cell Biol 162, 809–820.

Croft JA, Bridger JM, Boyle S, Perry P, Teague P, Bickmore WA (1999). Differences in the localization and morphology of chromosomes in the human nucleus. J Cell Biol 145, 1119–1131.

De Marzo AM, Marchi VL, Epstein JI, Nelson WG (1999). Proliferative inflammatory atrophy of the prostate: implications for prostatic carcinogenesis. Am J Pathol 155, 1985–1992.

Draisma G, Etzioni R, Tsodikov A, Mariotto A, Wever E, Gulati R, Feuer E, de Koning H (2009). Lead time and overdiagnosis in prostate-specific antigen screening: importance of methods and context. J Natl Cancer Inst 101, 374–383.

Egeblad M, Werb Z (2002). New functions for the matrix metalloproteinases in cancer progression. Nat Rev Cancer 2, 161–174.

Ferrai C, de Castro IJ, Lavitas L, Chotalia M, Pombo A (2010). Gene positioning. Cold Spring Harb Perspect Biol 2, a000588.

Ferte C, Andre F, Soria JC (2010). Molecular circuits of solid tumors: prognostic and predictive tools for bedside use. Nat Rev Clin Oncol 7, 367–380.

Foster HA, Griffin DK, Bridger JM (2012). Interphase chromosome positioning in in vitro porcine cells and ex vivo porcine tissues. BMC Cell Biol 13, 30.

Harewood L, Schutz F, Boyle S, Perry P, Delorenzi M, Bickmore WA, Reymond A (2010). The effect of translocation-induced nuclear reorganization on gene expression. Genome Res 20, 554–564.

Hiratani I, Ryba T, Itoh M, Yokochi T, Schwaiger M, Chang CW, Lyou Y, Townes TM, Schubeler D, Gilbert DM (2008). Global reorganization of replication domains during embryonic stem cell differentiation. PLoS Biol 6, e245.

Johnson TR, Koul S, Kumar B, Khandrika L, Venezia S, Maroni PD, Meacham RB, Koul HK (2010). Loss of PDEF, a prostate-derived Ets factor is associated with aggressive phenotype of prostate cancer: regulation of MMP 9 by PDEF. Mol Cancer 9, 148.

Kind J, Pagie L, Ortabozkoyun H, Boyle S, de Vries SS, Janssen H, Amendola M, Nolen LD, Bickmore WA, van Steensel B (2013). Single-cell dynamics of genome-nuclear lamina interactions. Cell 153, 178–192.

Knight M, Ittiprasert W, Odoemelam EC, Adema CM, Miller A, Raghavan N, Bridger JM (2011). Non-random organization of the Biomphalaria glabrata genome in interphase Bge cells and the spatial repositioning of activated genes in cells co-cultured with Schistosoma mansoni. Int J Parasitol 41, 61–70.

Kosak ST, Skok JA, Medina KL, Riblet R, Le Beau MM, Fisher AG, Singh H (2002). Subnuclear compartmentalization of immunoglobulin loci during lymphocyte development. Science 296, 158–162.

Kozubek S, Lukasova E, Jirsova P, Koutna I, Kozubek M, Ganova A, Bartova E, Falk M, Pasekova R (2002). 3D Structure of the human genome: order in randomness. Chromosoma 111, 321–331.

Lawrence MG, Lai J, Clements JA (2010). Kallikreins on steroids: structure, function, and hormonal regulation of prostate-specific antigen and the extended kallikrein locus. Endocr Rev 31, 407–446.

Li C, Shi Z, Zhang L, Huang Y, Liu A, Jin Y, Yu Y, Bai J, Chen D, Gendron C, *et al.* (2010). Dynamic changes of territories 17 and 18 during EBV-infection of human lymphocytes. Mol Biol Rep 37, 2347–2354.

Lin C, Yang L, Tanasa B, Hutt K, Ju BG, Ohgi K, Zhang J, Rose DW, Fu XD, Glass CK, Rosenfeld MG (2009). Nuclear receptor-induced chromosomal proximity and DNA breaks underlie specific translocations in cancer. Cell 139, 1069–1083.

Mani RS, Tomlins SA, Callahan K, Ghosh A, Nyati MK, Varambally S, Palanisamy N, Chinnaiyan AM (2009). Induced chromosomal proximity and gene fusions in prostate cancer. Science 326, 1230.

Meaburn KJ (2010). Fluorescence in situ hybridization on 3D cultures of tumor cells. Methods Mol Biol 659, 323–336.

Meaburn K, Burman B, Misteli T (2016). Spatial genome organization and disease. In: The Functional Nucleus, ed. G Dellaire and D Basett-Jones, New York: Springer (*in press*).

Meaburn KJ, Cabuy E, Bonne G, Levy N, Morris GE, Novelli G, Kill IR, Bridger JM (2007). Primary laminopathy fibroblasts display altered genome organization and apoptosis. Aging Cell 6, 139–153.

Meaburn KJ, Gudla PR, Khan S, Lockett SJ, Misteli T (2009). Disease-specific gene repositioning in breast cancer. J Cell Biol 187, 801–812.

Meaburn KJ, Misteli T (2008). Locus-specific and activity-independent gene repositioning during early tumorigenesis. J Cell Biol 180, 39–50.

Mehta IS, Eskiw CH, Arican HD, Kill IR, Bridger JM (2011). Farnesyltransferase inhibitor treatment restores chromosome territory positions and active chromosome dynamics in Hutchinson-Gilford progeria syndrome cells. Genome Biol 12, R74.

Mewborn SK, Puckelwartz MJ, Abuisneineh F, Fahrenbach JP, Zhang Y, MacLeod H, Dellefave L, Pytel P, Selig S, Labno CM, *et al.* (2010). Altered chromosomal positioning, compaction, and gene expression with a lamin A/C gene mutation. PLoS One 5, e14342.

Mikelsaar R, Paves H, Org K, Mikelsaar AV (2014). Chromosome variant 1qh- and its influence on the 3D organization of chromosome 1 heterochromatin in interphase nucleus of patients with endometriosis. J Genet 93, 219–223.
Morey C, Kress C, Bickmore WA (2009). Lack of bystander activation shows that localization exterior to chromosome territories is not sufficient to up-regulate gene expression. Genome Res 19, 1184–1194.
Murata S, Nakazawa T, Ohno N, Terada N, Iwashina M, Mochizuki K, Kondo T, Nakamura N, Yamane T, Iwasa S, *et al.* (2007). Conservation and alteration of chromosome territory arrangements in thyroid carcinoma cell nuclei. Thyroid 17, 489–496.
Parada L, McQueen P, Misteli T (2004). Tissue-specific spatial organization of genomes. Genome Biol 7, R44.
Parada LA, McQueen PG, Munson PJ, Misteli T (2002). Conservation of relative chromosome positioning in normal and cancer cells. Curr Biol 12, 1692–1697.
Paulo P, Barros-Silva JD, Ribeiro FR, Ramalho-Carvalho J, Jeronimo C, Henrique R, Lind GE, Skotheim RI, Lothe RA, Teixeira MR (2012). FLI1 is a novel ETS transcription factor involved in gene fusions in prostate cancer. Genes Chromosomes Cancer 51, 240–249.
Paz N, Felipe-Blanco I, Royo F, Zabala A, Guerra-Merino I, Garcia-Orad A, Zugaza JL, Parada LA (2015). Expression of the DYRK1A gene correlates with its 3D positioning in the interphase nucleus of Down syndrome cells. Chromosome Res 23, 285–298.
Peric-Hupkes D, Meuleman W, Pagie L, Bruggeman SW, Solovei I, Brugman W, Graf S, Flicek P, Kerkhoven RM, van Lohuizen M, *et al.* (2010). Molecular maps of the reorganization of genome-nuclear lamina interactions during differentiation. Mol Cell 38, 603–613.
Rafique S, Thomas JS, Sproul D, Bickmore WA (2015). Estrogen-induced chromatin decondensation and nuclear re-organization linked to regional epigenetic regulation in breast cancer. Genome Biol 16, 145.
Shachar S, Voss TC, Pegoraro G, Sciascia N, Misteli T (2015). Identification of gene positioning factors using high-throughput imaging mapping. Cell 162, 911–923.
Shen MM, Abate-Shen C (2010). Molecular genetics of prostate cancer: new prospects for old challenges. Genes Dev 24, 1967–2000.
Siegel RL, Miller KD, Jemal A (2015). Cancer statistics, 2015. CA Cancer J Clin 65, 5–29.
Takizawa T, Gudla PR, Guo L, Lockett S, Misteli T (2008a). Allele-specific nuclear positioning of the monoallelically expressed astrocyte marker GFAP. Genes Dev 22, 489–498.
Takizawa T, Meaburn KJ, Misteli T (2008b). The meaning of gene positioning. Cell 135, 9–13.
Therizols P, Illingworth RS, Courilleau C, Boyle S, Wood AJ, Bickmore WA (2014). Chromatin decondensation is sufficient to alter nuclear organization in embryonic stem cells. Science 346, 1238–1242.
Timme S, Schmitt E, Stein S, Schwarz-Finsterle J, Wagner J, Walch A, Werner M, Hausmann M, Wiech T (2011). Nuclear position and shape deformation of chromosome 8 territories in pancreatic ductal adenocarcinoma. Anal Cell Pathol (Amst) 34, 21–33.
Tomlins SA, Rhodes DR, Perner S, Dhanasekaran SM, Mehra R, Sun XW, Varambally S, Cao X, Tchinda J, Kuefer R, *et al.* (2005). Recurrent fusion of TMPRSS2 and ETS transcription factor genes in prostate cancer. Science 310, 644–648.
Towbin BD, Gonzalez-Aguilera C, Sack R, Gaidatzis D, Kalck V, Meister P, Askjaer P, Gasser SM (2012). Step-wise methylation of histone H3K9 positions heterochromatin at the nuclear periphery. Cell 150, 934–947.
Veltri RW, Christudass CS (2014). Nuclear morphometry, epigenetic changes, and clinical relevance in prostate cancer. Adv Exp Med Biol 773, 77–99.
Wiech T, Stein S, Lachenmaier V, Schmitt E, Schwarz-Finsterle J, Wiech E, Hildenbrand G, Werner M, Hausmann M (2009). Spatial allelic imbalance of BCL2 genes and chromosome 18 territories in nonneoplastic and neoplastic cervical squamous epithelium. Eur Biophys J 38, 793–806.
Wiech T, Timme S, Riede F, Stein S, Schuricke M, Cremer C, Werner M, Hausmann M, Walch A (2005). Human archival tissues provide a valuable source for the analysis of spatial genome organization. Histochem Cell Biol 123, 229–238.
Williams RR, Azuara V, Perry P, Sauer S, Dvorkina M, Jorgensen H, Roix J, McQueen P, Misteli T, Merkenschlager M, Fisher AG (2006). Neural induction promotes large-scale chromatin reorganisation of the Mash1 locus. J Cell Sci 119, 132–140.
Zeitz MJ, Ay F, Heidmann JD, Lerner PL, Noble WS, Steelman BN, Hoffman AR (2013). Genomic interaction profiles in breast cancer reveal altered chromatin architecture. PLoS One 8, e73974.

Tissue-of-origin-specific gene repositioning in breast and prostate cancer

Karen J. Meaburn, Olufunmilayo Agunloye, Michelle Devine, Marc Leshner, Gregory W. Roloff, Lawrence D. True & Tom Misteli

Histochemistry and Cell Biology

ISSN 0948-6143
Volume 145
Number 4

Histochem Cell Biol (2016) 145:433-446
DOI 10.1007/s00418-015-1401-8

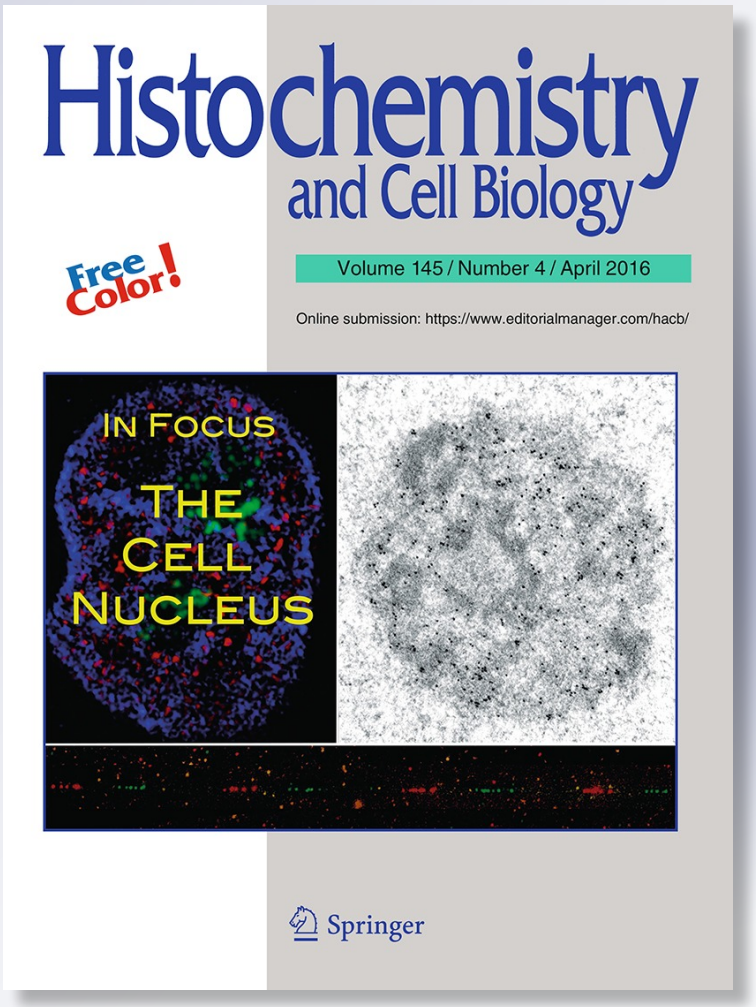

Springer

Histochem Cell Biol (2016) 145:433–446
DOI 10.1007/s00418-015-1401-8

ORIGINAL PAPER

Tissue-of-origin-specific gene repositioning in breast and prostate cancer

Karen J. Meaburn[1] · Olufunmilayo Agunloye[1] · Michelle Devine[1] · Marc Leshner[1] · Gregory W. Roloff[1] · Lawrence D. True[2] · Tom Misteli[1]

Accepted: 23 December 2015 / Published online: 20 January 2016

Abstract Genes have preferential non-random spatial positions within the cell nucleus. The nuclear position of a subset of genes differ between cell types and some genes undergo repositioning events in disease, including cancer. It is currently unclear whether the propensity of a gene to reposition reflects an intrinsic property of the locus or the tissue. Using quantitative FISH analysis of a set of genes which reposition in cancer, we test here the tissue specificity of gene repositioning in normal and malignant breast or prostate tissues. We find tissue-specific organization of the genome in normal breast and prostate with 40 % of genes occupying differential positions between the two tissue types. While we demonstrate limited overlap between gene sets that repositioned in breast and prostate cancer, we identify two genes that undergo disease-related gene repositioning in both cancer types. Our findings indicate that gene repositioning in cancer is tissue-of-origin specific.

Keywords Nuclear architecture · Spatial gene positioning · Breast cancer · Prostate cancer · Tissue specificity

Abbreviations

BAC	Bacterial artificial chromosome
EDT	Euclidean distance transform
FFPE	Formalin-fixed, paraffin embedded
GPBs	Gene positioning biomarkers
HSA	Human chromosome
KS test	Kolmogorov–Smirnov test
MMU	Mouse chromosome
NAT	Normal adjacent to tumor
PND	Pooled normal distribution
RRD	Relative radial distribution
TMA	Tissue microarray

Introduction

The genome is non-randomly organized within the interphase nucleus (Ferrai et al. 2010; Meaburn et al. 2016). There is a general tendency for gene-rich and gene-poor genomic regions, ranging from whole chromosomes to chromatin domains, to be spatially separate from each other (Boutanaev et al. 2005; Boyle et al. 2001; Croft et al. 1999; Guelen et al. 2008; Lieberman-Aiden et al. 2009; Shopland et al. 2006). While this trend is maintained across species and between cell types, the preferred nuclear locations of specific chromosomes and genes can be variable depending on cellular context. Spatial reorganization of the genome occurs, for example, with changes in proliferation status, during differentiation, between cell types and in disease (Ferrai et al. 2010; Meaburn et al. 2016). It is currently unclear how the spatial arrangements of the genome are established and maintained, although epigenetic modifications, chromatin remodeling, gene expression and replication timing have been implicated in the positioning of some genes (Ferrai et al. 2010; Hiratani et al. 2008; Kosak

Electronic supplementary material The online version of this article (doi:10.1007/s00418-015-1401-8) contains supplementary material, which is available to authorized users.

✉ Karen J. Meaburn
meaburnk@mail.nih.gov

✉ Tom Misteli
mistelit@mail.nih.gov

[1] National Cancer Institute, NIH, Bethesda, MD 20892, USA

[2] Department of Pathology, University of Washington, Seattle, WA 98195, USA

et al. 2002; Meaburn et al. 2016; Peric-Hupkes et al. 2010; Therizols et al. 2014; Towbin et al. 2012; Volpi et al. 2000; Williams et al. 2002).

The organization of the genome between terminally differentiated cell types is remarkably similar despite profound differences in function, gene expression profiles and nuclear shape. For instance, most human chromosomes (HSAs) occupy similar radial positions in lymphoblast and dermal fibroblast nuclei, with only HSA 8, HSA 20 and HSA 21 in different positions (Boyle et al. 2001; Meaburn et al. 2008). This phenomenon is not limited to humans, as there is also a high level of conservation in chromosomal positioning patterns between porcine lymphoblasts and fibroblasts, where chromosome 17 is the only differentially positioned chromosome (Foster et al. 2012). In mice, three of six chromosomes analyzed position similarly between lymphoblasts and fibroblasts (Mayer et al. 2005). Comparisons of positioning patterns of chromosomes between other cell types are less extensive; however, there is conservation in positioning patterns for at least some chromosomes. The positioning of HSA 18 and HSA 19 is broadly maintained in a wide range of cell types, including fibroblasts, keratinocytes, lymphocytes and epithelial cells from multiple tissues (Boyle et al. 2001; Cremer et al. 2003; Murata et al. 2007). Moreover, porcine chromosome 17, 13, 5 and X are similarly positioned between kidney, lung and brain tissue (Foster et al. 2012) and mouse chromosome (MMU) 14 is similarly positioned in lung and kidney cells (Parada et al. 2004). However, tissue-specific positioning of specific chromosomes does also occur. All six mouse chromosomes analyzed in freshly isolated small and large lung cells, liver, kidney, lymphocytes and myeloblasts cells are in differential positions in at least three tissue types (Parada et al. 2004). For example, MMU 12 and MMU 15 are in distinct positions in lung and kidney cells, yet are in similar positions in lymphocytes and myeloblasts (Parada et al. 2004). Moreover, MMU 5 is the only of several analyzed chromosome in a different spatial position between lymphocytes and myeloblasts, whereas MMU 1, MMU 5, MMU 6 and MMU 12 are differentially positioned between liver and myeloblasts (Parada et al. 2004). These observations point to partial conservation of positioning patterns among tissue types.

Similar, yet distinct, spatial arrangement of the genome between differentiated cell types is also consistent with genome-wide analyses (Battulin et al. 2015; Peric-Hupkes et al. 2010). Approximately 80 % of genomic regions that associate with the nuclear lamina protein lamin B1, used as a marker of the nuclear periphery, in *in vitro* differentiated mouse astrocytes also preferentially associate with the nuclear lamina in embryonic fibroblasts (Peric-Hupkes et al. 2010). Moreover, despite the highly compact and haploid nature of DNA in sperm, the genome-wide spatial organization of DNA is similar in mouse sperm and fibroblast nuclei when analyzed by Hi-C genome-wide crosslinking methods (Battulin et al. 2015). The organization is, however, not fully identical. For example, there is a higher frequency of long-range interactions in sperm compared to fibroblasts (Battulin et al. 2015). Additionally, in other cell types, some gene loci have tissue-specific positions. For example, human *CFTR* is more peripherally positioned in lymphocytes and embryonic kidney cells compared to nasal epithelial cells, and *CORTBP2* is more peripherally positioned in embryonic kidney cells compared to lymphocytes (Zink et al. 2004). Furthermore, the spatial position of a gene with respect to the chromosome it resides on may also vary between cell types. Some gene-rich clusters of functionally related genes, such as the epidermal differentiation complex or the major histocompatibility complex, loop out from the bulk of their chromosome territory more frequently in cell types where they are highly expressed (Volpi et al. 2000; Williams et al. 2002). Other genes, such as *PAX6*, *WT1*, *DMD*, *FLNA* and *BCL2*, however, remain within the chromosome territory in different cell types, independent of transcription status (Kurz et al. 1996; Mahy et al. 2002; Scheuermann et al. 2004).

Spatial reorganization of the genome is also associated with disease (Borden and Manuelidis 1988; Meaburn et al. 2007; Mehta et al. 2011; Mewborn et al. 2010; Mikelsaar et al. 2014; Paz et al. 2015), including cancer (Cremer et al. 2003; Leshner et al. 2015; Meaburn et al. 2009; Meaburn and Misteli 2008; Murata et al. 2007; Wiech et al. 2009; Zeitz et al. 2013). Much like between tissue types, changes in genome organization are not global and only subsets of gene loci alter their nuclear location (Borden and Manuelidis 1988; Leshner et al. 2015; Meaburn et al. 2007, 2009; Meaburn and Misteli 2008; Zeitz et al. 2013). We have previously identified two sets of genes that reposition in malignant breast or prostate tissue, respectively, compared to their normal counterparts (Leshner et al. 2015; Meaburn et al. 2009). These repositioning events are specific to the malignant state and do not commonly occur in non-malignant disease, and they are not accounted for by inter-individual variations nor do they correlate with numerical genome abnormalities, gene ontology, the local gene density surrounding the loci or changes in gene expression (Leshner et al 2015; Meaburn et al. 2009; Meaburn and Misteli 2008). In line with partial repositioning of genomes in cancer, the majority of genes do not change radial positioning in neither breast nor prostate cancer, suggesting gene-specific repositioning events (Leshner et al. 2015; Meaburn et al. 2009; Meaburn and Misteli 2008).

A key question that emerges from these observations is whether the same genes reposition in multiple cancers or whether the set of repositioned genes is tissue specific. Previous analysis has found repositioning of HSA 18 and HSA 19 in many types of cancer, including Hodgkin's lymphoma,

melanoma, colon, cervical and thyroid carcinomas, suggesting a lack of tissue-of-origin specificity (Cremer et al. 2003; Murata et al. 2007; Wiech et al. 2009). However, in contrast to the other types of cancers studied, HSA 18 is more peripherally located in a cervical squamous carcinoma tissue (Wiech et al. 2009). Moreover, *BCL2* is relocated to a more peripheral nuclear position in a BCL2 expressing cervical squamous carcinoma (Wiech et al. 2009), but its position is unaffected in breast cancer (Meaburn et al. 2009), prostate cancer (Leshner et al. 2015) and in a BCL2 negative cervical squamous carcinoma (Wiech et al. 2009), pointing to tissue-specific differences in repositioning behavior.

To more systematically determine whether cancer-associated gene repositioning is gene- or tissue-of-origin specific, we have here compared the nuclear positions of a set of eleven genes, which we have previously identified to robustly reposition in either breast or prostate cancers (Leshner et al. 2015; Meaburn et al. 2009). We find that the repositioned genes are largely distinct in each tissue type with only two genes repositioning in both types of cancer. These results point to tissue-of-origin specificity for gene repositioning in cancer.

Materials and methods

Tissue FISH

To generate fluorescence in situ hybridization (FISH) probes, bacterial artificial chromosome (BAC) clones (BACPAC resource center) (Suppl. Table S1) were label with either biotin- or digoxigenin-conjugated dUTPs (Roche) by nick translation, as previously described (Meaburn 2010; Meaburn et al. 2009). FISH was performed on 4- to 5-µm-thick FFPE de-identified human tissue sections (Suppl. Table S2), as previously described in Meaburn et al. (2009) and using the following modifications: the 60 °C slide baking step was not performed, tissue sections were incubated in 0.25 mg/ml proteinase K (Sigma-Aldrich) for 15–20 min, except for single tissue slides from Biomax Inc, where 0.5 mg/ml proteinase K was typically required. Tissue sections and tissue microarrays (TMAs) were purchased from US Biomax Inc, Imgenex Corporation, Folio Bioscience and Biochain Institute or were acquired from the University of Washington under the guidelines and approval of the Institutional Review Board of the University of Washington (#00-3449) (Suppl. Table S2). The prostate tissues from the University of Washington were reviewed by a genitourinary pathologist (L.D.T.). The panel of tissues included twelve breast cancers, six benign breast tissues (hyperplasia and fibroadenoma), six normal breast tissues, 20 prostate cancers, four hyperplasic prostate tissues and 24 histologically benign (normal) prostate specimens (Suppl. Table S2).

Image acquisition and FISH analysis

Image accusation was performed as previously described (Leshner et al. 2015; Meaburn et al. 2009). Briefly, all imaging was performed on a wide-field IX70 (Olympus) Deltavision (Applied Precision) microscope system, equipped with a 60 × 1.42 N oil objective lens (Olympus). An auxiliary magnification of 1.5 and a *z*-step size of 0.5 µm were used to acquire image stacks. Most tissue sections or TMA tissue cores contained predominantly a single morphology (e.g., malignant tissue only), and regions of epithelial nuclei were randomly imaged over the slide or tissue core. The prostate tissues from the University of Washington, however, often contained multiple morphologies on the same slide. In these cases, malignant and non-malignant glands were imaged and analyzed separately, after examination of the tissue at low resolution (10× lens; Olympus) and consultation of hematoxylin and eosin-stained slides, which had been annotated by a pathologist (L.D.T.). Images of epithelial nuclei were then randomly acquired within the predetermined regions of benign or malignant tissue. Before image analysis, 2D maximum intensity projections were generated from deconvolved image stacks, using SoftWoRx (Applied Precision) as previously described (Meaburn et al. 2009).

Analysis to map the spatial position of FISH signals was performed as previously described (Leshner et al. 2015; Meaburn et al. 2009). Briefly, 89–169 interphase epithelial nuclei, which had been manually segmented in Photoshop 7.0 (Adobe) based on DAPI staining, were run though custom image analysis algorithms (Meaburn et al. 2009), which were executed in MATLAB (The Mathsworks Inc.) and utilized DIPImage and PRTools toolboxes (Deft University). To determine the radial position of each FISH signal, the distance to the nearest nuclear boundary was determined for each pixel in a cell nucleus using Euclidean distance transform (EDT) and the geometric gravity center of each FISH signal was determined automatically. Next, the EDT value for a FISH signal was normalized to the maximal nuclear EDT for the corresponding nucleus to normalize for variations in nuclear size and shape. To generate a relative radial distribution (RRD) for a gene in a given specimen, the normalized FISH signal EDT for every allele from that tissue was combined and a cumulative frequency distribution was produced. For each gene a PND was also created. To this end, the normalized EDTs from all allele in each normal tissue, for a given gene, were combined. Table 1 details the number of normal tissues analyzed for each gene, and Suppl. Table S1 details the number of nuclei used to produce each PND. Finally, to statistically compare a gene's positioning patterns between individuals and between histological states, cumulative RRDs between tissues were cross-compared using the

nonparametric two-sample 1D Kolmogorov–Smirnov (KS) test, with $P < 0.01$ considered significant.

Some previously reported data were included in the current analysis for comparison of the positioning pattern of a gene between normal breast and prostate tissues. The RRDs for *AKT1, CSF1R, ERBB2, FOSL2, HES5, HSP90AA1, MYC, TGFB3, BCL2, CCND1, MMP1* and *VEGFA* in normal breast tissues were reported in Meaburn et al. (2009) and the RRDs for *FLI1, MMP9, MMP9, BCL2, CCND1, MMP1* and *VEGF* in prostate tissue are as reported in Leshner et al. (2015).

Results

We have previously identified a set of eight genes (*AKT1*, *CSF1R*, *ERBB2*, *FOL2*, *HES5*, *HSP90AA1*, *MYC* and *TGFB3*) that reposition in breast cancer (Meaburn et al. 2009) and a set of three genes (*FLI1*, *MMP2* and *MMP9*) that reposition in prostate cancer (Leshner et al. 2015). We refer to these gene sets as breast GBPs (gene positioning biomarkers) and prostate GPBs, respectively. To determine whether the observed repositioning events between normal and cancerous tissues are tissue specific, we sought to cross-compare prostate GPBs and breast GPBs in their heterologous tissues. To this end, we performed FISH to visualize the GPBs (Suppl. Table S1) in 4- to 5-μm-thick formalin-fixed, paraffin-embedded (FFPE) human tissues (Suppl. Table S2). We positioned prostate GPBs in benign (normal, hyperplasia, fibroadenoma) and malignant breast tissues and, conversely, we positioned breast GPBs in normal, normal adjacent to tumor (NAT) and adenocarcinoma prostate tissues (Suppl. Table S2). Typically 100–150 randomly selected epithelial nuclei were analyzed per tissue for each gene as previously described (Leshner et al. 2015; Meaburn et al. 2009). The radial position of each allele, normalized to nuclear size, was determined from projections of image stacks using EDT, as previously described (see *Materials and Methods* for details; Leshner et al. 2015; Meaburn et al. 2009). The normalized positions for each allele in a tissue were then combined to generate a cumulative RRD for each gene. Statistical differences between samples were assessed using the two-sample 1-D KS test as described (see "Materials and methods" ; Leshner et al.

Fig. 1 Tissue-specific spatial organization of the genome. **a** FISH was used to detect gene loci in FFPE tissue sections. *FLI1* (*green*) in a normal breast tissue and *HES5* (*green*) in a normal prostate tissue. *Blue*, DAPI nuclear counterstain. *Scale bar* 5 μm. Projected image stacks are shown. **b**, **c** Heat maps representing the pairwise statistical comparisons of the positioning patterns of the indicated genes between normal breast tissues (B-N1–B-N17; see Suppl. Tables S2, S3) and normal prostate tissues (P-N1–P-N31; see Suppl. Tables S2, S3), using the two-sample 1D KS test. **b** Genes that reposition in either breast or prostate cancer (or both). **c** Genes that do not significantly reposition in either breast or prostate cancer. For these comparisons, the RRDs for *AKT1, CSF1R, ERBB2, FOSL2, HES5, HSP90AA1, MYC, TGFB3, BCL2, CCND1, MMP1* and *VEGFA* in normal breast tissues are from Meaburn et al. (2009) and the RRDs for *FLI1, MMP9, MMP2, BCL2, CCND1, MMP1* and *VEGF* in prostate tissue are from Leshner et al. (2015)

Table 1 Comparison of gene positioning patterns between normal breast and normal prostate tissues

Gene	% (and number) of SD cross comparison between individual normal breast and prostate tissues	Tissue-specific positioning?[a]
AKT1	39.3 % (11/28)[b]	No
CSF1R	64.9 % (50/77)[b]	Yes
ERBB2	30.6 % (11/36)[b]	No
FLI1	20.8 % (10/48)[c]	No
FOSL2	46.0 % (29/63)[b]	No
HES5	14.3 % (6/42)[b]	No
HSP90AA1	61.2 % (26/42)[b]	Yes
MMP2	28.1 % (9/32)[c]	No
MMP9	86.7 % (52/60)[c]	Yes
MYC	97.2 % (35/36)[b]	Yes
TGFB3	25.0 % (12/48)[b]	No
BCL2	100.0 % (12/12)[b,c]	Yes
CCND1	37.5 % (6/16)[b,c]	No
MMP1	66.7 % (4/6)[b,c]	Yes
VEGF	9.6 % (5/52)[b,c]	No

SD significantly different, based on a two-sample 1D KS test, $P < 0.01$

[a] Between normal breast and prostate tissue. [b, c] These comparisons utilize positioning RRDs (position distributions) previously generated, specifically: [b] RRDs from breast tissues were previously published in Meaburn et al. (2009) and [c] prostate tissue RRDs are from Leshner et al. (2015)

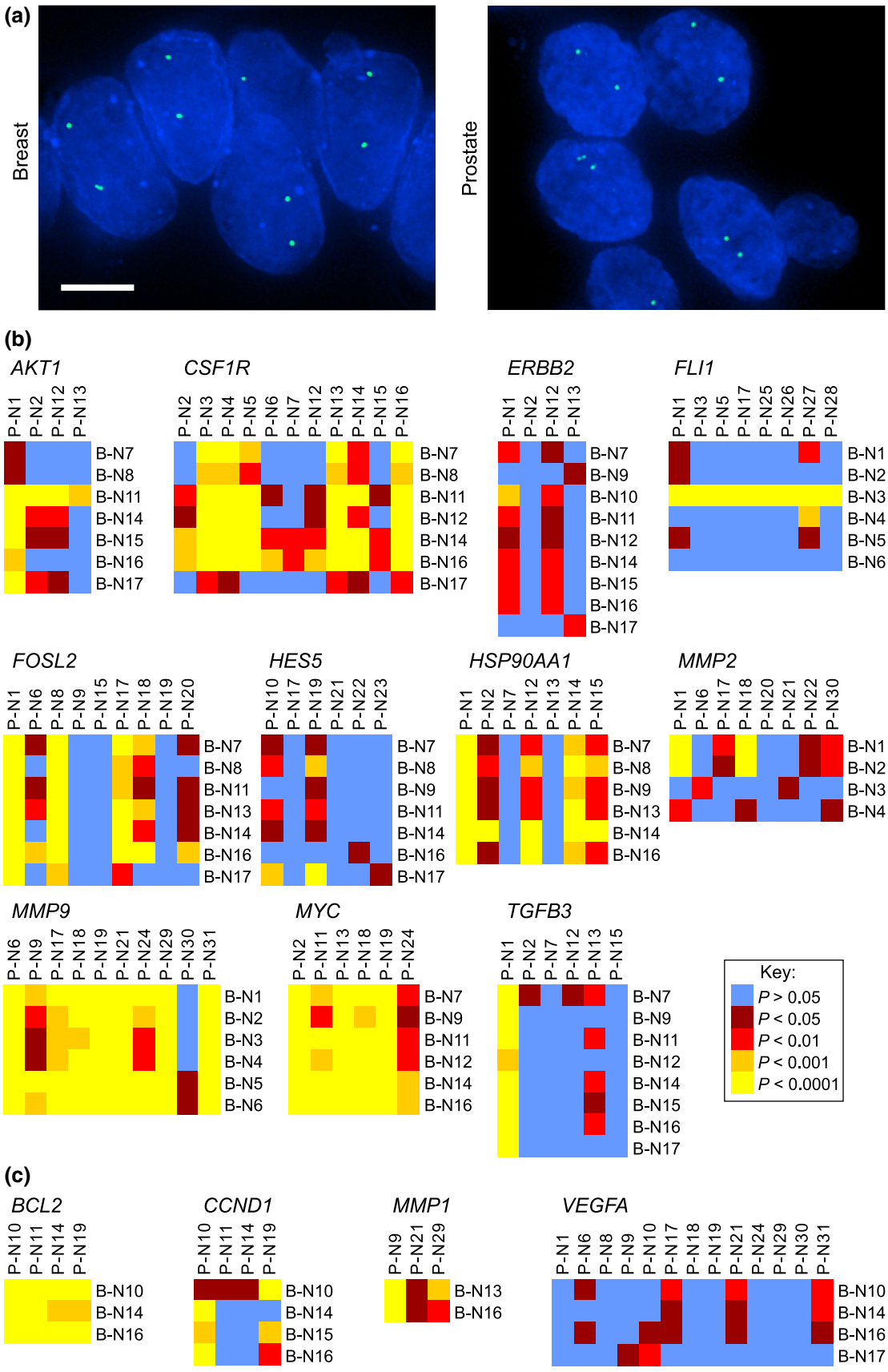

2015; Meaburn et al. 2009), and $P < 0.01$ was considered significant.

Tissue-specific spatial organization in normal tissues

To first determine tissue specificity of gene positioning in normal tissues, we compared the positioning patterns of the full set of eleven genes between multiple normal breast and prostate tissues (Table 1, Suppl. Tables S2-S3; Fig. 1a, b, Suppl. Fig. S1a). To increase the number of genes compared between the tissue types, for this analysis we included three additional genes that do not reposition significantly in breast or prostate cancer (*BCL2*, *CCND1* and *MMP1*) and *VEGF,* which repositioned in approximately half of both prostate and breast cancers (Table 1, Suppl. Table S4; Fig. 1c, Suppl. Fig. S1b). Many genes exhibited significantly overlapping distributions between normal breast and prostate tissues. For six genes (40 %; *VEGFA, HES5, FLI1, TGFB3, MMP2* and *ERBB2*) less than a third of the pairwise cross comparisons of RRDs between normal breast and prostate tissue were significantly different and for an additional three genes (20 %; *CCND1, AKT1* and *FOSL2*) 37.5–46.0 % of the cross comparisons between the tissue types were significant (Table 1; Fig. 1, Suppl. Fig. S1). On the other hand, six of the 15

Fig. 2 Positioning patterns in cancer compared to normal tissue. **a** ▶ *MMP9* (*green*) was detected by FISH in normal and cancerous breast FFPE tissue sections. *Blue*, DAPI nuclear counterstain. *Scale bar*, 5 µm. Projected image stacks are shown. **b** Cumulative RRDs for the indicated genes in cancer (*red*), normal tissues (*black*) and the pooled normal distribution (*blue*). The tissue type is specified in each graph. *RRP* relative radial position

Table 2 Cross comparisons between individual tissues

Gene	Tissue	Number of tissues		% (and number) of SD cross comparison between	
		Normal	Cancer	Individual normal tissues	Individual normal and cancer tissues
FLI1	Breast	6	10	33.3 % (5/15)	66.7 % (40/60)
MMP9	Breast	6	12	6.7 % (1/15)	66.7 % (48/72)
MMP2	Breast	4	6	50.0 % (3/6)	37.5 % (9/24)
AKT1	Prostate	4	6	16.7 % (1/6)	37.5 % (9/24)
CSF1R	Prostate	11	9	41.8 % (23/55)	38.4% (38/99)
ERBB2	Prostate	4	5	33.3 % (2/6)	35.0 % (7/20)
FOSL2	Prostate	9	7	38.9 % (14/36)	47.6 % (30/63)
HES5	Prostate	6	6	20.0 % (3/15)	27.8 % (10/36)
HSP90AA1	Prostate	7	4	57.1 % (12/21)	46.4 % (13/28)
MYC	Prostate	6	5	6.7 % (1/15)	3.3 % (1/30)
TGFB3	Prostate	6	4	33.3 % (5/15)	25.0 % (6/24)

SD significantly different, based on a two-sample 1D KS test, $P < 0.01$

Table 3 Comparison of individual tissues to a pooled normal distribution

Gene	Tissue	% (and number) of SD cross comparison between	
		Individual normal tissues and pooled normal	Individual cancer tissues and pooled normal
FLI1	Breast	16.7 % (1/6)	100.0 % (10/10)
MMP9	Breast	0.0 % (0/6)	83.3 % (10/12)
MMP2	Breast	25.0 % (1/4)	0.0 % (0/6)
AKT1	Prostate	0.0 % (0/4)	50.0 % (3/6)
CSF1R	Prostate	27.3 % (3/11)	44.4 % (4/9)
ERBB2	Prostate	0.0 % (0/4)	40.0 % (2/5)
FOSL2	Prostate	33.3 % (3/9)	42.9 % (3/7)
HES5	Prostate	0.0 % (0/6)	33.3 % (2/6)
HSP90AA1	Prostate	42.9 % (3/7)	50.0 % (2/4)
MYC	Prostate	0.0 % (0/6)	0.0 % (0/5)
TGFB3	Prostate	16.7 % (1/6)	25.0 % (1/4)

SD significantly different, based on a two-sample 1D KS test, $P < 0.01$

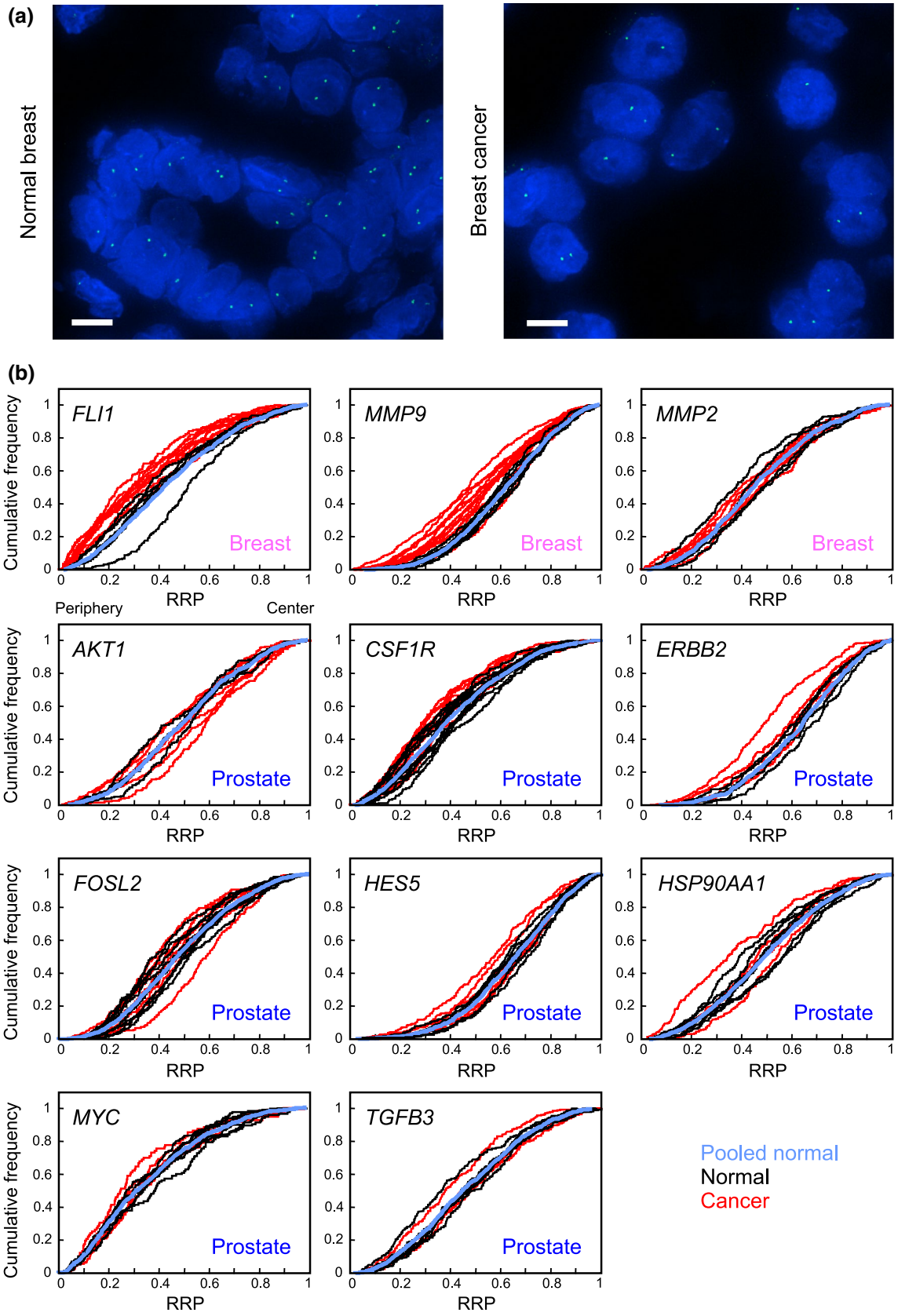

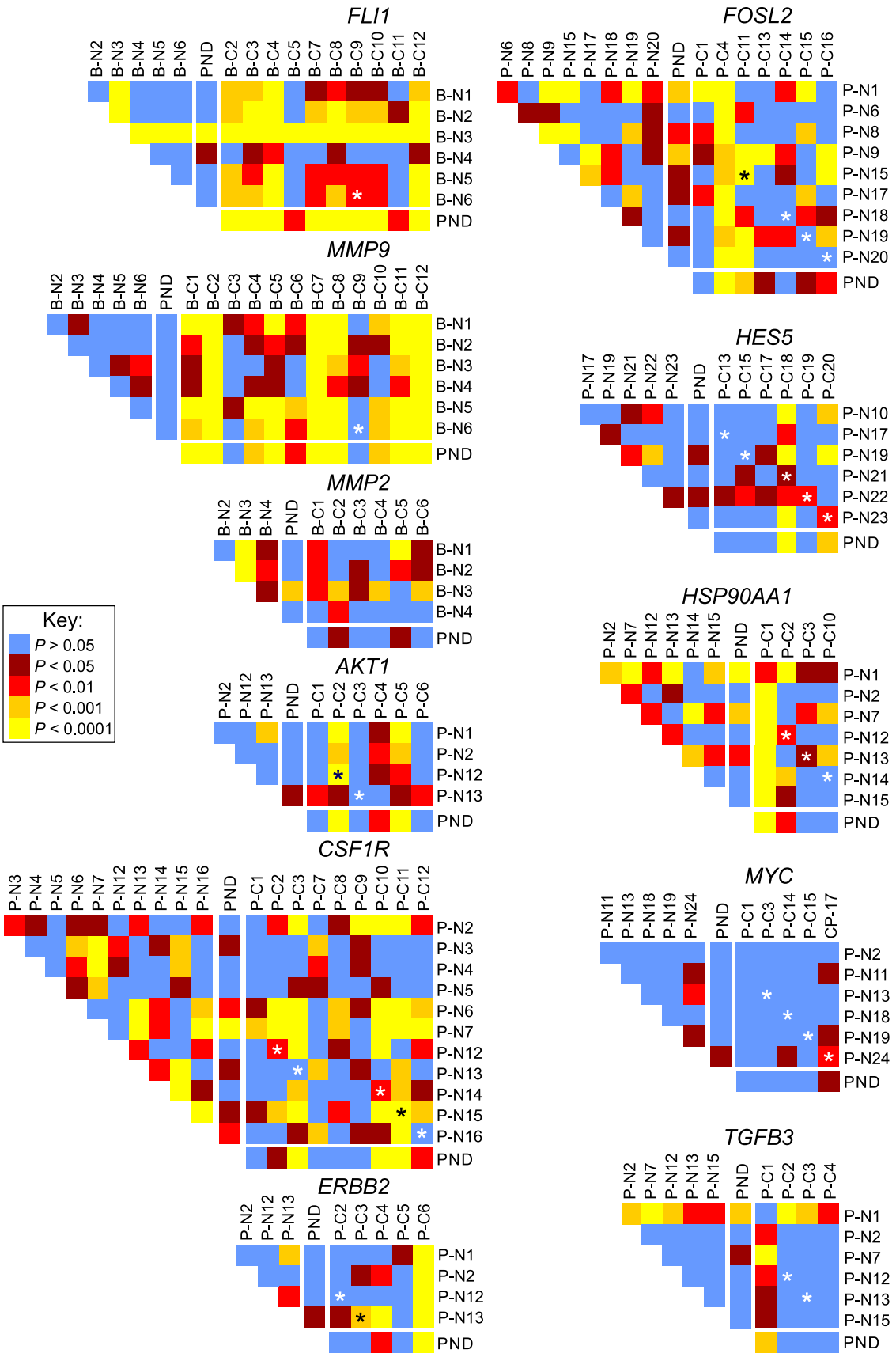

◀**Fig. 3** Statistical cross comparisons of gene positioning in cancer tissues. Heat maps representing the pairwise statistical comparisons of positioning patterns of indicated genes between tissues, using the two-sample 1D KS test. B-N1–B-N6, normal breast tissues (see Suppl. Table S2); B-C1–B-C12, cancerous breast tissues; P-N1–P-N24, normal prostate tissues; P-C1–P-C20, cancerous prostate tissues; *PND* pooled normal distribution. *Black* or *white asterisks* indicate a cross comparison between a normal and cancer specimen from the same individual

genes (40 %; *HSP90AA1, CSF1R, MMP1, MMP9, MYC,* and *BCL2*) displayed distinct tissue-specific positioning, with 61.2–100 % of the pairwise comparisons between normal breast and prostate tissue being significantly different (Table 1; Fig. 1, Suppl. Fig. S1). These observations point to a partial conservation of gene positioning between breast and prostate tissues.

Distinct subsets of genes reposition in breast and prostate cancer

To address if similar repositioning events occur in multiple cancer types or if distinct sets of genes reposition in cancers originating from different tissues, we compared the repositioning behavior of breast GPBs in prostate cancer and *vice versa*. To this end, we first compared the RRDs of the prostate GPBs, *FLI1, MMP9* and *MMP2,* in malignant breast tissues to individual normal breast tissues and to a pooled normal distribution (PND; Tables 2, 3; Figs. 2, 3), which was generated by averaging the RRDs from all normal tissues, of a given tissue-type, analyzed into a single distribution for each gene as previously described (Leshner et al. 2015; Meaburn et al. 2009; *see Materials and methods*). We find that *MMP2* was similarly positioned in breast cancer and normal breast tissue with 37.5 % (9/24) of individual cross comparisons between normal and malignant breast tissues significantly different. In addition, the distribution of *MMP2* was not statistically significantly different from the PND in all six breast cancer tissues (Tables 2, 3; Figs. 2b, 3). Furthermore, the position of *MMP2* was more different among normal tissues than when normal and cancer tissue was compared (Tables 2, 3; Figs. 2b, 3). In contrast to *MMP2*, the prostate GPBs *FLI1* and *MMP9* also repositioned in breast cancer (Tables 2, 3; Figs. 2, 3). For both genes, 66.7 % (40/60 and 48/72, respectively) of cross comparisons between normal breast and breast cancer were significantly different. Moreover, compared to the PND, *FLI1* was repositioned in all ten breast cancers and *MMP9* was repositioned in 83.3 % (10/12) of breast cancers. Importantly, *FLI1* and *MMP9* were both similarly positioned among normal breast tissues, with only 33.3 % (5/15) and 6.7 % (1/15), respectively, of individual cross comparisons between normal breast tissues reaching significance. Finally, compared to their PNDs, *FLI1* was repositioned in a single (1/6) normal tissue and *MMP9* was repositioned in none (0/6) of the normal breast tissues (Tables 2, 3; Figs. 2b, 3).

In an analogous fashion, we next determined how many of the previously identified breast GPBs (*AKT1*, *CSF1R*, *ERBB2*, *FOL2*, *HES5*, *HSP90AA1*, *MYC* and *TGFB3*) reposition in prostate cancer. We find that none of these breast GPBs robustly reposition in prostate cancer tissue (Tables 2, 3; Figs. 2b, 3). The majority of cross comparisons between normal and prostate cancer tissues were not significantly different for any of the genes with between 3.3–47.6 % cross comparisons being significantly different. For most genes, the number of significantly different cross comparisons between normal and malignant prostate tissues was similar or less than the proportion (16.7–57.1 %) of cross comparisons between normal tissues that were significantly different, suggesting that the repositioning was not cancer specific but rather related to the variability in positioning patterns between individuals (Table 2; Figs. 2b, 3). Comparing the position of genes in prostate cancer specimens to their PND also identified only a limited amount of repositioning of these genes in prostate cancer (Table 3; Figs. 2b, 3). *MYC, TGFB3* and *HES5* repositioned in 0–33.3 % prostate adenocarcinomas compared to their PNDs and *ERBB2, FOL2, CSF1R*, *AKT1* and *TGFB3* in 40.0–50.0 % of cancer tissues compared to their PND (Table 3; Fig. 3).

The radial positions of genes in breast tissues are highly conserved between individuals (Figs. 2b, 3; Meaburn et al. 2009). In contrast, we have previously identified several genes that occupy more variable positions between individuals in prostate tissue (Leshner et al. 2015). It is unclear whether this is a feature of the individual loci or reflects differences in the degree of overall positional conservation between breast and prostate tissue. In keeping with their positioning patterns in breast tissue, for five of the breast GPBs there was little variability in the positioning pattern of normal prostate tissues between individuals, with 16.7–33.3 % of individual cross comparisons among normal prostate tissues being significantly different (Table 2; Figs. 2b, 3). Moreover, for four of these genes, none of the normal tissues were significantly different to the PND, and for *TGFB3* only a single normal tissue (16.7 %; 1/6 tissues) was significantly different to the PND (Table 3; Figs. 2b, 3). Conversely, in contrast to their positioning profiles in breast tissue, the positions of three genes (*FOL2*, *CSF1R* and *HSP90AA1*) were more variable between individuals, with 38.9–57.4 % of individual cross comparisons reaching significance, and 27.3–42.9 % of normal tissues significantly different to the PND (Tables 2, 3; Figs. 2b, 3). These data suggest that differences in the extent of inter-individual variations of gene positioning patterns are tissue specific rather than gene specific.

Table 4 Comparison of gene positioning in benign tissues

Gene	Tissue	% (and number) of SD cross comparison between		
		Individual benign tissues	Individual normal and benign tissues	Individual benign tissues and pooled normal
FLI1	Breast	10.0 % (1/10)	26.7 % (8/30)	40.0 % (2/5)
MMP9	Breast	10.0 % (1/10)	20.0 % (6/30)	20.0 % (1/5)
MMP2	Breast	0.0 % (0/10)	45.0 % (9/20)	40.0 % (2/5)
CSF1R	Prostate	0.0 % (0/6)	18.2 % (8/44)	0.0 % (0/4)

SD significantly different, based on a two-sample 1D KS test, $P < 0.01$

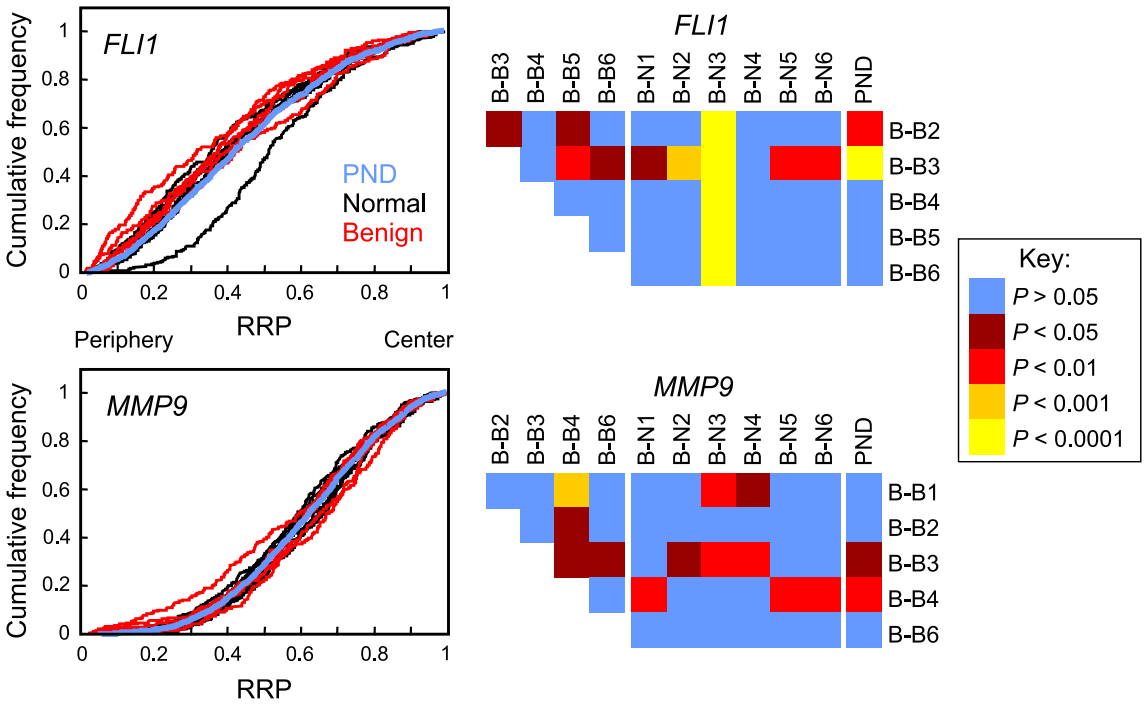

Fig. 4 Gene positioning in non-malignant disease resembles normal tissue. Positions of indicated genes were compared between benign breast disease (hyperplasia: B-B1–B-B3; fibroadenoma: B-B4–B-B6; see Suppl. Table S2) and normal breast tissue (B-N1–B-N6). *Left-hand panel* cumulative RRDs for the indicated genes in benign (*red*), normal tissues (*black*) and the pooled normal distribution (PND; *blue*). *Right-hand panel* pairwise statistical comparisons of RRDs between benign and normal tissues and among benign tissues, using the two-sample 1D KS test. *RRP* relative radial position

We conclude that only two of the eleven marker genes (18.2 %; *MMP9* and *FLI1;* Suppl. Table S4) reposition in both breast and prostate cancer, demonstrating that cancer-related repositioning is not a gene-intrinsic feature but that distinct sets of genes reposition in cancer in a tissue-of-origin-specific manner.

The spatial repositioning of *FLI1* and *MMP9* is specific to cancer

In addition to cancer, we have shown that genes can reposition in breast and prostate tissue with abnormal but non-malignant histology (Leshner et al. 2015; Meaburn et al. 2009). Therefore, to ascertain if the repositioning of the prostate GPBs markers *FLI1* and *MMP9* in breast cancer tissues was specific to cancer or also occurred in abnormal, but non-malignant, breast tissue, we positioned these genes in benign hyperplasia and fibroadenoma breast tissues (Table 4, Suppl. Table S2; Fig. 4). The positions of both *FLI1* and *MMP9* were similar in the non-malignant diseased tissues with only a single cross comparison reaching significance for each gene (1/10; Table 4; Fig. 4). There was also only limited repositioning of *FLI1* and *MMP9* when the non-malignant diseased tissues were compared to normal breast tissues, with 20–26.7 % of cross comparisons to individual normal tissues and 20–40 % (1/5 and 2/5, respectively) of comparisons to the PND being significant (Table 4; Fig. 4). These data suggest that *FLI1* and *MMP9*

Table 5 False-positive and false-negative rates

Gene	Tissue	Normal tissue false positives	Benign tissue false positives	Total false positives	False-negative rate
FLI1	Breast	16.7 % (1/6)	40.0 % (2/5)	27.3 % (3/11)	0.0 % (0/10)
MMP9	Breast	0.0 % (0/6)	20.0 % (1/5)	9.1 % (1/11)	16.7 % (2/12)
MMP2	Breast	25.0 % (1/4)	40.0 % (2/5)	33.3 % (3/9)	100.0 % (6/6)
AKT1	Prostate	0.0 % (0/4)	ND	0.0 % (0/4)	50.0 % (3/6)
CSF1R	Prostate	27.3 % (3/11)	0.0 % (0/4)	20.0 % (3/15)	55.6 % (5/9)
ERBB2	Prostate	0.0 % (0/4)	ND	0.0 % (0/4)	60.0 % (3/5)
FOSL2	Prostate	33.3 % (3/9)	ND	33.3 % (3/9)	57.1 % (4/7)
HES5	Prostate	0.0 % (0/6)	ND	0.0 % (0/6)	66.7 % (4/6)
HSP90AA1	Prostate	42.9 % (3/7)	ND	42.9 % (3/7)	50.0 % (2/4)
MYC	Prostate	0.0 % (0/6)	ND	0.0 % (0/6)	100.0 % (5/5)
TGFB3	Prostate	16.7 % (1/6)	ND	16.7 % (1/6)	75.0 % (3/4)

The percentage (and number) of tissues that give a false-positive or false-negative result. A false positive is scored when a gene has a statistically significantly different RRD in a normal, fibroadenoma or hyperplasic tissue compared to the pooled normal ($P < 0.01$; KS test). A false negative is scored when a gene has a similar RRD in a cancer tissue to that of the pooled normal distribution (KS test, $P > 0.01$)

ND not determined

repositioning is specific to cancer and not a general feature of a diseased phenotype.

Since *MMP2* repositioned in hyperplasic prostate tissue (Leshner et al. 2015), we also positioned it in benign breast disease. *MMP2* was positioned identically among all the non-malignant diseased tissues (Table 4; Suppl. Fig. S2) and showed a low level of repositioning in the non-malignant diseased breast tissues compared to normal tissue with 45.0 % (9/20) of the cross comparisons to individual normal tissues reaching significance and only two (40 %) of non-malignant diseased tissues significantly different to the PND tissues (Table 4; Suppl. Fig. S2), further demonstrating the tissue-specific nature of the *MMP2* repositioning event.

Normal and NAT prostate tissue often contain small areas of mild hyperplasic morphology. Therefore, as a control to ensure the heterogeneity in positioning patterns for some genes in normal prostate tissues was not a reflection of the inclusion of abnormal tissue, we positioned *CSF1R*, which displayed a high level of variability between individuals in hyperplasic prostate tissues. *CSF1R* was positioned identically among all hyperplasic prostate tissues (Table 4; Suppl. Fig. S2). Similarly, the position of *CSF1R* was also similar between hyperplasic and normal tissues with all four hyperplasic prostate tissues distributions statistically similar to the PND and only 18.2 % (8/44) of cross comparisons between hyperplasic and individual normal tissues being significantly different (Table 4; Suppl. Fig. S2). This suggests that the presence of hyperplasic nuclei within a normal tissue RRD is not skewing spatial positioning patterns.

Finally, the high rate of repositioning of *FLI1* and *MMP9* in breast cancer tissue combined with the low level of repositioning in benign tissues make these two genes potential breast GPBs for diagnostic applications. To assess their suitability, we determined false-positive and false-negative rates for these two genes in breast cancer tissues (Table 5). A false positive is defined as spatial repositioning of a gene in a non-malignant tissue compared to the PND, which would incorrectly classify the tissue as cancer. Conversely, a false negative is defined as a cancer tissue where the given gene did not reposition, which would incorrectly classify the tissue as non-malignant. Both *FLI1* and *MMP9* had low false-negative rates in breast cancer of 0 % (0/10) and 16.7 % (2/12), respectively (Table 5), and had false positive rates of 27.3 % (3/11) and 9.1 % (1/11), respectively (Table 5). These results suggest that *FLI1* and *MMP9*, in addition to being prostate GPBs, are also potential candidates as breast cancer biomarkers.

Discussion

We report here a systematic comparison of the spatial positioning patterns of a diverse set of gene loci in both normal and malignant breast and prostate tissues. For many genes, we find conservation of positioning patterns between non-malignant breast and prostate tissues. We identify only two genes that are repositioned in both breast and prostate cancer, compared to their normal counterparts. These observations demonstrate that cancer-related gene repositioning events are tissue-of-origin specific.

Consistent with previous studies in other tissues and cell types (Battulin et al. 2015; Boyle et al. 2001; Cremer et al. 2003; Foster et al. 2012; Mayer et al. 2005; Parada et al. 2004; Peric-Hupkes et al. 2010), we find considerable

conservation of spatial positioning patterns between normal breast and prostate tissues, with 60 % of the 15 genes analyzed in similar radial positions between the two organs. The observed differential positioning patterns of some genes between breast and prostate are unlikely to reflect global genome reorganization or repositioning of whole chromosomes, but appear to reflect changes at the level of individual genes. In support, while the position of *MMP1* was dependent on tissue type, two other genes on HSA 11, *FLI1* and *CCND1*, are similarly positioned between breast and prostate tissue. Similarly, of the three genes on HSA 14, only *HSP90AA1* differs between breast and prostate tissue.

Our study extends growing evidence, from multiple tissue types including brain, thyroid, breast and prostate, that the spatial positioning of the genome is largely conserved between individuals (Borden and Manuelidis 1988; Leshner et al. 2015; Meaburn et al. 2009; Murata et al. 2007; Timme et al. 2011; Wiech et al. 2005). We find that 18 genes analyzed in multiple morphologically normal breast tissues all displayed a high level of conservation of positioning between individuals (this study and Meaburn et al. 2009). In addition, in prostate tissues 44/48 (91.7 %) of genes have similar positioning patterns among individuals (this study and Leshner et al. 2015). However, some inter-individual variability was found, particularly in prostate. Unlike in breast (Meaburn et al. 2009), we find that radial distributions of *FOSL2*, *CSF1R* and *HSP90AA1* are variable between individual prostate tissues. Similarly, the position of *CCND1* was similar between breast tissues (Meaburn et al. 2009), yet variable among prostate tissues from multiple individuals (Leshner et al. 2015). This observation leads to the possibility that some tissues have a higher degree of intrinsic variability in spatial genome organization patterns. Due to the high prevalence of benign hyperplasia of the prostate, another possible explanation is that the variability in positioning patterns between prostates reflects a varying amount of hyperplasic nuclei included in the analysis of "normal" tissue, although our observation of similar positioning of *CSF1R* in hyperplasic and normal argues against this scenario. It is also possible that the extent of other benign morphologies, such as proliferative inflammatory atrophy or prostatic intraepithelial neoplasia, may affect positioning patterns between individuals.

We have previously identified eight genes that reposition in breast cancer tissues (Meaburn et al. 2009). By testing prostate GPBs in breast tissue as part of our cross comparison, we have identified two additional genes (*FLI1* and *MMP9*) that reposition in breast cancer, but not benign breast tissues. When we combine our current findings with our previous studies (Leshner et al. 2015; Meaburn et al. 2009), we find that 6.4 % (3/47) of analyzed genes reposition in prostate cancer and 43.5 % (10/23) of tested genes reposition in breast cancer. It is unclear why the proportion of repositioning genes is considerably lower in prostate cancer, although the higher inter-individual variability in prostate may be a contributing factor. Future studies employing high-throughput imaging to map a larger number of genes should determine if this difference is due to the limited number of tested genes or reflects underlying biological properties or both. The molecular properties that determine whether a gene repositions between normal and cancer tissues are currently unknown. Analysis of repositioned genes in breast and prostate cancer has demonstrated that cancer-related repositioning does not correlate with their gene expression status, gene copy number or local gene density (Leshner et al. 2015; Meaburn et al. 2009; Meaburn and Misteli 2008).

We find that a particular gene can behave differently in cancers from different tissues. Of the eleven genes previously identified to reposition in either breast (Meaburn et al. 2009) or prostate cancer (Leshner et al. 2015), only two (*FLI1* and *MMP9*) spatially reposition in both breast and prostate cancer. In keeping with our finding, *BCL2* has previously been identified to reposition in some cervical squamous carcinomas (Wiech et al. 2009), but not breast (Meaburn et al. 2009) or prostate (Leshner et al. 2015) cancer. This suggests that distinct groups of genes reposition in cancers from different tissues. While breast and prostate cancer share biological features such as their origin from epithelial cells and dependence on sex steroid hormones (Risbridger et al. 2010), it will be interesting to determine in future studies how general the repositioning of *FLI1* and *MMP9* is in other cancers.

The fact that different genes spatially reposition in different cancer types may have implications for diagnostics as it suggests a correlation between non-random repositioning of the genome during carcinogenesis with the specific biology of the cancer. This leads to the possibility that differential positioning patterns for specific genes may occur even within cancers originating from the same tissue, including among subtypes of tumors. Identification of subtype-specific positioning biomarkers may be valuable in cancer prognostics, for example in distinguishing indolent from aggressive cancers.

Acknowledgments We thank Prabhakar Gudla and Stephen Lockett for assistance with image analysis; Delft University, the Netherlands, for providing the DIPImage and PRTools toolboxes; and Tatiana Karpova for microscopy support. Fluorescence imaging was performed at the National Cancer Institute Fluorescence Imaging Facility. We also thank Ms. Kathy Doan for help in identifying and obtaining prostate tissue used for this study.

Funding This work was supported by a Department of Defense Idea Awards (W81XWH-12-1-0224 and W81XWH-12-1-0295), by NCI, National Institutes of Health (NIH) under award Pacific Northwest Prostate Cancer SPORE Grant (P50CA097186), and in part by the Intramural Research Program of the NIH, NCI, Center for Cancer Research.

Compliance with ethical standards

Conflict of interest The authors declare that they have no conflict of interest.

Ethical approval All procedures performed in studies involving human participants were in accordance with the ethical standards of the institutional and/or national research committee and with the 1964 Helsinki Declaration and its later amendments or comparable ethical standards.

Informed consent Informed consent was obtained from all individual participants included in the study.

References

Battulin N et al (2015) Comparison of the 3D organization of sperm and fibroblast genomes using the Hi-C approach. Genome Biol 16:77. doi:10.1186/s13059-015-0642-0

Borden J, Manuelidis L (1988) Movement of the X chromosome in epilepsy. Science 242:1687–1691

Boutanaev AM, Mikhaylova LM, Nurminsky DI (2005) The pattern of chromosome folding in interphase is outlined by the linear gene density profile. Mol Cell Biol 25:8379–8386

Boyle S, Gilchrist S, Bridger JM, Mahy NL, Ellis JA, Bickmore WA (2001) The spatial organization of human chromosomes within the nuclei of normal and emerin-mutant cells. Hum Mol Genet 10:211–219

Cremer M et al (2003) Inheritance of gene density-related higher order chromatin arrangements in normal and tumor cell nuclei. J Cell Biol 162:809–820

Croft JA, Bridger JM, Boyle S, Perry P, Teague P, Bickmore WA (1999) Differences in the localization and morphology of chromosomes in the human nucleus. J Cell Biol 145:1119–1131

Ferrai C, de Castro IJ, Lavitas L, Chotalia M, Pombo A (2010) Gene positioning. Cold Spring Harbor Perspect Biol 2:a000588. doi:10.1101/cshperspect.a000588

Foster HA, Griffin DK, Bridger JM (2012) Interphase chromosome positioning in in vitro porcine cells and ex vivo porcine tissues. BMC Cell Biol 13:30. doi:10.1186/1471-2121-13-30

Guelen L et al (2008) Domain organization of human chromosomes revealed by mapping of nuclear lamina interactions. Nature 453:948–951. doi:10.1038/nature06947

Hiratani I et al (2008) Global reorganization of replication domains during embryonic stem cell differentiation. PLoS Biol 6:e245. doi:10.1371/journal.pbio.0060245

Kosak ST, Skok JA, Medina KL, Riblet R, Le Beau MM, Fisher AG, Singh H (2002) Subnuclear compartmentalization of immunoglobulin loci during lymphocyte development. Science 296:158–162

Kurz A et al (1996) Active and inactive genes localize preferentially in the periphery of chromosome territories. J Cell Biol 135:1195–1205

Leshner M, Devine M, Roloff GW, True LD, Misteli T, Meaburn KJ (2015) Locus-specific gene repositioning in prostate cancer. Mol Biol Cell. doi:10.1091/mbc.E15-05-0280

Lieberman-Aiden E et al (2009) Comprehensive mapping of long-range interactions reveals folding principles of the human genome. Science 326:289–293. doi:10.1126/science.1181369

Mahy NL, Perry PE, Gilchrist S, Baldock RA, Bickmore WA (2002) Spatial organization of active and inactive genes and noncoding DNA within chromosome territories. J Cell Biol 157:579–589

Mayer R, Brero A, von Hase J, Schroeder T, Cremer T, Dietzel S (2005) Common themes and cell type specific variations of higher order chromatin arrangements in the mouse. BMC Cell Biol 6:44

Meaburn KJ (2010) Fluorescence in situ hybridization on 3D cultures of tumor cells. Methods Mol Biol 659:323–336. doi:10.1007/978-1-60761-789-1_25

Meaburn KJ, Misteli T (2008) Locus-specific and activity-independent gene repositioning during early tumorigenesis. J Cell Biol 180:39–50

Meaburn KJ et al (2007) Primary laminopathy fibroblasts display altered genome organization and apoptosis. Aging cell 6:139–153. doi:10.1111/j.1474-9726.2007.00270.x

Meaburn KJ, Newbold RF, Bridger JM (2008) Positioning of human chromosomes in murine cell hybrids according to synteny. Chromosoma 117:579–591. doi:10.1007/s00412-008-0175-3

Meaburn KJ, Gudla PR, Khan S, Lockett SJ, Misteli T (2009) Disease-specific gene repositioning in breast cancer. J Cell Biol 187:801–812. doi:10.1083/jcb.200909127

Meaburn KJ, Burman B, Misteli T (2016) Spatial genome organization and disease. In: Dellaire G, Basett-Jones D (eds) The functional nucleus. Springer DE (in press)

Mehta IS, Eskiw CH, Arican HD, Kill IR, Bridger JM (2011) Farnesyltransferase inhibitor treatment restores chromosome territory positions and active chromosome dynamics in Hutchinson-Gilford progeria syndrome cells. Genome Biol 12:R74. doi:10.1186/gb-2011-12-8-r74

Mewborn SK et al (2010) Altered chromosomal positioning, compaction, and gene expression with a lamin A/C gene mutation. PLoS One 5:e14342. doi:10.1371/journal.pone.0014342

Mikelsaar R, Paves H, Org K, Mikelsaar AV (2014) Chromosome variant 1qh- and its influence on the 3D organization of chromosome 1 heterochromatin in interphase nucleus of patients with endometriosis. J Genet 93:219–223

Murata S et al (2007) Conservation and alteration of chromosome territory arrangements in thyroid carcinoma cell nuclei. Thyroid 17:489–496. doi:10.1089/thy.2006.0328

Parada L, McQueen P, Misteli T (2004) Tissue-specific spatial organization of genomes. Genome Biol 7:R44

Paz N et al (2015) Expression of the DYRK1A gene correlates with its 3D positioning in the interphase nucleus of Down syndrome cells. Chromosome Res. doi:10.1007/s10577-015-9467-7

Peric-Hupkes D et al (2010) Molecular maps of the reorganization of genome-nuclear lamina interactions during differentiation. Mol Cell 38:603–613. doi:10.1016/j.molcel.2010.03.016

Risbridger GP, Davis ID, Birrell SN, Tilley WD (2010) Breast and prostate cancer: more similar than different. Nat Rev Cancer 10:205–212. doi:10.1038/nrc2795

Scheuermann MO, Tajbakhsh J, Kurz A, Saracoglu K, Eils R, Lichter P (2004) Topology of genes and nontranscribed sequences in human interphase nuclei. Exp Cell Res 301:266–279

Shopland LS et al (2006) Folding and organization of a contiguous chromosome region according to the gene distribution pattern in primary genomic sequence. J Cell Biol 174:27–38

Therizols P, Illingworth RS, Courilleau C, Boyle S, Wood AJ, Bickmore WA (2014) Chromatin decondensation is sufficient to alter nuclear organization in embryonic stem cells. Science 346:1238–1242. doi:10.1126/science.1259587

Timme S et al (2011) Nuclear position and shape deformation of chromosome 8 territories in pancreatic ductal adenocarcinoma. Anal Cell Pathol 34:21–33. doi:10.3233/ACP-2011-0004

Towbin BD et al (2012) Step-wise methylation of histone H3K9 positions heterochromatin at the nuclear periphery. Cell 150:934–947. doi:10.1016/j.cell.2012.06.051

Volpi EV et al (2000) Large-scale chromatin organization of the major histocompatibility complex and other regions of human chromosome 6 and its response to interferon in interphase nuclei. J Cell Sci 113(Pt 9):1565–1576

Wiech T et al (2005) Human archival tissues provide a valuable source for the analysis of spatial genome organization. Histochem Cell Biol 123:229–238

Wiech T et al (2009) Spatial allelic imbalance of BCL2 genes and chromosome 18 territories in nonneoplastic and neoplastic cervical squamous epithelium. Eur Biophys J 38:793–806

Williams RR, Broad S, Sheer D, Ragoussis J (2002) Subchromosomal positioning of the epidermal differentiation complex (EDC) in keratinocyte and lymphoblast interphase nuclei. Exp Cell Res 272:163–175

Zeitz MJ, Ay F, Heidmann JD, Lerner PL, Noble WS, Steelman BN, Hoffman AR (2013) Genomic interaction profiles in breast cancer reveal altered chromatin architecture. PLoS One 8:e73974. doi:10.1371/journal.pone.0073974

Zink D et al (2004) Transcription-dependent spatial arrangement of CFTR and adjacent genes in human cell nuclei. J Cell Biol I166:815–825

Spatial genome organization and disease

Karen J. Meaburn*, Bharat Burman and Tom Misteli*

*Corresponding authors

K. Meaburn* and T. Misteli*:

National Cancer Institute, NIH, Bethesda, MD 20892, USA

E-mail: meaburnk@mail.nih.gov; mistelit@mail.nih.gov

Tel: 301 451 5118; 301 402 3959

B. Burman:

National Cancer Institute, NIH, Bethesda, MD 20892, USA; Program in Cell, Molecular and Developmental Biology, Tufts University, Sackler School of Biomedical Sciences, Boston, MA, USA

E-mail: burmanb@mail.nih.gov

Key Words: Genome organization; Chromosome territories; Nuclear architecture; Spatial positioning; Gene positioning; Disease; Cancer; Translocations; Chromatin structure

Table of Contents

x.1 Abstract

The nucleus is a complex organelle that performs a wide array of critical functions. Within the nucleus the genome is highly organized. Individual chromosomes form discrete chromosome territories. The organization of the genome is correlated with function, for example gene expression. Each chromosome and gene has a preferential spatial location, which can vary by cell type, differentiation stage and during disease. Active and inactive chromatin tends to be spatially separated, both within the 3D nuclear space and within a chromosome territory. The molecular mechanisms that determine genome organization are currently poorly understood. However, it is known that the proximity of gene loci can contribute to translocation partner choice. The recent development of a plethora of new molecular techniques and imaging strategies, combined with fluorescent in situ hybridization, is being applied to both normal and diseased cells. Such studies will bring us closer to understanding the implications of genome organization and the molecules and mechanisms that determine it.

x.2 Introduction

The basic principles underlying how chromosomes behave and organize themselves during mitosis, compacting into tightly condensed X-shaped structures, aligning and then separating into daughter nuclei, have been appreciated since the late 1800's. The interphase nucleus, however, has historically been far more of a black box with regards to its compartmentalization and organization. Yet cells, and consequently chromosomes, spend most of their time in interphase. It is during this time that they perform the majority of their functions.

Ground-breaking work over the last several decades has revealed that the nucleus is highly compartmentalized and that chromosomes persist as distinct nuclear subdomains, known as chromosome territories (CTs) (fig. x.1). These territories persist throughout the cell cycle, and remain largely separate from each other occupying reproducible positions within interphase nuclei (Cremer and Cremer 2001; Meaburn and Misteli 2007). The first evidence that chromosomes occupy discrete territories came in the 1970's and early 80's from a series of UV-laser microbeam experiments (Cremer and Cremer 2001; Cremer et al. 2014). A microlaser was used to create DNA damage to a small volume of the interphase nucleus. The sites of damage detected in the subsequent metaphase were limited to only a few chromosomes per cell, indicating that chromosomes occupy discrete domains in the nucleus since damage to many more chromosomes would have been expected if the DNA from each chromosome was dispersed throughout the nucleus. The first direct visualization of CTs came in 1985, when total human genomic DNA was used as a probe to reveal the location of human DNA in interphase nuclei of human:rodent hybrid cells, which contained either one or a few human chromosomes (Cremer et al. 2014). However, it was not until the development and expanded use of DNA fluorescent in situ hybridization (FISH) in interphase cells in the 1980's (Cremer and Cremer 2001; Cremer et al. 2014) that it became possible to truly elucidate interphase chromosome topography, and to begin to probe the relationship between the spatial organization of the genome and nuclear function. In FISH whole chromosomes or individual genomic regions are "painted" with fluorescent labels enabling the visualization of specific sub-regions of the genome. More

recently, a host of complementary biochemical techniques have been devised to probe genome organization, such as chromatin conformation capture (3C)-based technologies and DNA adenine methyltransferase identification (DamID). These techniques are now confirming conclusions drawn from FISH experiments on a genome-wide scale and are yielding further insights into spatial genome organization (Bickmore and van Steensel 2013; van Steensel and Dekker 2010). The group of 3C-technologies measure the contact frequency of pairs of genomic loci in fixed nuclei, to determine regions that are in close 3D spatial proximity within a population of cells (reviewed in (van Steensel and Dekker 2010)) The different C-techniques are variations on the same basic principle, differing mainly by how much of the genome they cover. 3C detects the contact frequencies of a known locus to selected target loci of interest, 4C takes this one step further and asks where a single “bait” locus contacts other chromatin regions across the whole genome. In a more unbiased approach, Hi-C maps all contacts in the genome. The resolution of these methods is limited by the sequencing depth. For example, 5C is a similar “all against all” approach as Hi-C, but uses a small, defined region as a target, thus increasing resolution (Bickmore and van Steensel 2013; van Steensel and Dekker 2010). DamID is a complementary tool for detecting genomic interaction (proximity) with nuclear sub-compartments. To this end, DNA adenine methyltransferase is fused to a protein of interest, such as the nuclear lamina protein lamin B. This fusion protein methylates adenines in DNA that is in proximity with the fusion protein, thus mapping associated genomic regions (reviewed in (van Steensel and Dekker 2010)).

While there is no question that the genome is highly organized within interphase nuclei, we are still a long way from fully understanding what this means functionally and what molecules are responsible for positioning and repositioning the genome. For the purpose of this review, we focus on mammalian genomes, but many properties of genome organization hold true for many other species, including plants, yeast, *C. elegans* and drosophila (Bickmore and van Steensel 2013; Del Prete et al. 2014; Egecioglu and Brickner 2011; Sexton et al. 2012; Sharma and Meister 2013; Zimmer and Fabre 2011).

x.3 Non-random genome organization

x.3.1 Spatial separation of gene-rich and gene-poor genomic regions

The genome is highly organized within interphase nuclei. Each chromosome and gene occupies a preferred nuclear position (fig x.1) (Boyle et al. 2001; Cremer and Cremer 2010; Meaburn and Misteli 2007). The prototypical example of this is human chromosomes (HSA) 18 and 19 in proliferating cells. The gene-rich HSA19 is located in the center of the nucleus, while the gene-poor HSA18 locates to the nuclear periphery (Boyle et al. 2001; Croft et al. 1999). Indeed, in proliferating human cells the radial position (position relative to the edge and center of the nucleus) is highly correlated with gene density, whereby CTs generally follow the pattern of HSA18 and 19, with the gene-rich chromosomes in the center of the nucleus and gene-poor chromosome towards the periphery (Boyle et al. 2001). Chromosome positioning patterns can also be correlated with chromosome size (Bolzer et al. 2005; Bridger et al. 2000; Sun et al.

2000). In this case, the small chromosomes tend to position to the nuclear interior and the larger chromosomes prefer the periphery.

Remarkably, even within a CT there is spatial separation of gene-rich and gene-poor DNA (fig x.2). Using FISH, it was demonstrated that gene-rich and gene-poor DNA within a 7MB domain of Drosophila chromosome 2 (Boutanaev et al. 2005) or a 4.3MB domain of mouse chromosome (MMU) 14 (Shopland et al. 2006) cluster separately from each other. This holds true at the whole CT level. The exome of the MMU2 chromosome is not found evenly throughout its CT, and instead localizes to the part of the CT which faces the nuclear interior, and beyond the bulk of the CT (Boyle et al. 2011). In the case of the HSAX chromosome, genes, regardless of their activity, locate to the periphery of the CT, while the non-genic DNA localizes to the interior of the territory (Clemson et al. 2006). Genome-wide analysis has shown this spatial separation is not limited to a few isolated cases. Early Hi-C analysis, at the resolution of 1Mb, revealed that gene-rich and transcriptionally active chromatin regions, and gene-rich chromosomes, tend to cluster together within the nuclear space, as do gene-poor, inactive chromatin regions. Moreover, gene-poor and gene-rich regions are far less likely to cluster with each other (Lieberman-Aiden et al. 2009). Hi-C and 4C have also shown that intra-chromosomal interactions are far more common than trans-chromosomal interactions, fitting with a genome organized into discrete CTs, and even the p and q arms of the same chromosome do not interact at high frequency (Bickmore and van Steensel 2013; Lieberman-Aiden et al. 2009). FISH data also reveals that CTs

are not completely isolated from each other. For example by cryo-FISH, ~40% of a given CT volume intermingles with other CTs (Branco and Pombo 2006).

At a higher resolution, Hi-C and 5C can resolve internal CT domains further and has revealed the presence of the so-called topologically associated domains (TADs)(Bickmore and van Steensel 2013; Dixon et al. 2012). TADs are discrete kb-Mb-sized domains, which are defined as genomic regions that are more likely to be spatially close to other loci within the same TAD than within another TAD (Bickmore and van Steensel 2013; Cavalli and Misteli 2013; Dixon et al. 2012). TADs are separated by sharp boundaries, and are conserved both between cell types and species (Dixon et al. 2012). TAD borders are characterized by enrichment for certain factors, such as CTCF binding sites, housekeeping genes and “active” histone modifications, and by depletion of heterochromatin marks such as H3K9me3 (Dixon et al. 2012). It has been suggested that the boundaries between TADs may function to prevent the spread of heterochromatin (Dixon et al. 2012). Despite the topological constraints imposed by such local domains, long range chromatin interactions still occur within the nucleus, particularly between promoters and distal regulatory elements (Dekker and Misteli 2015).

Spatial positioning due to gene density and/or size cannot be the full story however, since the positioning patterns of chromosomes are not identical in all cells. For example, some, but not all, CTs are differentially positioned in proliferating and non-proliferating cells, as indicated by HSA18 and 13 that are peripheral in proliferating cells but

internally positioned in G_0 cells (Bridger et al. 2000; Meaburn and Misteli 2008; Mehta et al. 2010). Similarly, although the organization of CTs is broadly similar across different tissues, some chromosomes occupy alternative positions in different cell types (Boyle et al. 2001; Foster et al. 2012; Parada et al. 2004; Zuleger et al. 2013), such as the small and gene-poor HSA21 which locates to the nuclear periphery in lymphoblasts but to the nuclear interior in fibroblasts (Boyle et al. 2001). Obviously, gene density and chromosome size are identical between these different cells, indicating other factors, such as differential gene expression or histone modifications, in CT positioning.

x.3.2 A link between gene activity and positioning

Generally, frequently transcribed genes congregate in euchromatin, or "active chromatin", and localize in the nuclear interior, while repressed genes reside in heterochromatin, or "inactive chromatin", and localize in the nuclear periphery (Bickmore 2013). At the individual gene level there is also a correlation with gene expression and nuclear position (Ferrai et al. 2010a; Takizawa et al. 2008b). This is strikingly shown by the differential position of the active and inactive *Gfap* and *Il4* alleles, where the inactive allele is in a more peripheral position than the active allele, at least in the vast majority of cells in the population (Takizawa et al. 2008a). Another example of this is *CFTR*, which moves from the nuclear periphery upon activation, while its neighbouring, still silent, genes remain at the periphery (Zink et al. 2004a). In fact many loci, particularly developmentally regulated loci, reposition concomitantly with activation or silencing (Ferrai et al. 2010a; Takizawa et al. 2008b). For example, *Igh* and *Mash1* move from the edge of the nucleus to a more internal position as they become

activated during lymphocyte and neuronal differentiation, respectively (Kosak et al. 2002; Williams et al. 2006). DamID, employing a lamin B fusion gene, found that the FISH studies on a limited number of genes coincided well at the genome-wide scale. In mammalian genomes there are 1,100-1400 lamin associated domains (LADs), which are predominantly gene-poor and lowly transcribed/silent regions of the genome and include many developmentally regulated regions (Guelen et al. 2008; Peric-Hupkes et al. 2010; Pickersgill et al. 2006; Zullo et al. 2012). LADs vary between cell types and differentiation stages, and a subset of genomic regions change association with the lamina as they change expression (Peric-Hupkes et al. 2010). Interestingly, numerous genes move away from the periphery during differentiation before they change expression (Peric-Hupkes et al. 2010), suggesting that repositioning is not a mere consequence of activity changes and involves separate mechanisms. While the majority of genes that associate with another lamina protein, lamin A/C, are also predominantly transcriptionally silent (Kubben et al. 2012), these observations should not be taken to mean that all silent genes locate to the nuclear periphery or that all peripheral genes are silent (fig x.2). Many silent genes are located within the interior of the nucleus. As an example, even though *Gfap* moves to a more internal location upon activation, even it is inactive state it does not associate with the nuclear periphery (Takizawa et al. 2008a). Additionally, within each individual nucleus only ~30% of the LAD domains are at the nuclear lamina (Kind et al. 2013). Conversely, numerous active genes locate to the nuclear periphery, often in association with nuclear pore complexes (Egecioglu and Brickner 2011), which may provide support for the “gene-gating” hypothesis put forward by Gunter Blobel nearly three decades ago (Blobel et al., 1985).

Many gene loci change their association with other nuclear sub-compartments correlating with changes in transcription. These include nuclear bodies such as transcription factories, splicing speckles, Cajal bodies, polycomb bodies and blocks of heterochromatin (reviewed in (Bickmore and van Steensel 2013; Ferrai et al. 2010a)). In at least some cases, this association is critical for gene expression (Khanna et al. 2014). Several examples have been reported of clustering of co-regulated genes, either in their active or inactive state, within the nuclear space, in many cases at nuclear bodies (Brown et al. 2008; Clowney et al. 2012; Fanucchi et al. 2013; Hakim et al. 2011; Rieder et al. 2014; Schoenfelder et al. 2010; Szczerbal and Bridger 2010; Takizawa et al. 2008a). Active genes may even loop away from the bulk of their CT in order to associate with co-regulated genes in “transcription factories” or splicing speckles (Branco and Pombo 2006; Brown et al. 2006; Ferrai et al. 2010b; Matarazzo et al. 2007; Morey et al. 2009). Splicing speckles are enriched in components of the splicing machinery and RNA polymerases. Transcription factories are sites of active transcription within the nucleus, which are enriched in RNA polymerases. Individual transcription factories have been suggested to be able to allow the simultaneous expression of several genes (Ferrai et al. 2010a).

x.3.3 Beyond gene expression

Changes in the spatial position of a gene may also occur in the absence of changes in gene expression (Harewood et al. 2010; Morey et al. 2009; Kubben et al. 2012; Kumaran and Spector 2008; Meaburn and Misteli 2008; Takizawa et al. 2008b; Williams

et al. 2006). For example, when the *Mash1* locus moves to the nuclear interior upon activation during murine neuronal cell differentiation, neighbouring genes also become more internally positioned despite remaining silent (Williams et al. 2006). Equally, when the active *Hoxb* locus loops out of its CT during mouse ES cell differentiation, flanking genes also move away from the bulk of the CT without an accompanying change in expression (Morey et al. 2009). Moreover, when loci are forced to change nuclear position, either by artificial tethering to the nuclear periphery or by chromosome translocation, some genes do alter expression, while others are unaffected (Finlan et al. 2008; Harewood et al. 2010; Kumaran and Spector 2008; Reddy et al. 2008). Conversely, another set of genes remain in the same nuclear position when their activity changes (Hakim et al. 2011; Hewitt et al. 2004; Meaburn and Misteli 2008), such as *Ifn³*, which remains at the periphery in mouse T helper cells when activated (Hewitt et al. 2004). To complicate things further, in mouse erythroid differentiation, *²-globin* becomes active, localizes with active polymerase II and then, at a later time, moves from the nuclear periphery simultaneously with polymerase II foci concentrating away from the periphery (Ragoczy et al. 2006). In this case, the repositioning could be a consequence of changes in expression. However, gene expression increases further after the loci repositions, suggesting that positioning patterns may aid modulation of expression (Ragoczy et al. 2006).

One explanation for these varying observations on individual genes is that some loci require specific positioning for expression and others do not, and that the latter loci are passively moved along with the neighbouring regions for which positioning is important.

Alternatively, other factors may also influence spatial positioning. It seems the genomic or regional neighbourhood a locus resides in is important for its behaviour (Takizawa et al. 2008b). In agreement with this, the same gene can behave differently between species when activated. For example, during erythroblast differentiation ±-*globin* and ²-*globin* loci co-localize, with ±-*globin* looping out of its CT in mice when the gene activates, but neither of these events occur in humans (Brown et al. 2008; Brown et al. 2006). The genomic neighbourhood for these two genes (e.g. local gene density) is divergent between mouse and human (Brown et al. 2008). These data suggest that the repositioning and resulting proximity of these two genes is not a requirement per se for the regulation of particular genes, and that genomic context matters. Further evidence that sequence does not intrinsically dictate position but that the local environment plays a role comes from human:mouse hybrid cells. In these hybrid cells, many human chromosomes do not assume the same position in the mouse nucleus as they do in the human cells they originate from (Meaburn et al. 2008). Such comparisons across multiple species and assessing the effects of manipulating the nuclear environment may shed light on the factors that are important in defining positioning patterns.

Transcription is only one of many functions the nucleus carries out. While gene activity does not fully account for genome organization, it could be that other nuclear activities, either alone or in combination with gene expression, influence positioning patterns. For example, replication timing, which in itself is linked to gene expression, correlates with nuclear positioning patterns (Meaburn et al. 2008). Moreover, in yeast cells, broken chromosome ends move to the nuclear periphery (Nagai et al. 2008). Although in

mammalian cells the position of broken DNA ends are generally positionally stable (Roukos and Misteli 2014), large scale DNA damage does seem to induce both decondensation of chromatin (Kruhlak et al., 2006; Dellaire et al., 2009) and a re-organization of the genome (Mehta et al. 2013). For example both UV-laser induced DNA damage (Kruhlak et al., 2006) and etoposide-induced DNA DSBs (Dellaire et al., 2009) can trigger large scale decondensation of chromatin. In another example, five chromosomes were shown to reposition in fibroblasts cells upon treatment with global DNA damaging agents, including gene-rich HSA17, 19 and 20 relocating to the nuclear periphery (Mehta et al. 2013).

Chromosome organization may also play a structural role by contributing to the function of the organ within which the individual cells reside. For example, a rather surprising apparent role for genome organization with respect to cellular function has been identified in the retina. In rod cells of nocturnal mammals there is an inversion of the position of eu- and heterochromatin, with heterochromatin locating in the center of cells (Solovei et al. 2009). This evolutionary adaptation is important for filtering low levels of light through nuclei to the photoreceptors to optimize night vision (Solovei et al. 2009). Surprisingly, this massive reorganization of chromatin does not affect transcriptional output (Solovei et al. 2009).

Despite the ample evidence of the existence of chromosomal movement, it remains unclear what mechanisms move chromatin in the nucleus. Several mechanisms have been suggested. For example, passage though mitosis and particularly early G_1 has

been associated with localizing some regions to the nuclear periphery, such as HSA18 as cells re-enter proliferation (Bridger et al. 2000). Similarly, the subset of LAD regions binding to the nuclear periphery are reset during early G_1, and are a different subset than the mother cell (Kind et al. 2013). Moreover, tethering of a reporter array to the periphery via lamin B also required passage through mitosis (Kumaran and Spector 2008). However, the observed repositioning of loci in quiescence (Bridger et al. 2000; Meaburn and Misteli 2008), by its very definition, cannot involve mitosis and early G_1. In fact, the repositioning of whole chromosomes in quiescent cells is remarkably quick, occurring within 15 min after cells are placed into low serum conditions, and requires ATP/GTP and nuclear myosin and actin (Mehta et al. 2010). Chromatin modifiers may also play a role is the positioning of the genome. In line with this, histone deacetylase 3 is important for the correct peripheral localization of certain gene loci (Demmerle et al. 2013; Zullo et al. 2012). Similarly, histone H3K9 di- and tri-methylation by Suv39H and G9a in mammalian cells (Bian et al. 2013; Kind et al. 2013) and by MET-2 and SET-25 in *C. elegans* (Towbin et al. 2012) are also important to anchor heterochromatin at the nuclear periphery. Non-coding RNA may also play a role in maintaining certain features of CT since it has recently been discovered that non-coding RNA from repetitive regions of the DNA coat CTs and appear to influence chromatin compaction (Hall et al. 2014). In addition, the long noncoding RNA Firre is necessary for the co-localization of specific trans-chromosomal loci (Hacisuleyman et al. 2014). The potential role of the nuclear envelope in positioning the genome will be discussed below (Section x.4.1).

x.4 Genome organization and disease

The fact that genome organization is linked to correct cellular function is highlighted by the findings that the genome is often reorganized in disease states. Disease generally does not result in global nuclear re-organization and instead leads to repositioning of subsets of genome regions. Studying genome positioning patterns in disease is giving deeper insight into what regulates genome organization, may provide clues to disease mechanisms and is paving the way for spatial positioning to be used as a diagnostic tool.

x.4.1 The nuclear envelope, laminopathies and genome organization

Laminopathies are a group of rare diseases caused by mutations in nuclear envelope (NE) proteins. The most prominent of these diseases result from mutations in lamin A/C and include Emery-Dreifuss muscular dystrophy (EDMD) and the premature aging disease Hutchison-Gilford progeria syndrome (HGPS) (Burke and Stewart 2013; Dittmer and Misteli 2011). The organization of CTs in proliferating fibroblasts from laminopathy patients resembles that of quiescent normal fibroblasts cells, with HSA13 and 18 no longer positioned at the nuclear periphery and HSA10 relocating to the periphery (Meaburn et al. 2007b; Mehta et al. 2011; Mewborn et al. 2010). These altered positioning patterns can be reversed. Treatment of HGPS fibroblasts with farnesyltransferase inhibitors (FTIs), which prevent the accumulation of mutant lamin A at the NE, rescues CT positioning back to normal (Mehta et al. 2011). Interestingly, the reorganization of CTs is similar for most laminopathy patients, irrespective of where the mutation maps to on the lamin A/C gene (*LMNA*), or what disease the patient suffers from (Meaburn et al. 2007a; Mewborn et al. 2010). The exceptions to this being *LMNA*

mutations delta303 and D596N, where HSA13 is more tightly associated with the nuclear periphery (Mewborn et al. 2010). Not all chromosomes change their association with the NE in laminopathy fibroblasts, however. Similar to quiescent control cells, HSA4 and X remain at the nuclear periphery of laminopathy cells (Meaburn et al. 2007a; Mehta et al. 2011). That said, the conformation of each chromosome does appear to change, at least in late passage HGPS cells. Using Hi-C, there is a loss of spatial separation between active and inactive chromosomal domains in late passage, senescing HGPS fibroblasts (passage-19), but not in a proliferating culture of HGPS (passage-17) (McCord et al. 2013). Since senescing normal fibroblasts were not used as a control, it remains unclear to what extent these changes are associated with senescence and what changes are directly linked to HGPS. Interestingly, changes in H3K27me3 and lamin A/C binding patterns were noted to occur before the large scale changes in chromatin contact frequencies in these cells, suggesting these are important determinants of chromatin organization (McCord et al. 2013).

The observations in laminopathies are in line with findings on the role of various NE proteins in genome organization. In mouse fibroblasts, the position of MMU18 to the nuclear periphery is dependent on lamin B1, while the central position of MMU19 is not (Malhas et al. 2007). As with lamins, several NE transmembrane proteins (NETs) influence the position of a specific subsets of chromosomes (Zuleger et al. 2013). NET29 and NET39 have a role in locating HSA5 and HSA13 to the nuclear periphery, whereas expression of NET5, NET45 and NET47 position HSA5 but not HSA13 to the periphery. Moreover, the presence of NET47 actually reduced HSA13's association with

the nuclear periphery. On the other hand, the internal position of HSA19 and HSA17 are not influenced by presence of these NETs (Zuleger et al. 2013).

Given that the NE of different cell types is composed of distinct complements of NE proteins, the variations between different NE proteins and the chromosomes they influences may account, in part, for the tissue-specificity of genome organization, (Solovei et al. 2013; Wong et al. 2014). For example, the expression of some NETs, including the five NETs mentioned above, are either restricted to only certain tissues or exhibit a wide range of expression levels between tissue types (Zuleger et al. 2013). In keeping with this, the positioning pattern of HSA5 in liver cells could be transformed into that of kidney cells by modifying the expression of NETs so that the NE better resembled the kidney NE (Zuleger et al. 2013). The differential influence of various NE proteins between different cell types is also highlighted in laminopathies. HSA13 and 18 remain peripheral in laminopathy patient lymphoblastiod cell lines, a cell type which does not require lamin A/C (Boyle et al. 2001; Meaburn et al. 2005). Consistent with this, in *C. elegans* an EDMD associated mutant lamin (Y59C) inhibited the release from the nuclear lamina, and full activation, of a muscle promoter array in muscle cells, but it did not interfere with an intestinal promoter containing array relocating to the nuclear interior during gut development (Mattout et al. 2011). Along with the tissue specific impairment of genome reorganization, the Y59C worms only had an aberrant muscle phenotype (Mattout et al. 2011). In the most detailed study to date of differences in NE composition between tissues and the consequences on spatial organization, NE proteins lamin B receptor (LBR) and lamin A/C were compared between rod nuclei from

39 different species and in 30 tissue types during mouse development (Solovei et al. 2013). Lack of both LBR and lamin A/C strongly correlated with a dramatic inversion of chromatin distribution, in which euchromatin shifts from an internal position to the periphery. In wild-type and LBR null mice inverted chromatin was only observed in cell types lacking both LBR and lamin A/C, suggesting that these proteins have roles in targeting heterochromatin to the nuclear periphery (Solovei et al. 2013). Indeed, Pelger–Huët anomaly, a disease in which LBR is mutated, is characterised by an altered heterochromatin distribution (Hoffmann et al. 2007). Developmentally regulated loss of LBR has also been implicated in the clustering of silenced olfactory receptor genes, away from the nuclear periphery, in olfactory neurons (Clowney et al. 2012).

The changes to genome organization in cells with either a mutation in a NE protein or with an altered complement of NE proteins may be due to a direct role of NE proteins in tethering chromatin. However, since these reorganizations occur in concert with misregulation of both gene expression and histone modifications (Malhas et al. 2007; McCord et al. 2013; Mewborn et al. 2010; Scaffidi and Misteli 2005; Shumaker et al. 2006), it cannot be ruled out that that the repositioning events are indirectly related to altered NE structure or function. Of course, direct roles via physical interaction and indirect roles of NE proteins in chromatin positioning are not mutually exclusive. It seems likely that genome repositioning events are a result of a release from tethering to the NE as well as due to changes in epigenetic modifications and gene expression that stem from alterations in NE interactions with other proteins. Several lines of evidence support a direct tethering role for NE proteins. These include the observation that NE

proteins, such as lamins and LBR, can directly bind to DNA and chromatin (Dittmer and Misteli 2011; Makatsori et al. 2004). Moreover, HSA13 and 18 are mis-positioned in asymptomatic carriers of *LMNA* mutation R527H+/- (Meaburn et al. 2007a), where presumably gene expression patterns and chromatin modifications are similar to control cells. In *LMNA* E145K mutant fibroblasts centromeres and telomeres are mis-localized only in nuclei that are lobulated (Taimen et al. 2009). Live cell imaging revealed that the reorganization of the centromeres and telomeres and lobulation occurred together as the NE reformed after mitosis, suggesting an altered attachment of centromeres and telomeres to lamins (Taimen et al. 2009). In further support of a direct tethering role, in mouse cardiac myocytes, knock-down of lamin A/C caused a subset of genes to move away from the nuclear periphery, in the absence of a change of expression for that gene (Kubben et al. 2012). It may be that several NE proteins are required to work in concert to tether chromatin to the NE. At least in rod cells, LEM domain proteins, such as emerin, are required with lamin A/C to tether chromatin to the periphery (Solovei et al. 2013). Conversely, LBR does not seem to require a mediator to tether heterochromatin (Solovei et al. 2013).

x.4.2 Altered genome organization in other non-cancerous diseases

Genome reorganization is not limited to diseases with altered NE. In one of the first studies of spatial genome organization in disease, Borden and Manuelidis established that the centromere of HSAX is relocated away from the nuclear periphery or the periphery of nucleoli in the epileptic focus of brain tissue from patients with chronic uncontrolled seizures. Conversely, loci mapping to 1q12, 9q12 and Yq12 remained

proximal to the NE and/or nucleolus in most patients (Borden and Manuelidis 1988). Some diseases also have an increased clustering of genomic loci. In cheek cells from Alzheimer's patients there is an altered telomere aggregation and clustering, possibly as the result of shortened telomeres and telomere dysfunction (Mathur et al. 2014) and in Down syndrome there is an increase clustering of HSA21 (Paz et al. 2013).

Furthering a link between spatial genome positioning and histone modifications, gene repositioning occurs in a disease associated with altered DNA methylation. Mutations in DNA methyltransferase 3B lead to immunodeficiency centromeric instability facial anomalies (ICF) syndrome, and several genomic loci are subjected to DNA hypomethylation and thus activation. One such site, *SYBL1,* which normally escapes X inactivation*,* loops out of the inactive X (X_i) in female ICF cells and the HSAY CT in male ICF cells, but it does not loop from the active X (Matarazzo et al. 2007). The normally methylated and silenced neighbouring gene *SPRY3* also loops out of the X_i CT, but not HSAY in ICF cells (Matarazzo et al. 2007). Both these differences point to the local genomic environment as an influential factor on positioning (see section x.3.3).

Altered spatial positioning patterns are also induced in cells infected with either viruses or parasites. For example, Epstein-Barr virus infection of lymphocytes results in HSA17 transiently moving closer to the periphery in the days following infection, while the position of HSA18 is unaffected (Li et al. 2010). Similarly, in snail Bge embryonic cells, infection with the parasite *Shistosoma manoni* results in temporal repositioning of gene loci (Knight et al. 2011). Again, the effect of infection varies between the loci studied.

Actin shifted toward the nuclear periphery within 30 minutes of infection, in the absence of a change in gene expression. However, in these cells, gene expression was altered at both earlier (15min) and later (2 hours) times after infection. Conversely, *ferritin* was displaced from the nuclear periphery, peaking at 5 hours and returning to a peripheral positioning by 24 hours, matching the temporal changes in its expression. This repositioning is dependent on an active infection, and not simply the presence of a cellular breach or foreign entity within the nuclei since irradiated (non-functional) parasites did not induce repositioning (Knight et al. 2011). Interestingly, both HSA17 and *actin* exhibited cycling of positioning to the periphery after infection, with both returning to the periphery again after internal positioning had been restored (Knight et al. 2011; Li et al. 2010).

x.4.3 Altered genome organization in cancer

Alterations in spatial genome organization have been prominently linked to cancer (Meaburn and Misteli 2007; Zink et al. 2004b). Indeed, distinctive alterations in chromatin staining patterns and nucleoli size and number, in addition to nuclear shape and tissue morphology, are used by pathologists to diagnose cancer. Yet these large scale changes at the chromatin level do not appear to reflect a global change in genomic spatial positioning patterns. For example, in pancreatic cancer tissues, HSA8 remains at the nuclear peripherally, although the CT shape changes (Timme et al. 2011; Wiech et al. 2005). Conversely, HSA18 and 19 change nuclear location in several cancers types, including cervical, colon and some thyroid cancers (Cremer et al. 2003; Murata et al. 2007). Cancer related repositioning is not limited to whole chromosomes.

For instance, in cervical squamous carcinoma, the *BCL2* locus repositions in a BCL2 positive tumor, but not in a BCL2 negative tumor (Wiech et al. 2009). The most extensively studied cancer to date, with respect to spatial genome positioning, is breast cancer. 4C data, and FISH validation, revealed *IGFBP3* changes long range interaction partners in breast cancer cell lines (Zeitz et al. 2013). Moreover, the centromere of HSA17 is more internally positioned in breast cancer (Wiech et al. 2005) and several genes reposition in breast cancer (Meaburn et al. 2009; Meaburn and Misteli 2008). In an in vitro mammary epithelial cell model of early breast cancer, four out of eleven tested genes (*AKT1*, *VEGF*, *BCL2* and *ERBB2*) significantly changed intranuclear position, but not their gene expression level, during carcinogenic transformation (Meaburn and Misteli 2008). Similarly, in breast cancer tissues, eight of 20 tested genes (*HES5*, *HSP90AA1*, *TGFB3*, *MYC*, *ERBB2*, *FOSL2*, *CSF1R* and *AKT1*) occupied significantly different positions in breast cancer tissues compared to normal tissues (Meaburn et al. 2009). These differences were not due to inter-sample variance since these genes were positioned in 11-14 cancers and 6-9 normal tissues and even though a wide range of breast cancers specimens were used, these genes repositioned in 64.3-100% of cancers (MEABURN 09). The differences in gene position were also not due to numerical chromosome abnormalities, and, for most genes, were not observed in the benign breast diseases hyperplasia and fibroadenoma or among normal tissues (Meaburn et al. 2009). These observations point to specific repositioning events of a subset of genes in breast cancer and they point to the possibility of using spatial positioning of the genome as a diagnostic biomarker for cancer detection (Meaburn et al. 2009; Meaburn and Misteli 2008).

X.5 The role of positioning and chromatin in translocation formation

X.5.1 Spatial proximity of translocation partners

While it is not entirely clear why the genome is positioned as it is within interphase cell and what functional role it has, the spatial positioning of the genome has emerged as an important factor in determining chromosome translocation partners (fig x.3)(Meaburn et al. 2007b; Misteli 2010; Roukos and Misteli 2014). It was initially noticed in FISH experiments that frequent translocation partners appeared to be frequently found in close spatial proximity. For example, peripheral chromosomes HSA4, 9, 13 and 18 are more likely to translocate with each other than with internally located chromosomes (Bickmore and Teague 2002). Moreover, chromosomes that form preferred clusters within certain tissues, such as MMU12, 14 and 15 in splenocytes or MMU5 and 6 in hepatocytes, are more likely to translocate in cancers derived from those tissues than chromosomes that are not part of these clusters (Parada et al. 2004; Parada et al. 2002). This data points to the role tissue specific genome organization may play in the prevalence of certain translocations in different tissues. In keeping with proximal chromosomes being more likely to be translocation partners, the amount of intermingling with neighbouring chromosomes in human lymphocytes correlates with translocation frequency (Branco and Pombo 2006).

Perhaps more importantly, beyond the level of entire chromosomes, genes that translocate are in close proximity, in the cell types where they translocate (Lukasova et al. 1997; Meaburn et al. 2007b; Misteli 2010; Neves et al. 1999; Roix et al. 2003;

Roukos and Misteli 2014). For instance, in androgen deprived prostate cell nuclei, *TMPRSS2*, *ERG* and *ETV1,* which are common translocation partners in prostate cancers, are generally found in distant locations (Lin et al. 2009; Mani et al. 2009). Upon androgen stimulation these genes reposition to become proximal neighbours, predisposing them as translocation partners, as indicated by a dramatic increase in translocation frequency upon irradiation (Lin et al. 2009; Mani et al. 2009). Along the same lines, in anaplastic large-cell lymphoma cells the close proximity of *ALK* and *NPM1* facilities the formation of the *ALK-NPM1* gene fusion upon irradiation (Mathas et al. 2009).

The caveat of these correlation studies is they may not reflect translocation formation per se, since only translocations that carry a growth advantage, and thus expand to high levels within the cancer cell population, are analyzed. Moreover, most of these studies were limited to a few genes and control regions. To address this, several genome-wide studies have been performed in mouse B lymphocytes, which, crucially, were carried out before cellular selection skewed the translocation detection frequency. Translocation frequencies across the genome were measured and mapped onto linear chromosomes (Chiarle et al. 2011; Klein et al. 2011) or compared to Hi-C (Zhang et al. 2012) or 4C (Hakim et al. 2012; Rocha et al. 2012) data, to account for 3D genomic proximity. These studies have confirmed a correlation between spatial proximity and translocation frequency. Nevertheless, a low frequency of translocations from genes that were distally located was also detected (Zhang et al. 2012). In addition to spatial proximity, not surprisingly, the amount of DNA damage was also implicated in

determining frequency of specific translocations (Hakim et al. 2012). These correlative studies were recently extended by direct observation of translocation formation (Roukos et al. 2013). For this, inducible DNA double strand break (DSB) sites, tagged with coloured fluorescently labels, were integrated into different mouse chromosomes. Upon DNA damage, the broken DNA ends where then tracked using live-cell imaging of individual cells. Consistent with both the FISH and genome-wide data, the vast majority of translocation forming breaks were proximal (within 2.5µm) before pairing, however, ~10% of translocations were formed from distant breaks (>4µm apart) (Roukos et al. 2013).

Given the fact the translocation partners tend to be proximal neighbours before translocation, it is not surprising that many fusion chromosomes resulting from the translocation event position similarly to their intact counterparts (Cremer et al. 2003; Croft et al. 1999; Meaburn et al. 2007b; Parada et al. 2002). Interestingly, the orientations within the derivative CT tend to reflect the positioning patterns of the individual intact chromosomes (Cremer et al. 2003; Croft et al. 1999), for example, within the CT of the t(18;19) derivative chromosome, the HSA18 DNA is more peripherally located than the HSA19 DNA, similar to the intact chromosomes (Croft et al. 1999). This is not to say the positions of all translocation chromosomes are unaffected. In lymphoblastoid cells from multiple individuals with the t(11;22)(q23;q11) balanced translocation, the HSA11 DNA on the fusion chromosome is more centrally located that intact HSA11. Similarly, the HSA22 portion of the fusion chromosome was more peripherally located than the intact HSA22 for the derivative 11 chromosome, but

was unaffected when it was part of the derivate 22 chromosome (Harewood et al. 2010). The repositioning of gene loci after translocation can also be variable depending on the translocation, with some translocated loci repositioning and others not (Meaburn et al. 2007b). In at least some case the repositioning reflects alterations to the local gene density around the fusion gene site (Harewood et al. 2010; Murmann et al. 2005) or aberrant expression at or around the fusion gene (Ballabio et al. 2009; Harewood et al. 2010).

x.5.2 Chromatin organization and translocations

While the spatial arrangement of the genome in vivo contributes to the formation of translocations, not all genomic loci are equally susceptible to translocation. Recently, evidence has emerged that points to higher-order chromatin structure as a key player in translocations formation, possibly by modulating DNA DSB susceptibility and repair (Misteli 2010). In support, genome-wide sequencing of translocation junctions after DSBs were experimentally induced found that most breakpoints localize within or near transcriptionally active regions (fig. x.3) (Chiarle et al. 2011; Klein et al. 2011). The break sites were enriched for histone modifications associated with active chromatin, such as H3K4me3, H3K36me3 and H3 acetylation (Klein et al. 2011). A link between transcriptional activity and translocation frequency has been demonstrated in prostate cancer, where the common translocation fusion-gene partners *TMPRSS2*, *ERG*, and *ETV1* contain binding sites for androgen receptor (AR), a potent transcriptional activator. Upon androgen treatment, AR was co-recruited with topoisomerase-II² to break sites, leading to a more open chromatin conformation and persistent DSBs

(Haffner et al. 2010; Lin et al. 2009). Similarly, the regions near translocation breakpoints in anaplastic large cell lymphoma were found to be transcriptionally activated prior to translocation (Mathas et al. 2009). Taken together, these observations suggest that genomic regions with altered chromatin structure and transcription factor binding may be more susceptible to DSBs that lead to translocations.

Chromatin organization within the nucleus also appears to determine the efficiency of DNA repair. After a DSB occurs, damaged chromatin around the break is thought to rapidly decondense to facilitate access of repair machineries, and then recondense as the repair process progresses. These events are orchestrated by chromatin remodelers that reposition nucleosomes, histone chaperone proteins that exchange core histones for specific histone variants, and histone modifying enzymes (Groth et al. 2007). Higher-order chromatin structure can drastically influence the progression of repair, possibly by impeding recruitment of these proteins. For example, radiation-induced DSBs in heterochromatin were observed to repair more slowly than breaks in euchromatin (Goodarzi et al. 2008). In the case of translocations, several chromatin modifications have been implicated in the inaccurate repair of DSBs. In prostate cancer cells treated with liganded AR, H3K79me2, a modification associated with DNA recombination, was found to be enriched near *TMPRSS2* and *ERG* breakpoints. Overexpression of H3K79-specific methyltransferase DOT1L significantly increased translocation frequency (Lin et al. 2009). Along the same lines, genome-wide conversion to an H4K20 monomethylation state in mice led to defective DSB repair, Ig class-switch recombination, and *IgH* translocations (Schotta et al. 2008). Finally, in the absence of

H2AX, a histone variant that is immediately phosphorylated after DSB formation, DSBs were shown to persist during Ig class-switch recombination, resulting in frequent translocations (Franco et al. 2006). These observations point to a potential, still poorly characterized, role of chromatin structure and histone modifications in determining translocation break points.

x.6 Summary

It has become increasingly apparent that the genome is non-randomly organized in interphase nuclei and that these positioning patterns generally correlate with nuclear function. Several recently developed technologies are driving forward our understanding of the extent and relevance of spatial genome organization. Combining genome-wide strategies and high-throughput siRNA screens with FISH will enable the identification of factors that directly regulate the position of genomic loci, the mechanisms of gene motion and will give a clearer understanding of the functional consequences of positioning patterns. In these studies it will be important to consider a given gene in the context of its neighbourhood. Comparisons of genome-wide data sets merging genome positioning information with gene expression, epigenetics, proteome, non-coding RNA expression and localisation, in multiple biological systems (different species, cell types, conditions, diseases) will be an important first step. Furthermore, studying the genome in live cells will continue to give important insights and allow the hypotheses generated from fixed cells to be tested in real time. New approaches, such as clustered regularly interspaced short palindromic repeats (CRISPR) (Chen et al. 2013), are adding to the arsenal of techniques for live cell imaging of specific regions of the genome, be it

endogenous loci or engineered arrays. The time is ripe to integrate data from of the new and old techniques to further elucidate important properties of the spatial organization of genomes.

Acknowledgments Work in the Misteli laboratory is supported by the Intramural Research Program of the National Institutes of Health (NIH), NCI, Center for Cancer Research. KM and BB are supported by Department of Defense Idea Awards (W81XWH-12-1-0224 and W81XWH-12-1-0295).

References

Ballabio E, Cantarella CD, Federico C, Di Mare P, Hall G, Harbott J, Hughes J, Saccone S, Tosi S (2009) Ectopic expression of the HLXB9 gene is associated with an altered nuclear position in t(7;12) leukaemias. Leukemia 23 (6):1179-1182. doi:10.1038/leu.2009.15

Bian Q, Khanna N, Alvikas J, Belmont AS (2013) beta-Globin cis-elements determine differential nuclear targeting through epigenetic modifications. The Journal of cell biology 203 (5):767-783. doi:10.1083/jcb.201305027

Bickmore WA (2013) The spatial organization of the human genome. Annual review of genomics and human genetics 14:67-84. doi:10.1146/annurev-genom-091212-153515

Bickmore WA, Teague P (2002) Influences of chromosome size, gene density and nuclear position on the frequency of constitutional translocations in the human population. Chromosome research : an international journal on the molecular, supramolecular and evolutionary aspects of chromosome biology 10 (8):707-715

Bickmore WA, van Steensel B (2013) Genome architecture: domain organization of interphase chromosomes. Cell 152 (6):1270-1284. doi:10.1016/j.cell.2013.02.001

Blobel G (1985) Gene gating: a hypothesis. Proceedings of the National Academy of Sciences of the United States of America 82 (24):8527-8529

Bolzer A, Kreth G, Solovei I, Koehler D, Saracoglu K, Fauth C, Muller S, Eils R, Cremer C, Speicher MR, Cremer T (2005) Three-dimensional maps of all chromosomes in human male fibroblast nuclei and prometaphase rosettes. PLoS Biol 3 (5):e157

Borden J, Manuelidis L (1988) Movement of the X chromosome in epilepsy. Science 242:1687-1691

Boutanaev AM, Mikhaylova LM, Nurminsky DI (2005) The pattern of chromosome folding in interphase is outlined by the linear gene density profile. Mol Cell Biol 25 (18):8379-8386

Boyle S, Gilchrist S, Bridger JM, Mahy NL, Ellis JA, Bickmore WA (2001) The spatial organization of human chromosomes within the nuclei of normal and emerin-mutant cells. Hum Mol Genet 10 (3):211-219

Boyle S, Rodesch MJ, Halvensleben HA, Jeddeloh JA, Bickmore WA (2011) Fluorescence in situ hybridization with high-complexity repeat-free oligonucleotide probes generated by massively

parallel synthesis. Chromosome research : an international journal on the molecular, supramolecular and evolutionary aspects of chromosome biology 19 (7):901-909. doi:10.1007/s10577-011-9245-0

Branco MR, Pombo A (2006) Intermingling of chromosome territories in interphase suggests role in translocations and transcription-dependent associations. PLoS Biol 4 (5):e138

Bridger JM, Boyle S, Kill IR, Bickmore WA (2000) Re-modelling of nuclear architecture in quiescent and senescent human fibroblasts. Curr Biol 10 (3):149-152

Brown JM, Green J, das Neves RP, Wallace HA, Smith AJ, Hughes J, Gray N, Taylor S, Wood WG, Higgs DR, Iborra FJ, Buckle VJ (2008) Association between active genes occurs at nuclear speckles and is modulated by chromatin environment. The Journal of cell biology 182 (6):1083-1097. doi:10.1083/jcb.200803174

Brown JM, Leach J, Reittie JE, Atzberger A, Lee-Prudhoe J, Wood WG, Higgs DR, Iborra FJ, Buckle VJ (2006) Coregulated human globin genes are frequently in spatial proximity when active. The Journal of cell biology 172 (2):177-187

Burke B, Stewart CL (2013) The nuclear lamins: flexibility in function. Nature reviews Molecular cell biology 14 (1):13-24. doi:10.1038/nrm3488

Cavalli G, Misteli T (2013) Functional implications of genome topology. Nature structural & molecular biology 20 (3):290-299. doi:10.1038/nsmb.2474

Chen B, Gilbert LA, Cimini BA, Schnitzbauer J, Zhang W, Li GW, Park J, Blackburn EH, Weissman JS, Qi LS, Huang B (2013) Dynamic imaging of genomic loci in living human cells by an optimized CRISPR/Cas system. Cell 155 (7):1479-1491. doi:10.1016/j.cell.2013.12.001

Chiarle R, Zhang Y, Frock RL, Lewis SM, Molinie B, Ho YJ, Myers DR, Choi VW, Compagno M, Malkin DJ, Neuberg D, Monti S, Giallourakis CC, Gostissa M, Alt FW (2011) Genome-wide translocation sequencing reveals mechanisms of chromosome breaks and rearrangements in B cells. Cell 147 (1):107-119. doi:10.1016/j.cell.2011.07.049

Clemson CM, Hall LL, Byron M, McNeil J, Lawrence JB (2006) The X chromosome is organized into a gene-rich outer rim and an internal core containing silenced nongenic sequences. Proceedings of the National Academy of Sciences of the United States of America 103 (20):7688-7693

Clowney EJ, LeGros MA, Mosley CP, Clowney FG, Markenskoff-Papadimitriou EC, Myllys M, Barnea G, Larabell CA, Lomvardas S (2012) Nuclear aggregation of olfactory receptor genes governs their monogenic expression. Cell 151 (4):724-737. doi:10.1016/j.cell.2012.09.043

Cremer M, Kupper K, Wagler B, Wizelman L, Hase Jv J, Weiland Y, Kreja L, Diebold J, Speicher MR, Cremer T (2003) Inheritance of gene density-related higher order chromatin arrangements in normal and tumor cell nuclei. The Journal of cell biology 162 (5):809-820

Cremer T, Cremer C (2001) Chromosome territories, nuclear architecture and gene regulation in mammalian cells. Nat Rev Genet 2 (4):292-301

Cremer T, Cremer C, Lichter P (2014) Recollections of a scientific journey published in human genetics: from chromosome territories to interphase cytogenetics and comparative genome hybridization. Human genetics 133 (4):403-416. doi:10.1007/s00439-014-1425-5

Cremer T, Cremer M (2010) Chromosome territories. Cold Spring Harbor perspectives in biology 2 (3):a003889. doi:10.1101/cshperspect.a003889

Croft JA, Bridger JM, Boyle S, Perry P, Teague P, Bickmore WA (1999) Differences in the localization and morphology of chromosomes in the human nucleus. J Cell Biol 145:1119-1131

Dekker J, Misteli T (2015) Long-range genome interactions Epigenetics 2edn. Cold Spring Harbor Laboratory Press,

Del Prete S, Arpon J, Sakai K, Andrey P, Gaudin V (2014) Nuclear Architecture and Chromatin Dynamics in Interphase Nuclei of Arabidopsis thaliana. Cytogenetic and genome research 143 (1-3):28-50. doi:10.1159/000363724

Dellaire G, Kepkay R, Bazett-Jones DP (2009) High resolution imaging of changes in the structure and spatial organization of chromatin, gamma-H2A.X and the MRN complex within etoposide-induced DNA repair foci. Cell cycle 8 (22):3750-3769

Demmerle J, Koch AJ, Holaska JM (2013) Emerin and histone deacetylase 3 (HDAC3) cooperatively regulate expression and nuclear positions of MyoD, Myf5, and Pax7 genes during myogenesis. Chromosome research : an international journal on the molecular, supramolecular and evolutionary aspects of chromosome biology 21 (8):765-779. doi:10.1007/s10577-013-9381-9

Dittmer TA, Misteli T (2011) The lamin protein family. Genome biology 12 (5):222. doi:10.1186/gb-2011-12-5-222

Dixon JR, Selvaraj S, Yue F, Kim A, Li Y, Shen Y, Hu M, Liu JS, Ren B (2012) Topological domains in mammalian genomes identified by analysis of chromatin interactions. Nature 485 (7398):376-380. doi:10.1038/nature11082

Egecioglu D, Brickner JH (2011) Gene positioning and expression. Current opinion in cell biology 23 (3):338-345. doi:10.1016/j.ceb.2011.01.001

Fanucchi S, Shibayama Y, Burd S, Weinberg MS, Mhlanga MM (2013) Chromosomal contact permits transcription between coregulated genes. Cell 155 (3):606-620. doi:10.1016/j.cell.2013.09.051

Ferrai C, de Castro IJ, Lavitas L, Chotalia M, Pombo A (2010a) Gene positioning. Cold Spring Harbor perspectives in biology 2 (6):a000588. doi:10.1101/cshperspect.a000588

Ferrai C, Xie SQ, Luraghi P, Munari D, Ramirez F, Branco MR, Pombo A, Crippa MP (2010b) Poised transcription factories prime silent uPA gene prior to activation. PLoS Biol 8 (1):e1000270. doi:10.1371/journal.pbio.1000270

Finlan LE, Sproul D, Thomson I, Boyle S, Kerr E, Perry P, Ylstra B, Chubb JR, Bickmore WA (2008) Recruitment to the nuclear periphery can alter expression of genes in human cells. PLoS genetics 4 (3):e1000039

Foster HA, Griffin DK, Bridger JM (2012) Interphase chromosome positioning in in vitro porcine cells and ex vivo porcine tissues. BMC cell biology 13:30. doi:10.1186/1471-2121-13-30

Franco S, Gostissa M, Zha S, Lombard DB, Murphy MM, Zarrin AA, Yan C, Tepsuporn S, Morales JC, Adams MM, Lou Z, Bassing CH, Manis JP, Chen J, Carpenter PB, Alt FW (2006) H2AX prevents DNA breaks from progressing to chromosome breaks and translocations. Molecular cell 21 (2):201-214. doi:10.1016/j.molcel.2006.01.005

Goodarzi AA, Noon AT, Deckbar D, Ziv Y, Shiloh Y, Lobrich M, Jeggo PA (2008) ATM signaling facilitates repair of DNA double-strand breaks associated with heterochromatin. Molecular cell 31 (2):167-177. doi:10.1016/j.molcel.2008.05.017

Groth A, Rocha W, Verreault A, Almouzni G (2007) Chromatin challenges during DNA replication and repair. Cell 128 (4):721-733. doi:10.1016/j.cell.2007.01.030

Guelen L, Pagie L, Brasset E, Meuleman W, Faza MB, Talhout W, Eussen BH, de Klein A, Wessels L, de Laat W, van Steensel B (2008) Domain organization of human chromosomes revealed by mapping of nuclear lamina interactions. Nature 453 (7197):948-951. doi:10.1038/nature06947

Hacisuleyman E, Goff LA, Trapnell C, Williams A, Henao-Mejia J, Sun L, McClanahan P, Hendrickson DG, Sauvageau M, Kelley DR, Morse M, Engreitz J, Lander ES, Guttman M, Lodish HF, Flavell R, Raj A, Rinn JL (2014) Topological organization of multichromosomal regions by the long intergenic noncoding RNA Firre. Nature structural & molecular biology 21 (2):198-206. doi:10.1038/nsmb.2764

Haffner MC, Aryee MJ, Toubaji A, Esopi DM, Albadine R, Gurel B, Isaacs WB, Bova GS, Liu W, Xu J, Meeker AK, Netto G, De Marzo AM, Nelson WG, Yegnasubramanian S (2010) Androgen-induced TOP2B-mediated double-strand breaks and prostate cancer gene rearrangements. Nat Genet 42 (8):668-675. doi:10.1038/ng.613

Hakim O, Resch W, Yamane A, Klein I, Kieffer-Kwon KR, Jankovic M, Oliveira T, Bothmer A, Voss TC, Ansarah-Sobrinho C, Mathe E, Liang G, Cobell J, Nakahashi H, Robbiani DF, Nussenzweig A, Hager GL, Nussenzweig MC, Casellas R (2012) DNA damage defines sites of recurrent chromosomal translocations in B lymphocytes. Nature 484 (7392):69-74. doi:10.1038/nature10909

Hakim O, Sung MH, Voss TC, Splinter E, John S, Sabo PJ, Thurman RE, Stamatoyannopoulos JA, de Laat W, Hager GL (2011) Diverse gene reprogramming events occur in the same spatial clusters of distal regulatory elements. Genome research 21 (5):697-706. doi:10.1101/gr.111153.110

Hall LL, Carone DM, Gomez AV, Kolpa HJ, Byron M, Mehta N, Fackelmayer FO, Lawrence JB (2014) Stable C0T-1 repeat RNA is abundant and is associated with euchromatic interphase chromosomes. Cell 156 (5):907-919. doi:10.1016/j.cell.2014.01.042

Harewood L, Schutz F, Boyle S, Perry P, Delorenzi M, Bickmore WA, Reymond A (2010) The effect of translocation-induced nuclear reorganization on gene expression. Genome research 20 (5):554-564. doi:10.1101/gr.103622.109

Hewitt SL, High FA, Reiner SL, Fisher AG, Merkenschlager M (2004) Nuclear repositioning marks the selective exclusion of lineage-inappropriate transcription factor loci during T helper cell differentiation. Eur J Immunol 34 (12):3604-3613

Hoffmann K, Sperling K, Olins AL, Olins DE (2007) The granulocyte nucleus and lamin B receptor: avoiding the ovoid. Chromosoma 116 (3):227-235. doi:10.1007/s00412-007-0094-8

Khanna N, Hu Y, Belmont AS (2014) HSP70 transgene directed motion to nuclear speckles facilitates heat shock activation. Curr Biol 24 (10):1138-1144. doi:10.1016/j.cub.2014.03.053

Kind J, Pagie L, Ortabozkoyun H, Boyle S, de Vries SS, Janssen H, Amendola M, Nolen LD, Bickmore WA, van Steensel B (2013) Single-cell dynamics of genome-nuclear lamina interactions. Cell 153 (1):178-192. doi:10.1016/j.cell.2013.02.028

Klein IA, Resch W, Jankovic M, Oliveira T, Yamane A, Nakahashi H, Di Virgilio M, Bothmer A, Nussenzweig A, Robbiani DF, Casellas R, Nussenzweig MC (2011) Translocation-capture sequencing reveals the extent and nature of chromosomal rearrangements in B lymphocytes. Cell 147 (1):95-106. doi:10.1016/j.cell.2011.07.048

Knight M, Ittiprasert W, Odoemelam EC, Adema CM, Miller A, Raghavan N, Bridger JM (2011) Non-random organization of the Biomphalaria glabrata genome in interphase Bge cells and the spatial repositioning of activated genes in cells co-cultured with Schistosoma mansoni. International journal for parasitology 41 (1):61-70. doi:10.1016/j.ijpara.2010.07.015

Kosak ST, Skok JA, Medina KL, Riblet R, Le Beau MM, Fisher AG, Singh H (2002) Subnuclear compartmentalization of immunoglobulin loci during lymphocyte development. Science 296 (5565):158-162

Kruhlak MJ, Celeste A, Dellaire G, Fernandez-Capetillo O, Muller WG, McNally JG, Bazett-Jones DP, Nussenzweig A (2006) Changes in chromatin structure and mobility in living cells at sites of DNA double-strand breaks. The Journal of cell biology 172 (6):823-834. doi:10.1083/jcb.200510015

Kubben N, Adriaens M, Meuleman W, Voncken JW, van Steensel B, Misteli T (2012) Mapping of lamin A- and progerin-interacting genome regions. Chromosoma 121 (5):447-464. doi:10.1007/s00412-012-0376-7

Kumaran RI, Spector DL (2008) A genetic locus targeted to the nuclear periphery in living cells maintains its transcriptional competence. The Journal of cell biology 180 (1):51-65

Li C, Shi Z, Zhang L, Huang Y, Liu A, Jin Y, Yu Y, Bai J, Chen D, Gendron C, Liu X, Fu S (2010) Dynamic changes of territories 17 and 18 during EBV-infection of human lymphocytes. Molecular biology reports 37 (5):2347-2354. doi:10.1007/s11033-009-9740-y

Lieberman-Aiden E, van Berkum NL, Williams L, Imakaev M, Ragoczy T, Telling A, Amit I, Lajoie BR, Sabo PJ, Dorschner MO, Sandstrom R, Bernstein B, Bender MA, Groudine M, Gnirke A,

Stamatoyannopoulos J, Mirny LA, Lander ES, Dekker J (2009) Comprehensive mapping of long-range interactions reveals folding principles of the human genome. Science 326 (5950):289-293. doi:10.1126/science.1181369

Lin C, Yang L, Tanasa B, Hutt K, Ju BG, Ohgi K, Zhang J, Rose DW, Fu XD, Glass CK, Rosenfeld MG (2009) Nuclear receptor-induced chromosomal proximity and DNA breaks underlie specific translocations in cancer. Cell 139 (6):1069-1083. doi:10.1016/j.cell.2009.11.030

Lukasova E, Kozubek S, Kozubek M, Kjeronska J, Ryznar L, Horakova J, Krahulcova E, Horneck G (1997) Localisation and distance between ABL and BCR genes in interphase nuclei of bone marrow cells of control donors and patients with chronic myeloid leukaemia. Human genetics 100 (5-6):525-535

Makatsori D, Kourmouli N, Polioudaki H, Shultz LD, McLean K, Theodoropoulos PA, Singh PB, Georgatos SD (2004) The inner nuclear membrane protein lamin B receptor forms distinct microdomains and links epigenetically marked chromatin to the nuclear envelope. The Journal of biological chemistry 279 (24):25567-25573. doi:10.1074/jbc.M313606200

Malhas A, Lee CF, Sanders R, Saunders NJ, Vaux DJ (2007) Defects in lamin B1 expression or processing affect interphase chromosome position and gene expression. The Journal of cell biology 176 (5):593-603. doi:10.1083/jcb.200607054

Mani RS, Tomlins SA, Callahan K, Ghosh A, Nyati MK, Varambally S, Palanisamy N, Chinnaiyan AM (2009) Induced chromosomal proximity and gene fusions in prostate cancer. Science 326 (5957):1230. doi:10.1126/science.1178124

Matarazzo MR, Boyle S, D'Esposito M, Bickmore WA (2007) Chromosome territory reorganization in a human disease with altered DNA methylation. Proceedings of the National Academy of Sciences of the United States of America 104 (42):16546-16551. doi:10.1073/pnas.0702924104

Mathas S, Kreher S, Meaburn KJ, Johrens K, Lamprecht B, Assaf C, Sterry W, Kadin ME, Daibata M, Joos S, Hummel M, Stein H, Janz M, Anagnostopoulos I, Schrock E, Misteli T, Dorken B (2009) Gene deregulation and spatial genome reorganization near breakpoints prior to formation of translocations in anaplastic large cell lymphoma. Proceedings of the National Academy of Sciences of the United States of America 106 (14):5831-5836. doi:10.1073/pnas.0900912106

Mathur S, Glogowska A, McAvoy E, Righolt C, Rutherford J, Willing C, Banik U, Ruthirakuhan M, Mai S, Garcia A (2014) Three-dimensional quantitative imaging of telomeres in buccal cells identifies mild, moderate, and severe Alzheimer's disease patients. Journal of Alzheimer's disease : JAD 39 (1):35-48. doi:10.3233/JAD-130866

Mattout A, Pike BL, Towbin BD, Bank EM, Gonzalez-Sandoval A, Stadler MB, Meister P, Gruenbaum Y, Gasser SM (2011) An EDMD mutation in C. elegans lamin blocks muscle-specific gene relocation and compromises muscle integrity. Curr Biol 21 (19):1603-1614. doi:10.1016/j.cub.2011.08.030

McCord RP, Nazario-Toole A, Zhang H, Chines PS, Zhan Y, Erdos MR, Collins FS, Dekker J, Cao K (2013) Correlated alterations in genome organization, histone methylation, and DNA-lamin A/C interactions in Hutchinson-Gilford progeria syndrome. Genome research 23 (2):260-269. doi:10.1101/gr.138032.112

Meaburn KJ, Cabuy E, Bonne G, Levy N, Morris GE, Novelli G, Kill IR, Bridger JM (2007a) Primary laminopathy fibroblasts display altered genome organization and apoptosis. Aging cell 6 (2):139-153. doi:10.1111/j.1474-9726.2007.00270.x

Meaburn KJ, Gudla PR, Khan S, Lockett SJ, Misteli T (2009) Disease-specific gene repositioning in breast cancer. The Journal of cell biology 187 (6):801-812. doi:10.1083/jcb.200909127

Meaburn KJ, Levy N, Toniolo D, Bridger JM (2005) Chromosome positioning is largely unaffected in lymphoblastoid cell lines containing emerin or A-type lamin mutations. Biochemical Society transactions 33 (Pt 6):1438-1440. doi:10.1042/BST20051438

Meaburn KJ, Misteli T (2007) Cell biology: chromosome territories. Nature 445 (7126):379-781. doi:10.1038/445379a

Meaburn KJ, Misteli T (2008) Locus-specific and activity-independent gene repositioning during early tumorigenesis. The Journal of cell biology 180 (1):39-50

Meaburn KJ, Misteli T, Soutoglou E (2007b) Spatial genome organization in the formation of chromosomal translocations. Seminars in cancer biology 17 (1):80-90. doi:10.1016/j.semcancer.2006.10.008

Meaburn KJ, Newbold RF, Bridger JM (2008) Positioning of human chromosomes in murine cell hybrids according to synteny. Chromosoma 117 (6):579-591. doi:10.1007/s00412-008-0175-3

Mehta IS, Amira M, Harvey AJ, Bridger JM (2010) Rapid chromosome territory relocation by nuclear motor activity in response to serum removal in primary human fibroblasts. Genome biology 11 (1):R5. doi:10.1186/gb-2010-11-1-r5

Mehta IS, Eskiw CH, Arican HD, Kill IR, Bridger JM (2011) Farnesyltransferase inhibitor treatment restores chromosome territory positions and active chromosome dynamics in Hutchinson-Gilford progeria syndrome cells. Genome biology 12 (8):R74. doi:10.1186/gb-2011-12-8-r74

Mehta IS, Kulashreshtha M, Chakraborty S, Kolthur-Seetharam U, Rao BJ (2013) Chromosome territories reposition during DNA damage-repair response. Genome biology 14 (12):R135. doi:10.1186/gb-2013-14-12-r135

Mewborn SK, Puckelwartz MJ, Abuisneineh F, Fahrenbach JP, Zhang Y, MacLeod H, Dellefave L, Pytel P, Selig S, Labno CM, Reddy K, Singh H, McNally E (2010) Altered chromosomal positioning, compaction, and gene expression with a lamin A/C gene mutation. PLoS ONE 5 (12):e14342. doi:10.1371/journal.pone.0014342

Misteli T (2010) Higher-order genome organization in human disease. Cold Spring Harbor perspectives in biology 2 (8):a000794. doi:10.1101/cshperspect.a000794

Morey C, Kress C, Bickmore WA (2009) Lack of bystander activation shows that localization exterior to chromosome territories is not sufficient to up-regulate gene expression. Genome research 19 (7):1184-1194. doi:10.1101/gr.089045.108

Murata S, Nakazawa T, Ohno N, Terada N, Iwashina M, Mochizuki K, Kondo T, Nakamura N, Yamane T, Iwasa S, Ohno S, Katoh R (2007) Conservation and alteration of chromosome territory arrangements in thyroid carcinoma cell nuclei. Thyroid : official journal of the American Thyroid Association 17 (6):489-496. doi:10.1089/thy.2006.0328

Murmann AE, Gao J, Encinosa M, Gautier M, Peter ME, Eils R, Lichter P, Rowley JD (2005) Local gene density predicts the spatial position of genetic loci in the interphase nucleus. Exp Cell Res 311 (1):14-26

Nagai S, Dubrana K, Tsai-Pflugfelder M, Davidson MB, Roberts TM, Brown GW, Varela E, Hediger F, Gasser SM, Krogan NJ (2008) Functional targeting of DNA damage to a nuclear pore-associated SUMO-dependent ubiquitin ligase. Science 322 (5901):597-602. doi:10.1126/science.1162790

Neves H, Ramos C, da Silva MG, Parreira A, Parreira L (1999) The nuclear topography of ABL, BCR, PML, and RARalpha genes: evidence for gene proximity in specific phases of the cell cycle and stages of hematopoietic differentiation. Blood 93 (4):1197-1207

Parada L, McQueen P, Misteli T (2004) Tissue-specific spatial organization of genomes. Genome biology 7:R44

Parada LA, McQueen PG, Munson PJ, Misteli T (2002) Conservation of relative chromosome positioning in normal and cancer cells. Curr Biol 12 (19):1692-1697

Paz N, Zabala A, Royo F, Garcia-Orad A, Zugaza JL, Parada LA (2013) Combined fluorescent-chromogenic in situ hybridization for identification and laser microdissection of interphase chromosomes. PLoS ONE 8 (4):e60238. doi:10.1371/journal.pone.0060238

Peric-Hupkes D, Meuleman W, Pagie L, Bruggeman SW, Solovei I, Brugman W, Graf S, Flicek P, Kerkhoven RM, van Lohuizen M, Reinders M, Wessels L, van Steensel B (2010) Molecular maps of the reorganization of genome-nuclear lamina interactions during differentiation. Molecular cell 38 (4):603-613. doi:10.1016/j.molcel.2010.03.016

Pickersgill H, Kalverda B, de Wit E, Talhout W, Fornerod M, van Steensel B (2006) Characterization of the Drosophila melanogaster genome at the nuclear lamina. Nat Genet 38 (9):1005-1014. doi:10.1038/ng1852

Ragoczy T, Bender MA, Telling A, Byron R, Groudine M (2006) The locus control region is required for association of the murine beta-globin locus with engaged transcription factories during erythroid maturation. Genes & development 20 (11):1447-1457

Reddy KL, Zullo JM, Bertolino E, Singh H (2008) Transcriptional repression mediated by repositioning of genes to the nuclear lamina. Nature 452 (7184):243-247

Rieder D, Ploner C, Krogsdam AM, Stocker G, Fischer M, Scheideler M, Dani C, Amri EZ, Muller WG, McNally JG, Trajanoski Z (2014) Co-expressed genes prepositioned in spatial neighborhoods stochastically associate with SC35 speckles and RNA polymerase II factories. Cellular and molecular life sciences : CMLS 71 (9):1741-1759. doi:10.1007/s00018-013-1465-3

Rocha PP, Micsinai M, Kim JR, Hewitt SL, Souza PP, Trimarchi T, Strino F, Parisi F, Kluger Y, Skok JA (2012) Close proximity to Igh is a contributing factor to AID-mediated translocations. Molecular cell 47 (6):873-885. doi:10.1016/j.molcel.2012.06.036

Roix JJ, McQueen PG, Munson PJ, Parada LA, Misteli T (2003) Spatial proximity of translocation-prone gene loci in human lymphomas. Nat Genet 34 (3):287-291

Roukos V, Misteli T (2014) The biogenesis of chromosome translocations. Nature cell biology 16 (4):293-300. doi:10.1038/ncb2941

Roukos V, Voss TC, Schmidt CK, Lee S, Wangsa D, Misteli T (2013) Spatial dynamics of chromosome translocations in living cells. Science 341 (6146):660-664. doi:10.1126/science.1237150

Scaffidi P, Misteli T (2005) Reversal of the cellular phenotype in the premature aging disease Hutchinson-Gilford progeria syndrome. Nature medicine 11 (4):440-445. doi:10.1038/nm1204

Schoenfelder S, Sexton T, Chakalova L, Cope NF, Horton A, Andrews S, Kurukuti S, Mitchell JA, Umlauf D, Dimitrova DS, Eskiw CH, Luo Y, Wei CL, Ruan Y, Bieker JJ, Fraser P (2010) Preferential associations between co-regulated genes reveal a transcriptional interactome in erythroid cells. Nat Genet 42 (1):53-61. doi:10.1038/ng.496

Schotta G, Sengupta R, Kubicek S, Malin S, Kauer M, Callen E, Celeste A, Pagani M, Opravil S, De La Rosa-Velazquez IA, Espejo A, Bedford MT, Nussenzweig A, Busslinger M, Jenuwein T (2008) A chromatin-wide transition to H4K20 monomethylation impairs genome integrity and programmed DNA rearrangements in the mouse. Genes & development 22 (15):2048-2061. doi:10.1101/gad.476008

Sexton T, Yaffe E, Kenigsberg E, Bantignies F, Leblanc B, Hoichman M, Parrinello H, Tanay A, Cavalli G (2012) Three-dimensional folding and functional organization principles of the Drosophila genome. Cell 148 (3):458-472. doi:10.1016/j.cell.2012.01.010

Sharma R, Meister P (2013) Nuclear organization in the nematode C. elegans. Current opinion in cell biology 25 (3):395-402. doi:10.1016/j.ceb.2013.02.002

Shopland LS, Lynch CR, Peterson KA, Thornton K, Kepper N, Hase J, Stein S, Vincent S, Molloy KR, Kreth G, Cremer C, Bult CJ, O'Brien TP (2006) Folding and organization of a contiguous chromosome region according to the gene distribution pattern in primary genomic sequence. The Journal of cell biology 174 (1):27-38

Shumaker DK, Dechat T, Kohlmaier A, Adam SA, Bozovsky MR, Erdos MR, Eriksson M, Goldman AE, Khuon S, Collins FS, Jenuwein T, Goldman RD (2006) Mutant nuclear lamin A leads to progressive

alterations of epigenetic control in premature aging. Proceedings of the National Academy of Sciences of the United States of America 103 (23):8703-8708. doi:10.1073/pnas.0602569103

Solovei I, Kreysing M, Lanctot C, Kosem S, Peichl L, Cremer T, Guck J, Joffe B (2009) Nuclear architecture of rod photoreceptor cells adapts to vision in mammalian evolution. Cell 137 (2):356-368. doi:10.1016/j.cell.2009.01.052

Solovei I, Wang AS, Thanisch K, Schmidt CS, Krebs S, Zwerger M, Cohen TV, Devys D, Foisner R, Peichl L, Herrmann H, Blum H, Engelkamp D, Stewart CL, Leonhardt H, Joffe B (2013) LBR and lamin A/C sequentially tether peripheral heterochromatin and inversely regulate differentiation. Cell 152 (3):584-598. doi:10.1016/j.cell.2013.01.009

Sun HB, Shen J, Yokota H (2000) Size-dependent positioning of human chromosomes in interphase nuclei. Biophys J 79 (1):184-190

Szczerbal I, Bridger JM (2010) Association of adipogenic genes with SC-35 domains during porcine adipogenesis. Chromosome research : an international journal on the molecular, supramolecular and evolutionary aspects of chromosome biology 18 (8):887-895. doi:10.1007/s10577-010-9176-1

Taimen P, Pfleghaar K, Shimi T, Moller D, Ben-Harush K, Erdos MR, Adam SA, Herrmann H, Medalia O, Collins FS, Goldman AE, Goldman RD (2009) A progeria mutation reveals functions for lamin A in nuclear assembly, architecture, and chromosome organization. Proceedings of the National Academy of Sciences of the United States of America 106 (49):20788-20793. doi:10.1073/pnas.0911895106

Takizawa T, Gudla PR, Guo L, Lockett S, Misteli T (2008a) Allele-specific nuclear positioning of the monoallelically expressed astrocyte marker GFAP. Genes & development 22 (4):489-498. doi:10.1101/gad.1634608

Takizawa T, Meaburn KJ, Misteli T (2008b) The meaning of gene positioning. Cell 135 (1):9-13. doi:10.1016/j.cell.2008.09.026

Timme S, Schmitt E, Stein S, Schwarz-Finsterle J, Wagner J, Walch A, Werner M, Hausmann M, Wiech T (2011) Nuclear position and shape deformation of chromosome 8 territories in pancreatic ductal adenocarcinoma. Analytical cellular pathology 34 (1-2):21-33. doi:10.3233/ACP-2011-0004

Towbin BD, Gonzalez-Aguilera C, Sack R, Gaidatzis D, Kalck V, Meister P, Askjaer P, Gasser SM (2012) Step-wise methylation of histone H3K9 positions heterochromatin at the nuclear periphery. Cell 150 (5):934-947. doi:10.1016/j.cell.2012.06.051

van Steensel B, Dekker J (2010) Genomics tools for unraveling chromosome architecture. Nature biotechnology 28 (10):1089-1095. doi:10.1038/nbt.1680

Wiech T, Stein S, Lachenmaier V, Schmitt E, Schwarz-Finsterle J, Wiech E, Hildenbrand G, Werner M, Hausmann M (2009) Spatial allelic imbalance of BCL2 genes and chromosome 18 territories in nonneoplastic and neoplastic cervical squamous epithelium. Eur Biophys J 38 (6):793-806

Wiech T, Timme S, Riede F, Stein S, Schuricke M, Cremer C, Werner M, Hausmann M, Walch A (2005) Human archival tissues provide a valuable source for the analysis of spatial genome organization. Histochem Cell Biol 123 (3):229-238. doi:10.1007/s00418-005-0768-3

Williams RR, Azuara V, Perry P, Sauer S, Dvorkina M, Jorgensen H, Roix J, McQueen P, Misteli T, Merkenschlager M, Fisher AG (2006) Neural induction promotes large-scale chromatin reorganisation of the Mash1 locus. J Cell Sci 119 (Pt 1):132-140

Wong X, Luperchio TR, Reddy KL (2014) NET gains and losses: the role of changing nuclear envelope proteomes in genome regulation. Current opinion in cell biology 28:105-120. doi:10.1016/j.ceb.2014.04.005

Zeitz MJ, Ay F, Heidmann JD, Lerner PL, Noble WS, Steelman BN, Hoffman AR (2013) Genomic interaction profiles in breast cancer reveal altered chromatin architecture. PLoS ONE 8 (9):e73974. doi:10.1371/journal.pone.0073974

Zhang Y, McCord RP, Ho YJ, Lajoie BR, Hildebrand DG, Simon AC, Becker MS, Alt FW, Dekker J (2012) Spatial organization of the mouse genome and its role in recurrent chromosomal translocations. Cell 148 (5):908-921. doi:10.1016/j.cell.2012.02.002

Zimmer C, Fabre E (2011) Principles of chromosomal organization: lessons from yeast. The Journal of cell biology 192 (5):723-733. doi:10.1083/jcb.201010058

Zink D, Amaral MD, Englmann A, Land S, Clarke LA, Rudolph C, Alt F, Luther K, Braz C, Sadoni N, Rosenecker J, Schindelhauer D (2004a) Transcription-dependent spatial arrangement of CFTR and adjacent genes in human cell nuclei. J Cell Biol I166:815-825

Zink D, Fische AH, Nickerson JA (2004b) Nuclear structure in cancer cells. Nat Rev Cancer 4 (9):677-687

Zuleger N, Boyle S, Kelly DA, de Las Heras JI, Lazou V, Korfali N, Batrakou DG, Randles KN, Morris GE, Harrison DJ, Bickmore WA, Schirmer EC (2013) Specific nuclear envelope transmembrane proteins can promote the location of chromosomes to and from the nuclear periphery. Genome biology 14 (2):R14. doi:10.1186/gb-2013-14-2-r14

Zullo JM, Demarco IA, Pique-Regi R, Gaffney DJ, Epstein CB, Spooner CJ, Luperchio TR, Bernstein BE, Pritchard JK, Reddy KL, Singh H (2012) DNA sequence-dependent compartmentalization and silencing of chromatin at the nuclear lamina. Cell 149 (7):1474-1487. doi:10.1016/j.cell.2012.04.035

Figures

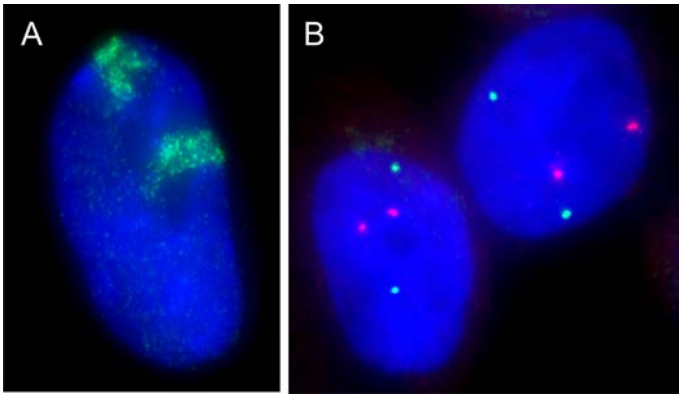

Fig. x.1. **Visualizing genomic loci.** (A) Individual chromosomes form discrete chromosome territories (CTs) in interphase cells. CTs can be visualized using fluorescence in situ hybridization (FISH), in this case, HSA11 is shown in a MCF10A breast epithelial cell nucleus. (B) Individual genes assume preferred spatial locations. FISH reveals the location of *MMP1* and *TGFB3* gene loci in MCF10A nuclei. DAPI to stain DNA in blue.

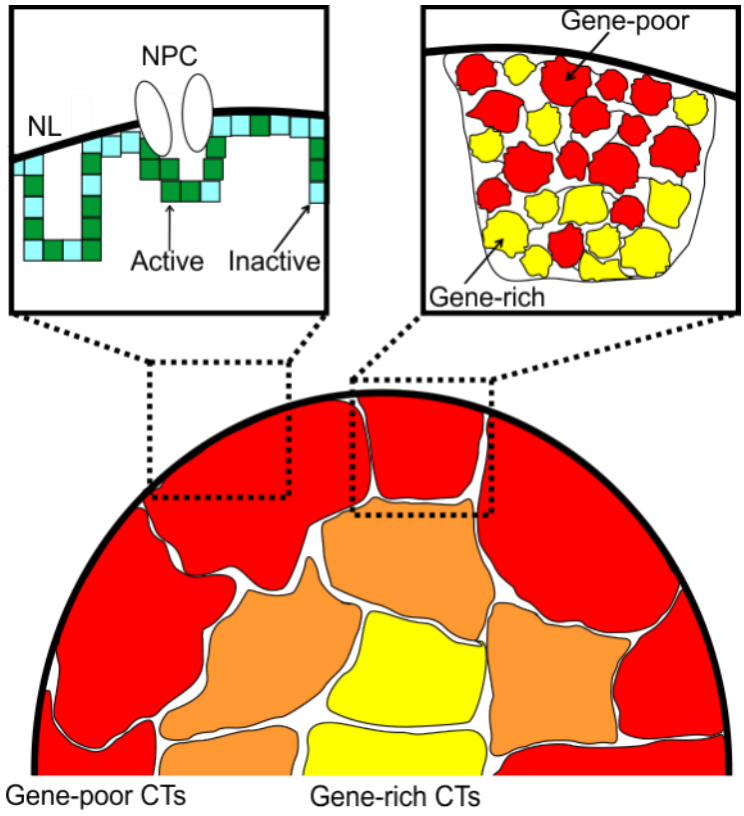

Fig. x.2: **The genome is non-randomly organized in interphase nucleus**. CTs occupy preferred positions with the nucleus both relative to the periphery of the nucleus and to other chromosomes. Smaller chromosomes tend to be more internally located. Gene-poor chromosomes have a preference for the nuclear periphery and gene-rich chromosomes for the nuclear interior, and chromosomes with intermediate gene densities are intermediately positioned. The nuclear lamina (NL) is associated with inactive chromatin, whereas the nuclear pore complex (NPC) can associate with active and inactive chromatin. Even within a CT, gene-rich and gene poor-chromatin regions tend to be spatially separated, with genic regions tending to favor both the edge of the CT and the part of the CT which faces the nuclear interior.

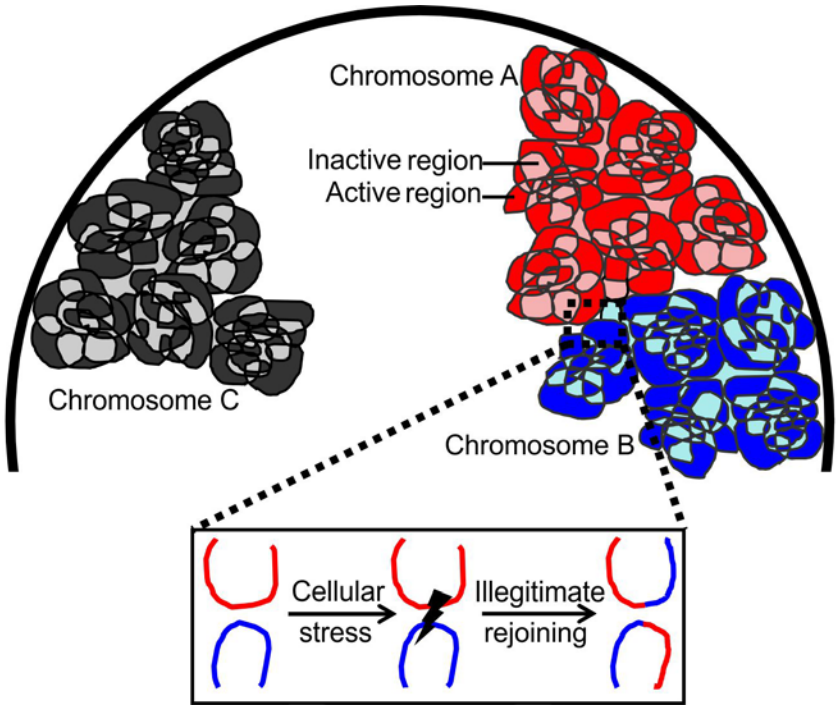

Fig. x.3. **Spatial positioning patterns influence translocation frequency**. Translocations can arise from DSBs induced by cellular stress in the forms of genotoxic, oxidative, replicative, or transcriptional stress. Illegitimate joining of DSBs can result in the formation of translocations. Proximal chromosomes A and B translocate at higher frequency than distal chromosomes A and C, or B and C. Chromatin features may also predispose certain genomic regions to translocation.

The Emerging Role of Spatial Genome Organization as a Potential Diagnosis Tool

Karen J. Meaburn[1]*

[1]Cell Biology of Genomes Group, National Cancer Institute, NIH, Bethesda, MD, USA.

*** Correspondence:** Karen J. Meaburn, Cell Biology of Genomes Group, National Cancer Institute, NIH, Bethesda, MD 20892, USA.

meaburnk@mail.nih.gov

Keywords: Genome organization; Nuclear architecture; Spatial positioning; Gene positioning; Disease; Cancer; Diagnosis

Word count: 9071

Number of Figures: 2

Abstract

In eukaryotic cells the genome is highly spatially organized. Functional relevance of higher order genome organization is implied by the fact that specific genes, and even whole chromosomes, alter spatial position in concert with functional changes within the nucleus, for example with modifications to chromatin or transcription. The exact molecular pathways that regulate spatial genome organization and the full implication to the cell of such an organization remain to be determined. However, there is a growing realization that the spatial organization of the genome can be used as a marker of disease. While global genome organization patterns remain largely conserved in disease, some genes and chromosomes occupy distinct nuclear positions in diseased cells compared to their normal counterparts, with the patterns of reorganization differing between diseases. Importantly, mapping the spatial positioning patterns of specific genomic loci can distinguish cancerous tissue from benign with high accuracy. Genome positioning is an attractive novel biomarker since additional quantitative biomarkers are urgently required in many cancer types. Current diagnostic techniques are often subjective and generally lack the ability to identify aggressive cancer from indolent, which can lead to over- or under-treatment of patients. Proof-of-principle for the use of genome positioning as a diagnostic tool has been provided based on small scale retrospective studies. Future large-scale studies are required to assess the feasibility of bringing spatial genome organization-based diagnostics to the clinical setting and to determine if the positioning patterns of specific loci can be useful biomarkers for cancer prognosis. Since spatial reorganization of the genome has been identified in multiple human diseases, it is likely that spatial genome positioning patterns as a diagnostic biomarker may be applied to many diseases.

A shortage of quantitative cancer biomarkers

Cancer is a major public health issue. In 2012 alone, across the globe approximately 14.1 million people were diagnosed with cancer and 8.2 million people lost their lives to it (Torre et al., 2015). In developed countries a third to a half of the population will be diagnosed with cancer during their lifetime (Ahmad et al., 2015;Siegel et al., 2016). Not only is cancer a leading cause of morbidity, it is also a leading cause of mortality. In fact, only heart disease accounts for more deaths than cancer; although cancer is the most frequent cause of death for 40-79 year olds (Siegel et al., 2016). Cancer is a heterogeneous collection of diseases. The most prevalent cancers are lung, breast, prostate and colorectal carcinomas, which, when combined account for ~43% of all new cancer diagnoses (Torre et al., 2015;Siegel et al., 2016). These four cancers are also leading causes of cancer-related mortality, contributing ~40% of the total (Torre et al., 2015;Siegel et al., 2016). Even cancers derived from the same organ can be quite heterogeneous from each other, and are further stratified based on morphological patterns, clinical features and/or molecular characteristics. This sub-grouping is important clinically because the appropriate treatment and the risk of recurrence or lethality differ between subgroups. For example, HER2 (also known as ERBB2) positive breast cancers have a poorer prognostic outlook than luminal breast cancers (Sorlie et al., 2001;Ferte et al., 2010), and many HER2-positive breast cancers respond well to trastuzumab (Herceptin) treatment, while endocrine therapy is an effective treatment option for the majority of luminal breast cancers (Ferte et al., 2010;Schnitt, 2010).

A key to the successful treatment of any disease is accurate diagnosis, preferably at an early stage in disease progression when treatments are generally more effective and less aggressive. However, early detection of cancer, particularly by population-based cancer screenings such as mammography or serum prostate-specific antigen (PSA) levels, often comes at the cost of overdiagnosis (Welch and Black, 2010;Bleyer and Welch, 2012;Sandhu and Andriole, 2012). Overdiagnosis is the detection of indolent cancers that will remain asymptomatic during the patient's lifetime and, as such, do not require treatment. Most commonly, cancer diagnosis is made following histological examination of biopsy or surgical tissue specimens. Unfortunately, in most instances there is a limit to the prognostic information that can be gleaned from histological analysis, and the pathologist is unable distinguish indolent from aggressive cancers with a high degree of certainty. Presently, due to a lack of additional markers to identify aggressive cancer, many overdiagnosed patients are being overtreated since they are receiving unnecessary therapies. Not only are these patients receiving no therapeutic benefit, as their cancer would never have significantly progressed, they are actually being harmed by the cancer treatment itself, because treatments can have both short-term and long-term effects that cause illness, reduce quality of life, create large financial burdens (for example by loss of income), and can even lead to death (Cooperberg et al., 2010;Welch and Black, 2010;Bleyer and Welch, 2012;Sandhu and Andriole, 2012). It has become a major focus of research to find markers that can distinguish between indolent and aggressive cancers, to aid the determination of the best possible treatment plan for the patient.

It is currently difficult to accurately assess how many cancers are overdiagnosed as directly measuring overdiagnosis would involve monitoring the progress of the cancer and the cause of death of cancer patients, without treating the individuals. The reported rate of overdiagnosis is also dependent on the precise definition of "clinically relevant" cancer. Nevertheless, for breast and prostate cancer, estimates suggest overdiagnosis is in the range of 22-67% of cancers (Draisma et al., 2009;Welch and Black, 2010;Bleyer and Welch, 2012;Sandhu and Andriole, 2012;Miller et al., 2014). Using prostate cancer mortality as an endpoint, as many as 84% of PSA screen-detected

prostate cancers may be overdiagnosed (McGregor et al., 1998). Breast and prostate cancers are highly prevalent, with almost 1.7 million women and 1.1 million men worldwide diagnosed with these cancers, respectively, in 2012 (Torre et al., 2015). In the USA, where population-based screening for breast and prostate cancer is common, over 240,000 women and more than 180,000 men per year are diagnosed, respectively (Siegel et al., 2016). Given these numbers, even taking the low estimate of overdiagnosis of 1 in 5 cancers additional prognostic markers could benefit hundreds of thousands of patients every year and reduce health care costs considerably.

Histological assessment of tissue specimens can be beneficial in the clinical setting to reduce overtreatment. For example, pathologists classify histological patterns within prostate cancer tissue according to the Gleason grading system, which broadly correlates with the differentiation status of the cancerous tissue (Montironi et al., 2005;Epstein et al., 2016). Gleason scores, particularly when used in combination with other clinical factors, including PSA level and clinical tumor stage, are the strongest markers of prostate cancer prognosis and progression currently available (D'Amico et al., 1998;Montironi et al., 2005;Cooperberg et al., 2009;Chang et al., 2014;Epstein et al., 2016). Part of the strength of the Gleason scoring system is that it takes into account intra-individual tumor heterogeneity (Van der Kwast, 2014;Epstein et al., 2016). A low Gleason score (Gleason score 6 or below) is highly indicative of an indolent cancer, and often monitoring the tumor (watchful-waiting/active surveillance) is recommend in place of treatment (Thompson et al., 2007). However, additional markers are required as both under- and over-treatment remain an issue (Cooperberg et al., 2010). Additionally, histological analysis of tissues is, by its very nature, subjective, which can lead to inter- and intra-observer variations. Taking the example of prostate cancer again, two pathologists will agree on the Gleason score 36-81% of the time (Montironi et al., 2005). Similarly, the same pathologist will derive an identical Gleason score for the same tissue specimen 43-78 % of the time (Montironi et al., 2005). Most frequently, the difference in score varies by a single Gleason grade, suggesting these small variations would make little difference to most patients. However, for men with Gleason score 6 or 7 cancers this could mean the difference between receiving treatment or not. The addition of quantitative diagnostic makers, to be used alongside histological analysis, would reduce inter- and intra-observer variations, and thus reduce overtreatment.

Targeting the nucleus in the search for clinically relevant biomarkers

Molecular markers, by their very nature, tend to be highly quantifiable, and are a good potential source of diagnostic and prognostic cancer biomarkers (Ferte et al., 2010). However, few molecular markers are currently in routine clinical practice (Ferte et al., 2010). An exciting area for exploration to identify novel biomarkers is cancer-related changes in the architecture of the cell nucleus (Veltri and Christudass, 2014). This is not without precedence and changes in nuclear structure, such as nuclear size, shape, prominence of nucleoli and chromatin texture, have long been used by pathologists as part of their criteria to identify cancerous cells (Zink et al., 2004b;Veltri and Christudass, 2014). Moreover, identifying chromosomal translocations is important for diagnosing hematological cancers, as specific translocations characterize the type of leukemia or lymphoma, are associated with distinct clinical features and are often indicative of the appropriate treatment (Mitelman et al., 2007). For example, chronic myeloid leukemia is diagnosed after the cytogenetic detection of t(9;22)(q34;q11), the Philadelphia chromosome, which results in a *BCR-ABL* fusion protein. Tyrosine kinase inhibitors (Imatinib/Gleevec) inhibit the activity of the resultant oncogenic fusion protein and use of this targeted therapy results in exceptionally high rates of remission for chronic myeloid leukemia patients (Hehlmann et al., 2007). Fluorescence *in situ* hybridization (FISH), a technique used to visualize selected sequences of DNA within interphase nuclei or on

mitotic chromosomes, is one method used in clinical practice to detect the presence of specific translocations (Muhlmann, 2002;Zink et al., 2004b;Hehlmann et al., 2007). FISH is also used clinically to detect other chromosomal aberrations in solid and hematological cancers, such as amplifications of the *ERBB2* locus in breast cancer, to aid diagnosis or as a prognostic marker (Muhlmann, 2002;Lambros et al., 2007;Hastings, 2010). Changes in gene expression profiles can also be useful diagnostically. For instance, there are several commercially available assays with prognostic value for various sub-types of breast cancer based on the gene expression profiles of between 2 and 97 genes (Dai et al., 2015).

Beyond gene expression changes and genomic aberrations, there are multiple other aspects of nuclear structure and function that are deregulated in cancer and could be exploited clinically. For example, alteration in nuclear shape, size, global levels and patterns of heterochromatin and/or histone modifications during carcinogenesis have been shown to be predictive of cancer progression (Zink et al., 2004b;Nielsen et al., 2008;Veltri and Christudass, 2014). Aberrant expression of A- and/or B-type lamins is a common feature of many types of cancer, including lung, breast, prostate, colorectal, skin and gut carcinomas (Broers et al., 1993;Moss et al., 1999;Venables et al., 2001;Willis et al., 2008;Belt et al., 2011;Kong et al., 2012;Wazir et al., 2013;Broers and Ramaekers, 2014;Saarinen et al., 2015). The majority of lamin proteins form the nuclear lamina, which underlies the nuclear envelope (NE), and an additional pool of intranuclear lamins exists (Dittmer and Misteli, 2011). Although highly variable between individual cancers and cancer sub-types, a broad generalization suggests cancers with lower expression levels of A-type lamins tend to have poorer outcomes and more aggressive phenotypes (Belt et al., 2011;Wazir et al., 2013;Saarinen et al., 2015). This is in line with findings that cells with a deficiency in A-type lamins can migrate more easily though narrow constrictions (Davidson et al., 2014), which may aid metastatic progression, and that reduced lamin A has been linked to a higher cellular proliferation rate (Venables et al., 2001). However, the associations between reduced lamin expression and prognosis tend to be weak or based on a low number of patients, and there are conflicting studies that find higher levels of A-type lamin expression to be predictive of a poor outcome (Willis et al., 2008;Kong et al., 2012). Since difference in lamin expression can vary between sub-groups of cancers, for example between small cell lung cancer and non-small cell lung cancer (Broers et al., 1993), future studies with more defined cohorts of patients may prove enlightening. It is not only changes in expression, mis-localization of lamins to the cytoplasm (Broers et al., 1993;Moss et al., 1999), or the nucleolus (Venables et al., 2001) have also been observed in some cancer specimens. The reduction and/or loss of lamin isoforms may be an early event in carcinogenesis as, at least in cervical cancer, it can occur before neoplasia is detectable (Capo-Chichi et al., 2016). Other nuclear bodies, including the nucleolus and PML bodies, are also disrupted in cancer, with the specific aberration detected depending on the type of cancer (Zink et al., 2004b).

While loss of genomic integrity, such as mutations, amplifications, deletions and translocations, are hallmarks of cancer and cancer progression (Mitelman et al., 2007;Hanahan and Weinberg, 2011), an additional feature of the genome is emerging as a potential cancer biomarker – namely the spatial organization of the genome within the interphase nucleus.

Non-random spatial organization of the genome in interphase nuclei

The genome is highly spatially organized within the nucleus, with, for the most part, each gene and chromosome occupying preferred nuclear positions (Cremer and Cremer, 2001;Ferrai et al., 2010;Dekker and Misteli, 2015;Meaburn et al., 2016a). Although the spatial organization of the

genome is non-random it does not mean that each cell within a population has an identical positioning pattern. In fact, spatial genome organization is probabilistic in nature with considerable cell-to-cell variability, and while in the majority of cells a certain position (e.g. internal, proximal to a nuclear speckle, etc.) will be favored, within the population of cells a specific genomic region can be found in any position within the cell (Parada et al., 2003;Bolzer et al., 2005;Goetze et al., 2007;Dekker and Misteli, 2015;Kind et al., 2015).

The nonrandom spatial positioning of genomic loci can be characterized in several ways, the most common being radial positioning and relative positioning (Figure 1). Radial positioning describes the position of a locus along a central axis between the nuclear periphery and the center of a nucleus. For instance, in many cell types human chromosome 18 preferentially locates to the nuclear periphery, and, conversely, chromosome 19 is positioned centrally (Croft et al., 1999;Boyle et al., 2001;Cremer et al., 2003). On the other hand, relative positioning measures the position of a gene or chromosome relative to another nuclear landmark, such to another gene or chromosome, association with the NE or with a nuclear body, including a transcription factory or a splicing speckle, or the position of a gene with respect to the rest of the chromosome it is located on. Relative positioning can measure either the frequency of close spatial proximity or the distance between the two objects. As an example of relative positioning, in human intermediate erythroblasts cells the ±-*globin* gene locus frequently loops out of its chromosome territory, and is often in close spatial proximity to the ²-*globin* gene at splicing factor-enriched nuclear speckles (Brown et al., 2006). Traditionally radial and proximal positioning are measured after FISH. More recently, biochemical methods have been developed to map the proximity of a locus to either other genomic regions (a range of chromatin conformation capture techniques, e.g. 3C, 4C, 5C, HiC) or to nuclear structures (e.g. DamID, ChIA-PET) (van Steensel and Dekker, 2010;Bickmore and van Steensel, 2013;Dekker and Misteli, 2015). These traditional and new methods are highly complementary, and it is their combined use that will drive forward our understanding of genome organization. Unlike FISH, the biochemical methods are population-based and the heterogeneity inherent in positioning, either between individual cells or between the two alleles of a gene within a single cell, is not captured. Conversely, as opposed to many of the biochemical methods, FISH is relatively low-throughput and candidate genes are required for analysis.

Correlations between spatial genome organization and transcription

The exact molecular mechanisms that regulate the spatial organization of the genome are currently not well elucidated. Moreover, it is not clear if the spatial organization of the genome is important to regulate proper nuclear function or if it is simply a byproduct of nuclear processes. Part of the difficulty in resolving this question is that it is virtually impossible to completely separate the various nuclear functions from each other and, therefore, determine cause and effect. It is also likely that different genes are regulated by different mechanisms; for every rule suggested to govern spatial genome organization there are multiple examples of exceptions. That said, there are several lines of evidence that suggest functional importance to spatial genome organization. The first hint comes from the fact that gene-rich regions of the genome are spatially separated from gene-poor regions (Boyle et al., 2001;Boutanaev et al., 2005;Clemson et al., 2006;Shopland et al., 2006;Simonis et al., 2006;Lieberman-Aiden et al., 2009;Boyle et al., 2011). For instance, gene-rich chromosomes are generally internally located whereas gene-poor chromosomes are enriched at the nuclear periphery (Boyle et al., 2001) and within individual chromosomes gene-poor and gene-rich chromatin are spatially separate, even at the Mb scale (Boutanaev et al., 2005;Shopland et al., 2006;Lieberman-Aiden et al., 2009). This suggests that the spatial organization of the genome is functionally

important for gene expression, or is at least dictated by gene expression. This hypothesis is supported by the observation of spatial clustering of some co-regulated genes, e.g. tRNA genes (Thompson et al., 2003), KLF1-regulated genes (Schoenfelder et al., 2010), STAT-regulated genes (Hakim et al., 2013) or olfactory receptor genes (Clowney et al., 2012). Further, genomic regions that are gene-poor and/or contain mostly inactive genes tend to cluster together, for example at the nuclear lamina, around the edge of the nucleolus or with peri-centromeric heterochromatin (Pickersgill et al., 2006;Guelen et al., 2008;Nemeth et al., 2010;Peric-Hupkes et al., 2010;van Koningsbruggen et al., 2010;Kind et al., 2013;Wijchers et al., 2015). Moreover, the spatial organization of the genome is different in cells with differing gene expression profiles, for example the genome reorganizes during differentiation and is different between different cell- and tissue-types (Kosak et al., 2002;Parada et al., 2004;Solovei et al., 2009;Peric-Hupkes et al., 2010;Foster et al., 2012;Hakim et al., 2013;Rao et al., 2014;Meaburn et al., 2016b). While specific loci often change nuclear positions, there is not a global spatial rearrangement of the genome between cell types. Positioning patterns are remarkably conserved between cell types and stages of differentiation, with only specific genomic regions in alternative positions. For instance, in human fibroblasts and lymphocytes most chromosomes are in similar radial positions and only the position of chromosomes 8, 20 and 21 differ (Boyle et al., 2001;Meaburn et al., 2008). Similarly, of the genomic regions that associated with the nuclear lamina in mouse embryonic stem cells and astrocytes, approximately 20% are lamina-associated in only one of the two cell types (Peric-Hupkes et al., 2010).

Most saliently, genes can relocate to different nuclear locations with changes in their transcriptional output (Fraser and Bickmore, 2007;Ferrai et al., 2010). For example, active *Gfap* and *Il4* alleles are generally more internally located than their silent counterparts (Takizawa et al., 2008a) and *CFTR*, *Mash1* and *IgH* display lower association with the nuclear periphery upon activation (Kosak et al., 2002;Zink et al., 2004a;Williams et al., 2006). Conversely, genes, such as *INO1*, *HXK1* and *GAL1* move to the nuclear pore complex (NPC), at the periphery of the nucleus, upon activation (Brickner and Walter, 2004;Taddei et al., 2006;Brickner et al., 2007) and some highly expressed gene-rich regions of the genome, including *major histocompatibility complex*, *epidermal differentiation complex* and *HoxB* loci loop out of the bulk of their chromosome territory when active (Volpi et al., 2000;Williams et al., 2002;Chambeyron and Bickmore, 2004). Not all loci alter nuclear location at the exact time of changes in expression. Some loci reposition before changes in gene expression, adopting poised positions in the days leading up to developmentally regulated activation of expression (Ragoczy et al., 2003;Chambeyron and Bickmore, 2004;Peric-Hupkes et al., 2010), suggesting, at least for some regions, changes in nuclear positions are not simply a consequence of the activation of gene expression. On the other hand, some genes move only after changes in expression, for example, during erythroid differentiation the mouse ^{2}*-globin* gene is activated prior to relocation away from the nuclear periphery (Ragoczy et al., 2006). In this case the movement of the locus might help modify the magnitude of transcription since expression is further increased with the repositioning (Ragoczy et al., 2006). It is not only upon activation genes alter nuclear location. Relocation to blocks of heterochromatin is associated with gene repression for some genes (Brown et al., 1997;Brown et al., 1999;Francastel et al., 1999;Wijchers et al., 2015); however, this is not a general rule as other silenced gene loci do not associate with blocks of heterochromatin (Moen et al., 2004;Takizawa et al., 2008a).

Lack of correlations between spatial genome organization and transcription

In addition to the discrepancy amongst genes on the timing of spatial repositioning in relation to altered transcription, there are a large number of studies demonstrating that for many genes changes

in nuclear position and gene expression are uncoupled (Scheuermann et al., 2004;Williams et al., 2006;Kumaran and Spector, 2008;Meaburn and Misteli, 2008;Takizawa et al., 2008b;Morey et al., 2009;Harewood et al., 2010;Hakim et al., 2011;Shachar et al., 2015). For instance, when a breast epithelial cell line, MCF10A, was grown under four different growth conditions there was no correlation between change in gene expression and change radial positioning pattern for any of the eleven genes analyzed (Meaburn and Misteli, 2008). There could be several reasons to explain this. Firstly, radial positioning is not an ideal measure to assess function (Takizawa et al., 2008b). With the exception of the NE, all radial locations within the nucleus are approximately equal with respect to function and gene expression. Transcription factories and active genes are equally distributed throughout the nucleus (Wansink et al., 1993;Takizawa et al., 2008a;Paz et al., 2015). Thus, changes in radial position do not necessary represent biologically relevant changes, as they do not correlate with moving a locus into a more or less transcriptionally active environment. Moreover, radial positioning can miss biologically relevant changes to positioning if it does not shift the locus to a different radial zone. Proximity to and association with nuclear bodies is likely to be far more important for gene expression and RNA processing than radial positioning. Indeed, for many genes changes in gene expression accompany changes in association with nuclear sub-compartments, including the lamina, nucleolus, transcription factories, heterochromatin, polycomb bodies, NPCs, Cajal bodies and nuclear speckles (Ahmed et al., 2010;Ferrai et al., 2010;Bickmore and van Steensel, 2013;Khanna et al., 2014;Dekker and Misteli, 2015;Wang et al., 2016). Furthermore, transient co-localization of X chromosomes during the establishment of X inactivation and co-localization of imprinted genes with imprinting control region loci suggest a critical role for spatial genome organization in establishing and maintaining mono-allelic expression in these regions (Fraser and Bickmore, 2007;MacDonald et al., 2016). However, radial positioning vs relative positioning cannot be the full story in explaining the differences between the studies because some genes spatially reposition in the absence of a change in expression. For example, *Mash1* relocates to a more internal nuclear position upon activation during neuronal differentiation, however, the repositioning is not specific to *Mash1* and several chromosomally neighboring genes also reposition despite remaining transcriptionally silent (Williams et al., 2006). This is not limited to transcriptionally silent genes; active genes can also change nuclear positions without modulating transcription. As an example, all four genes (*AKT1*, *BCL2*, *ERBB2* and *VEGF)* identified to change radial position after *in vitro* induction of early breast cancer were expressed at similar levels in the normal as compared to tumor cells (Meaburn and Misteli, 2008).

It could be that some genes are more sensitive to their nuclear position for expression than others, and the genes that require specific positioning patterns for their correct expression drive the relocation of neighboring regions by “pulling” them along. Consistent with this, when loci are forced into a different nuclear environment, either by being artificially tethered or due to a chromosomal translocation, the expression of some but not all genes is affected (Finlan et al., 2008;Kumaran and Spector, 2008;Reddy et al., 2008;Harewood et al., 2010;Wijchers et al., 2015). Additionally, the type of expression change may be an important factor. Most of the genes that have been identified to alter nuclear location in parallel with changes in gene expression are genes that are being activated or silenced during development and differentiation, i.e. are genes associated with a more or less permanent change in expression, and although these expression changes occur in a coordinated manner, it does not need to be rapid. Thus, it could be that a specific nuclear environment is required for this activation/repression, and time can be taken for a locus to be relocated to this environment, but once a gene is permanently induced or silenced the environment can change without affecting the expression of that region. In support, transient homologous pairing of *Oct4* alleles occurs during mouse ESC differentiation only as *Oct4* becomes permanently repressed (Hogan et al., 2015). It is

also likely that ongoing transcription is not required to maintain spatial positioning patterns, since long-range DNA interactions of active *²-globin* and *Rad23a* genes are maintained after the inhibition of RNA polymerase II transcription (Palstra et al., 2008). Precise spatial positioning, especially radial positioning, may not have a significant role for all genes beyond switching on/off. For genes that turn on and off rapidly in response to changing environmental signals, for example upon stimulation by a hormone or stress signals, rapid induction may be enhanced by proximal spatial positioning of sets of co-regulated genes prior to the stimulation, i.e. in a permanently poised position. In keeping with this, glucocorticoid receptor responsive genes cluster in the absence of glucocorticoid, and (re)stimulation with glucocorticoid does not significantly change positioning patterns (Hakim et al., 2011). Direct evidence for the concept of a more rapid activation of expression for genes already in the correct nuclear environment comes from yeast studies. The NPC associates with active regions of the genome, with specific genes recruited to the NPC upon activation (Egecioglu and Brickner, 2011;Liang and Hetzer, 2011). Even after the stimulation has been removed and the expression from these genes has been repressed several genes, including *HXK1*, *GAL1* and *INO1*, remain at the nuclear periphery and these peripheral loci are activated more quickly upon future re-stimulation (Brickner et al., 2007;Tan-Wong et al., 2009).

Additional players and functions

Remodeling of chromatin is intimately linked to gene expression. Thus, it is possible that chromatin remodelers and the resulting alterations to histones and chromatin compaction are an important part of the molecular machinery that reorganizes the genome, rather than gene transcription itself. Emerging evidence suggests this may well be the case. Decondensation of chromatin in the absence of altered gene expression, even for silent genes, is sufficient for a locus to spatially reposition (Chambeyron and Bickmore, 2004;Therizols et al., 2014). Similarly, modifications to histones are important for anchoring loci to the nuclear periphery, independently of a role in gene repression these modifications are associated with (Harr et al., 2016). For example, histone acetyltransferase SAGA (Dultz et al., 2016), histone deacetylases (Zullo et al., 2012;Demmerle et al., 2013;Dultz et al., 2016) and histone H3K9 di- and tri-methylation by histone methyltransferase (Towbin et al., 2012;Bian et al., 2013;Kind et al., 2013;Harr et al., 2015) are required to localize at least some genes to the nuclear periphery. It is most likely that chromatin remodelers work in tandem and that it is specific combination of histone marks that are required to target a genomic region to the nuclear periphery (Harr et al., 2016). It is also likely that chromatin remodelers play a role in targeting genes within the nucleoplasm, away from the NE, since chromatin remodelers EZH2 and SUV39H1 have been demonstrated to be critical for local chromatin clustering into sub-domains (Wijchers et al., 2016) and knocking down a range of chromatin remodelers and histone modifiers affected the position of several non-NE associated genes (Shachar et al., 2015).

In addition to gene expression and chromatin state, many other nuclear factors have been linked to a role in correct spatial organization of the genome, these include actin, myosin (Chuang et al., 2006;Dundr et al., 2007;Mehta et al., 2010), NE proteins, include A-type lamins (Meaburn et al., 2007;Mewborn et al., 2010;Mehta et al., 2011;Kubben et al., 2012;Solovei et al., 2013;Harr et al., 2015), B-type lamins (Malhas et al., 2007;Ranade et al., 2016), lamin B receptor (Clowney et al., 2012;Solovei et al., 2013), emerin (Demmerle et al., 2013) and several other NE transmembrane proteins (Zuleger et al., 2013), NPC proteins (Ahmed et al., 2010;Dultz et al., 2016) and non-coding RNAs (Hacisuleyman et al., 2014).

Interestingly, different genes can be targeted to the same nuclear compartment via different protein complexes and pathways, and the use of the different mechanisms may add an additional layer of control over the speed of inducing or enhancing gene expression (Randise-Hinchliff et al., 2016). Moreover, different genes require different proteins complexes for their correct nuclear location. SiRNA screening of 669 nuclear proteins, combined with mapping the radial position of 3-4 genes by FISH, identified 50 proteins with roles in spatially organizing the genome. However, of these proteins, only knocking down one, *CACNG1*, repositioned all four genes studied. Moreover, half of the hits affected the position of only a single gene (Shachar et al., 2015).

At some level underlying DNA sequence must play a role in the spatial positioning of the genome. Transcription factors bind to specific sequences in the genome, thereby, activating a specific set of genes, and genes regulated by specific transcription factors can spatially cluster (Schoenfelder et al., 2010;Hakim et al., 2011;Hakim et al., 2013). Some specific DNA sequences have been demonstrated to have a direct role in targeting genes to specific locations within the nucleus. In *S. cerevisiae*, two short gene recruitment sequences, within gene promotors, are required to target inducible genes to the NPC, allowing an enhanced transcriptional output (Ahmed et al., 2010). It has recently been proposed that the association between repetitive sequences, in particular homotypic associations between short interspersed retrotransposable elements (SINEs), which are enriched in gene-rich regions of the genome, or long interspersed retrotransposable elements (LINEs), which are enriched in gene-poor regions, may be a key underling factor responsible for the spatial separation of gene-rich and gene-poor regions of the genome (Cournac et al., 2016;Solovei et al., 2016). However, spatial positioning patterns cannot be an intrinsic feature of a piece of DNA, since, as discussed above, genes and chromosomes can alter position without changes in DNA sequence, e.g. between cell types or upon activation. Additionally, some human chromosomes, including chromosome X, adopt different nuclear positions when they are in a mouse nucleus compared to when they are within their endogenous human cell (Meaburn et al., 2008). It is also unlikely all repeat sequences direct spatial organization, as pericentromeric satellite repeats migrate to existing heterochromatin compartments during differentiation rather than drive the aggregation of heterochromatin (Wijchers et al., 2015).

Replication has also been linked to the spatial organization of the genome. Genomic regions change nuclear location as they change replication timing during development and disruptions to replication can affect the radial position of some genes (Hiratani et al., 2008;Shachar et al., 2015). Similarly, mitosis and NE reformation in early G_1 are important for some loci to establish nuclear location, especially for gene-poor and inactive regions when associating with the NE (Bridger et al., 2000;Kumaran and Spector, 2008;Kind et al., 2013) or during muscle differentiation (Neems et al., 2016). However, once more, these cannot be general mechanisms for all genes. Firstly, several genes and chromosomes reposition as cells exit the cell cycle and become quiescent or senescent, which clearly occurs in the absence of replication, mitosis and NE reformation (Bridger et al., 2000;Solovei et al., 2004;Meaburn et al., 2007;Meaburn and Misteli, 2008). Secondly, an alternative mechanism must be required for genes that move rapidly after stimulation. For example, relocation to the NPC occurs within 15-60 mins of activation in 60% of nuclei (Randise-Hinchliff et al., 2016). This timing is too fast for replication, mitosis or NE reformation to play a major role.

The spatial organization of the genome may also have a role in DNA repair, since whole chromosomes can reposition after DNA damage (Mehta et al., 2013;Ioannou et al., 2015), however, given that in mammalian cells broken DNA ends do not significantly move (Kruhlak et al., 2006;Soutoglou et al., 2007;Roukos et al., 2013), the function of this repositioning is not clear. What

is clear, however, is the role the spatial organization plays in the partner choice when oncogenic chromosomal translocations form, after the DNA breaks have occurred. Translocations preferentially form between loci that are in close spatial proximity prior to damage (Lukasova et al., 1997;Neves et al., 1999;Roix et al., 2003;Lin et al., 2009;Mani et al., 2009;Mathas et al., 2009;Chiarle et al., 2011;Klein et al., 2011;Hakim et al., 2012;Roukos et al., 2013). In a similar vein, the spatial organization of the genome also helps dictate the integration sites of HIV-1 virus DNA into the human genome after infection. HIV-1 integrates preferentially into highly transcribing genes that associated with the NPC (Lelek et al., 2015;Marini et al., 2015). A direct functional role for spatial genome positioning has not only been shown for disease progression. In the rod cells of nocturnal mammals a redistribution of heterochromatin to the center of the nucleus and euchromatin to the nuclear periphery aids night vision by optimizing the diffraction of light though the retina (Solovei et al., 2009).

Thus, while trends are emerging as to how and why the genome is spatially organized, no "one size fits all model" has yet to clearly present itself. This is not surprising given the complexity of the nucleus. Most likely it will be a combination of molecular strategies working in concert, and differing depending on the gene and the cellular context, that optimizes correct nuclear function and organization.

Spatial reorganization of the genome in non-malignant disease

Even though many mechanistic and functional aspects of the spatial organization of the genome have yet to be resolved, it is becoming increasingly evident that genomic spatial positioning patterns can be used as markers of disease. In a wide variety of diseases, including cancer, individual genes, genomic regions and/or whole chromosomes reposition (Figure 2) (Ferrai et al., 2010;Bridger et al., 2014;Meaburn et al., 2016a). This phenomenon was first identified in the 1980s in brain tissues of epilepsy patients (Borden and Manuelidis, 1988). The centromere of chromosome X redistributes away from the NE or edge of nucleoli in neurons from the epileptic seizure focus as compared to normal neurons from unaffected areas of the brain from the same individuals (Figure 2) (Borden and Manuelidis, 1988). This repositioning is not common to other heterochromatin regions, as neither the pericentromeric heterochromatin regions on chromosomes 1 (1q12) and 9 (9q12) nor the large heterochromatin block mapping to Yq12 reposition (Borden and Manuelidis, 1988). Generally speaking, different loci have been positioned in different diseases, with very few loci studied in more than one affliction, making it unclear how general the disease-related repositioning of a given locus is. At least some repositioning events are different between different diseases, however. While 1q12 is not repositioned in epilepsy, in the lymphocytes from patients with endometriosis 1q12 is more peripherally located, compared to control individuals, (Mikelsaar et al., 2014) and more internally located in Immunodeficiency, Centromere instability and Facial anomalies syndrome (ICF) patient lymphocytes (Jefferson et al., 2010;Dupont et al., 2012). Additional genomic regions were also found to reposition in ICF, including a reduced association of chromosome 16's pericentromeric heterochromatin region with the NE, and an increased incidence of *human pseudoautosomal region 2* genes looping out of their chromosome territories (chromosome Y and the inactive X) (Matarazzo et al., 2007;Jefferson et al., 2010). Similarly to epilepsy, loci-specific repositioning was observed in ICF, with other regions on chromosome 1 (*BTG2*, *CNN3*, *ID3*, and *RGS1*) and the pericentromeric heterochromatin of chromosome 9 not repositioning in ICF (Jefferson et al., 2010;Dupont et al., 2012). Pericentromeric loci are not the only repeat sequences to be spatially affected in disease. Aberrant telomere clustering has been identified in several diseases, including cancer and

Alzheimer's, often due to telomere dysfunction, and the degree of clustering can reflect the aggressiveness of the disease (Chuang et al., 2004;Gadji et al., 2010;Mathur et al., 2014).

Loci-specific repositioning also occurs in laminopathies (Figure 2) (Meaburn et al., 2007;Taimen et al., 2009;Mewborn et al., 2010;Mattout et al., 2011;Mehta et al., 2011;McCord et al., 2013), a wide ranging group of diseases characterized by mutations in lamin A/C, and includes Emery-Dreifuss muscular dystrophy and the premature aging disease Hutchinson-Gilford progeria syndrome (HGPS) (Dittmer and Misteli, 2011). The organization of chromosomes in proliferating laminopathy fibroblasts cells mimics that of normal quiescent cells, with chromosomes 13 and 18 shifted to a more internal position, chromosome 10 repositioning towards the nuclear periphery, and chromosome 4 and X remaining at the nuclear periphery (Meaburn et al., 2007;Mewborn et al., 2010;Mehta et al., 2011). Generally, the spatial reorganization of the genome very similar between different laminopathy patients, regardless of the disease or mutation present (Meaburn et al., 2007;Mewborn et al., 2010), the exception being that chromosome 13 is more peripheral in patients with " 303 or D596N *LMNA* mutations (Mewborn et al., 2010). Moreover, the spatial organization of the genome in asymptomatic laminopathy carriers is very similar to the laminopathy patients (Meaburn et al., 2007). Taken together, this suggests that repositioning results from the presence of aberrant A-type lamin rather than the specific disease *per se*. The release of chromosome 13 and 18 from the nuclear periphery may be linked to changes in chromatin status, since there is a reduction of heterochromatin-specific markers, including HP1± and histone H3K9 methylation, in HGPS fibroblasts (Scaffidi and Misteli, 2005), or it may be due to an uncoupling of cell-cycle regulation and spatial positioning patterns (Meaburn et al., 2007). In progeria at least, the redistribution of the genome may be progressive. An abnormal clustering of centromeres associated with the *LMNA* E145K mutation only occurs in nuclei with aberrant shapes, and the prevalence increases with increased time in culture (Taimen et al., 2009). Compared to proliferating normal fibroblasts, a dramatic genome-wide reduction in the spatial separation of active and inactive chromatin was observed in senescent HGPS fibroblasts, but not in proliferating HGPS cultures (McCord et al., 2013). Some of these differences in interaction frequencies were senescence- rather than disease-related as they were also detected in normal senescent fibroblasts, however, differences between senescent normal and HGPS cells were detected (Chandra et al., 2015). It remains unclear how disease related these differences are, as it could be more a reflection of the type of senescence being compared. The HGPS cells used had reached (early) replicative senescence by continued culture (McCord et al., 2013), whereas senescence was induced in the normal cells by oncogene activation, which, unlike replicative senescence, forms senescence-associated heterochromatin foci (Chandra et al., 2015). The laminopathy-related spatial positioning patterns are tissue-specific, and chromosomal positioning abnormalities have not been detected in laminopathy patient lymphoblasts, a cell-type that does not require A-type lamins (Boyle et al., 2001;Meaburn et al., 2005). Further, in a *C. elegans* model of Emery-Dreifuss muscular dystrophy, a muscle-specific promotor was retained at the NE in the muscles of diseased animals, however, the release from the NE of a gut-specific promotor was not affected in gut tissue (Mattout et al., 2011).

In benign prostate hyperplasia tissues *MMP2* shifts to a more peripheral position than normal prostate tissue, whereas the positions of *MMP9* and *FLI1* are unaffected (Figure 2) (Leshner et al., 2016). In lymphocytes from Down syndrome patients, two (or three) copies of chromosome 21 clusters together more frequently than in diploid control cells (Figure 2) (Paz et al., 2013;Paz et al., 2015). Moreover, *SOD1*, which is located on chromosome 21, is more peripherally located in Down syndrome (Paz et al., 2015). This altered position is not simply a consequence of the presence of an additional chromosome 21, however, as the radial position of *DYRK1A*, which also maps to

chromosome 21, is unaffected (Paz et al., 2015). It is not only chronic diseases that are associated with a spatial reorganization of the genome. Short-term repositioning of some, but not all, genes or chromosomes occurs after viral or parasitic infection (Li et al., 2010;Knight et al., 2011;Arican-Goktas et al., 2014). Chromosome 17, but not 18, relocates to a more peripheral position in human lymphocytes within 24 hours of Epstein-Barr virus infection (Li et al., 2010). Similarly, dynamic radial repositioning of *actin*, *ferritin* and *hsp70*, occurs in both cultured snail cells and in intact live snails within hours of active parasitic infection, with the repositioning correlating to changes in gene expression (Knight et al., 2011;Arican-Goktas et al., 2014).

Local disruptions to hierarchical genome organization can be important for disease progression. High-resolution mapping of the 3D genome has revealed that beyond a spatial separation of gene-rich and gene-poor chromatin, chromosomes further fold into a succession of ten to hundreds of kb long self-associating globular domains, known as topologically associating domains (TADs) (Dixon et al., 2012;Nora et al., 2012;Sexton et al., 2012). Individual TADs are stably conserved between species and cell types and are separated by sharp boundaries that are enriched in histone marks associated with active genes, SINEs, binding sites for the chromatin-binding protein CTCF and housekeeping genes (Dixon et al., 2012). TAD boundaries are believed to be important for gene regulation, by acting as insulators, inhibiting the expansion of either heterochromatin or active chromatin into a neighboring TADs and by increasing the frequency of specific regulatory interactions by confining certain promoters and enhances into a single TAD (Dixon et al., 2012;Sexton et al., 2012;Narendra et al., 2015). Consentient with this, genes within TAD domains are co-expressed during differentiation and disruption of TAD boundaries results in a partial or complete fusion of neighboring TADs and altered gene expression (Nora et al., 2012;Lupianez et al., 2015;Narendra et al., 2015;Hnisz et al., 2016). Disruption to the TAD boundary near the *EPHA4* locus by deletion, duplication or inversion of DNA sequences at the boundary results in limb deformation syndromes (Lupianez et al., 2015). In normal limb development *EPHA4* is active but genes in neighboring TADs are silent. The loss of the TAD boundary allows enhancer-promoter interactions between regulatory sequences normally separated into different TADs, and consequently results in the spuriously activation of the neighboring genes in the mis-fused TAD (Lupianez et al., 2015). Similarly, cancer-associated micro-deletions or mutations at TAD boundaries can activate oncogenes, and may represent a common mechanism of gene mis-regulation in multiple cancers (Hnisz et al., 2016). The study of TADs is still in its infancy, and most likely disruption to TAD boundaries will be detected as functionally important in many other diseases.

Spatial genome organization in cancer

Despite the high level of genomic instability associated with many cancers, which could conceivably be expected to result in a large scale disruption to the spatial organization of the genome, there is a general conservation of spatial positioning patterns in cancer, with the majority of genes and chromosomes not altering nuclear position (Kozubek et al., 2002;Parada et al., 2002;Cremer et al., 2003;Meaburn and Misteli, 2008;Meaburn et al., 2009;Timme et al., 2011;Zeitz et al., 2013;Leshner et al., 2016;Meaburn et al., 2016b). For example, 44 of 47 (94%) genes spatially mapped in human prostate tissues do not alter radial position in prostate cancer and the radial positions of 13 out of 23 (57%) genes are conserved in breast cancer (Meaburn et al., 2009;Leshner et al., 2016;Meaburn et al., 2016b). While genome positioning patterns remain largely conserved in cancer, some genes and chromosomes occupy distinct nuclear positions in cancerous cells compared to their normal or benign counterparts, with the patterns of reorganization differing between different cancers (Figure 2) (Cremer et al., 2003;Murata et al., 2007;Meaburn and Misteli, 2008;Meaburn et al., 2009;Wiech et

al., 2009;Zeitz et al., 2013;Leshner et al., 2016;Meaburn et al., 2016b). For instance, the radial positions of chromosomes 18 and 19 are affected in many cancer types, including thyroid, colon and cervical cancer, with a tendency for chromosome 18 to become more internally located and chromosome 19 to shift away from the center of the nucleus (Cremer et al., 2003;Murata et al., 2007;Wiech et al., 2009). However, in some cervical cancers, chromosome 18 becomes more internally located (Wiech et al., 2009). In breast cancer cell lines there is a significant change to the set of genes that are close spatial neighbors of *IGFBP3* (Zeitz et al., 2013). Moreover, ten genes (*FLI1, HES5, MMP9, HSP90AA1, TGFB3, MYC, ERBB2, FOSL2, CSF1R* and *AKT1*) have been identified to radially reposition in epithelial cells of breast cancer tissues (Meaburn et al., 2009;Meaburn et al., 2016b) and *FLI1, MMP9* and *MMP2* occupy alternative radial locations in prostate cancer (Leshner et al., 2016).

Interestingly, of the eleven genes so far reported with altered radial position in either breast or prostate cancer, only *MMP9* and *FLI1* robustly reposition in both types of cancer (Figure 2) (Leshner et al., 2016;Meaburn et al., 2016b). This suggests cancer-type specific repositioning, with different sets of genes repositioning in breast and prostate cancer. Similarly, *BCL2* repositions in a BCL2-positive cervical squamous carcinoma, but not in a BCL2-negative cervical squamous carcinoma (Wiech et al., 2009), nor in breast (Meaburn et al., 2009) or prostate cancer (Leshner et al., 2016). When taken together with the findings discussed above that a genomic region can behave differently, with respect to repositioning between different non-cancerous diseases, it suggests that the overall organization of the genome in disease is, mostly, specific to the disease and not a consequence of a more general “stress” response. In keeping with this, of the genes that occupy distinct radial positions in breast and/or prostate cancer, only *MMP2* is also commonly repositioned in non-malignant disease; but even for this gene it cannot be a general disease response as *MMP2* repositions in prostate but not breast cancer (Figure 2) (Leshner et al., 2016;Meaburn et al., 2016b).

It is interesting to note that many of the factors implicated in influencing gene positioning patterns are often altered in cancer, e.g lamins, gene expression, proliferation status, chromatin status and histone modifications. However, the precise mechanisms involved in the mis-organization of the genome in cancer are unclear. It would seem that, for the radially repositioned genes at least, transcription of the locus itself is not the key to the repositioning. No correlation was found for the repositioning of a given gene and its transcriptional output in a model of early cancer (Meaburn and Misteli, 2008). Moreover, cancer-associated genes, that are known to have altered expression in cancer, often did not reposition in breast or prostate cancer (Meaburn and Misteli, 2008;Meaburn et al., 2009;Leshner et al., 2016). Even for the cancer-associated genes that do reposition in cancer, it may not be altered transcription of the loci that is driving the alternative positioning pattern. For example, although elevated expression of *MMP9* and *MMP2* is a marker of poor prognosis in prostate cancer, and linked to metastasis, their expression is from tumor-associated stroma cells and not from the cancerous epithelial cells, where the gene repositioning was detected (Egeblad and Werb, 2002;Leshner et al., 2016). This does not rule out gene expression as a factor in repositioning, and further studies are required that measure gene expression changes in extended chromosomal regions of the repositioned gene.

An increase in proliferation is a hallmark of cancer. The spatial reorganization of the genome in cancer does not seem to simply be a reflection of a transition from quiescent normal breast or prostate tissue to a proliferating tumor. Spatial genome organization in cancer cells do not mimic proliferating (or quiescent) breast epithelial cells (Meaburn and Misteli, 2008). This is not surprising, given the fact that the majority of cells within a cancerous tumor are actually not proliferating. Ki-67 is

commonly used as a marker of cellular proliferation, since it is present in all stages of the cell cycle with the exception of G_0. Breast cancers that contain ≥30% Ki-67 positive cells are classified as highly proliferative cancers, and the majority of breast cancers, almost 60%, have only 10% or less of cells positive for Ki-67 (de Azambuja et al., 2007;Jonat and Arnold, 2011). In fact, no feature of a genomic locus has yet been identified that enables the prediction of whether a gene will reposition or not in cancer (Meaburn et al., 2009;Leshner et al., 2016;Meaburn et al., 2016b).

Clinical biomarker potential

Regardless of why the genome is spatially reorganized in the nuclei of cancer cells, the small scale studies so far performed suggest that these differences in positioning patterns have the potential to be exploited for diagnostic use (Meaburn et al., 2009;Leshner et al., 2016;Meaburn et al., 2016b). Distinguishing cancer from normal tissue by spatial gene positioning patterns could practically be integrated into clinical use because it requires only a small tissue sample for analysis (100-1000 cells), meaning it will not require additional invasive procedures for the patient. Moreover, FISH is currently already used in diagnostic labs, thus, the infrastructure for such analysis already exists in the clinic. Importantly for clinical applications, for most genes tested in breast and prostate tissues false positive rates were low since for the vast majority of genes spatial positioning patterns are highly similar between individuals in non-diseased tissue (Borden and Manuelidis, 1988;Wiech et al., 2005;Murata et al., 2007;Meaburn et al., 2009;Leshner et al., 2016;Meaburn et al., 2016b) and repositioning events did not generally occur in non-malignant breast and prostate disease (Meaburn et al., 2009;Leshner et al., 2016;Meaburn et al., 2016b). There were a few notable exceptions, *MMP2* repositions in both cancer and non-malignant disease, and the radial position of a few genes, such as *CCND1* and *TIMP3*, were highly variable between normal prostate tissues. This highlights that each candidate marker gene must be rigorously tested to eliminate genes with high false positive rates, as is standard practice for any marker brought to the clinic. Critically, particularly when genes are used in combination, spatial positioning patterns can detect breast or prostate cancer with high accuracy (Meaburn et al., 2009;Leshner et al., 2016;Meaburn et al., 2016b). When genes are used as markers singularly, between 64-100% of samples are correctly identified as cancer based on radial positioning patterns. Multiplexing genes improved the accuracy of cancer detection for genes with lower sensitivities, reducing false negative rates (Meaburn et al., 2009;Leshner et al., 2016;Meaburn et al., 2016b). Repositioning events are independent of variations in copy number and even in the background of highly variable, and in some cases large scale, genomic instability between cancer specimens, it is possible to use gene positioning to accurately detect cancers (Meaburn et al., 2009;Leshner et al., 2016;Meaburn et al., 2016b).

Although these studies represent the largest analysis of genome organization in cancerous tissues performed to date, the eleven genes identified as potential breast or prostate cancer biomarkers were analyzed in a low number of individuals (11-19 cancers, 6-10 normal tissues and 5 non-malignant disease tissues) (Meaburn et al., 2009;Leshner et al., 2016;Meaburn et al., 2016b). Larger scale follow up studies are required to assess the sensitivity and specificity of these markers, to determine if they are strong enough for clinical use. It will be important to compare gene-positioning biomarkers to existing diagnostic methodologies and to establish if using the various methods in combination, or alone, improves diagnostic accuracy. Additionally, the original studies were not designed to determine if the spatial organization of the genome in cancer has prognostic value. Some of the genes so far identified are unlikely to be useful for prognostics. For example, *FLI1* repositions in 100% (10/10) of breast cancers and 92.9% (13/14) of prostate cancers (Leshner et al., 2016;Meaburn et al., 2016b), rates far too high to suggest they can be used to stratify indolent and

aggressive cancers. Future screening studies are required, using a highly defined set of indolent and aggressive cancers. Given the fact that the position of a gene can vary between cancers derived from the same organ, and between cancers from different organs (Meaburn et al., 2009;Wiech et al., 2009;Leshner et al., 2016;Meaburn et al., 2016b), it suggests the possibility that the spatial organization of the genome can be used to sub-type cancers for prognostic purposes. It is "simply" a matter of finding the right genes. Since spatial reorganization of the genome has been identified in multiple human diseases, it is likely that the same principle of using spatial genome positioning patterns as a diagnostic biomarker could be applied to any disease.

Summery

There is no doubt that the genome is non-randomly organized in interphase nuclei. However, a deep understanding of the functional relevance of the spatial organization of the genome and the molecular mechanisms required to correctly position genes and chromosomes has proved more elusive. Until recently, due to practical constraints, loci could only realistically be studied in virtual isolation. Yet it is increasingly emerging that there is likely multiple mechanisms important for positioning a loci, and that the mechanism employed depends on the individual gene and the cellular context. With the rapidly reducing cost of sequencing and the advent of multiple biochemical methods to analyze genome organization on a larger scale, the tools are now in place to study the spatial organization of chromatin on a genome wide scale. It will be important to compare these positioning maps to gene expression data, epigenetic maps, proteome data, non-coding RNA, replication timings etc, in combination. Moreover, it will be important to not only ask what is changing at the level of an individual locus, it will be vital to consider the chromosomal neighborhood at large. The new technologies will not make FISH obsolete; in fact, quite the opposite. It will be critical to study candidate regions, identified by population-based biochemical methods, in greater detail using single cell FISH analysis. For example, in how many cells is a given positioning patterns found? Do both alleles of a gene behave in the same manner? Are positioning patterns found in the population mutually exclusive at the single cell level? From here, loci or nuclear factors can then be manipulated to determine the true functional relevance, beyond correlation.

The genome is spatially reorganized in disease. Accumulating evidence suggests that these repositioning patterns can be exploited for diagnostic use. Currently, there is no way to predict which genes will reposition in cancer. As we gain a better understanding of how spatial positioning is regulated in a normal cell, it may become easier to predict regions that will be diagnostically interesting. The reverse is also true. Comparing positioning patterns between normal and diseased cells will inform our understanding of spatial genome organization. While it is exciting that proof-of-principle studies have identified spatial positioning of the genome as a potentially sensitive and specific biomarker of cancer, much work is yet to be done. large-scale follow-up studies are required to determine the feasibility and usefulness of spatial genome organization-based diagnostic in the clinical setting. Moreover, while additional diagnostic tests have their use, there is urgent need for biomarkers that can distinguish aggressive cancers from indolent ones. These markers would have a tremendous impact on cancer patients, by guiding clinicians to the best treatment regime for an individual and reducing both under and over-treatment. As such, as future studies relating to genome organization for clinical use should focus on prognostic rather than simply diagnostic.

Abbreviation list

FISH = Fluorescence *in situ* hybridization
ICF = Immunodeficiency, Centromere instability and Facial anomalies syndrome
HGPS = Hutchinson-Gilford progeria syndrome
NE = Nuclear envelope
NPC = Nuclear pore complex
PSA = Prostate-specific antigen
TAD = Topologically associating domain

Author Contributions

KM wrote the review and prepared the figures.

Acknowledgments

The author thanks Drs Tom Misteli, Elizabeth Finn, Iain Sawyer and Sara Snyder (CCR, NCI, NIH) for critical reading of the manuscript and thoughtful suggestions.

Funding: This work was supported by Department of Defense Idea Awards (W81XWH-12-1-0224, W81XWH-15-1-0322).

Conflict of Interest Statement

Patent: Misteli T.A. and Meaburn K. (2009). Method for detection of cancer based on spatial genome organization. US Patent App. 13/062,247, European patent number 2321428. The authors declare that the research was conducted in the absence of any other commercial or financial relationships that could be construed as a potential conflict of interest.

References

Ahmad, A.S., Ormiston-Smith, N., and Sasieni, P.D. (2015). Trends in the lifetime risk of developing cancer in Great Britain: comparison of risk for those born from 1930 to 1960. *Br J Cancer* 112**,** 943-947. doi: 10.1038/bjc.2014.606.

Ahmed, S., Brickner, D.G., Light, W.H., Cajigas, I., McDonough, M., Froyshteter, A.B., Volpe, T., and Brickner, J.H. (2010). DNA zip codes control an ancient mechanism for gene targeting to the nuclear periphery. *Nat Cell Biol* 12**,** 111-118. doi: 10.1038/ncb2011.

Arican-Goktas, H.D., Ittiprasert, W., Bridger, J.M., and Knight, M. (2014). Differential spatial repositioning of activated genes in Biomphalaria glabrata snails infected with Schistosoma mansoni. *PLoS Negl Trop Dis* 8**,** e3013. doi: 10.1371/journal.pntd.0003013.

751 Belt, E.J., Fijneman, R.J., van den Berg, E.G., Bril, H., Delis-van Diemen, P.M., Tijssen, M., van
752 Essen, H.F., de Lange-de Klerk, E.S., Belien, J.A., Stockmann, H.B., Meijer, S., and Meijer,
753 G.A. (2011). Loss of lamin A/C expression in stage II and III colon cancer is associated with
754 disease recurrence. *Eur J Cancer* 47**,** 1837-1845. doi: 10.1016/j.ejca.2011.04.025.

755 Bian, Q., Khanna, N., Alvikas, J., and Belmont, A.S. (2013). beta-Globin cis-elements determine
756 differential nuclear targeting through epigenetic modifications. *J Cell Biol* 203**,** 767-783. doi:
757 10.1083/jcb.201305027.

758 Bickmore, W.A., and van Steensel, B. (2013). Genome architecture: domain organization of
759 interphase chromosomes. *Cell* 152**,** 1270-1284. doi: 10.1016/j.cell.2013.02.001.

760 Bleyer, A., and Welch, H.G. (2012). Effect of three decades of screening mammography on breast-
761 cancer incidence. *N Engl J Med* 367**,** 1998-2005. doi: 10.1056/NEJMoa1206809.

762 Bolzer, A., Kreth, G., Solovei, I., Koehler, D., Saracoglu, K., Fauth, C., Muller, S., Eils, R., Cremer,
763 C., Speicher, M.R., and Cremer, T. (2005). Three-dimensional maps of all chromosomes in
764 human male fibroblast nuclei and prometaphase rosettes. *PLoS Biol* 3**,** e157.

765 Borden, J., and Manuelidis, L. (1988). Movement of the X chromosome in epilepsy. *Science* 242**,**
766 1687-1691.

767 Boutanaev, A.M., Mikhaylova, L.M., and Nurminsky, D.I. (2005). The pattern of chromosome
768 folding in interphase is outlined by the linear gene density profile. *Mol Cell Biol* 25**,** 8379-
769 8386.

770 Boyle, S., Gilchrist, S., Bridger, J.M., Mahy, N.L., Ellis, J.A., and Bickmore, W.A. (2001). The
771 spatial organization of human chromosomes within the nuclei of normal and emerin-mutant
772 cells. *Hum Mol Genet* 10**,** 211-219.

773 Boyle, S., Rodesch, M.J., Halvensleben, H.A., Jeddeloh, J.A., and Bickmore, W.A. (2011).
774 Fluorescence in situ hybridization with high-complexity repeat-free oligonucleotide probes
775 generated by massively parallel synthesis. *Chromosome Res* 19**,** 901-909. doi:
776 10.1007/s10577-011-9245-0.

777 Brickner, D.G., Cajigas, I., Fondufe-Mittendorf, Y., Ahmed, S., Lee, P.C., Widom, J., and Brickner,
778 J.H. (2007). H2A.Z-mediated localization of genes at the nuclear periphery confers epigenetic
779 memory of previous transcriptional state. *PLoS Biol* 5**,** e81. doi:
780 10.1371/journal.pbio.0050081.

781 Brickner, J.H., and Walter, P. (2004). Gene recruitment of the activated INO1 locus to the nuclear
782 membrane. *PLoS Biol* 2**,** e342.

783 Bridger, J.M., Arican-Gotkas, H.D., Foster, H.A., Godwin, L.S., Harvey, A., Kill, I.R., Knight, M.,
784 Mehta, I.S., and Ahmed, M.H. (2014). The non-random repositioning of whole chromosomes
785 and individual gene loci in interphase nuclei and its relevance in disease, infection, aging, and
786 cancer. *Adv Exp Med Biol* 773**,** 263-279. doi: 10.1007/978-1-4899-8032-8_12.

787 Bridger, J.M., Boyle, S., Kill, I.R., and Bickmore, W.A. (2000). Re-modelling of nuclear architecture
788 in quiescent and senescent human fibroblasts. *Curr Biol* 10**,** 149-152.

789 Broers, J.L., and Ramaekers, F.C. (2014). The role of the nuclear lamina in cancer and apoptosis. *Adv*
790 *Exp Med Biol* 773**,** 27-48. doi: 10.1007/978-1-4899-8032-8_2.

Broers, J.L., Raymond, Y., Rot, M.K., Kuijpers, H., Wagenaar, S.S., and Ramaekers, F.C. (1993). Nuclear A-type lamins are differentially expressed in human lung cancer subtypes. *Am J Pathol* 143**,** 211-220.

Brown, J.M., Leach, J., Reittie, J.E., Atzberger, A., Lee-Prudhoe, J., Wood, W.G., Higgs, D.R., Iborra, F.J., and Buckle, V.J. (2006). Coregulated human globin genes are frequently in spatial proximity when active. *J Cell Biol* 172**,** 177-187.

Brown, K.E., Baxter, J., Graf, D., Merkenschlager, M., and Fisher, A.G. (1999). Dynamic repositioning of genes in the nucleus of lymphocytes preparing for cell division. *Mol. Cell* 3**,** 207-217.

Brown, K.E., Guest, S.S., Smale, S.T., Hahm, K., Merkenschlager, M., and Fisher, A.G. (1997). Association of transcriptionally silent genes with Ikaros complexes at centromeric heterochromatin. *Cell* 91**,** 845-854.

Capo-Chichi, C.D., Aguida, B., Chabi, N.W., Cai, Q.K., Offrin, G., Agossou, V.K., Sanni, A., and Xu, X.X. (2016). Lamin A/C deficiency is an independent risk factor for cervical cancer. *Cell Oncol (Dordr)* 39**,** 59-68. doi: 10.1007/s13402-015-0252-6.

Chambeyron, S., and Bickmore, W.A. (2004). Chromatin decondensation and nuclear reorganization of the HoxB locus upon induction of transcription. *Genes Dev* 18**,** 1119-1130. doi: 10.1101/gad.292104.

Chandra, T., Ewels, P.A., Schoenfelder, S., Furlan-Magaril, M., Wingett, S.W., Kirschner, K., Thuret, J.Y., Andrews, S., Fraser, P., and Reik, W. (2015). Global reorganization of the nuclear landscape in senescent cells. *Cell Rep* 10**,** 471-483. doi: 10.1016/j.celrep.2014.12.055.

Chang, A.J., Autio, K.A., Roach, M., 3rd, and Scher, H.I. (2014). High-risk prostate cancer-classification and therapy. *Nat Rev Clin Oncol* 11**,** 308-323. doi: 10.1038/nrclinonc.2014.68.

Chiarle, R., Zhang, Y., Frock, R.L., Lewis, S.M., Molinie, B., Ho, Y.J., Myers, D.R., Choi, V.W., Compagno, M., Malkin, D.J., Neuberg, D., Monti, S., Giallourakis, C.C., Gostissa, M., and Alt, F.W. (2011). Genome-wide translocation sequencing reveals mechanisms of chromosome breaks and rearrangements in B cells. *Cell* 147**,** 107-119. doi: 10.1016/j.cell.2011.07.049.

Chuang, C.H., Carpenter, A.E., Fuchsova, B., Johnson, T., de Lanerolle, P., and Belmont, A.S. (2006). Long-range directional movement of an interphase chromosome site. *Curr Biol* 16**,** 825-831. doi: 10.1016/j.cub.2006.03.059.

Chuang, T.C., Moshir, S., Garini, Y., Chuang, A.Y., Young, I.T., Vermolen, B., van den Doel, R., Mougey, V., Perrin, M., Braun, M., Kerr, P.D., Fest, T., Boukamp, P., and Mai, S. (2004). The three-dimensional organization of telomeres in the nucleus of mammalian cells. *BMC Biol* 2**,** 12.

Clemson, C.M., Hall, L.L., Byron, M., McNeil, J., and Lawrence, J.B. (2006). The X chromosome is organized into a gene-rich outer rim and an internal core containing silenced nongenic sequences. *Proc Natl Acad Sci U S A* 103**,** 7688-7693.

Clowney, E.J., LeGros, M.A., Mosley, C.P., Clowney, F.G., Markenskoff-Papadimitriou, E.C., Myllys, M., Barnea, G., Larabell, C.A., and Lomvardas, S. (2012). Nuclear aggregation of olfactory receptor genes governs their monogenic expression. *Cell* 151**,** 724-737. doi: 10.1016/j.cell.2012.09.043.

833 Cooperberg, M.R., Broering, J.M., and Carroll, P.R. (2009). Risk assessment for prostate cancer
834 metastasis and mortality at the time of diagnosis. *J Natl Cancer Inst* 101**,** 878-887. doi:
835 10.1093/jnci/djp122.

836 Cooperberg, M.R., Broering, J.M., and Carroll, P.R. (2010). Time trends and local variation in
837 primary treatment of localized prostate cancer. *J Clin Oncol* 28**,** 1117-1123. doi:
838 10.1200/JCO.2009.26.0133.

839 Cournac, A., Koszul, R., and Mozziconacci, J. (2016). The 3D folding of metazoan genomes
840 correlates with the association of similar repetitive elements. *Nucleic Acids Res* 44**,** 245-255.
841 doi: 10.1093/nar/gkv1292.

842 Cremer, M., Kupper, K., Wagler, B., Wizelman, L., Hase Jv, J., Weiland, Y., Kreja, L., Diebold, J.,
843 Speicher, M.R., and Cremer, T. (2003). Inheritance of gene density-related higher order
844 chromatin arrangements in normal and tumor cell nuclei. *J Cell Biol* 162**,** 809-820.

845 Cremer, T., and Cremer, C. (2001). Chromosome territories, nuclear architecture and gene regulation
846 in mammalian cells. *Nat Rev Genet* 2**,** 292-301.

847 Croft, J.A., Bridger, J.M., Boyle, S., Perry, P., Teague, P., and Bickmore, W.A. (1999). Differences
848 in the localization and morphology of chromosomes in the human nucleus. *J. Cell Biol.* 145**,**
849 1119-1131.

850 D'Amico, A.V., Whittington, R., Malkowicz, S.B., Schultz, D., Blank, K., Broderick, G.A.,
851 Tomaszewski, J.E., Renshaw, A.A., Kaplan, I., Beard, C.J., and Wein, A. (1998).
852 Biochemical outcome after radical prostatectomy, external beam radiation therapy, or
853 interstitial radiation therapy for clinically localized prostate cancer. *JAMA* 280**,** 969-974.

854 Dai, X., Li, T., Bai, Z., Yang, Y., Liu, X., Zhan, J., and Shi, B. (2015). Breast cancer intrinsic
855 subtype classification, clinical use and future trends. *Am J Cancer Res* 5**,** 2929-2943.

856 Davidson, P.M., Denais, C., Bakshi, M.C., and Lammerding, J. (2014). Nuclear deformability
857 constitutes a rate-limiting step during cell migration in 3-D environments. *Cell Mol Bioeng* 7**,**
858 293-306. doi: 10.1007/s12195-014-0342-y.

859 de Azambuja, E., Cardoso, F., de Castro, G., Jr., Colozza, M., Mano, M.S., Durbecq, V., Sotiriou, C.,
860 Larsimont, D., Piccart-Gebhart, M.J., and Paesmans, M. (2007). Ki-67 as prognostic marker
861 in early breast cancer: a meta-analysis of published studies involving 12,155 patients. *Br J*
862 *Cancer* 96**,** 1504-1513. doi: 10.1038/sj.bjc.6603756.

863 Dekker, J., and Misteli, T. (2015). *Long-range genome interactions* Cold Spring Harbor Laboratory
864 Press.

865 Demmerle, J., Koch, A.J., and Holaska, J.M. (2013). Emerin and histone deacetylase 3 (HDAC3)
866 cooperatively regulate expression and nuclear positions of MyoD, Myf5, and Pax7 genes
867 during myogenesis. *Chromosome Res* 21**,** 765-779. doi: 10.1007/s10577-013-9381-9.

868 Dittmer, T.A., and Misteli, T. (2011). The lamin protein family. *Genome Biol* 12**,** 222. doi:
869 10.1186/gb-2011-12-5-222.

870 Dixon, J.R., Selvaraj, S., Yue, F., Kim, A., Li, Y., Shen, Y., Hu, M., Liu, J.S., and Ren, B. (2012).
871 Topological domains in mammalian genomes identified by analysis of chromatin interactions.
872 *Nature* 485**,** 376-380. doi: 10.1038/nature11082.

873 Draisma, G., Etzioni, R., Tsodikov, A., Mariotto, A., Wever, E., Gulati, R., Feuer, E., and de Koning,
874 H. (2009). Lead time and overdiagnosis in prostate-specific antigen screening: importance of
875 methods and context. *J Natl Cancer Inst* 101**,** 374-383. doi: 10.1093/jnci/djp001.

876 Dultz, E., Tjong, H., Weider, E., Herzog, M., Young, B., Brune, C., Mullner, D., Loewen, C., Alber,
877 F., and Weis, K. (2016). Global reorganization of budding yeast chromosome conformation in
878 different physiological conditions. *J Cell Biol* 212**,** 321-334. doi: 10.1083/jcb.201507069.

879 Dundr, M., Ospina, J.K., Sung, M.H., John, S., Upender, M., Ried, T., Hager, G.L., and Matera, A.G.
880 (2007). Actin-dependent intranuclear repositioning of an active gene locus in vivo. *J Cell Biol*
881 179**,** 1095-1103. doi: 10.1083/jcb.200710058.

882 Dupont, C., Guimiot, F., Perrin, L., Marey, I., Smiljkovski, D., Le Tessier, D., Lebugle, C.,
883 Baumann, C., Bourdoncle, P., Tabet, A.C., Aboura, A., Benzacken, B., and Dupont, J.M.
884 (2012). 3D position of pericentromeric heterochromatin within the nucleus of a patient with
885 ICF syndrome. *Clin Genet* 82**,** 187-192. doi: 10.1111/j.1399-0004.2011.01697.x.

886 Egeblad, M., and Werb, Z. (2002). New functions for the matrix metalloproteinases in cancer
887 progression. *Nat Rev Cancer* 2**,** 161-174. doi: 10.1038/nrc745.

888 Egecioglu, D., and Brickner, J.H. (2011). Gene positioning and expression. *Curr Opin Cell Biol* 23**,**
889 338-345. doi: 10.1016/j.ceb.2011.01.001.

890 Epstein, J.I., Egevad, L., Amin, M.B., Delahunt, B., Srigley, J.R., Humphrey, P.A., and Grading, C.
891 (2016). The 2014 International Society of Urological Pathology (ISUP) Consensus
892 Conference on Gleason Grading of Prostatic Carcinoma: Definition of Grading Patterns and
893 Proposal for a New Grading System. *Am J Surg Pathol* 40**,** 244-252. doi:
894 10.1097/PAS.0000000000000530.

895 Ferrai, C., de Castro, I.J., Lavitas, L., Chotalia, M., and Pombo, A. (2010). Gene positioning. *Cold*
896 *Spring Harb Perspect Biol* 2**,** a000588. doi: 10.1101/cshperspect.a000588.

897 Ferte, C., Andre, F., and Soria, J.C. (2010). Molecular circuits of solid tumors: prognostic and
898 predictive tools for bedside use. *Nat Rev Clin Oncol* 7**,** 367-380. doi:
899 10.1038/nrclinonc.2010.84.

900 Finlan, L.E., Sproul, D., Thomson, I., Boyle, S., Kerr, E., Perry, P., Ylstra, B., Chubb, J.R., and
901 Bickmore, W.A. (2008). Recruitment to the nuclear periphery can alter expression of genes in
902 human cells. *PLoS Genet* 4**,** e1000039.

903 Foster, H.A., Griffin, D.K., and Bridger, J.M. (2012). Interphase chromosome positioning in in vitro
904 porcine cells and ex vivo porcine tissues. *BMC Cell Biol* 13**,** 30. doi: 10.1186/1471-2121-13-
905 30.

906 Francastel, C., Walters, M.C., Groudine, M., and Martin, D.I. (1999). A functional enhancer
907 suppresses silencing of a transgene and prevents its localization close to centrometric
908 heterochromatin. *Cell* 99**,** 259-269.

909 Fraser, P., and Bickmore, W. (2007). Nuclear organization of the genome and the potential for gene
910 regulation. *Nature* 447**,** 413-417. doi: 10.1038/nature05916.

911 Gadji, M., Fortin, D., Tsanaclis, A.M., Garini, Y., Katzir, N., Wienburg, Y., Yan, J., Klewes, L.,
912 Klonisch, T., Drouin, R., and Mai, S. (2010). Three-dimensional nuclear telomere architecture
913 is associated with differential time to progression and overall survival in glioblastoma
914 patients. *Neoplasia* 12**,** 183-191.

915 Goetze, S., Mateos-Langerak, J., and van Driel, R. (2007). Three-dimensional genome organization
916 in interphase and its relation to genome function. *Semin Cell Dev Biol* 18**,** 707-714. doi:
917 10.1016/j.semcdb.2007.08.007.

918 Guelen, L., Pagie, L., Brasset, E., Meuleman, W., Faza, M.B., Talhout, W., Eussen, B.H., de Klein,
919 A., Wessels, L., de Laat, W., and van Steensel, B. (2008). Domain organization of human
920 chromosomes revealed by mapping of nuclear lamina interactions. *Nature* 453**,** 948-951. doi:
921 10.1038/nature06947.

922 Hacisuleyman, E., Goff, L.A., Trapnell, C., Williams, A., Henao-Mejia, J., Sun, L., McClanahan, P.,
923 Hendrickson, D.G., Sauvageau, M., Kelley, D.R., Morse, M., Engreitz, J., Lander, E.S.,
924 Guttman, M., Lodish, H.F., Flavell, R., Raj, A., and Rinn, J.L. (2014). Topological
925 organization of multichromosomal regions by the long intergenic noncoding RNA Firre. *Nat*
926 *Struct Mol Biol* 21**,** 198-206. doi: 10.1038/nsmb.2764.

927 Hakim, O., Resch, W., Yamane, A., Klein, I., Kieffer-Kwon, K.R., Jankovic, M., Oliveira, T.,
928 Bothmer, A., Voss, T.C., Ansarah-Sobrinho, C., Mathe, E., Liang, G., Cobell, J., Nakahashi,
929 H., Robbiani, D.F., Nussenzweig, A., Hager, G.L., Nussenzweig, M.C., and Casellas, R.
930 (2012). DNA damage defines sites of recurrent chromosomal translocations in B
931 lymphocytes. *Nature* 484**,** 69-74. doi: 10.1038/nature10909.

932 Hakim, O., Sung, M.H., Nakayamada, S., Voss, T.C., Baek, S., and Hager, G.L. (2013). Spatial
933 congregation of STAT binding directs selective nuclear architecture during T-cell functional
934 differentiation. *Genome Res* 23**,** 462-472. doi: 10.1101/gr.147652.112.

935 Hakim, O., Sung, M.H., Voss, T.C., Splinter, E., John, S., Sabo, P.J., Thurman, R.E.,
936 Stamatoyannopoulos, J.A., de Laat, W., and Hager, G.L. (2011). Diverse gene
937 reprogramming events occur in the same spatial clusters of distal regulatory elements.
938 *Genome Res* 21**,** 697-706. doi: 10.1101/gr.111153.110.

939 Hanahan, D., and Weinberg, R.A. (2011). Hallmarks of cancer: the next generation. *Cell* 144**,** 646-
940 674. doi: 10.1016/j.cell.2011.02.013.

941 Harewood, L., Schutz, F., Boyle, S., Perry, P., Delorenzi, M., Bickmore, W.A., and Reymond, A.
942 (2010). The effect of translocation-induced nuclear reorganization on gene expression.
943 *Genome Res* 20**,** 554-564. doi: 10.1101/gr.103622.109.

944 Harr, J.C., Gonzalez-Sandoval, A., and Gasser, S.M. (2016). Histones and histone modifications in
945 perinuclear chromatin anchoring: from yeast to man. *EMBO Rep* 17**,** 139-155. doi:
946 10.15252/embr.201541809.

947 Harr, J.C., Luperchio, T.R., Wong, X., Cohen, E., Wheelan, S.J., and Reddy, K.L. (2015). Directed
948 targeting of chromatin to the nuclear lamina is mediated by chromatin state and A-type
949 lamins. *J Cell Biol* 208**,** 33-52. doi: 10.1083/jcb.201405110.

950 Hastings, R. (2010). Quality control in FISH as part of a laboratory's quality management system.
951 *Methods Mol Biol* 659**,** 249-259. doi: 10.1007/978-1-60761-789-1_18.

952 Hehlmann, R., Hochhaus, A., Baccarani, M., and European, L. (2007). Chronic myeloid leukaemia.
953 *Lancet* 370**,** 342-350. doi: 10.1016/S0140-6736(07)61165-9.

954 Hiratani, I., Ryba, T., Itoh, M., Yokochi, T., Schwaiger, M., Chang, C.W., Lyou, Y., Townes, T.M.,
955 Schubeler, D., and Gilbert, D.M. (2008). Global reorganization of replication domains during
956 embryonic stem cell differentiation. *PLoS Biol* 6**,** e245. doi: 10.1371/journal.pbio.0060245.

957 Hnisz, D., Weintraub, A.S., Day, D.S., Valton, A.L., Bak, R.O., Li, C.H., Goldmann, J., Lajoie, B.R.,
958 Fan, Z.P., Sigova, A.A., Reddy, J., Borges-Rivera, D., Lee, T.I., Jaenisch, R., Porteus, M.H.,
959 Dekker, J., and Young, R.A. (2016). Activation of proto-oncogenes by disruption of
960 chromosome neighborhoods. *Science*. doi: 10.1126/science.aad9024.

961 Hogan, M.S., Parfitt, D.E., Zepeda-Mendoza, C.J., Shen, M.M., and Spector, D.L. (2015). Transient
962 pairing of homologous Oct4 alleles accompanies the onset of embryonic stem cell
963 differentiation. *Cell Stem Cell* 16**,** 275-288. doi: 10.1016/j.stem.2015.02.001.

964 Ioannou, D., Kandukuri, L., Quadri, A., Becerra, V., Simpson, J.L., and Tempest, H.G. (2015).
965 Spatial positioning of all 24 chromosomes in the lymphocytes of six subjects: evidence of
966 reproducible positioning and spatial repositioning following DNA damage with hydrogen
967 peroxide and ultraviolet B. *PLoS One* 10**,** e0118886. doi: 10.1371/journal.pone.0118886.

968 Jefferson, A., Colella, S., Moralli, D., Wilson, N., Yusuf, M., Gimelli, G., Ragoussis, J., and Volpi,
969 E.V. (2010). Altered intra-nuclear organisation of heterochromatin and genes in ICF
970 syndrome. *PLoS One* 5**,** e11364. doi: 10.1371/journal.pone.0011364.

971 Jonat, W., and Arnold, N. (2011). Is the Ki-67 labelling index ready for clinical use? *Ann Oncol* 22**,**
972 500-502. doi: 10.1093/annonc/mdq732.

973 Khanna, N., Hu, Y., and Belmont, A.S. (2014). HSP70 transgene directed motion to nuclear speckles
974 facilitates heat shock activation. *Curr Biol* 24**,** 1138-1144. doi: 10.1016/j.cub.2014.03.053.

975 Kind, J., Pagie, L., de Vries, S.S., Nahidiazar, L., Dey, S.S., Bienko, M., Zhan, Y., Lajoie, B., de
976 Graaf, C.A., Amendola, M., Fudenberg, G., Imakaev, M., Mirny, L.A., Jalink, K., Dekker, J.,
977 van Oudenaarden, A., and van Steensel, B. (2015). Genome-wide maps of nuclear lamina
978 interactions in single human cells. *Cell* 163**,** 134-147. doi: 10.1016/j.cell.2015.08.040.

979 Kind, J., Pagie, L., Ortabozkoyun, H., Boyle, S., de Vries, S.S., Janssen, H., Amendola, M., Nolen,
980 L.D., Bickmore, W.A., and van Steensel, B. (2013). Single-cell dynamics of genome-nuclear
981 lamina interactions. *Cell* 153**,** 178-192. doi: 10.1016/j.cell.2013.02.028.

982 Klein, I.A., Resch, W., Jankovic, M., Oliveira, T., Yamane, A., Nakahashi, H., Di Virgilio, M.,
983 Bothmer, A., Nussenzweig, A., Robbiani, D.F., Casellas, R., and Nussenzweig, M.C. (2011).
984 Translocation-capture sequencing reveals the extent and nature of chromosomal
985 rearrangements in B lymphocytes. *Cell* 147**,** 95-106. doi: 10.1016/j.cell.2011.07.048.

986 Knight, M., Ittiprasert, W., Odoemelam, E.C., Adema, C.M., Miller, A., Raghavan, N., and Bridger,
987 J.M. (2011). Non-random organization of the Biomphalaria glabrata genome in interphase
988 Bge cells and the spatial repositioning of activated genes in cells co-cultured with
989 Schistosoma mansoni. *Int J Parasitol* 41**,** 61-70. doi: 10.1016/j.ijpara.2010.07.015.

990 Kong, L., Schafer, G., Bu, H., Zhang, Y., Zhang, Y., and Klocker, H. (2012). Lamin A/C protein is
991 overexpressed in tissue-invading prostate cancer and promotes prostate cancer cell growth,
992 migration and invasion through the PI3K/AKT/PTEN pathway. *Carcinogenesis* 33**,** 751-759.
993 doi: 10.1093/carcin/bgs022.

994 Kosak, S.T., Skok, J.A., Medina, K.L., Riblet, R., Le Beau, M.M., Fisher, A.G., and Singh, H.
995 (2002). Subnuclear compartmentalization of immunoglobulin loci during lymphocyte
996 development. *Science* 296**,** 158-162.

997 Kozubek, S., Lukasova, E., Jirsova, P., Koutna, I., Kozubek, M., Ganova, A., Bartova, E., Falk, M.,
998 and Pasekova, R. (2002). 3D Structure of the human genome: order in randomness.
999 *Chromosoma* 111**,** 321-331. doi: 10.1007/s00412-002-0210-8.

Kruhlak, M.J., Celeste, A., Dellaire, G., Fernandez-Capetillo, O., Muller, W.G., McNally, J.G., Bazett-Jones, D.P., and Nussenzweig, A. (2006). Changes in chromatin structure and mobility in living cells at sites of DNA double-strand breaks. *J Cell Biol* 172**,** 823-834. doi: 10.1083/jcb.200510015.

Kubben, N., Adriaens, M., Meuleman, W., Voncken, J.W., van Steensel, B., and Misteli, T. (2012). Mapping of lamin A- and progerin-interacting genome regions. *Chromosoma* 121**,** 447-464. doi: 10.1007/s00412-012-0376-7.

Kumaran, R.I., and Spector, D.L. (2008). A genetic locus targeted to the nuclear periphery in living cells maintains its transcriptional competence. *J Cell Biol* 180**,** 51-65.

Lambros, M.B., Natrajan, R., and Reis-Filho, J.S. (2007). Chromogenic and fluorescent in situ hybridization in breast cancer. *Hum Pathol* 38**,** 1105-1122. doi: 10.1016/j.humpath.2007.04.011.

Lelek, M., Casartelli, N., Pellin, D., Rizzi, E., Souque, P., Severgnini, M., Di Serio, C., Fricke, T., Diaz-Griffero, F., Zimmer, C., Charneau, P., and Di Nunzio, F. (2015). Chromatin organization at the nuclear pore favours HIV replication. *Nat Commun* 6**,** 6483. doi: 10.1038/ncomms7483.

Leshner, M., Devine, M., Roloff, G.W., True, L.D., Misteli, T., and Meaburn, K.J. (2016). Locus-specific gene repositioning in prostate cancer. *Mol Biol Cell* 27**,** 236-246. doi: 10.1091/mbc.E15-05-0280.

Li, C., Shi, Z., Zhang, L., Huang, Y., Liu, A., Jin, Y., Yu, Y., Bai, J., Chen, D., Gendron, C., Liu, X., and Fu, S. (2010). Dynamic changes of territories 17 and 18 during EBV-infection of human lymphocytes. *Mol Biol Rep* 37**,** 2347-2354. doi: 10.1007/s11033-009-9740-y.

Liang, Y., and Hetzer, M.W. (2011). Functional interactions between nucleoporins and chromatin. *Curr Opin Cell Biol* 23**,** 65-70. doi: 10.1016/j.ceb.2010.09.008.

Lieberman-Aiden, E., van Berkum, N.L., Williams, L., Imakaev, M., Ragoczy, T., Telling, A., Amit, I., Lajoie, B.R., Sabo, P.J., Dorschner, M.O., Sandstrom, R., Bernstein, B., Bender, M.A., Groudine, M., Gnirke, A., Stamatoyannopoulos, J., Mirny, L.A., Lander, E.S., and Dekker, J. (2009). Comprehensive mapping of long-range interactions reveals folding principles of the human genome. *Science* 326**,** 289-293. doi: 10.1126/science.1181369.

Lin, C., Yang, L., Tanasa, B., Hutt, K., Ju, B.G., Ohgi, K., Zhang, J., Rose, D.W., Fu, X.D., Glass, C.K., and Rosenfeld, M.G. (2009). Nuclear receptor-induced chromosomal proximity and DNA breaks underlie specific translocations in cancer. *Cell* 139**,** 1069-1083. doi: 10.1016/j.cell.2009.11.030.

Lukasova, E., Kozubek, S., Kozubek, M., Kjeronska, J., Ryznar, L., Horakova, J., Krahulcova, E., and Horneck, G. (1997). Localisation and distance between ABL and BCR genes in interphase nuclei of bone marrow cells of control donors and patients with chronic myeloid leukaemia. *Hum Genet* 100**,** 525-535.

Lupianez, D.G., Kraft, K., Heinrich, V., Krawitz, P., Brancati, F., Klopocki, E., Horn, D., Kayserili, H., Opitz, J.M., Laxova, R., Santos-Simarro, F., Gilbert-Dussardier, B., Wittler, L., Borschiwer, M., Haas, S.A., Osterwalder, M., Franke, M., Timmermann, B., Hecht, J., Spielmann, M., Visel, A., and Mundlos, S. (2015). Disruptions of topological chromatin domains cause pathogenic rewiring of gene-enhancer interactions. *Cell* 161**,** 1012-1025. doi: 10.1016/j.cell.2015.04.004.

MacDonald, W.A., Sachani, S.S., White, C.R., and Mann, M.R. (2016). A role for chromatin topology in imprinted domain regulation. *Biochem Cell Biol* 94**,** 43-55. doi: 10.1139/bcb-2015-0032.

Malhas, A., Lee, C.F., Sanders, R., Saunders, N.J., and Vaux, D.J. (2007). Defects in lamin B1 expression or processing affect interphase chromosome position and gene expression. *J Cell Biol* 176**,** 593-603. doi: 10.1083/jcb.200607054.

Mani, R.S., Tomlins, S.A., Callahan, K., Ghosh, A., Nyati, M.K., Varambally, S., Palanisamy, N., and Chinnaiyan, A.M. (2009). Induced chromosomal proximity and gene fusions in prostate cancer. *Science* 326**,** 1230. doi: 10.1126/science.1178124.

Marini, B., Kertesz-Farkas, A., Ali, H., Lucic, B., Lisek, K., Manganaro, L., Pongor, S., Luzzati, R., Recchia, A., Mavilio, F., Giacca, M., and Lusic, M. (2015). Nuclear architecture dictates HIV-1 integration site selection. *Nature* 521**,** 227-231. doi: 10.1038/nature14226.

Matarazzo, M.R., Boyle, S., D'Esposito, M., and Bickmore, W.A. (2007). Chromosome territory reorganization in a human disease with altered DNA methylation. *Proc Natl Acad Sci U S A* 104**,** 16546-16551. doi: 10.1073/pnas.0702924104.

Mathas, S., Kreher, S., Meaburn, K.J., Johrens, K., Lamprecht, B., Assaf, C., Sterry, W., Kadin, M.E., Daibata, M., Joos, S., Hummel, M., Stein, H., Janz, M., Anagnostopoulos, I., Schrock, E., Misteli, T., and Dorken, B. (2009). Gene deregulation and spatial genome reorganization near breakpoints prior to formation of translocations in anaplastic large cell lymphoma. *Proc Natl Acad Sci U S A* 106**,** 5831-5836. doi: 10.1073/pnas.0900912106.

Mathur, S., Glogowska, A., McAvoy, E., Righolt, C., Rutherford, J., Willing, C., Banik, U., Ruthirakuhan, M., Mai, S., and Garcia, A. (2014). Three-dimensional quantitative imaging of telomeres in buccal cells identifies mild, moderate, and severe Alzheimer's disease patients. *J Alzheimers Dis* 39**,** 35-48. doi: 10.3233/JAD-130866.

Mattout, A., Pike, B.L., Towbin, B.D., Bank, E.M., Gonzalez-Sandoval, A., Stadler, M.B., Meister, P., Gruenbaum, Y., and Gasser, S.M. (2011). An EDMD mutation in C. elegans lamin blocks muscle-specific gene relocation and compromises muscle integrity. *Curr Biol* 21**,** 1603-1614. doi: 10.1016/j.cub.2011.08.030.

McCord, R.P., Nazario-Toole, A., Zhang, H., Chines, P.S., Zhan, Y., Erdos, M.R., Collins, F.S., Dekker, J., and Cao, K. (2013). Correlated alterations in genome organization, histone methylation, and DNA-lamin A/C interactions in Hutchinson-Gilford progeria syndrome. *Genome Res* 23**,** 260-269. doi: 10.1101/gr.138032.112.

McGregor, M., Hanley, J.A., Boivin, J.F., and McLean, R.G. (1998). Screening for prostate cancer: estimating the magnitude of overdetection. *CMAJ* 159**,** 1368-1372.

Meaburn, K., Burman, B., and Misteli, T. (2016a). "Spatial genome organization and disease," in *The functional Nucleus,* eds. G. Dellaire & D. Bazett-Jones. Springer DE), in press.

Meaburn, K.J., Agunloye, O., Devine, M., Leshner, M., Roloff, G.W., True, L.D., and Misteli, T. (2016b). Tissue-of-origin-specific gene repositioning in breast and prostate cancer. *Histochem Cell Biol* 145**,** 433-446. doi: 10.1007/s00418-015-1401-8.

Meaburn, K.J., Cabuy, E., Bonne, G., Levy, N., Morris, G.E., Novelli, G., Kill, I.R., and Bridger, J.M. (2007). Primary laminopathy fibroblasts display altered genome organization and apoptosis. *Aging Cell* 6**,** 139-153. doi: 10.1111/j.1474-9726.2007.00270.x.

1085 Meaburn, K.J., Gudla, P.R., Khan, S., Lockett, S.J., and Misteli, T. (2009). Disease-specific gene
1086 repositioning in breast cancer. *J Cell Biol* 187**,** 801-812. doi: 10.1083/jcb.200909127.

1087 Meaburn, K.J., Levy, N., Toniolo, D., and Bridger, J.M. (2005). Chromosome positioning is largely
1088 unaffected in lymphoblastoid cell lines containing emerin or A-type lamin mutations.
1089 *Biochem Soc Trans* 33**,** 1438-1440. doi: 10.1042/BST20051438.

1090 Meaburn, K.J., and Misteli, T. (2008). Locus-specific and activity-independent gene repositioning
1091 during early tumorigenesis. *J Cell Biol* 180**,** 39-50.

1092 Meaburn, K.J., Newbold, R.F., and Bridger, J.M. (2008). Positioning of human chromosomes in
1093 murine cell hybrids according to synteny. *Chromosoma* 117**,** 579-591. doi: 10.1007/s00412-
1094 008-0175-3.

1095 Mehta, I.S., Amira, M., Harvey, A.J., and Bridger, J.M. (2010). Rapid chromosome territory
1096 relocation by nuclear motor activity in response to serum removal in primary human
1097 fibroblasts. *Genome Biol* 11**,** R5. doi: 10.1186/gb-2010-11-1-r5.

1098 Mehta, I.S., Eskiw, C.H., Arican, H.D., Kill, I.R., and Bridger, J.M. (2011). Farnesyltransferase
1099 inhibitor treatment restores chromosome territory positions and active chromosome dynamics
1100 in Hutchinson-Gilford progeria syndrome cells. *Genome Biol* 12**,** R74. doi: 10.1186/gb-2011-
1101 12-8-r74.

1102 Mehta, I.S., Kulashreshtha, M., Chakraborty, S., Kolthur-Seetharam, U., and Rao, B.J. (2013).
1103 Chromosome territories reposition during DNA damage-repair response. *Genome Biol* 14**,**
1104 R135. doi: 10.1186/gb-2013-14-12-r135.

1105 Mewborn, S.K., Puckelwartz, M.J., Abuisneineh, F., Fahrenbach, J.P., Zhang, Y., MacLeod, H.,
1106 Dellefave, L., Pytel, P., Selig, S., Labno, C.M., Reddy, K., Singh, H., and McNally, E.
1107 (2010). Altered chromosomal positioning, compaction, and gene expression with a lamin A/C
1108 gene mutation. *PLoS One* 5**,** e14342. doi: 10.1371/journal.pone.0014342.

1109 Mikelsaar, R., Paves, H., Org, K., and Mikelsaar, A.V. (2014). Chromosome variant 1qh- and its
1110 influence on the 3D organization of chromosome 1 heterochromatin in interphase nucleus of
1111 patients with endometriosis. *J Genet* 93**,** 219-223.

1112 Miller, A.B., Wall, C., Baines, C.J., Sun, P., To, T., and Narod, S.A. (2014). Twenty five year
1113 follow-up for breast cancer incidence and mortality of the Canadian National Breast
1114 Screening Study: randomised screening trial. *BMJ* 348**,** g366. doi: 10.1136/bmj.g366.

1115 Mitelman, F., Johansson, B., and Mertens, F. (2007). The impact of translocations and gene fusions
1116 on cancer causation. *Nat Rev Cancer* 7**,** 233-245. doi: 10.1038/nrc2091.

1117 Moen, P.T., Jr., Johnson, C.V., Byron, M., Shopland, L.S., de la Serna, I.L., Imbalzano, A.N., and
1118 Lawrence, J.B. (2004). Repositioning of muscle-specific genes relative to the periphery of
1119 SC-35 domains during skeletal myogenesis. *Mol Biol Cell* 15**,** 197-206. doi:
1120 10.1091/mbc.E03-06-0388.

1121 Montironi, R., Mazzuccheli, R., Scarpelli, M., Lopez-Beltran, A., Fellegara, G., and Algaba, F.
1122 (2005). Gleason grading of prostate cancer in needle biopsies or radical prostatectomy
1123 specimens: contemporary approach, current clinical significance and sources of pathology
1124 discrepancies. *BJU Int* 95**,** 1146-1152. doi: 10.1111/j.1464-410X.2005.05540.x.

Morey, C., Kress, C., and Bickmore, W.A. (2009). Lack of bystander activation shows that localization exterior to chromosome territories is not sufficient to up-regulate gene expression. *Genome Res* 19**,** 1184-1194. doi: 10.1101/gr.089045.108.

Moss, S.F., Krivosheyev, V., de Souza, A., Chin, K., Gaetz, H.P., Chaudhary, N., Worman, H.J., and Holt, P.R. (1999). Decreased and aberrant nuclear lamin expression in gastrointestinal tract neoplasms. *Gut* 45**,** 723-729.

Muhlmann, M. (2002). Molecular cytogenetics in metaphase and interphase cells for cancer and genetic research, diagnosis and prognosis. Application in tissue sections and cell suspensions. *Genet Mol Res* 1**,** 117-127.

Murata, S., Nakazawa, T., Ohno, N., Terada, N., Iwashina, M., Mochizuki, K., Kondo, T., Nakamura, N., Yamane, T., Iwasa, S., Ohno, S., and Katoh, R. (2007). Conservation and alteration of chromosome territory arrangements in thyroid carcinoma cell nuclei. *Thyroid* 17**,** 489-496. doi: 10.1089/thy.2006.0328.

Narendra, V., Rocha, P.P., An, D., Raviram, R., Skok, J.A., Mazzoni, E.O., and Reinberg, D. (2015). CTCF establishes discrete functional chromatin domains at the Hox clusters during differentiation. *Science* 347**,** 1017-1021. doi: 10.1126/science.1262088.

Neems, D.S., Garza-Gongora, A.G., Smith, E.D., and Kosak, S.T. (2016). Topologically associated domains enriched for lineage-specific genes reveal expression-dependent nuclear topologies during myogenesis. *Proc Natl Acad Sci U S A*. doi: 10.1073/pnas.1521826113.

Nemeth, A., Conesa, A., Santoyo-Lopez, J., Medina, I., Montaner, D., Peterfia, B., Solovei, I., Cremer, T., Dopazo, J., and Langst, G. (2010). Initial genomics of the human nucleolus. *PLoS Genet* 6**,** e1000889. doi: 10.1371/journal.pgen.1000889.

Neves, H., Ramos, C., da Silva, M.G., Parreira, A., and Parreira, L. (1999). The nuclear topography of ABL, BCR, PML, and RARalpha genes: evidence for gene proximity in specific phases of the cell cycle and stages of hematopoietic differentiation. *Blood* 93**,** 1197-1207.

Nielsen, B., Albregtsen, F., and Danielsen, H.E. (2008). Statistical nuclear texture analysis in cancer research: a review of methods and applications. *Crit Rev Oncog* 14**,** 89-164.

Nora, E.P., Lajoie, B.R., Schulz, E.G., Giorgetti, L., Okamoto, I., Servant, N., Piolot, T., van Berkum, N.L., Meisig, J., Sedat, J., Gribnau, J., Barillot, E., Bluthgen, N., Dekker, J., and Heard, E. (2012). Spatial partitioning of the regulatory landscape of the X-inactivation centre. *Nature* 485**,** 381-385. doi: 10.1038/nature11049.

Palstra, R.J., Simonis, M., Klous, P., Brasset, E., Eijkelkamp, B., and de Laat, W. (2008). Maintenance of long-range DNA interactions after inhibition of ongoing RNA polymerase II transcription. *PLoS One* 3**,** e1661. doi: 10.1371/journal.pone.0001661.

Parada, L., McQueen, P., and Misteli, T. (2004). Tissue-specific spatial organization of genomes. *Genome Biology* 7**,** R44.

Parada, L.A., McQueen, P.G., Munson, P.J., and Misteli, T. (2002). Conservation of relative chromosome positioning in normal and cancer cells. *Curr Biol* 12**,** 1692-1697.

Parada, L.A., Roix, J.J., and Misteli, T. (2003). An uncertainty principle in chromosome positioning. *Trends Cell Biol* 13**,** 393-396.

Paz, N., Felipe-Blanco, I., Royo, F., Zabala, A., Guerra-Merino, I., Garcia-Orad, A., Zugaza, J.L., and Parada, L.A. (2015). Expression of the DYRK1A gene correlates with its 3D positioning

in the interphase nucleus of Down syndrome cells. *Chromosome Res*. doi: 10.1007/s10577-015-9467-7.

Paz, N., Zabala, A., Royo, F., Garcia-Orad, A., Zugaza, J.L., and Parada, L.A. (2013). Combined fluorescent-chromogenic in situ hybridization for identification and laser microdissection of interphase chromosomes. *PLoS One* 8**,** e60238. doi: 10.1371/journal.pone.0060238.

Peric-Hupkes, D., Meuleman, W., Pagie, L., Bruggeman, S.W., Solovei, I., Brugman, W., Graf, S., Flicek, P., Kerkhoven, R.M., van Lohuizen, M., Reinders, M., Wessels, L., and van Steensel, B. (2010). Molecular maps of the reorganization of genome-nuclear lamina interactions during differentiation. *Mol Cell* 38**,** 603-613. doi: 10.1016/j.molcel.2010.03.016.

Pickersgill, H., Kalverda, B., de Wit, E., Talhout, W., Fornerod, M., and van Steensel, B. (2006). Characterization of the Drosophila melanogaster genome at the nuclear lamina. *Nat Genet* 38**,** 1005-1014. doi: 10.1038/ng1852.

Ragoczy, T., Bender, M.A., Telling, A., Byron, R., and Groudine, M. (2006). The locus control region is required for association of the murine beta-globin locus with engaged transcription factories during erythroid maturation. *Genes Dev* 20**,** 1447-1457.

Ragoczy, T., Telling, A., Sawado, T., Groudine, M., and Kosak, S.T. (2003). A genetic analysis of chromosome territory looping: diverse roles for distal regulatory elements. *Chromosome Res* 11**,** 513-525.

Ranade, D., Koul, S., Thompson, J., Prasad, K.B., and Sengupta, K. (2016). Chromosomal aneuploidies induced upon Lamin B2 depletion are mislocalized in the interphase nucleus. *Chromosoma*. doi: 10.1007/s00412-016-0580-y.

Randise-Hinchliff, C., Coukos, R., Sood, V., Sumner, M.C., Zdraljevic, S., Meldi Sholl, L., Garvey Brickner, D., Ahmed, S., Watchmaker, L., and Brickner, J.H. (2016). Strategies to regulate transcription factor-mediated gene positioning and interchromosomal clustering at the nuclear periphery. *J Cell Biol*. doi: 10.1083/jcb.201508068.

Rao, S.S., Huntley, M.H., Durand, N.C., Stamenova, E.K., Bochkov, I.D., Robinson, J.T., Sanborn, A.L., Machol, I., Omer, A.D., Lander, E.S., and Aiden, E.L. (2014). A 3D map of the human genome at kilobase resolution reveals principles of chromatin looping. *Cell* 159**,** 1665-1680. doi: 10.1016/j.cell.2014.11.021.

Reddy, K.L., Zullo, J.M., Bertolino, E., and Singh, H. (2008). Transcriptional repression mediated by repositioning of genes to the nuclear lamina. *Nature* 452**,** 243-247.

Roix, J.J., McQueen, P.G., Munson, P.J., Parada, L.A., and Misteli, T. (2003). Spatial proximity of translocation-prone gene loci in human lymphomas. *Nat Genet* 34**,** 287-291.

Roukos, V., Voss, T.C., Schmidt, C.K., Lee, S., Wangsa, D., and Misteli, T. (2013). Spatial dynamics of chromosome translocations in living cells. *Science* 341**,** 660-664. doi: 10.1126/science.1237150.

Saarinen, I., Mirtti, T., Seikkula, H., Bostrom, P.J., and Taimen, P. (2015). Differential Predictive Roles of A- and B-Type Nuclear Lamins in Prostate Cancer Progression. *PLoS One* 10**,** e0140671. doi: 10.1371/journal.pone.0140671.

Sandhu, G.S., and Andriole, G.L. (2012). Overdiagnosis of prostate cancer. *J Natl Cancer Inst Monogr* 2012**,** 146-151. doi: 10.1093/jncimonographs/lgs031.

Scaffidi, P., and Misteli, T. (2005). Reversal of the cellular phenotype in the premature aging disease Hutchinson-Gilford progeria syndrome. *Nat Med* 11**,** 440-445. doi: 10.1038/nm1204.

Scheuermann, M.O., Tajbakhsh, J., Kurz, A., Saracoglu, K., Eils, R., and Lichter, P. (2004). Topology of genes and nontranscribed sequences in human interphase nuclei. *Exp Cell Res* 301**,** 266-279.

Schnitt, S.J. (2010). Classification and prognosis of invasive breast cancer: from morphology to molecular taxonomy. *Mod Pathol* 23 Suppl 2**,** S60-64. doi: 10.1038/modpathol.2010.33.

Schoenfelder, S., Sexton, T., Chakalova, L., Cope, N.F., Horton, A., Andrews, S., Kurukuti, S., Mitchell, J.A., Umlauf, D., Dimitrova, D.S., Eskiw, C.H., Luo, Y., Wei, C.L., Ruan, Y., Bieker, J.J., and Fraser, P. (2010). Preferential associations between co-regulated genes reveal a transcriptional interactome in erythroid cells. *Nat Genet* 42**,** 53-61. doi: 10.1038/ng.496.

Sexton, T., Yaffe, E., Kenigsberg, E., Bantignies, F., Leblanc, B., Hoichman, M., Parrinello, H., Tanay, A., and Cavalli, G. (2012). Three-dimensional folding and functional organization principles of the Drosophila genome. *Cell* 148**,** 458-472. doi: 10.1016/j.cell.2012.01.010.

Shachar, S., Voss, T.C., Pegoraro, G., Sciascia, N., and Misteli, T. (2015). Identification of Gene Positioning Factors Using High-Throughput Imaging Mapping. *Cell* 162**,** 911-923. doi: 10.1016/j.cell.2015.07.035.

Shopland, L.S., Lynch, C.R., Peterson, K.A., Thornton, K., Kepper, N., Hase, J., Stein, S., Vincent, S., Molloy, K.R., Kreth, G., Cremer, C., Bult, C.J., and O'Brien, T.P. (2006). Folding and organization of a contiguous chromosome region according to the gene distribution pattern in primary genomic sequence. *J Cell Biol* 174**,** 27-38.

Siegel, R.L., Miller, K.D., and Jemal, A. (2016). Cancer statistics, 2016. *CA Cancer J Clin* 66**,** 7-30. doi: 10.3322/caac.21332.

Simonis, M., Klous, P., Splinter, E., Moshkin, Y., Willemsen, R., de Wit, E., van Steensel, B., and de Laat, W. (2006). Nuclear organization of active and inactive chromatin domains uncovered by chromosome conformation capture-on-chip (4C). *Nat Genet* 38**,** 1348-1354. doi: 10.1038/ng1896.

Solovei, I., Kreysing, M., Lanctot, C., Kosem, S., Peichl, L., Cremer, T., Guck, J., and Joffe, B. (2009). Nuclear architecture of rod photoreceptor cells adapts to vision in mammalian evolution. *Cell* 137**,** 356-368. doi: 10.1016/j.cell.2009.01.052.

Solovei, I., Schermelleh, L., During, K., Engelhardt, A., Stein, S., Cremer, C., and Cremer, T. (2004). Differences in centromere positioning of cycling and postmitotic human cell types. *Chromosoma* 112**,** 410-423.

Solovei, I., Thanisch, K., and Feodorova, Y. (2016). How to rule the nucleus: divide et impera. *Curr Opin Cell Biol* 40**,** 47-59. doi: 10.1016/j.ceb.2016.02.014.

Solovei, I., Wang, A.S., Thanisch, K., Schmidt, C.S., Krebs, S., Zwerger, M., Cohen, T.V., Devys, D., Foisner, R., Peichl, L., Herrmann, H., Blum, H., Engelkamp, D., Stewart, C.L., Leonhardt, H., and Joffe, B. (2013). LBR and lamin A/C sequentially tether peripheral heterochromatin and inversely regulate differentiation. *Cell* 152**,** 584-598. doi: 10.1016/j.cell.2013.01.009.

Sorlie, T., Perou, C.M., Tibshirani, R., Aas, T., Geisler, S., Johnsen, H., Hastie, T., Eisen, M.B., van de Rijn, M., Jeffrey, S.S., Thorsen, T., Quist, H., Matese, J.C., Brown, P.O., Botstein, D., Lonning, P.E., and Borresen-Dale, A.L. (2001). Gene expression patterns of breast

carcinomas distinguish tumor subclasses with clinical implications. *Proc Natl Acad Sci U S A* 98**,** 10869-10874. doi: 10.1073/pnas.191367098.

Soutoglou, E., Dorn, J.F., Sengupta, K., Jasin, M., Nussenzweig, A., Ried, T., Danuser, G., and Misteli, T. (2007). Positional stability of single double-strand breaks in mammalian cells. *Nat Cell Biol* 9**,** 675-682. doi: 10.1038/ncb1591.

Taddei, A., Van Houwe, G., Hediger, F., Kalck, V., Cubizolles, F., Schober, H., and Gasser, S.M. (2006). Nuclear pore association confers optimal expression levels for an inducible yeast gene. *Nature* 441**,** 774-778.

Taimen, P., Pfleghaar, K., Shimi, T., Moller, D., Ben-Harush, K., Erdos, M.R., Adam, S.A., Herrmann, H., Medalia, O., Collins, F.S., Goldman, A.E., and Goldman, R.D. (2009). A progeria mutation reveals functions for lamin A in nuclear assembly, architecture, and chromosome organization. *Proc Natl Acad Sci U S A* 106**,** 20788-20793. doi: 10.1073/pnas.0911895106.

Takizawa, T., Gudla, P.R., Guo, L., Lockett, S., and Misteli, T. (2008a). Allele-specific nuclear positioning of the monoallelically expressed astrocyte marker GFAP. *Genes Dev* 22**,** 489-498. doi: 10.1101/gad.1634608.

Takizawa, T., Meaburn, K.J., and Misteli, T. (2008b). The meaning of gene positioning. *Cell* 135**,** 9-13. doi: 10.1016/j.cell.2008.09.026.

Tan-Wong, S.M., Wijayatilake, H.D., and Proudfoot, N.J. (2009). Gene loops function to maintain transcriptional memory through interaction with the nuclear pore complex. *Genes Dev* 23**,** 2610-2624. doi: 10.1101/gad.1823209.

Therizols, P., Illingworth, R.S., Courilleau, C., Boyle, S., Wood, A.J., and Bickmore, W.A. (2014). Chromatin decondensation is sufficient to alter nuclear organization in embryonic stem cells. *Science* 346**,** 1238-1242. doi: 10.1126/science.1259587.

Thompson, I., Thrasher, J.B., Aus, G., Burnett, A.L., Canby-Hagino, E.D., Cookson, M.S., D'Amico, A.V., Dmochowski, R.R., Eton, D.T., Forman, J.D., Goldenberg, S.L., Hernandez, J., Higano, C.S., Kraus, S.R., Moul, J.W., Tangen, C.M., and Panel, A.U.A.P.C.C.G.U. (2007). Guideline for the management of clinically localized prostate cancer: 2007 update. *J Urol* 177**,** 2106-2131. doi: 10.1016/j.juro.2007.03.003.

Thompson, M., Haeusler, R.A., Good, P.D., and Engelke, D.R. (2003). Nucleolar clustering of dispersed tRNA genes. *Science* 302**,** 1399-1401.

Timme, S., Schmitt, E., Stein, S., Schwarz-Finsterle, J., Wagner, J., Walch, A., Werner, M., Hausmann, M., and Wiech, T. (2011). Nuclear position and shape deformation of chromosome 8 territories in pancreatic ductal adenocarcinoma. *Anal Cell Pathol (Amst)* 34**,** 21-33. doi: 10.3233/ACP-2011-0004.

Torre, L.A., Bray, F., Siegel, R.L., Ferlay, J., Lortet-Tieulent, J., and Jemal, A. (2015). Global cancer statistics, 2012. *CA Cancer J Clin* 65**,** 87-108. doi: 10.3322/caac.21262.

Towbin, B.D., Gonzalez-Aguilera, C., Sack, R., Gaidatzis, D., Kalck, V., Meister, P., Askjaer, P., and Gasser, S.M. (2012). Step-wise methylation of histone H3K9 positions heterochromatin at the nuclear periphery. *Cell* 150**,** 934-947. doi: 10.1016/j.cell.2012.06.051.

Van der Kwast, T.H. (2014). Prognostic prostate tissue biomarkers of potential clinical use. *Virchows Arch* 464**,** 293-300. doi: 10.1007/s00428-014-1540-7.

van Koningsbruggen, S., Gierlinski, M., Schofield, P., Martin, D., Barton, G.J., Ariyurek, Y., den Dunnen, J.T., and Lamond, A.I. (2010). High-resolution whole-genome sequencing reveals that specific chromatin domains from most human chromosomes associate with nucleoli. *Mol Biol Cell* 21**,** 3735-3748. doi: 10.1091/mbc.E10-06-0508.

van Steensel, B., and Dekker, J. (2010). Genomics tools for unraveling chromosome architecture. *Nat Biotechnol* 28**,** 1089-1095. doi: 10.1038/nbt.1680.

Veltri, R.W., and Christudass, C.S. (2014). Nuclear morphometry, epigenetic changes, and clinical relevance in prostate cancer. *Adv Exp Med Biol* 773**,** 77-99. doi: 10.1007/978-1-4899-8032-8_4.

Venables, R.S., McLean, S., Luny, D., Moteleb, E., Morley, S., Quinlan, R.A., Lane, E.B., and Hutchison, C.J. (2001). Expression of individual lamins in basal cell carcinomas of the skin. *Br J Cancer* 84**,** 512-519. doi: 10.1054/bjoc.2000.1632.

Volpi, E.V., Chevret, E., Jones, T., Vatcheva, R., Williamson, J., Beck, S., Campbell, R.D., Goldsworthy, M., Powis, S.H., Ragoussis, J., Trowsdale, J., and Sheer, D. (2000). Large-scale chromatin organization of the major histocompatibility complex and other regions of human chromosome 6 and its response to interferon in interphase nuclei. *J Cell Sci* 113 (Pt 9)**,** 1565-1576.

Wang, Q., Sawyer, I.A., Sung, M.H., Sturgill, D., Shevtsov, S.P., Pegoraro, G., Hakim, O., Baek, B., Hager, G.L., and Dundr, M. (2016). Cajal bodies are linked to genome conformation. *Nature Communications* in press. doi: 10.1038/ncomms10966.

Wansink, D.G., Schul, W., van der Kraan, I., van Steensel, B., van Driel, R., and de Jong, L. (1993). Fluorescent labelling of nascent RNA reveals transcription by RNA polymerase II in domains scattered throughout the nucleus. *J. Cell Biol.* 122**,** 282-293.

Wazir, U., Ahmed, M.H., Bridger, J.M., Harvey, A., Jiang, W.G., Sharma, A.K., and Mokbel, K. (2013). The clinicopathological significance of lamin A/C, lamin B1 and lamin B receptor mRNA expression in human breast cancer. *Cell Mol Biol Lett* 18**,** 595-611. doi: 10.2478/s11658-013-0109-9.

Welch, H.G., and Black, W.C. (2010). Overdiagnosis in cancer. *J Natl Cancer Inst* 102**,** 605-613. doi: 10.1093/jnci/djq099.

Wiech, T., Stein, S., Lachenmaier, V., Schmitt, E., Schwarz-Finsterle, J., Wiech, E., Hildenbrand, G., Werner, M., and Hausmann, M. (2009). Spatial allelic imbalance of BCL2 genes and chromosome 18 territories in nonneoplastic and neoplastic cervical squamous epithelium. *Eur Biophys J* 38**,** 793-806.

Wiech, T., Timme, S., Riede, F., Stein, S., Schuricke, M., Cremer, C., Werner, M., Hausmann, M., and Walch, A. (2005). Human archival tissues provide a valuable source for the analysis of spatial genome organization. *Histochem Cell Biol* 123**,** 229-238.

Wijchers, P.J., Geeven, G., Eyres, M., Bergsma, A.J., Janssen, M., Verstegen, M., Zhu, Y., Schell, Y., Vermeulen, C., de Wit, E., and de Laat, W. (2015). Characterization and dynamics of pericentromere-associated domains in mice. *Genome Res* 25**,** 958-969. doi: 10.1101/gr.186643.114.

Wijchers, P.J., Krijger, P.H., Geeven, G., Zhu, Y., Denker, A., Verstegen, M.J., Valdes-Quezada, C., Vermeulen, C., Janssen, M., Teunissen, H., Anink-Groenen, L.C., Verschure, P.J., and de

1334 Laat, W. (2016). Cause and Consequence of Tethering a SubTAD to Different Nuclear
1335 Compartments. *Mol Cell* 61**,** 461-473. doi: 10.1016/j.molcel.2016.01.001.

1336 Williams, R.R., Azuara, V., Perry, P., Sauer, S., Dvorkina, M., Jorgensen, H., Roix, J., McQueen, P.,
1337 Misteli, T., Merkenschlager, M., and Fisher, A.G. (2006). Neural induction promotes large-
1338 scale chromatin reorganisation of the Mash1 locus. *J Cell Sci* 119**,** 132-140.

1339 Williams, R.R., Broad, S., Sheer, D., and Ragoussis, J. (2002). Subchromosomal positioning of the
1340 epidermal differentiation complex (EDC) in keratinocyte and lymphoblast interphase nuclei.
1341 *Exp Cell Res* 272**,** 163-175.

1342 Willis, N.D., Cox, T.R., Rahman-Casans, S.F., Smits, K., Przyborski, S.A., van den Brandt, P., van
1343 Engeland, M., Weijenberg, M., Wilson, R.G., de Bruine, A., and Hutchison, C.J. (2008).
1344 Lamin A/C is a risk biomarker in colorectal cancer. *PLoS One* 3**,** e2988. doi:
1345 10.1371/journal.pone.0002988.

1346 Zeitz, M.J., Ay, F., Heidmann, J.D., Lerner, P.L., Noble, W.S., Steelman, B.N., and Hoffman, A.R.
1347 (2013). Genomic interaction profiles in breast cancer reveal altered chromatin architecture.
1348 *PLoS One* 8**,** e73974. doi: 10.1371/journal.pone.0073974.

1349 Zink, D., Amaral, M.D., Englmann, A., Land, S., Clarke, L.A., Rudolph, C., Alt, F., Luther, K., Braz,
1350 C., Sadoni, N., Rosenecker, J., and Schindelhauer, D. (2004a). Transcription-dependent
1351 spatial arrangement of CFTR and adjacent genes in human cell nuclei. *J. Cell Biol.* I166**,** 815-
1352 825.

1353 Zink, D., Fische, A.H., and Nickerson, J.A. (2004b). Nuclear structure in cancer cells. *Nat Rev*
1354 *Cancer* 4**,** 677-687.

1355 Zuleger, N., Boyle, S., Kelly, D.A., de Las Heras, J.I., Lazou, V., Korfali, N., Batrakou, D.G.,
1356 Randles, K.N., Morris, G.E., Harrison, D.J., Bickmore, W.A., and Schirmer, E.C. (2013).
1357 Specific nuclear envelope transmembrane proteins can promote the location of chromosomes
1358 to and from the nuclear periphery. *Genome Biol* 14**,** R14. doi: 10.1186/gb-2013-14-2-r14.

1359 Zullo, J.M., Demarco, I.A., Pique-Regi, R., Gaffney, D.J., Epstein, C.B., Spooner, C.J., Luperchio,
1360 T.R., Bernstein, B.E., Pritchard, J.K., Reddy, K.L., and Singh, H. (2012). DNA sequence-
1361 dependent compartmentalization and silencing of chromatin at the nuclear lamina. *Cell* 149**,**
1362 1474-1487. doi: 10.1016/j.cell.2012.04.035.

1363
1364

Figure legends

Figure 1: Non-random organization of the genome. The spatial organization of the genome is characterized in several ways: **(A)** Radial positioning describes the position of a locus relative to the center and periphery of the nucleus. Gene-poor chromosomes (yellow) generally locate to the nuclear periphery, whilst gene-rich chromosomes have a preference for the nuclear interior. **(B-E)** Relative positioning describes the position of a locus relative to another nuclear landmark. **(B)** The position of a locus relative to another locus. The yellow and orange chromosomes are in close spatial proximity, whereas the orange and red chromosomes are distal. **(C)** Association with the nuclear envelope (NE). Some genes co-localize with the NE at high frequency (yellow gene). **(D)** Association with a nuclear body such as a splicing speckle. **(E)** The position of gene relative its own chromosome territory. Some gene rich loci loop out of the bulk of the chromosome territory when highly expressed.

Figure 2: Loci-specific reorganization of the genome in disease. Certain loci adopt alternative nuclear positions in disease (tick) compared to normal cells, whilst the positions of other loci are conserved in disease (cross). Moreover, the repositioning of some loci is disease specific, and although a gene repositions in one disease, it may not in another disease. Blue = Nucleus; NE = Nuclear envelope; Cent. = Centromere.

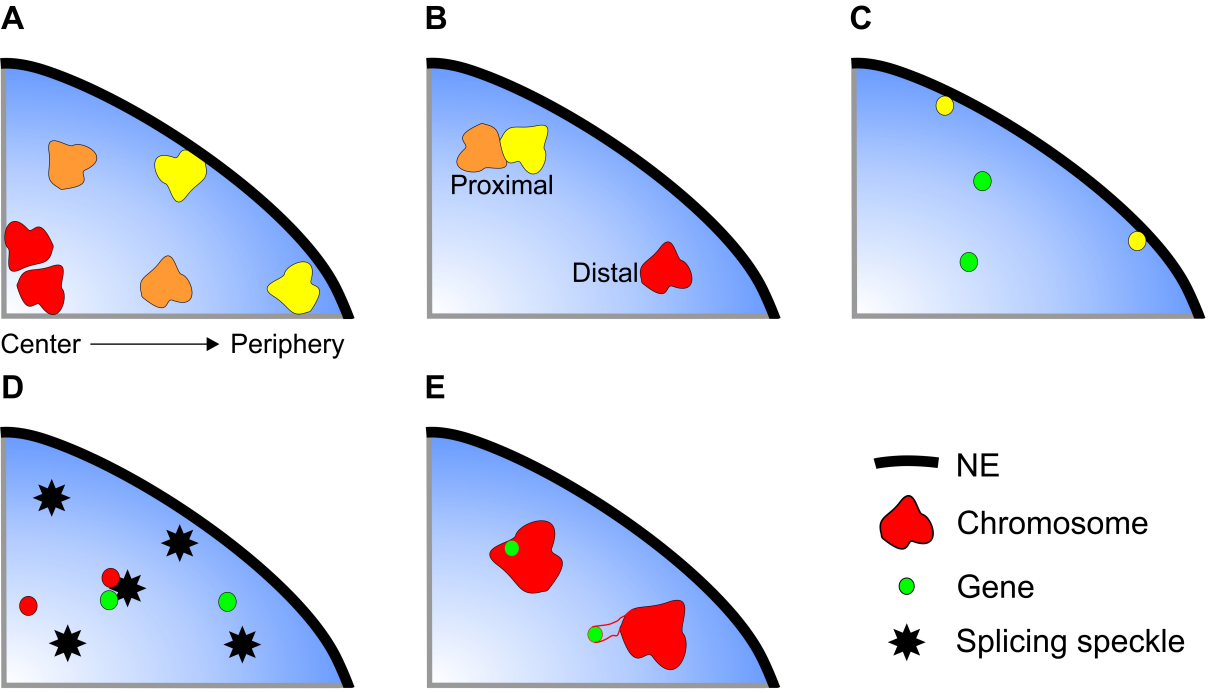
A
B
C
Proximal
Distal
Center
Periphery
D
E
NE
Chromosome
Gene
Splicing speckle

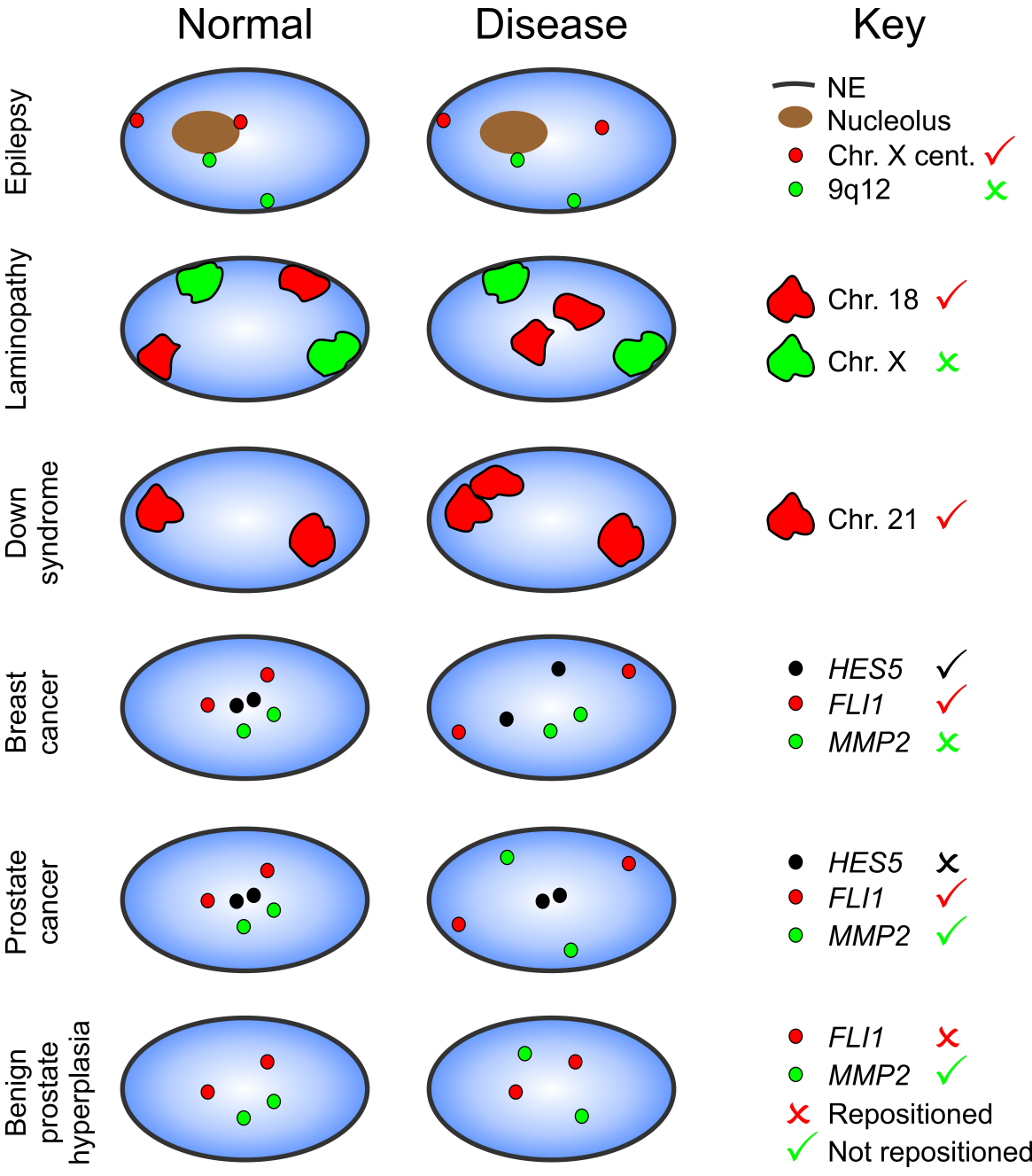
Normal
Disease
Key
Epilepsy
Laminopathy
Down syndrome
Breast cancer
Prostate cancer
Benign prostate hyperplasia
NE
Nucleolus
Chr. X cent.
9q12
Chr. 18
Chr. X
Chr. 21
HES5
FLI1
MMP2
HES5
FLI1
MMP2
FLI1
MMP2
Repositioned
Not repositioned